Stochastic Systems Approaches to Disease Control

Martin Knight

Doctor of Philosophy

University of York

Environment and Geography

March 2021

Abstract

Recent developments in network theory have provided new avenues for studying the spread of disease within populations. However, there is a need to develop dynamic generative models of networks that can capture the dynamic nature of many real-world systems that typical models cannot account for.

Models of the spread of livestock disease have frequently employed traditional network approaches, but with the availability of highly detailed animal movement datasets, there is unprecedented scope to develop generative models of livestock trade parameterised by these data and exploring the spread of disease modulated by trade. Livestock diseases incur significant financial burdens on farms and governments, and the presence of disease remains a constant issue, so developing new insights and novel control strategies is vital.

Analytically tractable generative models of livestock trade, parameterised to the Scottish cattle trading system, are developed, incorporating dynamics such as time-varying trading partnerships that, to date, have not been accounted for. Expressions for the basic reproduction number R_0 are obtained and manipulations to trading behaviour are shown to reduce R_0 while maintaining farm business requirements.

Extended models, accounting for time-varying trading behaviours, are developed. Individual-based adaptation in response to changes in trading propensities is shown to mitigate the prevalence reducing potential of such changes, highlighting the need to account for behavioural responses when modelling disease spread. Typical disease control measures, such as post-movement testing and risk aversion are shown to be effective in controlling disease, but can perturb the trading system. When parameterised to the Scottish cattle trade system, the impact of these control measures on prevalence is explored.

The models presented here are a first attempt at analysing trade and its effect on disease spread at a national scale for a highly heterogeneous system using a generative network modelling approach, and can be extended to other real-world systems.

Contents

List of Tables **5**

List of Figures **6**

Acknowledgements **26**

Author's Declaration **27**

1 Introduction **28**

1.1 Livestock diseases within cattle herds 29

1.1.1 Bovine Tuberculosis 29

1.1.2 Paratuberculosis 31

1.1.3 Foot-and-Mouth Disease 32

1.2 Demographics of livestock movements 33

1.3 Networks 35

1.3.1 Static networks 35

1.3.2 Temporal networks 37

1.4 Modelling disease dynamics 38

1.4.1 Compartmental and mass action models 38

1.4.2 Disease spread on networks 39

1.4.3 Stochastic simulation of disease processes 41

1.5 Network-based approaches to modelling disease spread on livestock trading systems 43

1.6 The thesis 46

1.6.1 Aims . . . 46
1.6.2 Thesis structure . . . 46

2 Generative models of network dynamics provide insight into the effects of trade on endemic livestock disease 48

2.1 Introduction . . . 48
2.2 Materials and methods . . . 51
2.2.1 Livestock trading model . . . 51
2.3 Results . . . 55
2.3.1 Farms' basic reproduction number . . . 55
2.3.2 The effect of changes to trading practices . . . 56
2.4 Case study: Scottish cattle trade industry . . . 59
2.4.1 Assessing the potential for trade practices to modulate endemic disease . . . 63
2.4.2 Impact of trade practices on a wide range of endemic diseases 65
2.4.3 Targeting the trade practices of large buyers . . . 66
2.4.4 Combining targeted changes to trading practices with targeted biosecurity . . . 68
2.5 Discussion . . . 69
2.6 Appendix . . . 73
2.6.1 Derivation of $p_{ij}(t)$ and $k_i^{in}(t)$ . . . 73
2.6.2 Derivation of R_0^i . . . 74
2.6.3 R_0^i in large ε_{trade} limit . . . 77
2.6.4 R_0^i in small ε_{ptnr} limit . . . 77
2.6.5 R_0^i in large ε_{ptnr} limit . . . 78
2.6.6 R_0^i in fully connected limit . . . 78
2.6.7 Comparison of theoretical predictions with stochastic simulation 78
2.6.8 Comparing changes to frequency and size of trades . . . 80
2.6.9 Comparing changes to duration of trading partnerships . . . 80
2.6.10 Comparing changes to number of concurrent trading partners 82
2.6.11 Overview of CTS data analysis . . . 83

2.6.12 Distributions of model quantities from CTS data 87
2.6.13 Distribution of trading partners' out-flows and partnership duration before and after modification to formation and cessation rates 90
2.6.14 Values of R_0 for varying trade patterns 94
2.6.15 Values of R_0 for varying disease parameterisations 95

3 A stochastic, adaptive systems view of livestock trading 97
3.1 Introduction 97
3.2 An individual-based systems model of trade dynamics 99
3.2.1 Mechanisms of stock generation and a global pricing strategy . 99
3.2.2 The dynamics of trade partnerships 103
3.2.3 The dynamics of trade 104
3.3 The adaptive system dynamics of trade 107
3.3.1 Exclusion of a pricing model can lead to divergent stock levels 107
3.3.2 Shocks in stock quantities 108
3.3.3 Effects of trade and partnership friction on system dynamics . 111
3.4 Disease control and trade in a complex adaptive system 118
3.4.1 The effect of friction on disease spread and control 123
3.4.2 Movement testing: impact on trading patterns and prevalence 129
3.4.3 Networked versus global information to inform risk aversion . 135
3.5 Discussion 145
3.6 Appendix 150
3.6.1 Plots for $\lambda = 0.05$, $\gamma = 1/3$ 150
3.6.2 Plots for $\lambda = 0.25$, $\gamma = 1.5$ 157

4 National-scale parameterisation of generative systems model for livestock trade and implications for disease control 164
4.1 Introduction 164
4.2 Parameterising systems model of trade dynamics using farm-to-farm movement data 166
4.2.1 Assessing model fit at global and farm level 169

4.2.2 Measuring farm stock quantities . . . 176
4.3 Disease spread on Scottish cattle trading system . . . 178
4.3.1 Impact of changes to propensities of trade . . . 180
4.3.2 Whole batch testing and rejecting . . . 186
4.3.3 Whole batch testing and rejecting with a global risk aversion strategy . . . 190
4.3.4 Whole batch testing and rejecting with a global risk aversion strategy and discounting of risk . . . 194
4.4 Discussion . . . 197

5 Discussion **201**
5.1 Aims of the thesis . . . 201
5.1.1 Chapter 2 . . . 203
5.1.2 Chapter 3 . . . 204
5.1.3 Chapter 4 . . . 207
5.2 The role of trade in disease spread . . . 209
5.3 Extensions and future work . . . 211

6 References **215**

List of Tables

2.1 Table of model quantities and their respective definitions 52

3.1 Table of quantities and parameters in the model 101
3.2 Table of system-level averages for trading quantities obtained from the Scottish trading system. 123

4.1 Table of correlation coefficients of trade quantities from simulation and data output for individual farms. 170
4.2 Table of K-S test maximum absolute difference between stochastic simulation output and data. 172
4.3 Table of sim-data ratios of trade quantities with their respective system-wide means, standard deviations, and MAPE, the mean absolute percentage error. 175
4.4 Table of the number (and percentages) of farms with sim-data ratios smaller than 0.8 and greater than 1.2. 176

List of Figures

1.1 Time trajectories of the deterministic (left) and stochastic (right) SIS disease model. 1000 stochastic realisations are generated for using the Gillespie SSA. 43

1.2 Distribution of equilibrium disease prevalence for the stochastic SIS model. 44

2.1 **Model fit to data**. For model with modifications to partnership formation and cessation rates. Panel (a) shows the average out-flow, ζ_j, of farms' trading partners, where blue points are obtained from data, and points from stochastic simulation, where simulations are performed using Gillespie Stochastic Simulation Algorithm. Bottom four panels show comparisons of simulation output and data for four statistics: annual in-flow (b), annual number of concurrent trading partners (c), annual number of partnership formations (d), and annual number of partnership cessations (e). 61

2.2 **Impact of trade behaviour and partnership dynamics.** Percentage change in R_0 for a persistent and high prevalence disease ($\lambda = \gamma = 0.2$) due to changes in the dynamics of trade and trade partnerships compared with the current dynamics of the Scottish trade system (grey squares). We consider changes to batch size and partnership duration (a), batch size and number of concurrent trading partners (b), and number of concurrent trading partners and partnership duration (c). 62

2.3 **Reducing endemic disease burden.** The percentage reduction in the system average R_0 for a range of disease parameterisations under specific trading and partnership dynamics changes, when compared with values of R_0 for current trading patterns in the Scottish trade system. Black points represent disease parameterisations in which $R_0 > 1$ before changes, and $R_0 < 1$ after changes are implemented. . . 64

2.4 **Targeting high risk farms.** Percentage reduction in R_0 compared to: current trading patterns (left); and 100% adoption of new trading patterns (right). The new trading patterns are those shown in the bottom right panel of Figure 2.3d, which provides percentage reduction at 100% (dashed lines). In both panels the x-axis indicates what percentage of the most frequent buyers (those making the largest number of trades annually) are adopting these changes. Different disease parameterisations are shown with dashed lines representing values of R_0 for: Case 1) $\lambda = 0.06$, $\gamma = 1$; Case 2) $\lambda = 0.15$, $\gamma = 0.4$; and Case 3) $\lambda = 0.25$, $\gamma = 0.2$. Initial R_0 values for current trading patterns are: Case 1) $R_0 = 1.19$, Case 2) $R_0 = 4.92$, and Case 3) $R_0 = 11.43$. . 66

2.5 **Comparing biosecurity with changes to trade patterns.** Percentage reduction in R_0 (disease parameters $\lambda = 0.25$ and $\gamma = 0.2$) for targeted changes to both trading practices and improved biosecurity (left), and due solely to targeted improvements to biosecurity (right). In both cases, x-axes indicate what percentage of the most frequent buyers adopt trade changes and largest sellers improve biosecurity. . . 68

2.6 Farm pair transition diagram. The farm pair can begin in either the $S-I$ state or the $S \cdot I$ state, corresponding to the presence or absence of a trading partnership, respectively. The presented states are the only ones relevant to obtaining the probability that the infected farm transmits infection to the susceptible farm, i.e. the probability of transitioning to the $I-I$ state, and are thus the only states relevant to obtaining R_0^i. 75

2.7 The system-average R_0 (top left), equilibrium disease prevalence (top right), percentage reduction in R_0 compared to the initial state (bottom left), and the percentage reduction in the equilibrium disease prevalence compared to the initial state (bottom right) as the average batch size is increased from an initial batch size of 1. Solid red lines represent the theoretical predictions for the homogeneous system, and solid black lines represent the output of the average of 2000 independent simulations for the homogeneous system. Dashed lines represent the same output for the Power-Law system, except in simulations each of the 200 farms is chosen to be the initial infected in 10 simulations. 81

2.8 The system-average R_0 (top left), equilibrium disease prevalence (top right), percentage reduction in R_0 compared to the initial state (bottom left), and the percentage reduction in the equilibrium disease prevalence compared to the initial state (bottom right) as the average trading partnership duration is increased from an initial duration of 1 time unit. Solid red lines represent the theoretical predictions for the homogeneous system, and solid black lines represent the output of the average of 2000 independent simulations for the homogeneous system. Dashed lines represent the same output for the Power-Law system, except in simulations each of the 200 farms is chosen to be the initial infected in 10 simulations. 82

2.9 The system-average R_0 (top left), equilibrium disease prevalence (top right), percentage reduction in R_0 compared to the initial state (bottom left), and the percentage reduction in the equilibrium disease prevalence compared to the initial state (bottom right) as the average number of concurrent trading partners is increased from an initial number of 0.1. Solid red lines represent the theoretical predictions for the homogeneous system, and solid black lines represent the output of the average of 2000 independent simulations for the homogeneous system. Dashed lines represent the same output for the Power-Law system, except in simulations each of the 200 farms is chosen to be the initial infected in 10 simulations. 83
2.10 Monthly total number of animal movements (a) and number of animals moved (b). In general, animal movements and flows are consistent year-on-year, though there is a notable decline in 2007, corresponding to the small FMD outbreak that occurred. 87
2.11 The distribution (a) and empirical cumulative distribution (b) of animal flows. 88
2.14 The distribution (a) and empirical cumulative distribution (b) of the average batch size. 88
2.12 The distribution (a) and empirical cumulative distribution (b) of the annual average number of trading partnerships. 89
2.13 The distribution (a) and empirical cumulative distribution (b) of the annual average number of trades. 89
2.15 Simulation output and data for the distribution (a), and density and empirical cumulative distribution (b) of the average out-flow of farms' trading partners under original functional forms for the partnership formation and cessation rates. 90
2.16 Simulation output and data for the distribution (a), and density and empirical cumulative distribution (b) of the average partnership duration of farms under original functional forms for the partnership formation and cessation rates. 91

2.17 Simulation output and data for the distribution (a), and density and empirical cumulative distribution (b) of the average out-flow of farms' trading partners under modified functional forms for the partnership formation and cessation rates. 92
2.18 Simulation output and data for the distribution (a), and density and empirical cumulative distribution (b) of the average partnership duration of farms under modified functional forms for the partnership formation and cessation rates. 93
2.19 System average R_0 for varying values of average batch size, average partnership duration, and average number of concurrent trading partners. We consider changes to batch size and partnership duration (top left), batch size and number of concurrent trading partnerships (top right), and number of concurrent trading partnerships and partnership duration (bottom left). Grey squares represent the current trading patterns of the Scottish trade system. In all cases we set $\lambda = \gamma = 0.2$. 94
2.20 The predicted system average R_0 for a range of disease parameterisations under current observed trading patterns in the Scottish trade system. 95
2.21 Percentage reduction in system average R_0 for singular changes to trade over a range of disease parameterisations. Changes considered are doubling the batch size, with an accompanying halving of the number of trades (top left), doubling the duration of trade partnerships (top right), and halving the number of concurrent trading partners (bottom left). Changes to the batch size are most effecitve for diseases characterised by high prevalence and short infectious periods, whereas changes to the duration and number of trading partnerships are most effective for diseases with high prevalence and long infectious periods. 96

3.1 **Sensitivity of price to stock imbalances** Price sensitivity to imbalances in global demand and supply (a) and stock generation rates for varying prices (b). In both cases we set $P^* = 5$, $\varepsilon_D = \varepsilon_S = 0.5$, and $\eta_i^* = \zeta_i^* = 1$. Each trajectory is obtained deterministically from Eqs. (3.8), (3.9), and (3.10) 102

3.2 **Price sensitivity on stock generation** Average stock generation rates and average price over time for varying values of the price sensitivity parameter σ. The special case $\sigma = 0$ represents the absence of a pricing model. For each parameter value, output is generated by averaging 20 independent realisations of the stochastic simulation. . . 108

3.3 **Price sensitivity on supply and demand stability** Average price against excess demand (left) and excess demand over time (right) for varying values of the price sensitivity parameter σ. The special case $\sigma = 0$ represents the absence of a pricing model, i.e. no fluctuations in price caused by excess demand. For each parameter value, output is generated by averaging 20 independent realisations of the stochastic simulation. 109

3.4 **Stock imbalances in the absence of price** Global excess demand for a number of independent stochastic simulations when a pricing model is absent ($\sigma = 0$). 110

3.5 **Shocks in demand impact price and stock generation** Global excess demand (top left), average price (top right), average demand generation rate $\eta(t)$ (bottom left), and average supply generation rate $\zeta(t)$ (bottom right) for varying shocks to global demand. For a given demand shock s, for all farms i, farm-level demand is updated to $\mathcal{D}_i(t) \to \mathcal{D}_i(t) + s$. In all cases, shocks occur at $t = 250$. 112

3.6 **Shocks in demand and response of trading system** Average per-farm demand (top left) and supply (top right), number of trading partners (middle left), number of trades (middle right), batch size (bottom left), and per unit-time animal in-flow (bottom right) for varying shocks to global demand. For a given demand shock s, for all farms i, farm-level demand is updated to $\mathcal{D}_i(t) \to \mathcal{D}_i(t) + s$. In all cases, shocks occur at $t = 250$. 113

3.7 **Shocks in supply impact price and stock generation** Global excess demand (top left), average price (top right), average demand generation rate $\eta(t)$ (bottom left), and average supply generation rate $\zeta(t)$ (bottom right) for varying shocks to global supply. For a given supply shock s, for all farms i, farm-level supply is updated to $\mathcal{S}_i(t) \to \mathcal{S}_i(t) + s$. In all cases, shocks occur at $t = 250$. 114

3.8 **Shocks in supply and response of trading system** Average per-farm demand (top left) and supply (top right), number of trading partners (middle left), number of trades (middle right), batch size (bottom left), and per unit-time animal in-flow (bottom right) for varying shocks to global supply. For a given supply shock s, for all farms i, farm-level supply is updated to $\mathcal{S}_i(t) \to \mathcal{S}_i(t) + s$. In all cases, shocks occur at $t = 250$. 115

3.9 **Removal of all stock does not alter price and stock generation** Global excess demand (top left), average price (top right), average demand generation rate $\eta(t)$ (bottom left), and average supply generation rate $\zeta(t)$ (bottom right) when global supply and demand are removed. In all cases, shocks occur at $t = 250$. 116

3.10 **Removal of all stock and response of trading system** Average per-farm demand (top left) and supply (top right), number of trading partners (middle left), number of trades (middle right), batch size (bottom left), and per unit-time animal in-flow (bottom right) when global supply and demand are removed. In all cases, shocks occur at $t = 250$. 117

3.11 **Impact of trade friction on price and stock generation** Global excess demand (top left), average price (top right), average demand generation rate $\eta(t)$ (bottom left), and average supply generation rate $\zeta(t)$ (bottom right) for varying values of the trade rate constant b, representing varying levels of trade friction. 119

3.12 **Impact of trade friction on trading system equilibria** Average per-farm demand (top left) and supply (top right), number of trading partners (middle left), number of trades (middle right), batch size (bottom left), and per unit-time animal in-flow (bottom right) for varying values of the trade rate constant b, representing varying levels of trade friction. 120

3.13 **Impact of partnership formation friction on trading system equilibria** Average per-farm demand (top left) and supply (top right), number of trading partners (middle left), number of trades (middle right), batch size (bottom left), and per unit-time animal in-flow (bottom right) for varying values of the partnership formation rate constant a, representing varying levels of friction in the formation of trade partnerships. 121

3.14 **Impact of partnership durations on trading system equilibria** Average per-farm demand (top left) and supply (top right), number of trading partners (middle left), number of trades (middle right), batch size (bottom left), and per unit-time animal in-flow (bottom right) for varying values of the partnership cessation rate δ, representing varying levels of propensities for farms to end trading partnerships. . 122

3.15 **Impact of trade friction on trade and disease prevalence** Average per-farm demand (top left) and supply (top middle), number of trading partners (top right), number of trades (middle left), batch size (middle middle), per unit-time animal in-flow (middle right), and system disease prevalence (bottom left) for varying values of ε_b, the scaling factor to the frictional component of trade, b. In all cases, disease is introduced at $t = 25$ and changes to trade at $t = 50$. 124

3.16 **Impact of trade friction on equilibrium values of trading system and disease prevalence** Average equilibrium per-farm demand (top left) and supply (top middle), number of trading partners (top right), number of trades (middle left), batch size (middle middle), per unit-time animal in-flow (middle right), and system disease prevalence (bottom left) for varying values of ε_b, the scaling factor to the frictional component of trade, b. 125

3.17 **Impact of partnership formation friction on trade and disease prevalence** Average per-farm demand (top left) and supply (top middle), number of trading partners (top right), number of trades (middle left), batch size (middle middle), per unit-time animal in-flow (middle right), and system disease prevalence (bottom left) for varying values of ε_a, the scaling factor to the frictional component of trade, a. In all cases, disease is introduced at $t = 25$ and changes to trade at $t = 50$. . 126

3.18 **Impact of partnership formation friction on equilibrium values of trading system and disease prevalence** Average equilibrium per-farm demand (top left) and supply (top middle), number of trading partners (top right), number of trades (middle left), batch size (middle middle), per unit-time animal in-flow (middle right), and system disease prevalence (bottom left) for varying values of ε_a, the scaling factor to the frictional component of trade, a. 127

3.19 **Impact of partnership durations on trade and disease prevalence** Average per-farm demand (top left) and supply (top middle), number of trading partners (top right), number of trades (middle left), batch size (middle middle), per unit-time animal in-flow (middle right), and system disease prevalence (bottom left) for varying values of ε_δ, the scaling factor to the partnership cessation rate, δ. In all cases, disease is introduced at $t = 25$ and changes to trade at $t = 50$. 128

3.20 **Impact of partnership durations on equilibrium values of trading system and disease prevalence** Average equilibrium per-farm demand (top left) and supply (top middle), number of trading partners (top right), number of trades (middle left), batch size (middle middle), per unit-time animal in-flow (middle right), and system disease prevalence (bottom left) for varying values of ε_δ, the scaling factor to the partnership cessation rate, δ. 129

3.21 **Impact of individual animal rejection on trading system and disease prevalence** Average per-farm demand (top left) and supply (top middle), number of trading partners (top right), number of trades (middle left), batch size (middle middle), per unit-time animal in-flow (middle right), price (bottom left), net income (bottom middle) and system disease prevalence (bottom right) for various test sensitivities under the test-and-reject individual animal regime. 132

3.22 **Impact of whole batch rejection on trading system and disease prevalence** Average per-farm demand (top left) and supply (top middle), number of trading partners (top right), number of trades (middle left), batch size (middle middle), per unit-time animal in-flow (middle right), price (bottom left), net income (bottom middle) and system disease prevalence (bottom right) for various test sensitivities under the test-and-reject whole batch regime. 133

3.23 **Equilibrium values of trading system and prevalence for both testing regimes** Equilibrium average per-farm demand (top left) and supply (top middle), number of trading partners (top right), number of trades (middle left), batch size (middle middle), per unit-time animal in-flow (middle right), price (bottom left), net income (bottom middle) and system disease prevalence (bottom right) for various test sensitivities under the test-and-reject individual animal regime (dashed lines) and test-and-reject batch regime (solid lines). 136

3.24 **Impact of individual-based risk aversion on trading system and disease prevalence** Average per-farm demand (top left) and supply (top middle), number of trading partners (top right), number of trades (middle left), batch size (middle middle), per unit-time animal in-flow (middle right), price (bottom left), net income (bottom middle) and system disease prevalence (bottom right) for various test sensitivities combining batch testing and removal with farm-level risk aversion, where we set the aversion parameter $\omega = 0.1$. Dashed lines in the disease prevalence plot represent the average per-farm perceived level of prevalence, defined as the fraction of the network with $\omega \neq 1$. 138

3.25 **Impact of global risk aversion on trading system and disease prevalence** Average per-farm demand (top left) and supply (top middle), number of trading partners (top right), number of trades (middle left), batch size (middle middle), per unit-time animal in-flow (middle right), price (bottom left), net income (bottom middle) and system disease prevalence (bottom right) for various test sensitivities combining batch testing and removal with global (system-wide) risk aversion, where we set the aversion parameter $\omega = 0.1$. Dashed lines in the disease prevalence plot represent the average per-farm perceived level of prevalence, defined as the fraction of the network with $\omega \neq 1$. 140

3.26 **Equilibrium values of trading system and prevalence for both risk aversion strategies** Equilibrium average per-farm demand (top left) and supply (top middle), number of trading partners (top right), number of trades (middle left), batch size (middle middle), per unit-time animal in-flow (middle right), price (bottom left), net income (bottom middle) and system disease prevalence (bottom right) for various test sensitivities under a test-and-reject batch regime only (black line), test-and-reject batch with individual risk aversion (red line), and test-and-reject batch with a global aversion strategy (blue line). In both aversion strategies we set the aversion parameter $\omega = 0.1$. 141

3.27 **Impact of discounting of risk for individual-based risk aversion on trading system and prevalence** Average per-farm demand (top left) and supply (top middle), number of trading partners (top right), number of trades (middle left), batch size (middle middle), per unit-time animal in-flow (middle right), price (bottom left), net income (bottom middle) and system disease prevalence (bottom right) for test sensitivity $\tau = 0.75$ combining batch testing and removal with individual risk aversion and an incremental increase in weights after various periods of no trades with a detected batch, where we set the aversion parameter $\omega = 0.1$ and weights increase in increments of ω. Dashed lines in the disease prevalence plot represent the average per-farm perceived level of prevalence, defined as the fraction of the network with $\omega \neq 1$. 143

3.28 **Impact of discounting of risk for global risk aversion on trading system and prevalence** Average per-farm demand (top left) and supply (top middle), number of trading partners (top right), number of trades (middle left), batch size (middle middle), per unit-time animal in-flow (middle right), price (bottom left), net income (bottom middle) and system disease prevalence (bottom right) for test sensitivity $\tau = 0.75$ combining batch testing and removal with global risk aversion and an incremental increase in weights after various periods of no trades with a detected batch, where we set the aversion parameter $\omega = 0.1$ and weights increase in increments of ω. Dashed lines in the disease prevalence plot represent the average per-farm perceived level of prevalence, defined as the fraction of the network with $\omega \neq 1$. 144

3.29 Average trade quantities and disease prevalence for varying values of ε_b, the scaling factor to the frictional component of trade, b, when $\lambda = 0.05$ and $\gamma = 1/3$. 150

3.30 Average equilibrium trade quantities and disease prevalence for varying values of ε_b, the scaling factor to the frictional component of trade, b, when $\lambda = 0.05$ and $\gamma = 1/3$. 150

3.31 Average trade quantities and disease prevalence for varying values of ε_a, the scaling factor to the frictional component of trade, a, when $\lambda = 0.05$ and $\gamma = 1/3$. 151
3.32 Average equilibrium trade quantities and disease prevalence for varying values of ε_a, the scaling factor to the frictional component of trade, a, when $\lambda = 0.05$ and $\gamma = 1/3$. 151
3.33 Average trade quantities and disease prevalence for varying values of ε_δ, the scaling factor to the partnership cessation rate, δ, when $\lambda = 0.05$ and $\gamma = 1/3$. 152
3.34 Average equilibrium trade quantities and disease prevalence for varying values of ε_δ, the scaling factor to the partnership cessation rate, δ, when $\lambda = 0.05$ and $\gamma = 1/3$. 152
3.35 Average trade quantities and disease prevalence for various test sensitivities under the test-and-reject individual animal regime, and when $\lambda = 0.05$ and $\gamma = 1/3$. 153
3.36 Average trade quantities and disease prevalence for various test sensitivities under the test-and-reject whole batch regime, and when $\lambda = 0.05$ and $\gamma = 1/3$. 153
3.37 Equilibrium average trade quantities and disease prevalence for various test sensitivities under the test-and-reject individual animal regime (dashed lines) and test-and-reject batch regime (solid lines), and when $\lambda = 0.05$ and $\gamma = 1/3$. 154
3.38 Average trade quantities and disease prevalence for various test sensitivities combining batch testing and removal with farm-level risk aversion, where we set the aversion parameter $\omega = 0.1$, and $\lambda = 0.05$ and $\gamma = 1/3$. Dashed lines in the disease prevalence plot represent the average per-farm perceived level of prevalence, defined as the fraction of the network with $\omega \neq 1$. 154

3.39 Average trade quantities and disease prevalence for various test sensitivities combining batch testing and removal with global (system-wide) risk aversion, where we set the aversion parameter $\omega = 0.1$, and $\lambda = 0.05$ and $\gamma = 1/3$. Dashed lines in the disease prevalence plot represent the average per-farm perceived level of prevalence, defined as the fraction of the network with $\omega \neq 1$. 155

3.40 Average equilibrium trade quantities and disease prevalence for various test sensitivities combining batch testing and removal with global (system-wide) risk aversion, where we set the aversion parameter $\omega = 0.1$, and $\lambda = 0.05$ and $\gamma = 1/3$. Dashed lines in the disease prevalence plot represent the average per-farm perceived level of prevalence, defined as the fraction of the network with $\omega \neq 1$. . . . 155

3.41 Average trade quantities and disease prevalence for various test sensitivities combining batch testing and removal with global (system-wide) risk aversion and natural incremental increase to weights, where we set the aversion parameter $\omega = 0.1$, and $\lambda = 0.05$ and $\gamma = 1/3$. Dashed lines in the disease prevalence plot represent the average per-farm perceived level of prevalence, defined as the fraction of the network with $\omega \neq 1$. 156

3.42 Average trade quantities and disease prevalence for various test sensitivities combining batch testing and removal with individual risk aversion and natural incremental increase to weights, where we set the aversion parameter $\omega = 0.1$, and $\lambda = 0.05$ and $\gamma = 1/3$. Dashed lines in the disease prevalence plot represent the average per-farm perceived level of prevalence, defined as the fraction of the network with $\omega \neq 1$. 156

3.43 Average trade quantities and disease prevalence for varying values of ε_b, the scaling factor to the frictional component of trade, b, when $\lambda = 0.25$ and $\gamma = 1.5$. 157

3.44 Average equilibrium trade quantities and disease prevalence for varying values of ε_b, the scaling factor to the frictional component of trade, b, when $\lambda = 0.25$ and $\gamma = 1.5$. 157
3.45 Average trade quantities and disease prevalence for varying values of ε_a, the scaling factor to the frictional component of trade, a, when $\lambda = 0.25$ and $\gamma = 1.5$. 158
3.46 Average equilibrium trade quantities and disease prevalence for varying values of ε_a, the scaling factor to the frictional component of trade, a, when $\lambda = 0.25$ and $\gamma = 1.5$. 158
3.47 Average trade quantities and disease prevalence for varying values of ε_δ, the scaling factor to the partnership cessation rate, δ, when $\lambda = 0.25$ and $\gamma = 1.5$. 159
3.48 Average equilibrium trade quantities and disease prevalence for varying values of ε_δ, the scaling factor to the partnership cessation rate, δ, when $\lambda = 0.25$ and $\gamma = 1.5$. 159
3.49 Average trade quantities and disease prevalence for various test sensitivities under the test-and-reject individual animal regime, and when $\lambda = 0.25$ and $\gamma = 1.5$. 160
3.50 Average trade quantities and disease prevalence for various test sensitivities under the test-and-reject whole batch regime, and when $\lambda = 0.25$ and $\gamma = 1.5$. 160
3.51 Equilibrium average trade quantities and disease prevalence for various test sensitivities under the test-and-reject individual animal regime (dashed lines) and test-and-reject batch regime (solid lines), and when $\lambda = 0.25$ and $\gamma = 1.5$. 161
3.52 Average trade quantities and disease prevalence for various test sensitivities combining batch testing and removal with farm-level risk aversion, where we set the aversion parameter $\omega = 0.1$, and $\lambda = 0.25$ and $\gamma = 1.5$. Dashed lines in the disease prevalence plot represent the average per-farm perceived level of prevalence, defined as the fraction of the network with $\omega \neq 1$. 161

3.53 Average trade quantities and disease prevalence for various test sensitivities combining batch testing and removal with global (system-wide) risk aversion, where we set the aversion parameter $\omega = 0.1$, and $\lambda = 0.25$ and $\gamma = 1.5$. Dashed lines in the disease prevalence plot represent the average per-farm perceived level of prevalence, defined as the fraction of the network with $\omega \neq 1$. 162

3.54 Average equilibrium trade quantities and disease prevalence for various test sensitivities combining batch testing and removal with global (system-wide) risk aversion, where we set the aversion parameter $\omega = 0.1$, and $\lambda = 0.25$ and $\gamma = 1.5$. Dashed lines in the disease prevalence plot represent the average per-farm perceived level of prevalence, defined as the fraction of the network with $\omega \neq 1$. 162

3.55 Average trade quantities and disease prevalence for various test sensitivities combining batch testing and removal with global (system-wide) risk aversion and natural incremental increase to weights, where we set the aversion parameter $\omega = 0.1$, and $\lambda = 0.25$ and $\gamma = 1.5$. Dashed lines in the disease prevalence plot represent the average per-farm perceived level of prevalence, defined as the fraction of the network with $\omega \neq 1$. 163

3.56 Average trade quantities and disease prevalence for various test sensitivities combining batch testing and removal with individual risk aversion and natural incremental increase to weights, where we set the aversion parameter $\omega = 0.1$, and $\lambda = 0.25$ and $\gamma = 1.5$. Dashed lines in the disease prevalence plot represent the average per-farm perceived level of prevalence, defined as the fraction of the network with $\omega \neq 1$. 163

4.1 **Model fits to data** The average number of trade partners (top left), number of trades (top middle), batch size (top right), animal in-flow (bottom left), and animal out-flow (bottom middle) comparing respective values obtained from data against average values from stochastic simulation, where each point represents a farm in the system. 170

4.2 **Time evolution of trading system** System average per-farm demand (top left), supply (top right), number of trade partners (middle left), trades (middle right), batch size (bottom left), and animal in-flow (bottom right). In all cases dashed horizontal lines represent system averages obtained from data. 171

4.3 **Autocorrelations of trading system** Autocorrelation function plots for simulation output of trade quantities as presented in Figure 4.2. Blue lines represent a 95% confidence interval centered at 0. 173

4.4 **Model distributions of trade quantities** Density distributions of average number of trade partners (top left), trades (top right), average batch size (middle left), average animal in-flow (middle right), and out-flow (bottom left). In all cases blue lines represent out from stochastic simulation, and black lines are obtained from the data. . . 174

4.5 **Assessing farm-level differences in model compared to data** Distributions of the per-farm ratios between simulation output and data for the average number of trade partners (top left), number of trades (top right), the average batch size (middle left), and the animal in- and out-flows (middle right and bottom left, respectively). In all cases, red dashed lines represent a ratio of 1, indicating the simulation perfectly represents the data. Note the scales of x-axes differ between panels, emphasising small differences in farm flows. 175

4.6 **Model distributions of supply and demand** Histogram of average farm-level demand (left) and supply (right) obtained from stochastic simulation of our trading system. 176

4.7 **Model cumulative distributions of supply and demand** Cumulative distribution of farm-level supply and demand stock, obtained from stochastic simulation of our trading system. 177

4.8 **Measuring model imbalances in supply and demand** The average system-wide excess demand (left) and the average ratio of demand to supply (right), obtained from stochastic simulation of our trading system. 179

4.9 **Impact of model and data differences on farm-level supply and demand** Per-farm average animal in-flow against demand and out-flow against supply averaged over a 45 year period. 180

4.10 **Impact of trade friction on Scottish trading system** System-averages for various trade quantities when each farm's trade rate constant b_i is scaled by various values of ε_b. Vertical dashed lines represent the point at which ε_b is changed, and horizontal dashed lines represent respective system-wide averages for various trade quantities as obtained from the CTS data. 182

4.11 **Impact of trade friction on disease prevalence** System-wide disease prevalence when each farm's trade rate constant b_i is scaled by various values of ε_b. Vertical dashed lines represent the point at which ε_b is changed. 183

4.12 **Impact of partnership formation friction on Scottish trading system** System-averages for various trade quantities when each farm's partnership formation rate constant a_i is scaled by various values of ε_a. Vertical dashed lines represent the point at which ε_a is changed, and horizontal dashed lines represent respective system-wide averages for various trade quantities as obtained from the CTS data. 184

4.13 **Impact of partnership formation friction on disease prevalence** System-wide disease prevalence when each farm's partnership formation rate constant a_i is scaled by various values of ε_a. Vertical dashed lines represent the point at which ε_a is changed. 185

4.14 **Impact of partnership durations on Scottish trading system** System-averages for various trade quantities when each farm's partnership cessation rate constant δ_i is scaled by various values of ε_δ. Vertical dashed lines represent the point at which ε_δ is changed, and horizontal dashed lines represent respective system-wide averages for various trade quantities as obtained from the CTS data. 186

4.15 **Impact of partnership durations on disease prevalence** System-wide disease prevalence when each farm's partnership cessation rate constant δ_i is scaled by various values of ε_δ. Vertical dashed lines represent the point at which ε_δ is changed. 187

4.16 **Impact of whole batch rejection on Scottish trading system** System-averages for various trade quantities when whole batch testing and rejecting is enforced, for various test sensitivities. 188

4.17 **Impact of whole batch rejection on disease prevalence** Effect of whole batch testing and rejecting on system-wide disease prevalence for various test sensitivities. 189

4.18 **Impact of whole batch rejection on stock imbalances** Impact of batch testing and rejection for various test sensitivities on imbalances in stock quantities (left) and the ratio of system-average demand to supply (right). 190

4.19 **Impact of global risk aversion on Scottish trading system** System-averages for various trade quantities when whole batch testing and rejecting is enforced which informs a global risk aversion strategy, for various test sensitivities. 191

4.20 **Impact of global risk aversion on disease prevalence** System-wide disease prevalence when whole batch testing and rejecting is enforced which informs a global risk aversion strategy, for various test sensitivities. Dashed lines represent system-wide perceived prevalence, the fraction of the system with weight $\omega < 1$. 192

4.21 **Impact of global risk aversion on stock imbalances** Impact of batch testing and rejection, and global risk aversion for various test sensitivities on imbalances in stock quantities (left) and the ratio of system-average demand to supply (right). 193
4.22 **Impact of discounting of risk on Scottish trading system** System-averages for various trade quantities when whole batch testing and rejecting is enforced which informs a global risk aversion strategy, for various test sensitivities. High-risk farms have their weights incrementally increased in steps of ω after a period, $\Delta t = 0.1$, in which no batches were detected to contain an infected animal. 195
4.23 **Impact of discounting of risk on disease prevalence** System-wide disease prevalence when whole batch testing and rejecting is enforced which informs a global risk aversion strategy, for various test sensitivities. High-risk farms have their weights incrementally increased in steps of ω after a period, $\Delta t = 0.1$, in which no batches were detected to contain an infected animal. 196
4.24 **Impact of discounting of risk on stock imbalances** Impact of batch testing and rejection, and global risk aversion with natural increments to weights for various test sensitivities on imbalances in stock quantities (left) and the ratio of system-average demand to supply (right). 197

Acknowledgements

The work presented in this thesis was funded by Biomathematics and Statistics Scotland, SRUC, University of York, and Mains of Loirston Charitable Trust.
This thesis would not have been possible without the guidance, assistance, and encouragement from my four supervisors, Glenn Marion, Mike Hutchings, Piran White, and Ross Davidson. Thank you for always being ready to help and see the bigger picture when necessary.
It goes without saying that the support of my family and friends have been invaluable during my time as a PhD student, and thank you for putting up with me when things got stressful!
Finally I would like to thank the number of friends I have made along the way, in particular the other PhD students with whom I shared an office. Our numerous conversations and discussions were always a great source of inspiration and comfort.

Author's Declaration

I declare the work in this thesis is my own and has not been submitted for any other degree or award.

The contents of Chapter 2 have been published in the journal Royal Society Open Science under the title *Generative models of network dynamics provide insight into the effects of trade on endemic livestock disease.*

The contents of Chapters 3 and 4 are currently being prepared to be submitted for publication.

Chapter 1

Introduction

The recent development of network theory has provided an effective framework for modelling the spread of disease within populations that exhibit heterogeneous contact patterns that are challenging (or impossible) to account for in traditional models of disease spread. Despite these developments, models of disease spread on highly dynamic and temporal networks are currently lacking, and the analysis of generative temporal networks (in which networks grow and develop based on individual- or system-level properties) is a promising avenue of study that may provide novel insight on disease spread within populations.

The spread of disease within livestock trading networks act as an ideal case study for the development and analysis of generative network models, due to the availability of long-term, highly detailed datasets in which the movements of individual animals between premises are recorded. The UK cattle tracing system (CTS) dataset is an example of one such dataset. This thesis is concerned with the development of novel generative trading models, and the analysis of the spread of disease modulated through trades between individuals, using the Scottish subset of the CTS dataset as a case study throughout. The models presented in this thesis are not confined to livestock trade, and may be adapted and applied to a number of dynamic network systems, such as the spread of computer viruses, or the spread of human diseases.

1.1 Livestock diseases within cattle herds

The maintenance and control of livestock diseases within cattle herds has been a constant issue for farmers and governments for a number of years. Since the beginning of the 21st century, there have already been a number of disease outbreaks within the UK, the most notable the 2001 Foot-and-Mouth disease (FMD) epidemic [45, 80]. Not only are there significant production costs due to the debilitating effects of these diseases [12, 68, 75, 102], there are harder to quantify impacts such as on farmers' emotional well-being [86] and public perception and trust of governments' handling of disease outbreaks [54, 105]. Thus controlling infectious diseases is of vital importance not only from a financial perspective, but from an ethical and welfare perspective too.

Below we give examples of some livestock diseases that are currently of national and international importance. We consider two endemic diseases (diseases that are persistent within farms and incur long-term financial burdens), Bovine Tuberculosis and Paratuberculosis, and an exotic epidemic disease (within the UK), Foot and Mouth disease.

1.1.1 Bovine Tuberculosis

Bovine Tuberculosis (bTB) is an endemic disease in cattle that is acquired via infection by the bacterium *Mycobacterium bovis* through close animal contacts [104], and has been estimated to cost the UK annually £100 million [4]. At a farm level, analysis has revealed that annual costs to individual farms in the UK due to the management of bTB are in the range of £505 to £3184, with the variation due to a number of factors, such as herd demographics [17]. Due to its impact on trade, the EU introduced legislation characterising nations as *officially tuberculosis free* if the national herd prevalence did not increase by more than 0.1% per year for six years [49]. A number of mainland EU states have achieved officially tuberculosis free status, including, Belgium, Czech Republic, Denmark, Germany, France, Luxembourg, Netherlands, Austria, Slovakia, Finland, and Sweden [49], with states such as Italy that are not yet officially tuberculosis free observing general downward trends in

prevalence [1, 110].

Conspicuously, the UK has not achieved officially tuberculosis free status, with between herd prevalence estimated at 5-6% in 2009 [4]. Moreover, trends of bTB prevalence in the UK have indicated that prevalence levels have been increasing consistently, with the exception of Scotland which has been officially tuberculosis free for a number of years [2]. There have been a number of suggested reasons why the UK has not been able to eradicate bTB, while other EU member states have. Perhaps most notably, the 2001 FMD epidemic lead to widespread disruption in bTB testing [2], and atypical animal movement dynamics following the outbreak due to replenishment of stock have altered the risk factors for bTB introduction in British farms [19, 116]. Moreover, there has been a general tendency for farms to consolidate and increase their herd sizes [2], contributing to the persistence of bTB due to herd size being a risk factor in bTB spread [16]. Another contributing factor is the presence of susceptible wildlife that have been suggested as environmental reservoirs of bTB, most notably badgers [103]. While the interactions between badgers and livestock are not fully understood, there is evidence that close proximity to an infected badger sett increases the herd-level risk of infection [82]. As the UK has higher badger density than mainland Europe [18], and with the badger population increasing over the years [61], attempts have been made to control the badger population in an effort to minimise bTB spread, for example through culling. Randomised badger culls have had mixed effects, with reduction in cattle bTB observed within the cull areas, but increased bTB observed in areas outside the cull areas [32]. However, despite these results culling has continued for many years. While there are trade links between Scotland and high prevalence areas of the rest of the UK, the use of pre- and post-movement testing has been an effective deterrent in the spread of bTB to Scotland from the rest of the UK [44]. This, combined with lower badger [61] and cattle densities (at herd level) [2], have been suggested as reasons for why Scotland has managed to remain officially tuberculosis free.

1.1.2 Paratuberculosis

Paratuberculosis (paraTB), also known as Johne's disease, is an endemic disease in cattle caused by the bacterium *Mycobacterium avium subsp. paratuberculosis*, linked to Crohn's disease in humans, and is often acquired by the faecal-oral route [108]. It is known to persist for long periods of time within the environment under the right conditions, making controlling this disease a challenge [121]. There is an economic incentive to control the disease, with losses due to reduced milk production and weight loss reducing slaughter value [12, 75, 107]. It has been estimated that annual losses per cow in the UK due to paraTB are £27 for dairy cattle [75] and £16 for beef cattle due to weight loss [53]. Control of the disease can be challenging owing to a long incubation period, allowing for unknowing disease spread and late-time detection [122, 123]. In addition, sensitivities of animal tests have a large degree of variation, resulting in failed detections of infected animals [60, 93, 120]. The potential role of rabbits in the spread and maintenance of paraTB is also not fully understood, however the presence of paraTB in rabbits has been observed in excreta, allowing for the possibility of grazing animals to ingest and become infected [23, 24]. Investigations into whether paraTB could be controlled via the culling of rabbits revealed that very high levels of culling (>90%) for a single cull and >40% for repeated long-term culling would be necessary to effectively control paraTB within the rabbit population [26].

The importance of controlling paraTB is not universally recognised, resulting in further challenges to effectively controlling the disease. International survey studies have found differing opinions on control programmes intended to reduce paraTB incidence, with those in favour citing animal health and reductions in production losses the primary reasons. Conversely, those not in favour of control programmes cite economic concerns, other diseases are of greater importance, and paraTB is not prevalent enough to be of concern [123]. Bulk milk tank samples of randomly selected dairy farms have provided estimates for herd-level prevalence of paraTB in Britain, finding approximately 68% of dairy farms to be classed as infected [112].

1.1.3 Foot-and-Mouth Disease

Foot-and-Mouth Disease (FMD) is a highly contagious viral disease that was once endemic to Britain, though is now considered an epidemic disease [70], however remains an endemic disease in many countries around the world [123]. Understanding the spread of FMD has become vitally important in the wake of the 2001 UK FMD epidemic, and has clearly highlighted the role of animal movements in the ability for disease to spread [51]. The epidemic was largely attributed initially to sheep movements to market, which seeded infection in other animals (including cattle) and lead to long-range disease dispersal, after which localised spreading was responsible for the majority of cases [45]. Upon detection of the disease, nationwide movement restrictions were imposed and premises suspected of being infected were subject to herd culling. As a result, approximately 10 million animals were slaughtered and estimated costs to the UK agricultural industry due to these stock losses has been calculated at around £3.1 billion [116]. There were other losses, not directly related to agriculture, such as to tourism due to the closing of the British countryside, amounting to approximately £3.2 billion [45]. Moreover, the management of the outbreak has been criticised due to the government's policy of slaughtering herds deemed at risk of being infected [105] and subsequent analysis has shown that more targeted culling strategies may have been more effective with less financial impact [64], although the control strategies employed during the outbreak were based on predictions of mathematical models [67].

Another FMD outbreak occurred in August 2007, though the impact was far less severe than the previous 2001 epidemic. This was due to a number of factors, including rapid detection of infected animals, and an immediate national restriction of livestock movements [7]. Another key factor was the timing of the outbreak, as the 2001 epidemic began in springtime, a period of the year in which animal movements are at their peak [45]. In total, 2160 animals were slaughtered in the 2007 outbreak and total costs to the UK were estimated to be £147 million [7].

The FMD outbreaks in the UK provide a clear example of the significant impact livestock diseases can have on animal health, economies, and disruption to

farm businesses. Moreover, the complex nature of trade influences the success of widespread infection (without animal movements, the 2001 FMD epidemic would not have achieved such widespread distribution [64]), highlighting the importance of understanding the demographics of animal movements in an attempt to control disease spread.

1.2 Demographics of livestock movements

The availability of large scale livestock movement databases allow for detailed analysis of the demography of livestock and livestock movements. An example of such a dataset in UK cattle trade is the Cattle Tracing System (CTS) data, which uniquely identifies premises and animals, as well as recording individual animal movements, and births and deaths at a daily timescale [113]. Analysis of this data for the years following the 2001 FMD outbreak revealed that the trend of movement characteristic within the UK were moving in directions speculated to permit greater disease persistence [109]. Simulation based studies have produced similar results, suggesting that the introduction of movement standstills following the 2001 FMD epidemic have altered the livestock trading system in ways that may lead to greater disease persistence [115]. More longer-term analyses, however, have shown that these trends have generally stabilised since 2005 and the UK cattle trading system has not significantly altered in recent years [38, 113].

An observed distributional property of the UK cattle trading system is that of so-called *scale-free* (or scale-free like) behaviour, in particular for the number of farms from whom and to whom a farm buys and sells animals annually [22, 38, 46]. Such distributions, also known as Power-Laws, frequently occur throughout nature and are characterised by long-tails, with the vast majority of individuals possessing few contacts, and a small fraction possessing disproportionately larger numbers of contacts [91]. However, it should be noted that in the real world, such scale-free properties are always subject to some cut-off due to system size. Furthermore, some authors dispute whether or not observed phenomena are truly scale-free or in fact deviate from true scale-free processes [33]. Nonetheless, scale-free like, or approximately scale-

free, phenomena are widely observed in many varied phenomena in the natural and human world. In the context of livestock trading, most farms buy a small number of animals, but a small number of farms buy a very large number of animals. Similarly, the vast majority of farms sell only a small number of animals with a small minority selling very large numbers. In terms of connectivity in the trade system, this means that a small number of farms play a major role. Such characteristics have also been observed in livestock trading systems of countries other than the UK [71, 76, 101]. Farms display some habitual trading behaviour in terms of from whom or to whom animals are bought or sold. While some trade partnerships persist, with repeated trades between buyers and sellers, the majority of movements (60%) are between farms that have never traded before and will not trade again. Approximately 33% of movements are the result of repeat trades in partnerships that have traded between 2 and 10 times [113].

Seasonal trading patterns are clearly evident in the UK cattle trading system, with defined peaks in April and October, corresponding to peaks in births in April, and movements to slaughter in October [84, 113]. As evidenced by the 2001 FMD epidemic, springtime movements were a key component in the initial spread of disease [45]. Seasonal trading patterns are examples of episodic or "bursty" activity; movements occur in concentrated bursts followed by periods of low activity [11]. Such activity patterns have been studied in the context of disease spread and have been found to alter the spreading capability of disease, slowing disease spread [78].

The UK cattle trading system is also characterised by the presence of livestock markets. These premises are generally small in number (617 in the UK compared with 138640 total premises) but are responsible for a significant number of animal movements [113]. This is in part because they enable trade between farms that may not otherwise be possible via direct movements, resulting in animal movements over distances that are disproportionately larger than typical direct farm-to-farm movements [84]. This role of markets was evident during the 2001 FMD epidemic, with initial market movements seeding infection into geographical locations that may not have otherwise been infected [45]. Analysis of contact chains in the UK

cattle trading system reveals the role of markets in connecting individual farms to many others, leading to very large contact chains, and geographically distant farms being connected by a few intermediate animal holdings [38].

The UK cattle trading system is highly complex and heterogeneous, with farms trading in different manners individually and over time. Accounting for disease spread on these systems is therefore a challenge and a theoretical framework that allows for individual heterogeneity would help in assessing the spread of disease on these complex systems. In the next section we give an outline of *networks* that have the potential of allowing for theoretical considerations of disease spread on livestock trading systems.

1.3 Networks

Farms in cattle trade systems do not trade uniformly with every other farm. Moreover, most farms are generally limited to a few contacts with a small number of farms in a given year [113], and farms may maintain trade relationships with specific farms over long periods. Mathematical models, therefore, should account for this heterogeneity in contact patterns, and the recent development of network theory has provided an avenue to do so [90]. A network, or graph, consists of nodes (representing individuals in a population or farm premises, for example) and edges connecting nodes that represent contacts or partnerships between nodes, where edges can be undirected (indicating a two-way relationship between nodes) or directed (an edge emanating from one node i to another j indicates the presence of a relationship from i to j, but not necessarily from j to i) [90]. Two common representations of systems in a network framework are described below.

1.3.1 Static networks

The static network is a network in which nodes and edges are permanent and non-changing. In static networks, the network can be characterised by the *adjacency matrix*, $\mathbf{A}$, whose elements indicate the presence of edges in the network. For an

undirected network, the element A_{ij} indicates the presence of an edge between i and j (and so $A_{ij} = A_{ji}$) and takes value 1 if there is an edge and 0 otherwise (weighted edges, in which elements of the adjacency matrix can have values larger than 1, are an extension that allow for greater characterisation of the importance of specific edges). In directed networks A_{ij} takes value 1 if there is a directed edge from i to j (so A_{ij} and A_{ji} are not necessarily equal) and 0 otherwise [90]. The number of edges of a node, called its *degree* for undirected networks, and in- and out-degree for directed networks, representing the fact that nodes may not have equal numbers of edges pointing at or emanating from them, can be distributed arbitrarily to form a so-called degree distribution, the probability that a randomly chosen node has a given number of edges [90]. Frequently in real-world networks, scale-free or Power-Law distributions are observed, characterised by long tails in which most nodes have a small degree, with a small number of nodes having a disproportionately larger degree [91].

For networks with nontrivial degree distributions, questions arise over the role and importance of specific nodes within the network. Measures from social network analysis have been developed to answer these questions, and are collectively known as *centrality measures* [50]. Node degree is a simple centrality measure, however a more sophisticated centrality measure is the *eigenvector centrality* which measures nodes' importance in connecting high degree nodes together. Distance-based centrality measures are useful in assessing the ability for traversal across the network. The *closeness centrality* measures the mean distance (shortest path) for a node i to reach any other node j, whereas the *betweenness centrality* is the fraction of paths between nodes that node i falls on and is a measure of the control of node i on network flow (livestock, for instance) [50].

The *components* of a network measure the sizes of subsets of the network in which nodes within the subset can all be reached [90]. In undirected networks, the largest of these subsets is called the *giant component*. For directed networks, there is a *giant strongly connected component*, the largest subset of the network in which a directed path in both directions exists between every node pair (strongly connected), and a

giant weakly connected component, the largest subset of the network in which the directed nature of edges is ignored (weakly connected) [90].

1.3.2 Temporal networks

Temporal networks differ from static networks in one key component; nodes and/or edges are not necessarily permanent, and can appear and disappear over time [57]. Individuals may cease contact with some and begin contact with others over time, representing edge fluctuation, or new individuals may be born and old individuals die, represent node appearance and disappearance. As with static networks, we can define a time-dependent adjacency matrix $\mathbf{A}(t)$, whose elements, $A_{ij}(t)$, indicate whether an edge (whether undirected or directed) is present at time t. The degree of an individual, can then be defined as the at time t number of edges of the node. Defining the degree distribution can be challenging due to the potential for the temporal dynamics of the network to alter the distribution of edges according to arbitrary rules, however attempts have been made to obtain analytical expressions for degree distributions for temporally evolving networks [40].

Centrality measures on temporal networks can be hard to quantify owing to the time-dependent nature of edges [57]. Attempts to generalise static centrality measures to temporal networks has often involved aggregating the network into discrete time steps, creating network snapshots in a given time interval, and calculating centralities in successive time steps [57, 69]. Choosing an adequate time step, however, may be challenging depending on the dynamic nature of the network [69].

Attempts to define temporal components in a network have been successful when aggregating the network into a series of temporal snapshots. Components are then defined for each temporal snapshot, with the *temporal* giant strongly connected component being the largest set of nodes such that each node is strongly connected to every other node at a given snapshot. Similarly, the temporal giant weakly connected component is the largest set of nodes in which every node is weakly connected to the other in a given snapshot [92]. Analysis of such temporal components has revealed large fluctuations in component sizes over time that may not be observed in static

networks [92].

Network models may therefore provide a useful framework for modelling livestock trade, owing to its ability to characterise individuals according to arbitrary properties and account for temporal variation in trade dynamics. While temporal networks provide a more realistic interpretation of real-world behaviour, there are few models of temporal networks and there is a pressing need for the development of generative models of temporal networks parameterised to real data so that characteristics of individuals are represented [57]. Attempting to address this issue is a critical aim/goal of this thesis.

1.4 Modelling disease dynamics

1.4.1 Compartmental and mass action models

Characterising disease states of individuals into discrete compartments is a frequently used and powerful tool in studying disease spread [8]. Epidemiological models of disease spread often reduce disease status to a number of key categories (e.g. susceptible, infected, recovered) and explore how the mechanisms of disease spread influence the transition of individuals between these categories. For simple disease models, transitions between disease states occur according to rates (for example an intrinsic rate of disease transmission β and rate of recovery from disease γ [8]), and an assumed demographic structure of the population, the simplest being the mass action assumption, whereby all individuals can come into contact with one another at any given time, and contacts occur between individuals proportionately to the density of individuals in each disease state [8].

Perhaps the simplest widely used compartmental model of disease spread is the SIR model, in which individuals are characterised as either susceptible to infection (S), currently infectious (I), or recovered from infection (R). Assuming the law of mass action, the time evolution of the densities of each disease category can be described by

$$\frac{d}{dt}S(t) = -\beta S(t)I(t),$$
$$\frac{d}{dt}I(t) = \beta S(t)I(t) - \gamma I(t),$$
$$\frac{d}{dt}R(t) = \gamma I(t).$$

This simple set of differential equations is nonetheless analytically intractable, i.e. an explicit solution for each of the disease state densities cannot be obtained, due to the nonlinear interaction terms. However, insightful information can be gleaned from these models, notably the reproductive ratio of the disease, R_0, defined as the expected number of secondary cases caused by a single infectious individual in an otherwise susceptible population in its infectious lifetime [29]. For the simple SIR model, R_0 is

$$R_0 = \frac{\beta}{\gamma}.$$

For deterministic systems, such as the simple SIR model above, the value of R_0 determines absolutely the ability for disease to persist within the population. If $R_0 < 1$ then the disease is unable to persist and dies out, if $R_0 > 1$ the disease will spread exponentially (initially). The critical point $R_0 = 1$ indicates the threshold value at which point the disease stability switches [55]. Assessing the value of R_0 is often used to inform forecasting and intervention strategies for disease control [118]. The law of mass action is unrealistic, however, and the effects of host and contact heterogeneity can have significant effects on disease spread [119]. The development of network theory has allowed epidemiologists to analyse the spread of disease within populations without requiring the mass action assumption and under arbitrary connectivity and contact patterns.

1.4.2 Disease spread on networks

Attempts to assess the spread of disease on networks has currently been mostly confined to static networks [10], though to great success. By assuming edges in

a network are distributed according to some arbitrary degree distribution, it has been shown that disease spread is significantly influenced by an individual's degree, with R_0 explicitly linked to the degree distribution of the system [89] and that disease can spread and persist within high degree nodes even if $R_0 < 1$ [118]. In terms of outbreaks, there is a clear link with outbreak sizes and the size of the giant component, with nodes outside the giant component unable to cause large-scale outbreaks, and the size of the outbreak is determined by the size of the giant component for infectious individuals inside the giant component [89]. Modelling the spread of disease on directed networks has been less frequent, however extensions of disease spread to directed networks shows that success of the spread of disease is influenced by the out component of the network [25], and models of semi-directed networks (networks comprising of both undirected and directed edges) have shown that epidemic thresholds are generally larger than for fully undirected networks [77]. Of interest is disease spread on scale-free networks, due to their ubiquity in real-world networks [91]. Significantly, it has been shown that for most real-world networks that exhibit scale-free like properties, there is no epidemic threshold, and disease can spread and persist even at low transmission rates [100]. An important property relevant to disease control is the effect of immunisation strategies in scale-free networks. In particular, it has been shown that random immunisation cannot remove disease even at very high immunisation levels. On the other hand, targeted immunisation of the most highly connected nodes is highly effective, with disease eradication possible even at low immunisation levels [99].

Attempts to model disease spread on temporal networks have produced some success. An example is the so-called *neighbour exchange model* [118, 119], in which individuals possess a fixed degree following an arbitrary degree distribution, however edges in the network switch with some rate. This model, intended to reflect that real-world network connections are not necessarily static, was successful in showing that R_0 was heavily influenced by the switching rate, indicating that static approximations of dynamic networks may be inadequate [118]. The neighbour exchange model was intended to complement a model of dynamic partnerships in which in-

dividuals form and end partnerships with arbitrary rates, and importantly, without the requirement that the degree of individuals was maintained [6]. By assuming a tree-like network, expressions for R_0 were obtained, highlighting the importance of time-varying partnerships. Extending this model to heterogeneous populations is covered in Chapter 2. A true, continuous time, analytically tractable network model of disease spread that accounts for variable contact patterns as well as time-varying, non-constrained, degree distributions appears to be lacking and is a fundamental future challenge.

1.4.3 Stochastic simulation of disease processes

Deterministic models of disease spread are useful in analysing typical properties of disease spread, such as long-run behaviour, however they do not necessarily account for random variation (stochasticity) that is present in the real world. Inclusion of stochasticity allows for random events that may hinder disease spread that a deterministic model would not account for, and stochastic simulation of disease outbreaks can more accurately capture the variability of a disease outbreak [65]. However, despite inclusion of stochasticity, typical system behaviour will closely resemble deterministic models in many cases.

In general, the time-evolution of stochastic systems behave according to a random-walk process and the state of the system at a point in time can be encapsulated by a single equation, the so-called *master equation* [5]. Unfortunately, for most systems, the master equation is analytically intractable, however the Gillespie Stochastic Simulation Algorithm (Gillespie SSA) generates trajectories of the system that are exact solutions of the master equation [47, 48]. Each trajectory represents a single realisation of the stochastic process defining the system, and obtaining multiple independent trajectories offers insight into average properties of the system, as well as the variance (and covariation) due to stochasticity.

The SSA assumes Poissonian dynamics and relies on the memory-less property of the exponential distribution to calculate the time jump between two events and also what the next event is. Given a system of x possible events, and associated event

rates E_k, $k \in \{1, \ldots, x\}$, with $E = \sum_{k=1}^{x} E_k$ being the total event rate, the algorithm behaves as follows:

1. Initialise the starting state of the system and set the time $t = 0$.

2. The time of the next event, $t + \Delta t$, is calculated by generating a Uniform random number, $r_1 \in [0, 1]$ and setting

$$\Delta t = \frac{-\ln(r_1)}{\sum_{k=1}^{x} E_k}.$$

3. The next event to occur is obtained by drawing a second Uniform random number r_2. Event k occurs if

$$\sum_{k=1}^{x-1} E_k < r_2 E \leq \sum_{k=1}^{x} E_k.$$

4. Perform event k, and update the state of the system. Recalculate the event rates of any events that were altered by event k. Set $t \to t + \Delta t$.

5. Repeat from Step 2 until either $t > t_{\max}$, or some other criteria is met (such as disease extinction).

As an example, consider the SIS disease model, in which susceptible individuals are infected by infectious individuals with rate βSI, and remain infectious until they recover and become susceptible again, which occurs with rate γ. Figure 1.1 compares the behaviour of the deterministic and stochastic systems for a population of $N = 100$ individuals, an initial state of $S = 99$ and $I = 1$ individuals, with disease parameters $\beta = 0.02$ and $\gamma = 0.2$. Clearly the general behaviour of the two systems is similar, however due to stochasticity, for some realisations of the stochastic model, there are varying times to reach equilibrium, and there is general variation around the equilibrium. An important observation is that for some stochastic realisations, the disease dies out, which is not permitted under the deterministic model (as parameterised). Figure 1.2 shows that the disease behaves in two ways: either the disease successfully spreads, in which case it reaches an equilibrium (with some variation around the equilibrium), or it does not spread and dies out. These two equilbria, the disease-free equilibrium and the endemic equilibrium, exist for the

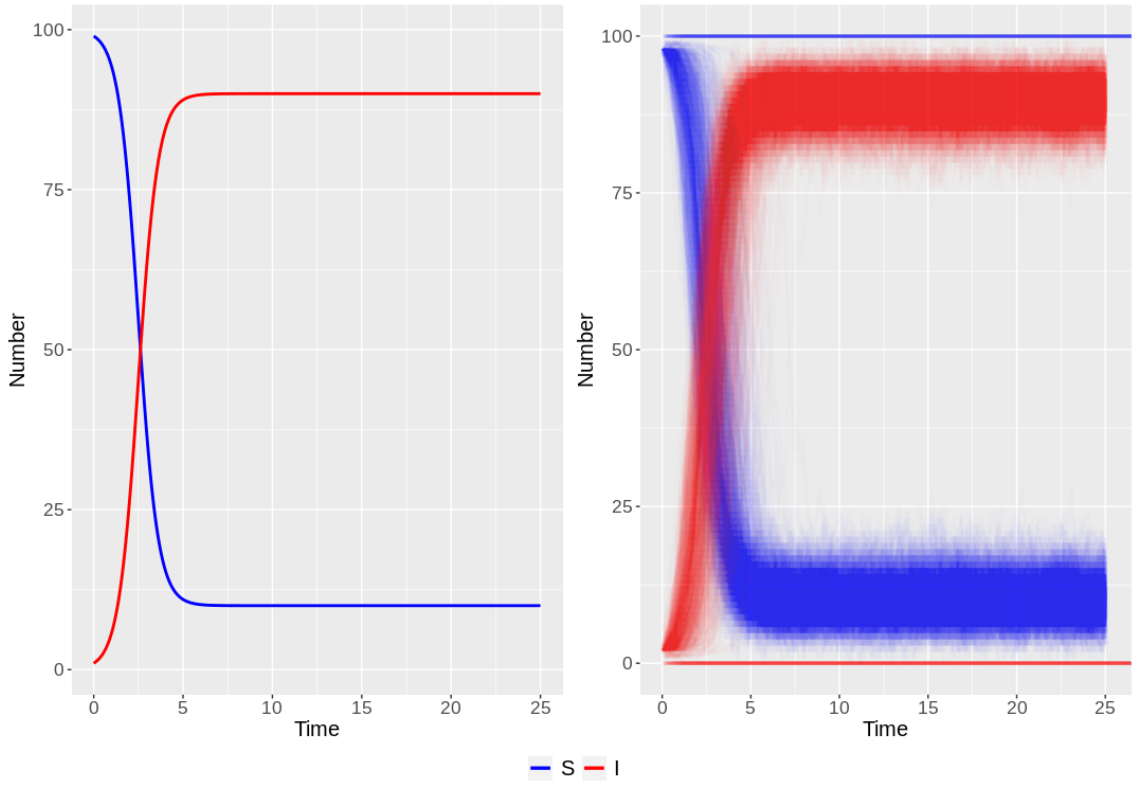

Figure 1.1: Time trajectories of the deterministic (left) and stochastic (right) *SIS* disease model. 1000 stochastic realisations are generated for using the Gillespie SSA.

deterministic model, however the disease-free equilibrium is unstable for the chosen parameterisation (thus the disease always spreads and persists). It should be noted that even in the persistent disease state, the stochastic system is only in very long-lived metastable state and that ultimately stochastic extinction will occur [74].

1.5 Network-based approaches to modelling disease spread on livestock trading systems

There has been much work on understanding disease spread on livestock trading systems. A common approach is to make use of large-scale animal movement datasets to recreate historic networks that match previously observed animal movements, and overlay a simulated disease process. A crucial finding of such studies is the identification of trading as a risk factor for introduction of disease into herds, for example for bTB [39, 46, 98], paraTB [13, 71], and FMD [37, 51, 97]. The 2001

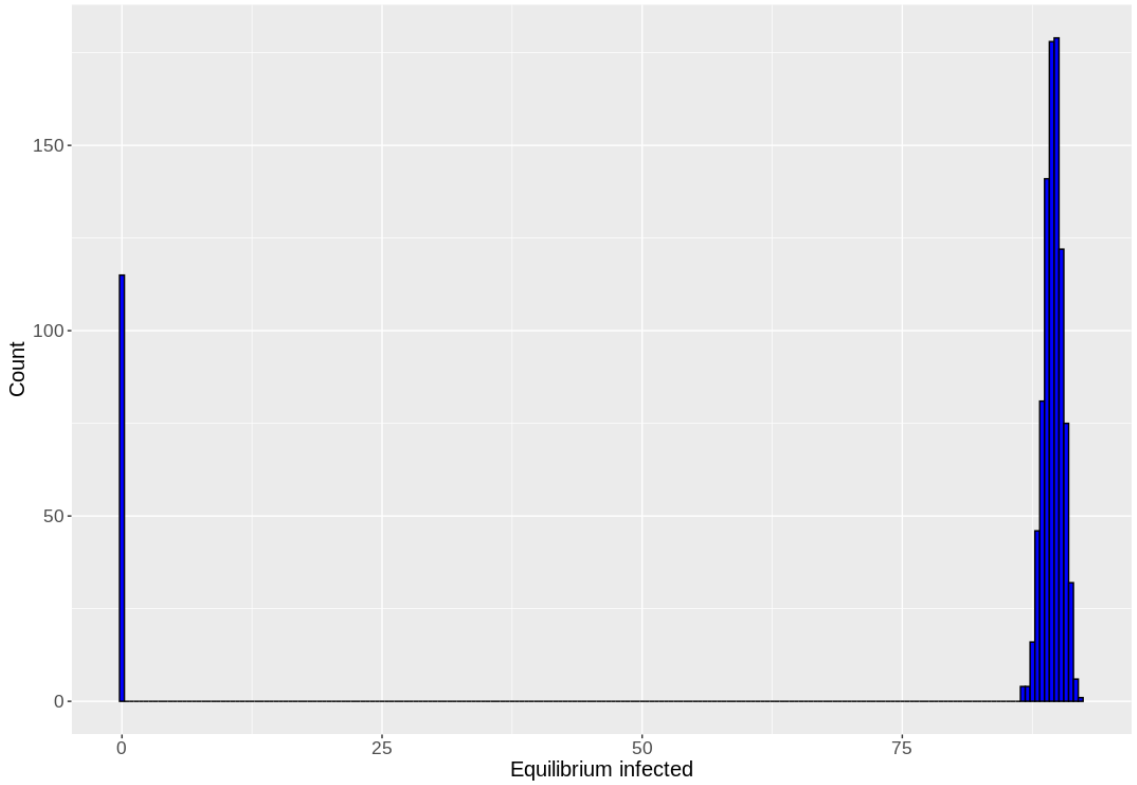

Figure 1.2: Distribution of equilibrium disease prevalence for the stochastic SIS model.

FMD epidemic is an example of how disease can alter network structure and have long-term consequences for disease control. Indeed, it has been shown through network analysis that control measures, such as animal testing, as a consequence of the FMD epidemic have altered trading behaviours in a way that increases the giant strong component of the network and permits greater disease spread, highlighting the complex nature of cattle trade and the challenges of modelling such systems [109, 115]. As a result of FMD control strategies, the role of animal movements as a risk factor for bTB spread has become more prominent [116].

Framing livestock trading in a network context has allowed for the exploration of the effect of changes to the structure of the network on the spread of livestock disease. In particular, exploitation of the highly heterogeneous and scale-free nature of livestock trading networks has shown that rewiring trading connections between farms based on network-level properties, such as centrality measures or by rewiring movements away from certain holdings like markets, can significantly reduce disease prevalence when targeted at a small number of farms [43, 85, 117]. In addition, effectively

removing certain connections in the network has been shown to alter the structure of the network and the size of the giant component in a way that may be effective in reducing disease persistence [62, 63]. Targeted vaccination strategies, such as based on farm size or other risk factors, may also potentially be an effective control strategy in combating disease spread [64, 66].

An important consideration when modelling trade by recreating networks from historic movement data is the temporal structure of the system. A general approach to analysing livestock movements is to assume some temporal snapshotting of the network, where connections between farms are static over some dicrete time period. Analysing the timescale of snapshots on livestock trading networks has shown that static network approximations hide important temporal characteristics of the real-world system, such as centrality, hindering the efficacy of disease control strategies [9]. For the UK network specifically, the importance of a dynamical network approach has been made clear, with static networks producing qualitatively different disease spreading properties compared with more dynamic representations of the network [114].

Models of disease spread that explicitly replicate observed animal movements are able to illustrate the potential for disease spread and even possible control measures. However, this is only in the historic context of past trading dynamics and it is challenging to use such an approach to generalise farm trading behaviour to ask "what if..." questions. Generative models that paramaterise a system at farm-level from these movement datasets would be a powerful tool in exploring the role of trade on disease spread while not being constrained to only replay past trading events, and there is currently a pressing need for the development of generative models of network dynamics in general [57]. Moreover, to date there have been few attempts at designing generative models of cattle trade, however those models that have been proposed have proved to be able to capture key system-wide properties of the trading networks they represent, as well as providing new insights into the role of trade on disease spread [58, 87]. In particular, manipulating the frequency of trade and size of animal batches, while conserving animal flows, has been show to

potentially reduce disease prevalence [87]. However, these models make a number of simplifying assumptions, such as constant trading patterns, or even neglecting trading relationships between farms, so there is scope for expanding these models to provide greater insight on the role of trade on disease spread. The development of more flexible and realistic generative models of network dynamics and disease spread on them is the aim of this thesis.

1.6 The thesis

1.6.1 Aims

The general aim of this thesis is to develop highly dynamic generative models of cattle trade that account for trading partnerships between farms and the movement of animals that occur between trading partners. With application to disease spread, this thesis aims to answer these questions: 1) can analytically tractable generative models of livestock trade be developed that capture farm-level properties? 2) can the dynamics of trade be exploited in such a way that disease persistence is reduced while maintaining farm-level animal flows? 3) can these models be expanded to account for time-varying farm-level stock quantities, dictating trading patterns? 4) do changes to trade affect stock quantities to such an extent that the trading system fundamentally changes? 5) under such scenarios, how does network adaptation impact disease spread? 6) how do traditional disease control measures, such as animal testing, impact the trading network, and how does that affect disease spread? 7) when applied to the Scottish cattle trade industry, do these results hold, and if so can effective disease control strategies be proposed?

1.6.2 Thesis structure

Chapter 2 introduces a novel generative livestock trading model that accounts for time-varying trading partnerships between farms. By considering the trading dynamics of farm pairs, per-farm expressions for R_0 are obtained that highlight the important role of trade frequency, batch size, and the dynamics of trading partnerships

on the ability for disease to spread and persist. This also shows that manipulation of trading patterns while conserving farm-level animal flows can positively alter R_0 such that disease is controlled. By parameterising this model to represent farms in the Scottish cattle trade industry so that average farm-level quantities reflect observations and are maintained under putative changes to trade behaviour, the effect of the above changes to trade are shown to be highly effective in reducing R_0.

Chapter 3 expands the model of Chapter 2 by introducing dynamic, time-varying, farm-level stock quantities that alter farms' propensities to trade and form trading partnerships at any given time. This reflects the idea that if a farm has just bought a batch of animals, its propensity to do so will be lowered for some period of time. The trading patterns are analysed and the effect of manipulations to trade similar to those explored in Chapter 2 are shown to be ineffective except in extreme scenarios. This difference results from the adaptive response of the system that leads to the network structure dynamically changing so that farm flows are maintained. Animal testing through trade is included and the effect of rejecting infected animals is shown to be positive, reducing disease prevalence but has transitory (and sometimes permanent) impacts on the trading sub-system. Linking testing to adaptive risk aversion, based on local and global information, is shown to be an effective strategy in reducing disease prevalence, and can eradicate disease in scenarios where testing alone is insufficient.

Chapter 4 outlines the method of parameterising the dynamic trading model of Chapter 3 to the Scottish cattle trade system, and the challenges that arise due to the presence of time-varying stock quantities that are not observed in the data. Successful parameterisations that successfully captures farm-level properties to large degree are obtained, and the resulting parameterised system is explored. The proposed disease control strategies explored in Chapter 3 are assessed on this real-world parameterised system.

Chapter 5 provides a discussion of the results of each chapter, and future avenues for research.

Chapter 2

Generative models of network dynamics provide insight into the effects of trade on endemic livestock disease

2.1 Introduction

The movement of animals via trade has long been considered a significant factor in the spread of disease within livestock populations [37, 42, 46, 51, 71, 94, 98, 108]. For example, animal movements resulting from restocking following the 2001 Foot-and-Mouth disease (FMD) outbreak in Great Britain has been suggested as a contributing factor to the subsequent surge in Bovine Tuberculosis (bTB) positive farms [19, 116]. The 2001 FMD outbreak itself spread widely, via animal movements [45], before detection led to national and international trade restrictions.

The contents of this chapter have been published in the journal Royal Society Open Science under the title *"Generative models of network dynamics provide insight into the effects of trade on endemic livestock disease"*[72]

While exotic disease incursions like *FMD* in 2001 incur large costs over short timescales (estimates for *FMD* 2001 include up to UK £3.1 billion for stock losses [116] and £3.2 billion related to tourism [45]), many endemic diseases impact production year-on-year. For example, paratuberculosis (*paraTB*) reduces milk production in dairy cattle and causes weight loss affecting beef quality [12, 75, 107], and bovine viral diarrhoea virus (*BVDV*) often reduces fertility, animal growth, and milk production [68]. These incur a significant cost to the agricultural industry (annually *paraTB* is estimated to cost £0.8 million, *BVDV* £39.6 million, and *bTB* £29.7 million [4, 14]). Unfortunately, controlling such diseases is a challenge due to a number of factors including animal movements, poorly understood transmission pathways (in particular the role of wildlife, e.g. rabbits and badgers in the spread of *paraTB* and *bTB*, respectively) [20, 24, 23, 30, 31, 52], long latent periods [123], and variable sensitivities of diagnostic tests [15, 93, 95].

Understanding the initial spread of disease is highly informative of its long-term ability to persist within a system, and can be captured by each disease's basic reproduction number R_0; the number of secondary infections caused by a single infected individual in an otherwise susceptible population [29]. If $R_0 < 1$ then the disease is unable to persist and the disease-free critical point is stable. Conversely, if $R_0 > 1$, the disease-free critical point is unstable, and introduction of a small number of cases will result in exponential growth (initially) towards a critical point in which the disease persists. The stability of these critical points switch as R_0 passes through the threshold point $R_0 = 1$ [55]. Thus, sufficiently accurate models that retain analytical tractability so that expressions for R_0 can be obtained are of great value to inform effective interventions against both persistent disease and outbreaks.

The increasing availability of animal movement datasets has shed light on the complex and highly heterogeneous nature of livestock trade [113], with developments in network theory enabling new insights into the dynamics of such complex systems [22, 38]. For example, the study of disease spread on such networks reveals that R_0 is heavily influenced by heterogeneity in the distribution of contacts [83, 89]. Thus,

to study the role of trade on disease spread, epidemiologists must develop models that adequately account for such complexities.

To date, attempts to assess the spread of disease in real-world cattle trade systems have largely consisted of replicating animal movements observed in data while overlaying simulated disease processes [71, 98, 76, 43, 117]. While these illustrate how past trade dynamics may have supported disease transmission, they cannot be generalised to ask "what if..." questions about what might occur under some future set of trades. In contrast, generative models capable of capturing key properties of such systems, while not being restricted to replaying historic movements, would allow far more general conclusions to be drawn. They would enable exploration of the potential impact of changes in movement patterns, highlighting novel avenues for intervention and control that move beyond standard approaches based on improvements to on-farm biosecurity or movement standstills. Thus far, attempts to develop mechanistic generative models of livestock trade systems have focussed on global properties [87] rather than considering trade between individual farms, or have modelled only the size and timing of animal movements on the frozen network of trade partnerships observed in the data [58].

To our knowledge here we present the first truly generative mechanistic model for livestock trading systems. This accounts for heterogeneity between farms and stochastically generates both movement of animals between trade partners and dynamically evolves the underlying partnership network (Section 2.2.1). Extending this to account for disease transmission via trade, we apply and extend the results of [6] to account for between-farm heterogeneities and derive a per-farm R_0, denoted R_0^i (Section 2.3.1). We subsequently use this analytic result to show large suppliers contribute disproportionately to disease spread and modifying trade dynamics could play a significant role in reducing disease burden (Section 2.3.2). With application to the Scottish cattle industry, we show that this parsimonious model can capture key features of the dynamics of a complex real-world trading system (Section 2.4). Subject to the condition that each farm maintains its annual in-flow of animals (representing maintenance of business requirements), we explore, for a broad spectrum

of endemic diseases, the impact on R_0, the system-average R_0^i, of changes to the way farms trade animals, including the formation of longer lasting trade partnerships. These results suggest that changes to trading practices are potentially effective in reducing both the burden of endemic disease and safeguarding against future disease outbreaks.

2.2 Materials and methods

2.2.1 Livestock trading model

We seek to model *animal movements* in terms of *trading practices* consisting of the formation and cessation of trade partnerships and trading between established partners. Connectivity relevant to disease transmission is therefore controlled by *partnership dynamics* (longevity of partnerships and number of concurrent partners) and *trading behaviour* (size and frequency of trades between partners). We assume a closed system of N farms and summarise between-farm heterogeneity in terms of a small number of farm-level constants. Firstly, annual in- and out-flows of animals measure farm-level demand and supply for farm i, and are denoted by η_i and ζ_i, respectively. Secondly, rates quantifying the propensity for farm i to form trading partnerships, a_i, end partnerships, d_i, and make trades, b_i. An outline of model quantities is given in Table 1 and are explained below in full. We note that in reality partnership dynamics and trade behaviour depend on a range of factors not considered here, e.g. social networks and capital, but farm-level propensities, supply and demand, capture much of the observed variation in the Scottish cattle trade system Section 2.4).

Dynamics of trading partnerships

The evolution of the topology of the modelled system is determined entirely by the formation and cessation of trading partnerships. Under the model, each farm possesses a dynamic list detailing which farms they can purchase animals from at a given time. Purchasing farms continually seek to optimise their trading partners by

Quantity	Definition
N	Number of farms
η_i	Per unit-time in-flow of animals for farm i
ζ_i	Per unit-time out-flow of animals for farm i
a_i	Rate describing farm i's propensity to form trading partnerships
d_i	Rate describing farm i's propensity to end trading partnerships
$\alpha_{ij} = a_i\eta_i\zeta_j/N$	Rate at which i forms a trading partnership with j
$\delta_{ij} = d_i/(\eta_i\zeta_j)$	Rate at which i ends a trading partnership with j
$p_{ij} = \frac{\alpha_{ij}}{\alpha_{ij}+\delta_{ij}}$	The probability that a trading partnership made by i with j is present
$k_i^{in} = \sum_{j\neq i}^{N} p_{ij}$	Expected instantaneous number of concurrent trading partners for farm i conditioned on zero partnerships at $t = 0$
b_i	Rate describing farm i's propensity to initiate trades with its trading partners
$\varphi_{ij} = b_i \min(\eta_i, \zeta_j)$	Rate at which i trades with its trading partner j
θ_i	Batch size for farm i
$V_i^{in} = \theta_i \sum_{j\neq i}^{N} \varphi_{ij}p_{ij}$	Expected unit-time equilibrium in-flow of animals for farm i
λ	Disease prevalence on an infected farm
$B(\theta_i) = 1 - (1-\lambda)^{\theta_i}$	Probability of at least one infected animal moves onto a susceptible farm i given batch size θ_i
$\beta_{ij} = \varphi_{ji}B(\theta_j)$	Transmission rate from infected farm i to susceptible farm j, given a trade partnership currently exists between farms i and j
γ	Disease recovery rate

Table 2.1: Table of model quantities and their respective definitions

preferentially forming partnerships with large suppliers, i.e. farms with large ζ_i, and preferentially ending partnerships with small suppliers, such that the system tends towards an equilibrium in which farms maintain long lasting partnerships with large suppliers. A farm i begins a trading partnership with another farm j, given no current partnership between them, at rate

$$\alpha_{ij} = \frac{a_i}{N}\eta_i\zeta_j \tag{2.1}$$

where constant a_i represents the propensity for farm i to form trading partnerships, summarising all factors that impact the ability of farm i to do so, e.g. the time required to search for partners. This process is uni-directional and, in general, asymmetric ($\alpha_{ij} \neq \alpha_{ji}$).

A current trading partnership between farms i and j ends at rate

$$\delta_{ij} = \frac{d_i}{\eta_i\zeta_j} \tag{2.2}$$

such that all farms tend to maintain longer partnerships with large suppliers compared with smaller suppliers. High demand farms are less likely to end trading partnerships in general compared to low demand farms. The constant d_i represents an intrinsic measure of the propensity for farm i to remove one of its traders, with larger values resulting in shorter duration trade partnerships, and vice versa.

The equilibrium probability of there being a trading partnership between i and j is p_{ij}, and the expected number of trading partners for farm i, k_i^{in}, are calculated as shown in Table 2.1 (see Appendix Section 2.6.1 for further details). The $1/N$ scaling of α_{ij} in Eq. (2.1) ensures that k_i^{in} does not scale linearly with the system size, N.

Movement of animals and trade flows

Animals are assumed to move between trading partners from j to i in batches (the number of individual animals moved in a single trade) of constant size θ_i with rate

$$\varphi_{ij} = b_i \min(\eta_i, \zeta_j), \tag{2.3}$$

where b_i is taken to represent any impediment to the movement of animals, for example delivery of livestock. The second term in Eq. (2.3) is referred to as the

reference transaction rate and is the maximum rate of exchange of indivisible goods (livestock), since $1/\eta_i$ is the expected time for i to generate new demand for animals and $1/\zeta_j$ the expected time for j to generate new supply [87, 58].

The per unit time in-flow of animals for farm i, when the system is at equilibrium, which is expected to equal η_i, is

$$V_i^{in} = \eta_i = \theta_i \sum_{j \neq i}^{N} \varphi_{ij} p_{ij}. \tag{2.4}$$

This expression is easily interpreted, since $\varphi_{ij} p_{ij}$ is the expected number of trades from j to i in a unit of time, and $\theta_i \varphi_{ij} p_{ij}$ is the total number of animals i purchases from j. Summed over the entire system, we obtain the total in-flow of animals per unit time for farm i. This expression for V_i^{in} allows us to alter the dynamics of trading partnerships and the movement of animals while maintaining each farm's in-flow of animals. We shall explore the effect of such conservative changes in Section 2.3.

Disease dynamics

The dynamics of disease are coupled with partnership dynamics and trade behaviour by assuming disease is driven entirely by animal movements, neglecting indirect transmission such as from external wildlife sources or distance modulated local infection.

We categorise disease status at farm level using a standard susceptible-infected-susceptible (SIS) model; susceptible farms become infected through trade with infected farms, and can themselves infect others, and, after an exponentially distributed infectious period with mean $1/\gamma$, recover to become susceptible once again. In addition to the infectious period, a given disease is also characterised by an effective on-farm prevalence level λ, assumed constant across infected farms and time. We therefore take λ to be the average prevalence of an infected farm over its infectious lifetime. We assume each animal moved off an infected farm i has a constant probability λ of infecting the susceptible buying farm and that off-farm movements do not alter herd prevalence on the selling farm. If an infected farm

sells θ animals in a trade to a susceptible farm, the total probability of transmission is $B(\theta) = 1 - (1 - \lambda)^\theta$, and the rate at which a farm j receives infection from its infectious trade partner i is $\beta_{ij} = \varphi_{ji} B(\theta_j)$, i.e. the rate at which j trades with i multiplied by the probability that the trade results in the transmission of disease. Thus, trades that occur with large size are more likely to result in the transmission of disease.

2.3 Results

2.3.1 Farms' basic reproduction number

Calculating R_0 for our model is challenging due to the heterogeneous nature of partnerhip dynamics and trading. Furthermore, the central role of the partnership network in mediating trade invalidates possible assumptions of homogeneous mixing. However, the methods outlined in [6] allows for an expression for R_0 to be obtained by considering the dynamics of farm pairs and calculating the probability of disease transmission. We extend these methods by incorporating farm heterogeneities and deriving a per-farm expression for R_0, R_0^i. Details of the calculation are provided in Appendix Section 2.6.2, but assume that the trading sub-system has reached an equilibrium (true for all simulations presented) and the partnership network is sufficiently sparse. The latter condition is satisfied since, for large systems, the probability of a two-way trading partnership scales as $1/N^2$. It is important to note that the results presented do not depend on the functional forms adopted above to describe partnership dynamics and trade behaviour and so offer general insights.

For a large system, R_0^i reduces to

$$\lim_{N\to\infty} R_0^i = \sum_{j\neq i}^{\infty} p_{ji} T_{ij} + \sum_{j\neq i}^{\infty} \frac{\alpha_{ji}}{\gamma} T_{ij}, \tag{2.5}$$

(see Appendix Section 2.6.2), where the transmissibility

$$T_{ij} = \frac{\beta_{ij}}{\beta_{ij} + \delta_{ji} + \gamma}$$

is the probability that farm i infects farm j if there is a trading partnership present, before the end of the infectious contact period, i.e. prior to either recovery or the

ending of the partnership [118]. The first term in Eq. (2.5) accounts for the number of current trade partnerships that result in the transmission of disease. The second term accounts for the number of new trade partnerships formed, before i recovers, that result in disease transmission before the end of the infectious contact period. This shows that partnership dynamics play a significant role in the ability for an infected farm to make infectious contacts. Indeed, even if the transmissibility was set to unity, so that farm i was guaranteed to pass infection onto its buyers following a trade, R_0^i would still be bounded by the rate at which buying farms sought out new trade partnerships with i, i.e. by α_{ji}.

2.3.2 The effect of changes to trading practices

We now use the above expression of R_0^i to rigorously explore the effects of modifying trading practices under the strong constraint Eq. (2.4) that farms maintain their expected in-flow of animals. Illustration of these results using stochastic simulations of example systems are presented in Appendix Section 2.6.7.

The role of trade behaviour

Consider first changes to the frequency and size of trades. Due to Eq. (2.4), and supposing the dynamics of trade partnerships are kept constant, a linear increase in the frequency of trade is accompanied by a proportional decrease in the size of trades, and vice versa. We introduce the scaling parameter ε_{trade} that determines the frequency and size of trades, and set

$$\varphi_{ij} \to \varepsilon_{trade}\varphi_{ij},$$
$$\theta_i \to \varepsilon_{trade}^{-1}\theta_i$$

for all i and j. Considering the case of large trades, substitution into the transmissibility, T_{ij}, reveals

$$\lim_{\varepsilon_{trade}\to 0} T_{ij} = \lim_{\varepsilon_{trade}\to 0} \left(\frac{\varepsilon_{trade}\varphi_{ji} B(\varepsilon_{trade}^{-1}\theta_j)}{\varepsilon_{trade}\varphi_{ji} B(\varepsilon_{trade}^{-1}\theta_j) + \delta_{ji} + \gamma} \right) = 0,$$

since $B(\varepsilon_{trade}^{-1}\theta_j)$ is bounded above by 1. It immediately follows that

$$\lim_{\varepsilon_{trade}\to 0} \lim_{N\to\infty} R_0^i = 0 \tag{2.6}$$

for all i. Thus, increasing the batch size reduces R_0. Similarly, in the case $\varepsilon_{trade} \to \infty$ where trades occur more frequently, but take ever smaller size, we find that R_0^i approaches a well-defined non-zero limit, further confirming that disease spread is inhibited by the dynamics of trade partnerships. This is due to the conservation of the in-flow of animals, so that the infection rate β_{ij} does not scale linearly with ε_{trade}, but rather approaches a limit given by $\varphi_{ji}\theta_j \ln(1/(1-\lambda))$, implying that although the number of trades increases significantly, the force of infection does not rise indefinitely due to the decrease in batch size. See Appendix Section 2.6.3 for details.

The role of partnership dynamics

We now explore the dynamics of trade partnerships when the frequency and size of trade is fixed. To do so, we introduce the scaling constant ε_{ptnr} and set

$$\alpha_{ij} \to \varepsilon_{ptnr}\alpha_{ij},$$
$$\delta_{ij} \to \varepsilon_{ptnr}\delta_{ij},$$

which allows for the dynamics of trade partnerships to be explored while maintaining a farm's expected instantaneous number of trading partners, k_i^{in}. As ε_{ptnr} increases, partnerships are formed increasingly frequently, however these partnerships last a decreasing period of time, and vice versa. In these limits we obtain

$$\lim_{\varepsilon_{ptnr}\to 0}\lim_{N\to\infty} R_0^i = \sum_{j\neq i}^{\infty} \frac{\alpha_{ji}}{\delta_{ji}} \frac{\beta_{ij}}{\beta_{ij}+\gamma} \tag{2.7}$$

for long duration partnerships, which is equivalent to the value of R_0 for a static directed network [83], so that the spread of disease is entirely dependent on the initial distribution of trade partnerships mediated by trade between them. We note that this is the scenario explored by [58]. Similarly, for small duration partnerships we obtain

$$\lim_{\varepsilon_{ptnr}\to\infty}\lim_{N\to\infty} R_0^i = \sum_{j\neq i}^{\infty} \frac{\widehat{\beta_{ij}}}{\gamma}, \tag{2.8}$$

where $\widehat{\beta_{ij}} = \beta_{ij}\alpha_{ji}/\delta_{ji}$, which is equivalent to the value of R_0 for a system under the mean-field assumption. Details of these results are provided in Appendix Sections

2.6.4 and 2.6.5. Comparing Eqs. (2.7) and (2.8), since $\beta_{ij} + \gamma > \gamma$ for all $\beta_{ij} > 0$, the disease is expected to spread more prolifically when trade partnerships are temporary, and a static network approximation offers a lower-bound on the early-time spread of disease, if all other components of the system are kept constant.

The role of the number of concurrent trading partners

Finally, we consider the effect on R_0^i of changes to the number of concurrent trading partners. Since there are an infinite number of combinations of α_{ij} and δ_{ij} that result in a given k_i^{in}, here we fix the duration of trade partnerships, i.e. keep δ_{ij} constant, and set

$$\alpha_{ij} \to \varepsilon^{ij}_{\#ptnr}\alpha_{ij}.$$

Note the i, j dependence of $\varepsilon^{ij}_{\#ptnr}$ in this case. We also note that conservation equation Eq. (2.4) implies a change in the number of trading partners must be accompanied by an inverse change in either the trade rate φ_{ij} or the batch size θ_i (or both). For simplicity, we herein maintain Eq. (2.4) by fixing the batch size and increasing/decreasing the trade rate when the number of trading partners is altered.

For a proportional change in k_i^{in} of x, we have

$$\varepsilon^{ij}_{\#ptnr} = \frac{x\alpha_{ij}}{(1-x)\alpha_{ij} + \delta_{ij}},$$

which can be verified by substitution into our expression for k_i^{in} (see Table 2.1). In the limit of a small number of concurrent trading partners we find

$$\lim_{\varepsilon^{ji}_{\#ptnr}\to 0} \lim_{N\to\infty} R_0^i = 0 \tag{2.9}$$

as expected since the system becomes entirely disconnected. For the scenario in which the number of concurrent trading partners goes to N, as N increases so too does R_0^i. As such, we use the expression for R_0^i for a system of finite size (see Appendix Section 2.6.6), and obtain

$$\lim_{\varepsilon^{ji}_{\#ptnr}\to\infty} R_0^i = \sum_{j\neq i}^{N} \frac{\beta_{ij}}{\beta_{ij} + \gamma}. \tag{2.10}$$

Note here that even for a finite system to reach this limit, $\varepsilon^{ij}_{\#ptnr}$ must go to infinity as the partnership cessation rate is fixed. Unsurprisingly, when the system is completely connected, the spread of disease is dependent solely on the dynamics of trade and the intrinsic disease parameters.

2.4 Case study: Scottish cattle trade industry

We demonstrate the potential of our modelling framework by application to the Scottish cattle trade system. We first show it is able to capture key features of this complex real-world system, and then use it to assess the potential impact of changes to trade patterns for the Scottish cattle industry. We use data from the Cattle Tracing System (CTS) for 2005-2013 inclusive, avoiding perturbations resulting from restocking following the UK 2001 Foot and Mouth Disease (FMD) outbreak [113]. We focus on the Scottish subset of this dataset featuring 15386 cattle farms which engage in a total of 135106 trades per year, with a total of 420931 animals move per year averaged over 2005-2013. We consider this a closed system, ignoring in-flow (representing approximately 10% of on-movements) and out-flow (approximately 14% of off-movements) of animals beyond Scotland, and consider only farm-to-farm movements grouped into dated batches. Animal flows through markets are maintained by treating such movements as transitory and replacing them with direct farm-to-farm movements. Movements to market are expected to play a small role in direct transmission endemic livestock disease [38, 13], but we acknowledge for epidemic spread of exotic or re-emerging diseases, market transmission may play a more significant role, for example in the 2001 FMD epidemic [45]. As such, we consider only slow spreading endemic diseases.

The farm-to-farm batch movement data described above are used to parameterise our model as follows (further details and distributions of trade quantities are presented in Appendix Section 2.6.11). Appendix Figure 2.10 shows trading patterns and animal flows are consistent year-on-year (movements at farm level are also known to be consistent year-on-year [38]), and we obtain annualised average in- and out-flows, η_i and ζ_i, for each farm by averaging observed yearly numbers of animals purchased

and sold, respectively. As above, the batch size for farm i, θ_i, is assumed constant, independent of the originating farm, and is estimated from data by averaging the total in-flow over the total number of trades for each farm.

Estimates for the trade partnership formation and cessation constants a_i and d_i are determined by evaluating partnerships on an annual basis, that is for a given year a partnership exists where two farms trade in that year. From the data we find that 83% of trade partnerships end after a single year, and 89% end after two years, emphasising the importance of accounting for partnership dynamics. To calculate a_i, we match observed new trading partners from year t to year $t+1$ with the partnership formation rate defined in Eq. (2.1), averaged over all years. Similarly, the constant d_i in the partnership cessation rate Eq. (2.2) is found by equating the number of partnership cessations occurring from one year to the next. Finally, the constant b_i in the trade rate Eq. (2.3) is obtained by solving the constraint equation Eq. (2.4) given estimates for all other quantities. Distributions across farms for each of these quantities can be found in Appendix Section 2.6.12.

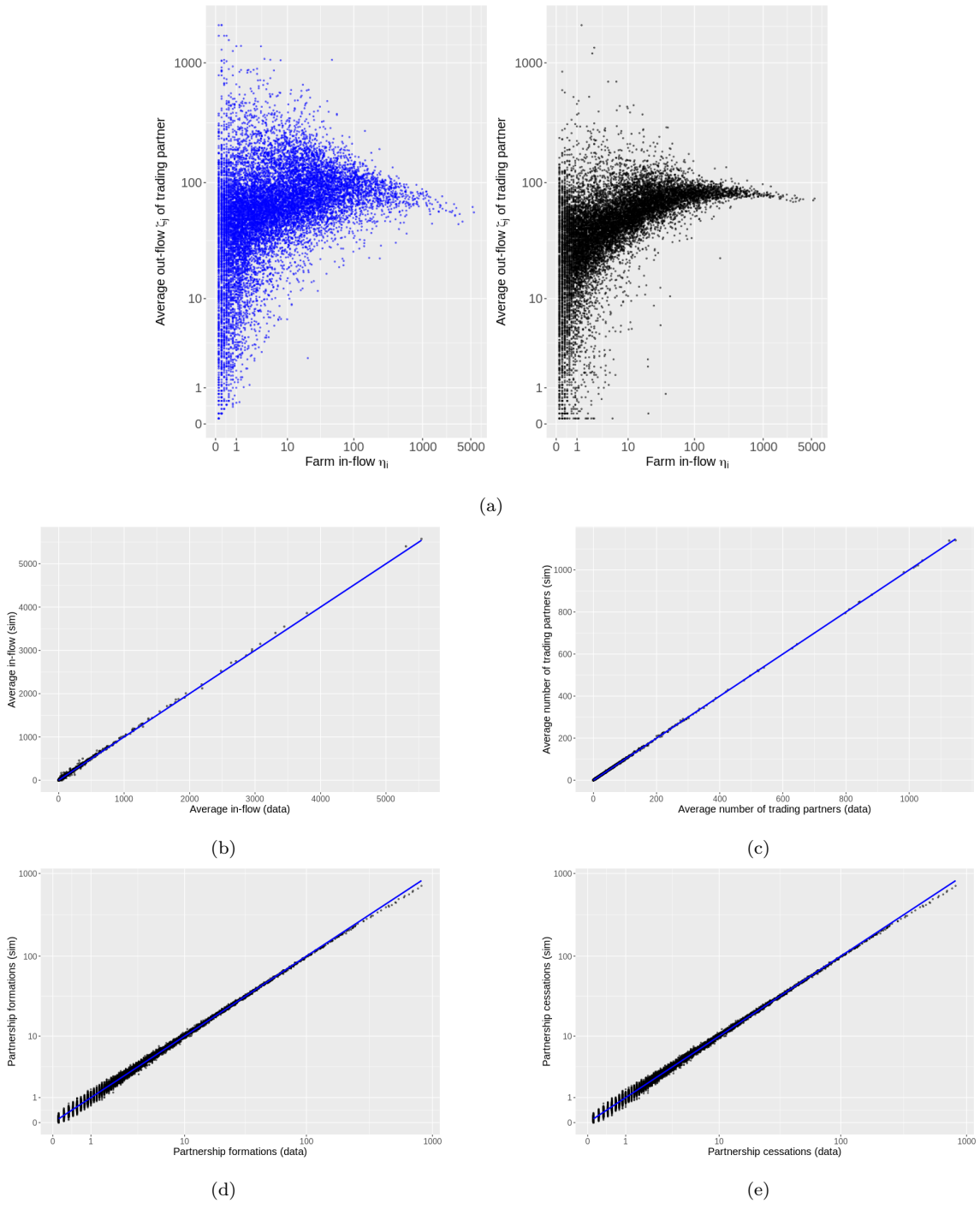

Figure 2.1: **Model fit to data**. For model with modifications to partnership formation and cessation rates. Panel (a) shows the average out-flow, ζ_j, of farms' trading partners, where blue points are obtained from data, and points from stochastic simulation, where simulations are performed using Gillespie Stochastic Simulation Algorithm. Bottom four panels show comparisons of simulation output and data for four statistics: annual in-flow (b), annual number of concurrent trading partners (c), annual number of partnership formations (d), and annual number of partnership cessations (e).

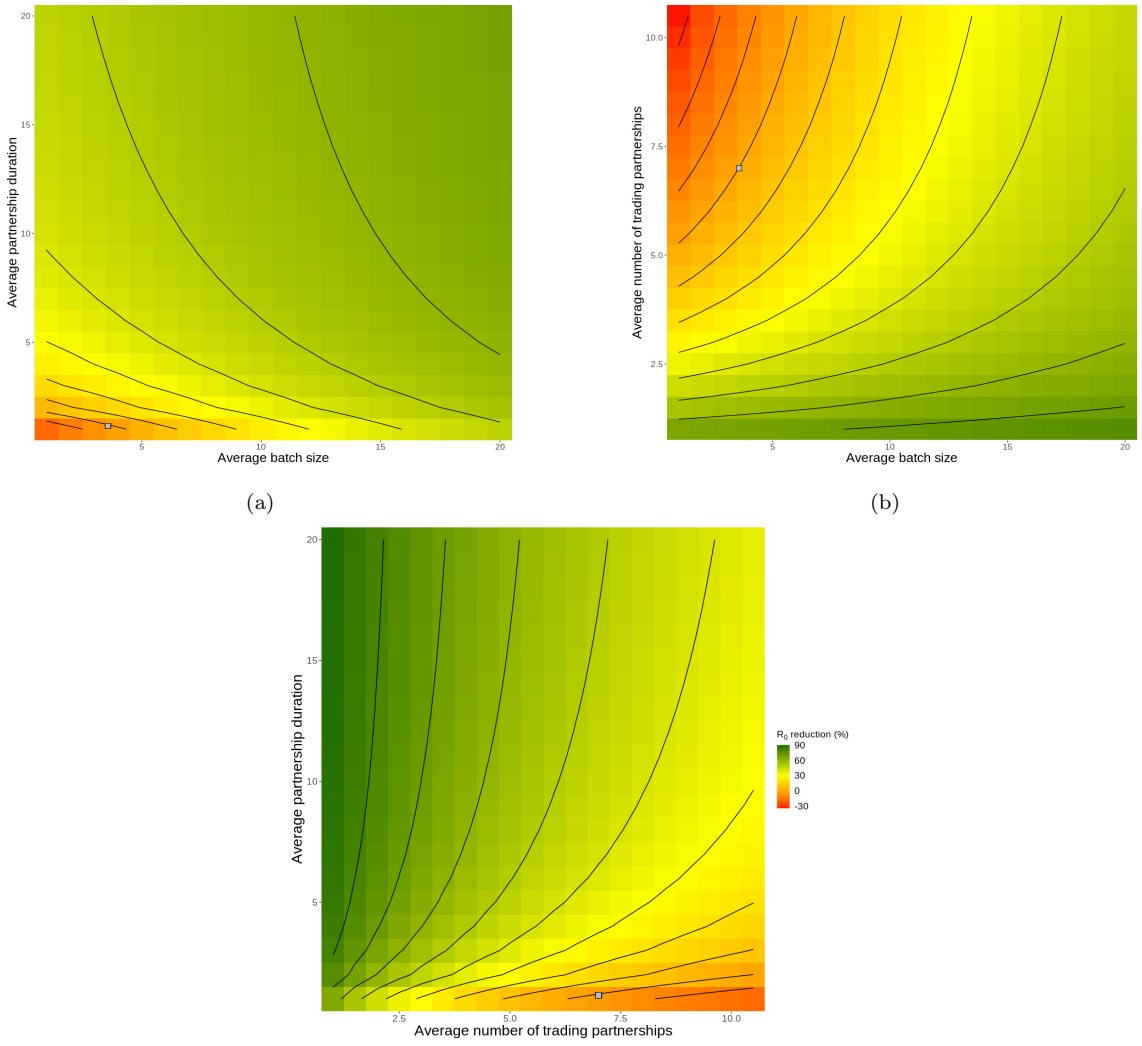

Figure 2.2: **Impact of trade behaviour and partnership dynamics.** Percentage change in R_0 for a persistent and high prevalence disease ($\lambda = \gamma = 0.2$) due to changes in the dynamics of trade and trade partnerships compared with the current dynamics of the Scottish trade system (grey squares). We consider changes to batch size and partnership duration (a), batch size and number of concurrent trading partners (b), and number of concurrent trading partners and partnership duration (c).

Initial results based on the above parameter estimates obtained for the model described in Section Section 2.2 reveal that our proposed trading partnership formation and cessation rates did not accurately replicate the distributions of the duration of trade partnerships or the joint distribution of farms' in-flows, η_i, and their traders'

out-flows, ζ_j. We therefore modified these rates to

$$\alpha_{ij} = \frac{a_i}{N}\left(\eta_i \zeta_j^m + w\right), \tag{2.11}$$

$$\delta_{ij} = \frac{d_i}{\eta_i}, \tag{2.12}$$

and find that setting $m = 0.75$ and $w = 75$ yields results closer to those observed in the data as shown in Figure 2.1 (initial fits are presented in Appendix Figures 2.15 and 2.16), while also replicating the values of higher-order statistics, e.g. annual in-flow, number of concurrent trading partners, and number of trades. This indicates the flexibility of our approach to represent real-world complexity in a parsimonious and tractable generative model framework. The required modifications to the model rates show that small buyers place greater weight on factors other than simply the size, ζ_i, of the prospective seller, but that larger buyers tend to buy from larger suppliers. Furthermore, large sellers are, in general, kept as trading partners for the same period of time as small sellers, again suggesting that farm sizes (the volume of animals bought/sold) are only one factor in selecting trade partners.

2.4.1 Assessing the potential for trade practices to modulate endemic disease

We now explore the effect of increased trade size, longer duration of trade partnerships, and reduced number of concurrent trading partners, subject to the constraint that farms' in-flows are maintained. To do so we focus on a fixed disease parameterisation $\lambda = 0.2$ and $1/\gamma = 5$ years, which is intended to represent a high prevalence, high persistence disease. For this hypothetical disease parameterisation and current Scottish trading patterns, our model predicts a system-average R_0^i $R_0 \approx 10$.

Figure 2.2 shows the percentage reduction in R_0 under varying changes to trade and trade partnership dynamics compared with current trading patterns (see Appendix Figure 2.19 for R_0 values). This shows that fewer, longer lasting trade partnerships yield the greatest reduction in R_0, with up to 90% reduction when farms maintain a single, near permanent trade partner. Fewer concurrent partnerships combined with fewer, larger trades reduces R_0 by up to 76%, however reducing the number

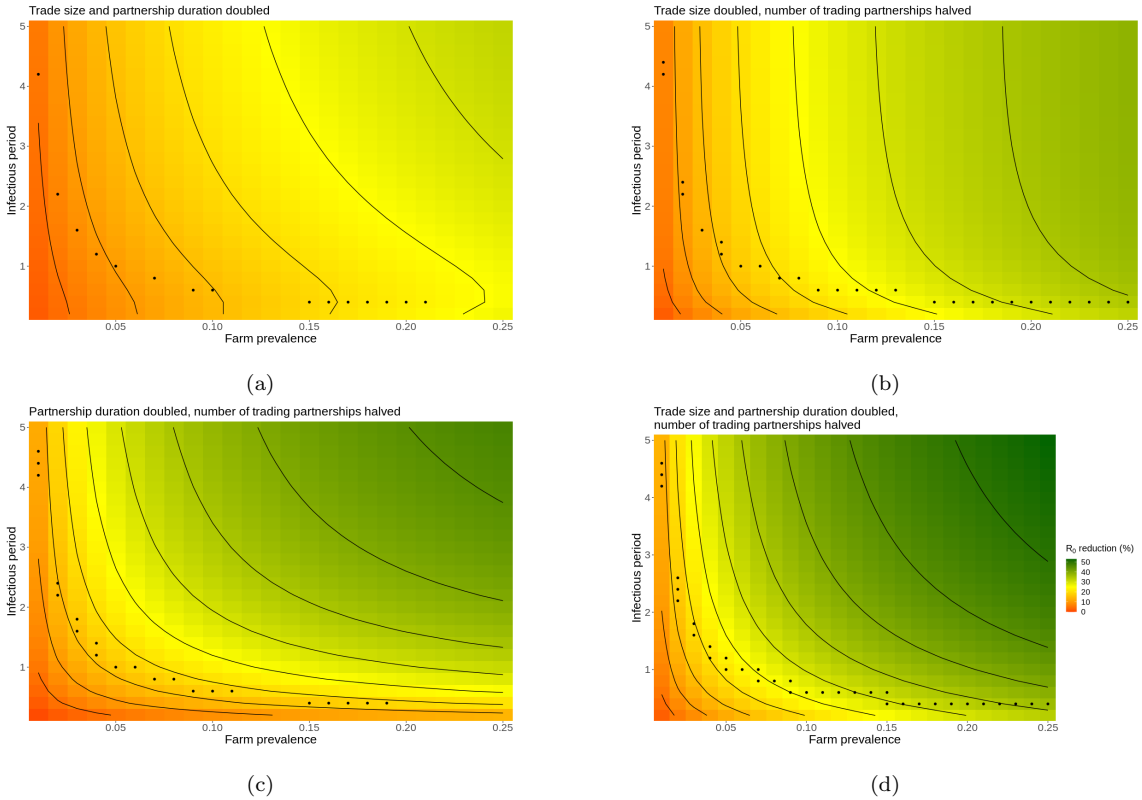

Figure 2.3: **Reducing endemic disease burden.** The percentage reduction in the system average R_0 for a range of disease parameterisations under specific trading and partnership dynamics changes, when compared with values of R_0 for current trading patterns in the Scottish trade system. Black points represent disease parameterisations in which $R_0 > 1$ before changes, and $R_0 < 1$ after changes are implemented.

of concurrent partnerships is responsible for most of this reduction. In the Scottish trading system, cattle farms average approximately 7.3 concurrent annual trading partners, and batches take average size of 3.58. Changes to current partnership dynamics and trading behaviour could yield both significant reductions and increases in R_0. For example, if the system-average number of concurrent trading partners and batch size were reduced by one, then R_0 would be reduced by approximately 12%. Conversely, if these were to be increased by one, then R_0 is increased by over 15%.

2.4.2 Impact of trade practices on a wide range of endemic diseases

We now explore the effect of specific changes to trade and partnership dynamics for a broad range of disease parameterisations (see Appendix Figure 2.20 for R_0 values). We consider halving the average number of concurrent trading partners, doubling the duration of trade partnerships, and doubling the average batch size, with each of these interventions considered under every possible combination (Figure 2.3) and in isolation (Appendix Figure 2.21). These changes are again made subject to conserving individual farms' in-flows of stock. Chosen farm-level prevalence, λ, ranges from 0.01 to 0.25, with infectious periods, $1/\gamma$, ranging from 6 months to 5 years.

Changes to the size and frequency of trades are most effective in reducing R_0 for high prevalence, small duration diseases, whereas changes to the duration and number of trade partnerships are most effective on high prevalence, long duration diseases (see Appendix Figure 2.21). This difference is explained by the fact that as the batch size increases, the inter-trade times increase, so that for small duration diseases the probability that an infected farm recovers before it is traded with increases. Changes to multiple aspects of trade patterns yield greater reductions in R_0 compared with changes to single elements. Encouraging fewer, longer lasting trade partnerships combined with fewer, larger trades provides the greatest reduction in R_0 (up to 53% for the highest prevalence and longest lasting diseases considered here) and also bring R_0 below 1 for a greater range of diseases. It is noteworthy that our suggested changes bring R_0 below 1 for diseases that are already close to this threshold, but also significantly reduce R_0 for high prevalence, long duration diseases, i.e. diseases that are extremely challenging to control and eradicate.

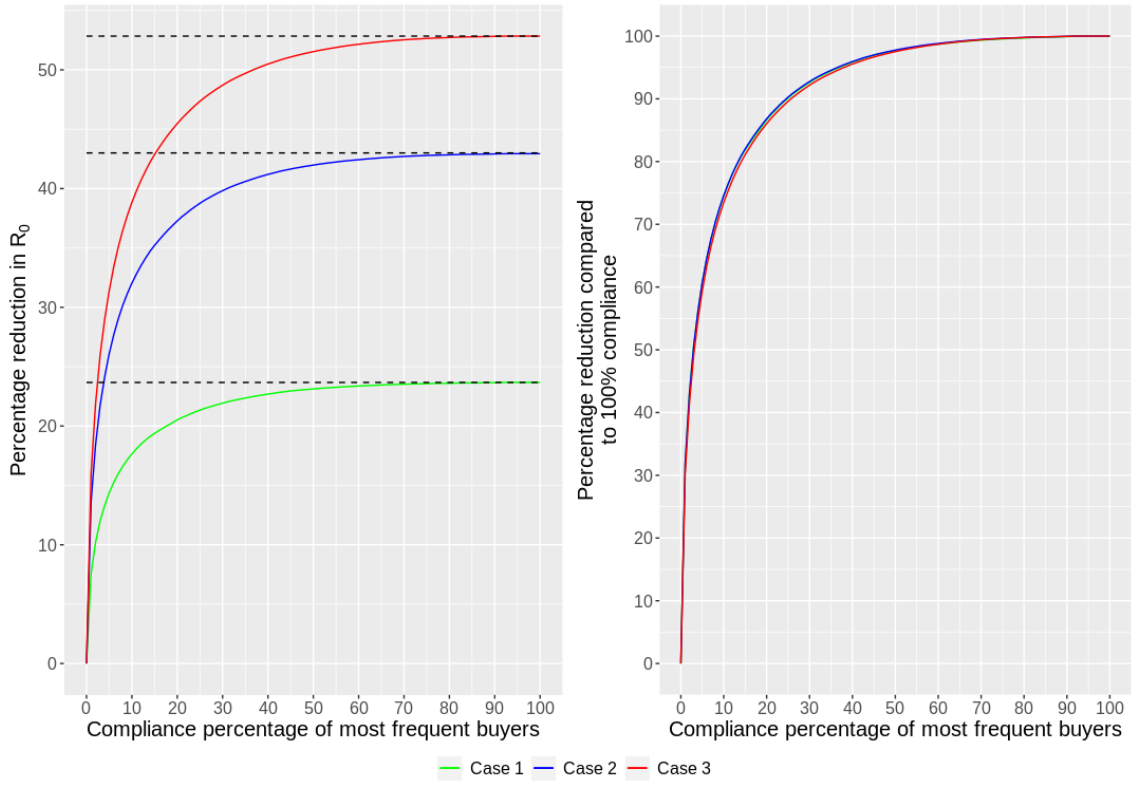

Figure 2.4: **Targeting high risk farms.** Percentage reduction in R_0 compared to: current trading patterns (left); and 100% adoption of new trading patterns (right). The new trading patterns are those shown in the bottom right panel of Figure 2.3d, which provides percentage reduction at 100% (dashed lines). In both panels the x-axis indicates what percentage of the most frequent buyers (those making the largest number of trades annually) are adopting these changes. Different disease parameterisations are shown with dashed lines representing values of R_0 for: Case 1) $\lambda = 0.06$, $\gamma = 1$; Case 2) $\lambda = 0.15$, $\gamma = 0.4$; and Case 3) $\lambda = 0.25$, $\gamma = 0.2$. Initial R_0 values for current trading patterns are: Case 1) $R_0 = 1.19$, Case 2) $R_0 = 4.92$, and Case 3) $R_0 = 11.43$.

2.4.3 Targeting the trade practices of large buyers

The results above show significant reductions in R_0 are attainable when all farms change their trade behaviour and partnership dynamics. However, consistent with other livestock markets [113, 58], the Scottish trading system exhibits scale-free like properties; a small number of farms trade much more frequently than the average and have a much larger annual number of concurrent trade partners (see Appendix Figures 2.12 and 2.13). Despite this, these outlying farms have average batch sizes similar to the mean batch size (and in some cases smaller, for example the 1% of

farms that make the largest number of trades make, on average, 363.5 trades per year, with average batch size 2.86, whereas the mean batch size is 3.58), suggesting there is scope for such farms to increase their average batch size. We therefore explore the potential for changes targeted at the most frequent buyers (those farms making the largest number of trades annually) and compare the resulting system average R_0 with the value of R_0 for current (i.e. no changes to) trade patterns, and with the value of R_0 obtained when all farms adopt the proposed changes.

Figure 2.4 shows the results from targeting the top $x\%$ of farms with x ranging from 0 to 100%. The changes to trading patterns considered are the composite changes that lead to the greatest reduction in R_0 in Figure 2.3. These changes are assessed under three disease parameterisations: Case 1) $\lambda = 0.06$, $\gamma = 1$, corresponding to a disease scenario in which our suggested changes in Section 2.4.2 brought R_0 below 1, Case 2) $\lambda = 0.15$, $\gamma = 0.4$, and Case 3) $\lambda = 0.25$, $\gamma = 0.2$, corresponding to the disease parameterisation that provided the greatest reduction in R_0 for the range of parameters we explored in Section 2.4.2.

In all disease scenarios 20% of the most frequent buyers are responsible for approximately 87% of the total possible reduction in R_0. Moreover, when 50% of the most frequent buyers adopt the proposed changes to trading patterns, we obtain approximately 98% of the reduction in R_0 that would be achievable if all farms comply. In Case 1) 8% compliance is sufficient to bring R_0 below 1, suggesting that for diseases with values of R_0 close to the threshold value, only a small fraction of farms would need to change their trading patterns to eradicate disease. For diseases that are challenging to control (Case 3), significant reductions are still achievable through the targeted approach, though stricter control measures may be necessary to bring R_0 below 1 for these diseases.

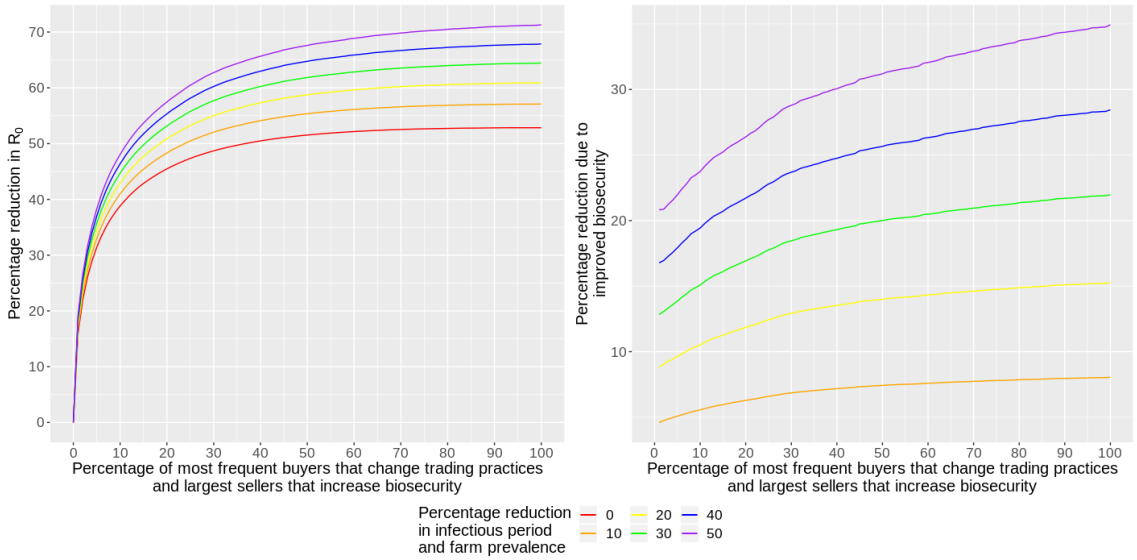

Figure 2.5: **Comparing biosecurity with changes to trade patterns.** Percentage reduction in R_0 (disease parameters $\lambda = 0.25$ and $\gamma = 0.2$) for targeted changes to both trading practices and improved biosecurity (left), and due solely to targeted improvements to biosecurity (right). In both cases, x-axes indicate what percentage of the most frequent buyers adopt trade changes and largest sellers improve biosecurity.

2.4.4 Combining targeted changes to trading practices with targeted biosecurity

So far we have considered only changes to buyers' trading patters, but now show that targeted changes in trade may be more impactful than similar targeting of standard on-farm biosecurity measures. We assess the impact of varying percentages of the largest sellers (those with the largest annual out-flow of animals) adopting on-farm biosecurity that is assumed to reduce prevalence λ and the infectious period $1/\gamma$ from a baseline ($\lambda = 0.25$ and $1/\gamma = 5$). These targeted biosecurity changes are assessed alone and in combination with changes to trading patterns targeted at the most frequent buyers, as above. Figure 2.5 shows that the combination further reduces system average R_0 compared to solely targeting trade patterns. However, these additional reductions increase relatively linearly as an increasing fraction of sellers adopt improved biosecurity. This is in stark contrast to the impact of an increasing fractions of the largest buyers changing trade practices (see Figure 2.4)

for which most of the potential reduction in R_0 is due to a small fraction of the most frequent buyers. This may be understood by considering that our analysis of the Scottish trading system suggests that formation and cessation of trading partnerships is determined by more factors than simply the size of the selling farm, i.e. their ζ_i. Thus, the out-flow of animals of a farm does not solely indicate whether that farm is a potential risk for the spread of disease.

2.5 Discussion

Animal movements via trade have long been considered a significant factor in the spread and persistence of diseases within national scale livestock disease systems [37, 42, 46, 51, 71, 94, 98, 108]. Recently available movement data has enabled modelling of disease spread to be superimposed on historic livestock movement patterns [51, 9, 109]. Network analysis of such data have also proved highly insightful. For example, using static networks to identify that fewer larger trades could improve disease control [88], or that highly connected 'hubs' are likely efficient targets for biocontrol [38]. Nonetheless, there is a pressing need to develop truly generative models of livestock movements to enable such data to better inform understanding and management of these complex systems. In this article we outline a generative approach with two components: a dynamic network which evolves via continuous formation and cessation of trading partnerships determining network topology at a given time; and a contact process on this network that represents animal movement (trades) and related disease spread between farms. Our approach goes beyond current state of the art models [58], for which only the size and timing of animal movements is modelled on a fixed network of trade partnerships, and is sufficiently powerful to represent key features of Scottish cattle movements as recorded by the Cattle Tracing System (CTS). Analysis of this model yields powerful insights into disease control, with limiting cases allowing re-derivation of known R_0 expressions, e.g. for static networks and well-mixed systems.

In the context of the Scottish cattle trading system we show that disease risks can be reduced in a way that minimises disruption by maintaining annual in-flows of animals

for all farms. Fewer, larger trades, and fewer, longer lasting trade partnerships yield the greatest reduction in system average R_0 when they are applied simultaneously, especially for diseases with high prevalence and persistence. Moreover, they can reduce R_0 below 1 for diseases close to this critical threshold under current trading patterns. Thus, changes in trade practices could eradicate certain diseases without other, potentially more disruptive and costly, control measures, and they could assist control of more persistent diseases that require multiple interventions. The fact that R_0 can be significantly reduced by simply changing the ways in which farms maintain their annual in-flow of animals is, we believe, a significant finding as this is potentially far less intrusive than other control strategies involving, for example, movement bans or restricting from whom a farm can purchase animals [43]. We note, however, that different network structures may effect the efficacy of each of our proposed changes to trade.

Our analysis also highlights the potential to exploit scale-free like properties of livestock trading systems for disease control. Targeted changes to the trade practices of only the farms with the highest trade volumes can significantly reduce R_0 and thus the burden of endemic disease and outbreak risk for the whole system. Further reductions result from combining changes to trade patterns with more standard biosecurity measures targeted on farms with the largest annual out-flows of animals. As such targeted modifications are expanded, resulting disease control benefits from changing trade practices scale much more favourably than do those of similarly targeted farm-level biosecurity (Figure 2.5). Given the current emphasis on farm-level biosecurity this is further evidence that the disease control potential of modifying trade deserves greater attention.

These results illustrate how mechanistic generative models, such as introduced here, can make a unique contribution to the study of livestock networks that complements existing network approaches. For example, our results agree with static network analysis identifying that fewer larger trades could improve disease control [87, 88], but go beyond these to show the impact of trade partnership dynamics. The scale-free properties of livestock trade are a common target for network analysis including

recent work on UK livestock trade that shows a fraction of farms are highly connected by contact chains involving multiple trades [38]. Although we do not explicitly identify such contact chains, their influence on disease transmission is integrated into our analysis and captured in our calculations of R_0 that account for trade and the formation of trade partnerships.

Naturally, the first implementation of our novel framework has made simplifying assumptions, the relaxation of which will be the subject of further work. Firstly, we assume trade occurs throughout the year, however animal movements generally occur in specific months [113]. Secondly, the rate at which farms trade is assumed constant, regardless of when the last trade was, but fluctuation in supply and demand is likely to play an important role in trade dynamics. However, we note that currently available generative mechanistic models of livestock trade make similar assumptions [87, 58]. Reformulating the trade rate to be a function of these stock quantities is a natural progression of our model which would resolve these issues, but could limit analytic tractability. Finally, the rates determining the formation and cessation of trade partnerships are based only on the annual in- and out-flows of farms, but our analysis suggests other factors may be at play. Distance-based metrics, farm types (beef, dairy, etc.), time-varying stock rates (see above), and socio-economic factors may enable better quantification of trading and partnership dynamics, and may also prove significant in the spread of disease.

In conclusion, we have introduced what we believe is the first generative modelling framework for livestock movements that is able to account for key features of complex national scale real-world systems. Analysis of resulting between-farm disease spread shows changes to trading patterns that conserve farm-level in-flow of animals provide a powerful approach to control of endemic disease and likely also mitigate outbreak risk. Attempts to adopt these novel approaches to disease control may reveal frictions in the ability of a real-world trading system to implement our proposed changes to trade and further work is needed to explore such barriers to uptake. For example, larger batch sizes (and fewer trades) may inhibit flexibility in adapting to changing conditions. Furthermore, there is evidence that some farmer behaviours

are determined by responses to external influences including extreme weather events and socially accepted farming practices [56]. This suggests that incentives, e.g. in the form of cooperatives, health schemes, or subsidies, may be required to encourage modification of farm-level trading behaviour. However, it is encouraging that reductions in disease burden resulting from targeted modification of trade practices scale much more favourably than those associated with improvements to farm biosecurity that are the usual focus of disease control policies.

2.6 Appendix

2.6.1 Derivation of $p_{ij}(t)$ and $k_i^{in}(t)$

We here derive the probability of a trade partnership between farms i and j, $p_{ij}(t)$, and the expected number of concurrent trade partners, $k_i^{in}(t)$.

The first-order differential equation governing the time-evolution of the probability of a trade partnership between i and j is given by

$$\frac{d}{dt}p_{ij}(t) = \alpha_{ij} - (\alpha_{ij} + \delta_{ij})p_{ij}(t), \tag{2.13}$$

which, under the assumption that the system begins in a disconnected state, i.e. $p_{ij}(0) = 0$, for all i and j, can be solved to yield

$$p_{ij}(t) = \frac{\alpha_{ij}}{\alpha_{ij} + \delta_{ij}} \left(1 - e^{-(\alpha_{ij}+\delta_{ij})t}\right). \tag{2.14}$$

At equilibrium, we obtain

$$p_{ij} = \lim_{t\to\infty} p_{ij}(t) = \frac{\alpha_{ij}}{\alpha_{ij} + \delta_{ij}}. \tag{2.15}$$

As the presence (or absence) of a trading partnership at time t is a Bernoulli random variable with probabilities differing between farm pairs, the expected number of trading partners for farm i at time t, $k_i^{in}(t)$, is a Poisson Binomial random variable with value

$$k_i^{in}(t) = \sum_{j\neq i}^{N} p_{ij}(t) \tag{2.16}$$

and the equilibrium number of concurrent trading partners is

$$k_i^{in} = \lim_{t\to\infty} k_i^{in}(t) = \sum_{j\neq i}^{N} p_{ij}. \tag{2.17}$$

2.6.2 Derivation of R_0^i

The disease transmissibility T_{ij} is calculated by solving

$$T_{ij} = \int_0^\infty P(i \text{ infects } j \mid \tau_{ij} = t)P(\tau_{ij} = t)dt, \tag{2.18}$$

where τ_{ij} is the infectious contact period, the period of time in which i is infected and is a supplier to j. Noting that the infectious contact period is a compound Poisson process, and since either recovery of cessation of the trading partnership ends the infectious contact period, which occurs with rate $\gamma + \delta_{ji}$, we have

$$\begin{aligned} P(\tau_{ij} = t) &= (\gamma + \delta_{ij})e^{-(\gamma+\delta_{ij})t}, \\ P(i \text{ infects } j \mid \tau_{ij} = t) &= 1 - e^{-\beta_{ij}t}, \end{aligned}$$

where β_{ij} is the rate at which i transmits infection to j. Upon substitution into Eq. (2.18) and integrating, we obtain

$$T_{ij} = \frac{\beta_{ij}}{\beta_{ij} + \delta_{ji} + \gamma}. \tag{2.19}$$

To calculate R_0^i, consider an initial infected farm i and another randomly chosen susceptible farm j. Referring to Figure 2.6, we define $S \cdot I$ as the state in which i is not a current trading partner of j. Similarly, $S - I$ is the state in which i is a current trading partner of j. We first calculate the probability that i transmits infection to j by calculating the probability that the farm pair transitions to the $I - I$ state, i.e. the state in which both farms are infected and i is a trading partner of j, before i recovers (represented by the transition to either the $S \cdot S$ or $S - S$ state). Now, since

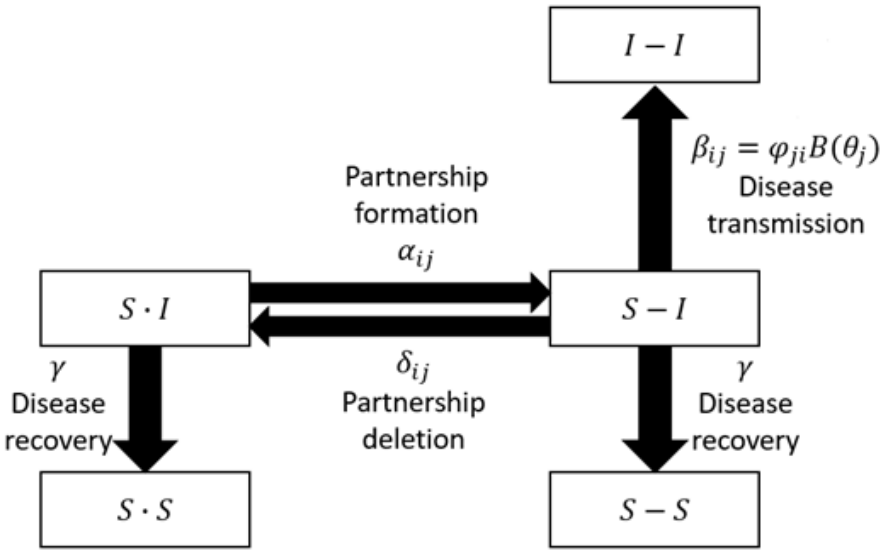

Figure 2.6: Farm pair transition diagram. The farm pair can begin in either the $S-I$ state or the $S \cdot I$ state, corresponding to the presence or absence of a trading partnership, respectively. The presented states are the only ones relevant to obtaining the probability that the infected farm transmits infection to the susceptible farm, i.e. the probability of transitioning to the $I-I$ state, and are thus the only states relevant to obtaining R_0^i.

j is chosen at random, the pair can begin in an initially connected or disconnected state, i.e. in the $S \cdot I$ or $S-I$ state, so we must calculate the conditional probabilities of transitioning to the $I-I$ state given their starting state, which we define as $A_{S \cdot I}$ and A_{S-I}, respectively. These conditional probabilities are related to each other by the following equations:

$$A_{S \cdot I} = \frac{\alpha_{ji}}{\alpha_{ji} + \gamma} A_{S-I},$$
$$A_{S-I} = T_{ij} + \frac{\delta_{ji}}{\beta_{ij}} T_{ij} A_{S \cdot I}$$

(these are obtained by considering the state transition diagram Figure 2.6). Upon solving we obtain

$$A_{S\cdot I} = \frac{\alpha_{ji}\beta_{ij}T_{ij}}{\beta_{ij}(\alpha_{ji}+\gamma) - \alpha_{ji}\delta_{ji}T_{ij}}, \tag{2.20}$$

$$A_{S-I} = \frac{(\alpha_{ji}+\gamma)\beta_{ij}T_{ij}}{\beta_{ij}(\alpha_{ji}+\gamma) - \alpha_{ji}\delta_{ji}T_{ij}}. \tag{2.21}$$

Defining the probability of transmission as ρ_{ij}, we have, by the Law of Total Probability,

$$\rho_{ij} = p_{ji}A_{S-I} + (1-p_{ji})A_{S\cdot I},$$

i.e. the probability that the pair start in a connected state and infection is successfully transmitted, plus the probability that the pair start in a disconnected state and infection is successfully transmitted. After substitution we obtain

$$\rho_{ij} = \frac{(\alpha_{ji}+\gamma p_{ji})\beta_{ij}T_{ij}}{\beta_{ij}(\alpha_{ji}+\gamma) - \alpha_{ji}\delta_{ji}T_{ij}}. \tag{2.22}$$

Disease transmission is Bernoulli random variable, and the probability of transmission differs between farm pairs but is independent. It follows that R_0^i is the mean of a Poisson Binomial distribution, given by

$$R_0^i = \sum_{j\neq i}^{N} \rho_{ij}. \tag{2.23}$$

Using the expression $\alpha_{ji} = a_j\eta_j\zeta_i/N$, substitution into Eq. (2.22) yields

$$\rho_{ij} = \frac{a_j\eta_j\zeta_i\beta_{ij}T_{ij}}{\beta_{ij}(a_j\eta_j\zeta_i+\gamma N) - a_j\eta_j\zeta_i\delta_{ji}T_{ij}} + \frac{\gamma p_{ji}\beta_{ij}T_{ij}}{\beta_{ij}(\alpha_{ji}+\gamma) - \alpha_{ji}\delta_{ji}T_{ij}}.$$

For a large system the denominator of the first term approaches $\beta_{ij}\gamma N$, the denominator of the second term approaches $\beta_{ij}\gamma$, and $p_{ji} \to \alpha_{ji}/\delta_{ji}$. Combining these we obtain

$$\lim_{N\to\infty} R_0^i = \sum_{j\neq i}^{\infty} \frac{\alpha_{ji}}{\gamma} T_{ij} + \sum_{j\neq i}^{\infty} p_{ji} T_{ij}. \tag{2.24}$$

2.6.3 R_0^i in large ε_{trade} limit

Under the scaling of the trade rate φ_{ij} and batch size θ_i by ε_{trade}, the infection rate β_{ij} does not scale linearly as ε_{trade} increases. The limit, rather, is given by

$$\lim_{\varepsilon_{trade}\to\infty} \beta_{ij} = \varphi_{ji} \lim_{\varepsilon_{trade}\to\infty} \varepsilon_{trade} B(\varepsilon_{trade}^{-1}\theta_j) = \varphi_{ji} \lim_{\varepsilon_{trade}\to\infty} \left(\varepsilon_{trade} \left(1 - (1-\lambda)^{\frac{\theta_j}{\varepsilon_{trade}}} \right) \right),$$

which is of indeterminate form. Application of L'Hôpital's Rule yields

$$\lim_{\varepsilon_{trade}\to\infty} \beta_{ij} = -\varphi_{ji}\theta_j \ln(1-\lambda) = \varphi_{ji}\theta_j \ln\left(\frac{1}{1-\lambda}\right). \tag{2.25}$$

Under this limit, the disease transmissibility is

$$T_{ij} = \frac{\varphi_{ji}\theta_j \ln\left(\frac{1}{1-\lambda}\right)}{\varphi_{ji}\theta_j \ln\left(\frac{1}{1-\lambda}\right) + \delta_{ji} + \gamma},$$

and the large N limit of R_0^i is of the same form as Eq. (2.24).

2.6.4 R_0^i in small ε_{ptnr} limit

Scaling the partnership formation and cessation rate, α_{ij} and δ_{ij}, by ε_{ptnr} and using the expression for the disease transmissibility Eq. (2.19), we have

$$\lim_{N\to\infty} R_0^i = \sum_{j\neq i}^{\infty} \frac{\varepsilon_{ptnr}\alpha_{ji}}{\gamma} \frac{\beta_{ij}}{\beta_{ij} + \varepsilon_{ptnr}\delta_{ji} + \gamma} + \sum_{j\neq i}^{\infty} p_{ji} \frac{\beta_{ij}}{\beta_{ij} + \varepsilon_{ptnr}\delta_{ji} + \gamma}. \tag{2.26}$$

In the small ε_{ptnr} limit, the first term vanished and we obtain

$$\lim_{\varepsilon_{ptnr}\to 0} \lim_{N\to\infty} R_0^i = \sum_{j\neq i}^{\infty} \frac{\alpha_{ji}}{\delta_{ji}} \frac{\beta_{ij}}{\beta_{ij} + \gamma}. \tag{2.27}$$

2.6.5 R_0^i in large ε_{ptnr} limit

In the large ε_{ptnr} limit the second term of Eq. (2.26) vanishes, but the first term is bounded and tends towards

$$\sum_{j\neq i}^{\infty} \frac{\alpha_{ji}}{\gamma} \frac{\beta_{ij}}{\delta_{ji}}.$$

After rearranging we obtain

$$\lim_{\varepsilon_{ptnr}\to\infty} \lim_{N\to\infty} R_0^i = \sum_{j\neq i}^{\infty} \frac{\alpha_{ji}}{\delta_{ji}} \frac{\beta_{ij}}{\gamma} = \sum_{j\neq i}^{\infty} \frac{\widehat{\beta}_{ij}}{\gamma}, \tag{2.28}$$

where $\widehat{\beta}_{ij} = \beta_{ij}\alpha_{ji}/\delta_{ji}$.

2.6.6 R_0^i in fully connected limit

Using the scaling factor $\varepsilon^{ji}_{\#ptnr}$ to scale the partnership formation rate α_{ji} as described in Section 2.3.2, and noting that $p_{ji} \to 1$ as $\varepsilon^{ji}_{\#ptnr} \to \infty$, we have, for a finite system, and using Eq. (2.23),

$$\lim_{\varepsilon^{ji}_{\#ptnr}\to\infty} R_0^i = \sum_{j\neq i}^{N} \frac{\beta_{ij}T_{ij}}{\beta_{ij} - \delta_{ji}T_{ij}},$$

which, upon substitution of the disease transmissibility Eq. (2.19) yields

$$\lim_{\varepsilon^{ji}_{\#ptnr}\to\infty} R_0^i = \sum_{j\neq i}^{N} \frac{\beta_{ij}}{\beta_{ij} + \gamma}. \tag{2.29}$$

2.6.7 Comparison of theoretical predictions with stochastic simulation

We compare our theoretical predictions of R_0, the system average R_0^i, for two trading systems: one in which trading patterns of farms distributed according to Power-Law distributions, and one in which all farms behave homogeneously, that is all quantities

in our system are equal across farms. In all cases we set the system size $N = 200$, farm prevalence $\lambda = 0.4$, and infection recovery rate $\gamma = 0.2$.

For the Power-Law system, trading quantities are of the form

$$p(Z = z) = Cx^{-\alpha},$$

where C normalises the distribution, and α determines the slope of the distribution. We distribute the in- and out-flows of farms, η_i and ζ_j, respectively, the number of concurrent trading partners, k_i^{in}, and the unit-time number of trades according to this distribution, and the value of α is chosen to obtain desired averages for each of these quantities. In the below scenarios, and in both systems, farms bring on and send out 2 animals per time unit, i.e. $\eta = \zeta = 2$, with an average of 2 trades from 2 concurrent trading partners.

We assume the constant a_i in the partnership formation rate is also distributed in such a way, and the partnership cessation constant d_i is thus determined by solving the expression for k_i^{in} (see Table 2.1). As an initial state, we desire the average partnership duration to be 1 unit of time, so a_i and d_i are rescaled to achieve this. The batch size, θ_i, is obtained by dividing the unit time in-flow, η_i, by the unit time number of trades for each farm, and the constant b_i in the rate of trade is found by solving our expression for the expected unit time in-flow of animals (see Eq. (2.4)). As with the duration of trade partnerships, we choose an initial state in which the average batch size is set to 1. Thus, b_i and θ_i are rescaled to achieve this.

For the homogeneous system, for comparison we set the values of farms' trading quantities to be equal to the means of the Power-Law system. For a homogeneous system, our expressions for R_0^i can be reduced to closed-form expressions. As our system is homogeneous, we drop subscripts from all quantities and summations over the system can be replaced with products, e.g.

$$\sum_{i}^{N} x = xN.$$

We note that $\sum_{j\neq i}^{N} p_{ij} = pN = k^{in}$, and that $k^{in} \to \alpha/\delta$ for large N. Thus,

$$R_0^i = R_0 = \frac{(\alpha N + \gamma k^{in})\beta T}{\beta(\alpha+\gamma) - \alpha\delta T}, \tag{2.30}$$

and

$$\lim_{N\to\infty} R_0 = \frac{\alpha N}{\gamma} T + k^{in} T. \tag{2.31}$$

Note that α is a function of the system size N so that αN is bounded for increasing N.

2.6.8 Comparing changes to frequency and size of trades

As predicted by Eq. (2.6), increasing the batch size and decreasing the frequency of trade has the desirable effect of reducing R_0 in both the Power-Law and homogeneous systems (see Figure 2.7). Both the theory and simulation are in good agreement, predicting similar behaviour qualitatively and quantitatively, although there are differences between the two systems, with the Power-Law system predicting slightly smaller values of R_0 than the homogeneous system, and a more pronounced decrease in the equilibrium disease prevalence as the batch size is increased. In both systems, however, complete removal of disease is possible when the batch size is increased to 6 for the Power-Law system and 8 for the homogeneous system.

2.6.9 Comparing changes to duration of trading partnerships

Increasing the average duration of trading partnerships reduces R_0 as predicted by Eq. (2.7), and both the theory and simulation output predict similar qualitative

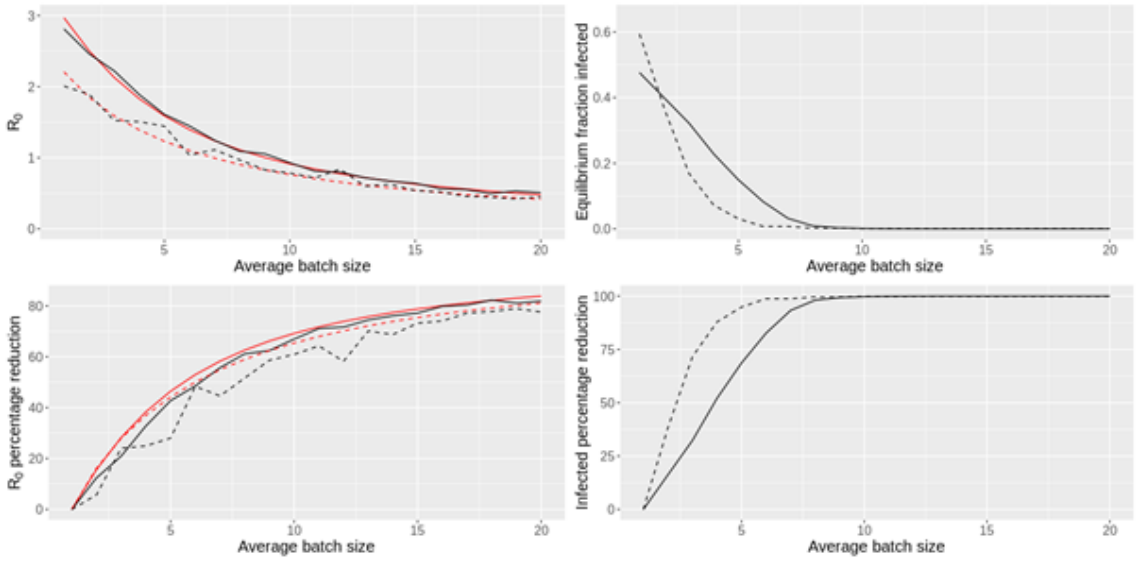

Figure 2.7: The system-average R_0 (top left), equilibrium disease prevalence (top right), percentage reduction in R_0 compared to the initial state (bottom left), and the percentage reduction in the equilibrium disease prevalence compared to the initial state (bottom right) as the average batch size is increased from an initial batch size of 1. Solid red lines represent the theoretical predictions for the homogeneous system, and solid black lines represent the output of the average of 2000 independent simulations for the homogeneous system. Dashed lines represent the same output for the Power-Law system, except in simulations each of the 200 farms is chosen to be the initial infected in 10 simulations.

behaviour, however the differences between the two are noticeable, in particular for the homogeneous system (see Figure 2.8). Encouraging longer lasting trading partnerships has a markedly larger effect on the equilibrium prevalence for the Power-Law system compared to the homogeneous system, with approximately 80% and 30% reduction when partnerships last an average of 20 time units for the Power-Law and homogeneous systems, respectively. We note that, while the value of R_0 can be reduced, altering the duration of trading partnerships may be insufficient in reducing R_0 below the threshold value of 1, and its ability to do so is determined by the intrinsic disease parameters and/or the frequency and size of trades.

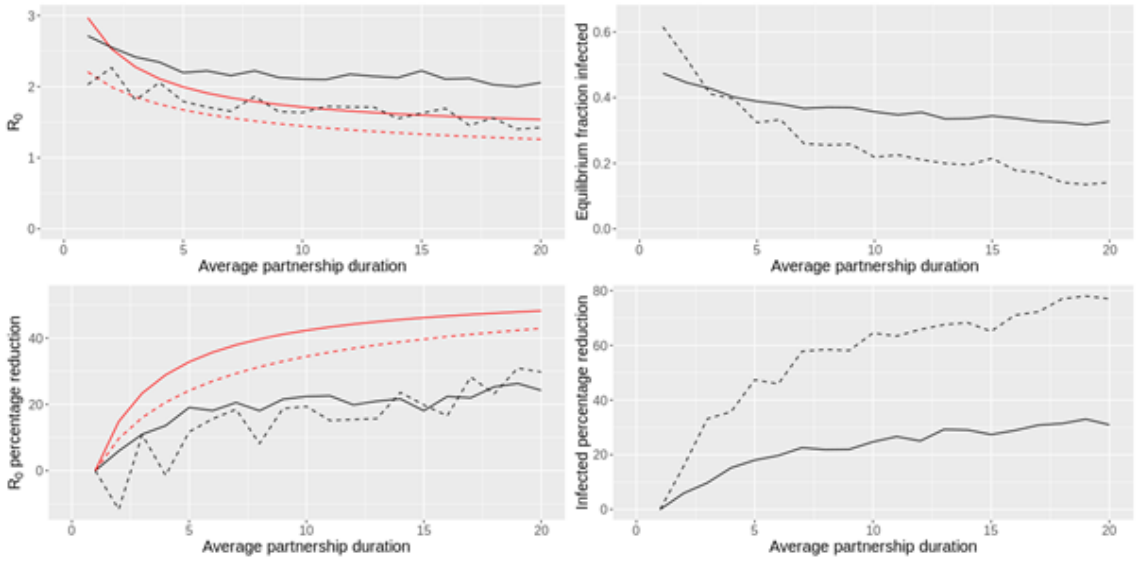

Figure 2.8: The system-average R_0 (top left), equilibrium disease prevalence (top right), percentage reduction in R_0 compared to the initial state (bottom left), and the percentage reduction in the equilibrium disease prevalence compared to the initial state (bottom right) as the average trading partnership duration is increased from an initial duration of 1 time unit. Solid red lines represent the theoretical predictions for the homogeneous system, and solid black lines represent the output of the average of 2000 independent simulations for the homogeneous system. Dashed lines represent the same output for the Power-Law system, except in simulations each of the 200 farms is chosen to be the initial infected in 10 simulations.

2.6.10 Comparing changes to number of concurrent trading partners

A reduction in the number of concurrent trading partners, accompanied by a proportional increase in the number of trades so that farms' in-flow of animals are maintained, yields a reduction in R_0 and the equilibrium prevalence, and, as with changes to the batch size, the theory and simulation predict similar qualitative and quantitative behaviour (see Figure 2.9). Complete eradication of disease is possible as the number of trading partners is brought closer to zero, and we note that for our two systems considered here that greater proportional reductions in the number of trading partners is required to reduce R_0 below 1 than is required if the batch size is increased. However, this may be a property of our chosen systems and not true in all cases, as evidenced by our analysis of the Scottish cattle trade industry where changes in the number of trading partners yielded greater reductions in R_0.

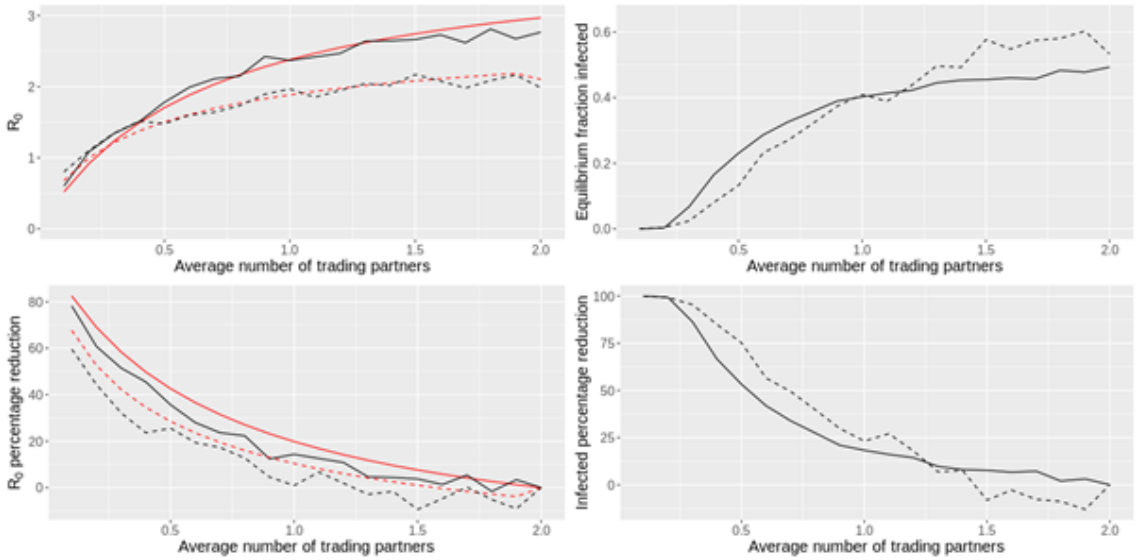

Figure 2.9: The system-average R_0 (top left), equilibrium disease prevalence (top right), percentage reduction in R_0 compared to the initial state (bottom left), and the percentage reduction in the equilibrium disease prevalence compared to the initial state (bottom right) as the average number of concurrent trading partners is increased from an initial number of 0.1. Solid red lines represent the theoretical predictions for the homogeneous system, and solid black lines represent the output of the average of 2000 independent simulations for the homogeneous system. Dashed lines represent the same output for the Power-Law system, except in simulations each of the 200 farms is chosen to be the initial infected in 10 simulations.

2.6.11 Overview of CTS data analysis

Our analysis of the Scottish trading system involves obtaining the distribution of quantities to apply to our model without explicitly matching the animal movements observed in the data. The Cattle Tracing System (CTS) dataset provides detailed records of individual cattle movements between premises, with each animal uniquely identified by an animal ID. We restrict our considerations solely to farms located within Scotland, and between years 2005-2013, inclusive. We choose not to include years prior to 2005 so that potential lingering perturbations to trade following the 2001 Foot-and-Mouth disease epidemic are minimised.

We remove seasonal trends by obtaining yearly averages for farm parameters and quantities, and since movements to markets are expected to play a small role in the spread of endemic diseases, we treat such movements as transitory and replace

them with direct farm-to-farm movements (thus maintaining the flow of animals through markets). Any movements to market that are not subsequently moved off that market are removed from the dataset. Additionally, any animal movement to a non-farm premises (defined as an agricultural holding in the data) is removed. This removes movements to slaughterhouses, here considered endpoints for infection. Our modelling assumption that disease transmits solely through trade implies that an animal holding that neither buys nor sells at least one animal in the time period considered makes no contribution to the spread of disease; consequently, these farms are also removed from the dataset. Finally, any farm-to-farm movement that originated or ended at a location not within Scotland was removed, so that we have a closed system of farms that trade solely within the population. Movements sent out of Scotland accounted for approximately 14% of all outgoing animal movements, and movements to Scotland accounted for approximately 10% of all incoming animal movements.

Our resulting dataset is closed system of the individual cattle movements of 15386 farms. We combine these individual cattle movements into batch movements between farms by matching the on- and off-location IDs for a given date. These batch movements allow us to obtain values for model quantities as follows. The yearly average in- and out-flow of animals for farms, η_i and ζ_i, respectively, are obtained by averaging the total observed number of animals purchased/solve over the time period we are considered, defined as T. Thus

$$\eta_i = \frac{1}{T}\sum_{t=1}^{T} V_i^{in}(t),$$
$$\zeta_i = \frac{1}{T}\sum_{t=1}^{T} V_i^{out}(t),$$

where $V_i^{in}(t)$ and $V_i^{out}(t)$ are the total in- and out-flows of animals for farm i in year t, respectively.

We make the modelling assumption that the batch size of a farm i, θ_i, is constant and independent of the farm whence the batch originated, so that all farms can

supply θ_i animals to farm i when a trade occurs. As such, we obtain θ_i by simply taking the average size of all trades observed for farm i:

$$\theta_i = \frac{1}{\Phi_i} \sum_{t=1}^{T} V_i^{in}(t),$$

where Φ_i is the total number of trades observed for farm i.

To obtain estimates for the partnership coefficients a_i and d_i, we assume that a farm that buys animals from another farm in year t and again in year $t+1$ maintained the trading partnership in both years. Conversely, if a trade is observed in year t but not in year $t+1$ then we assume the partnership ended at the end of year t. Thus, we evaluate trading partnerships on an annual basis and our analysis revealed that approximately 83% of partnerships ended after a single year, and 89% after two years.

To calculate a_i, we match the observed new trading partnerships from year t to $t+1$ with the partnership formation rate defined in Eq. (2.1). We do this for each year, as the number of potential new trading partners varies over the years depending on who is currently a trading partner. Thus we define $a_i(t)$ for year t, which is found by equating

$$\begin{aligned} a_i(t) \sum_{j \notin K_i^{in}(t-1)} \frac{\eta_i \zeta_j}{N} &= A_i(t-1,t) \\ \Rightarrow a_i(t) &= \frac{A_i(t-1,t)N}{\sum_{j \notin K_i^{in}(t-1)} \eta_i \zeta_j}, \end{aligned}$$

where $A_i(t-1,t)$ is the number of observed trading partnerships formed by i in year t that were not observed in year $t-1$. In the subscript of the summation we take $K_i^{in}(t-1)$ to be the trading partners of farm i in year $t-1$. We then calculate a_i as

$$a_i = \frac{1}{T} \sum_{t=1}^{T} a_i(t).$$

Note that for any farm in which $\zeta_i = 0$ we set $a_i = 0$.

We obtain d_i in a similar manner by equating the number of partnership cessations occurring from one year to the next with the partnership cessation rate at defined by Eq. (2.2). Thus

$$d_i(t) \sum_{j \in K_i^{in}(t-1)} \frac{1}{\eta_i \zeta_j} = D_i(t-1,t),$$
$$\Rightarrow d_i(t) = \frac{\eta_i D_i(t-1,t)}{\sum_{j \in K_i^{in}(t-1)} \zeta_j^{-1}},$$

where $D_i(t-1,t)$ is the number of observed partnerships in year $t-1$ that were not observed in year t. Note that the denominator is only defined for non-zero $K_i^{in}(t)$, i.e. in years in which farm i had at least one trading partner. Thus, to obtain d_i, we average over the years in which i had at least one trading partner, defined as Y_i. Therefore

$$d_i = \frac{1}{Y_i} \sum_{t=1}^{Y_i} d_i(t).$$

Finally, we obtain the trade rate coefficient b_i by solving Eq. (2.4) so that

$$b_i = \frac{\eta_i}{\theta_i \sum_{j \neq i}^{N} p_{ij} \cdot \min(\eta_i, \zeta_j)}.$$

2.6.12 Distributions of model quantities from CTS data

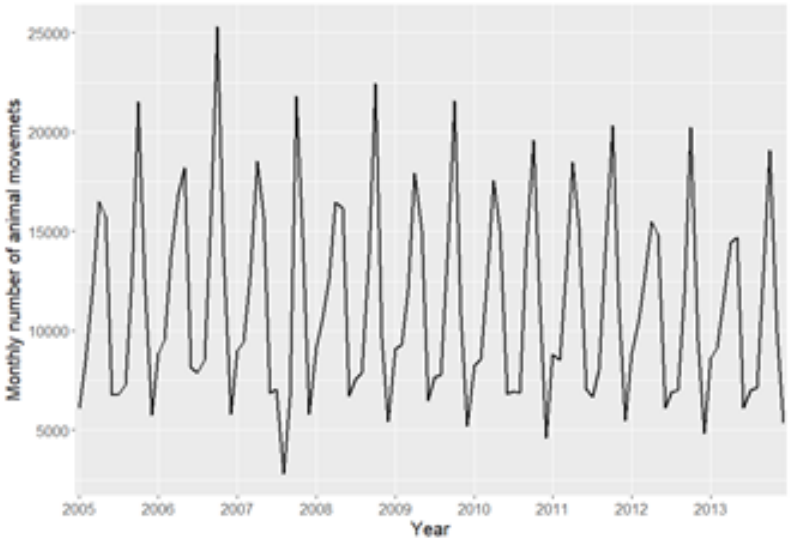

(a)

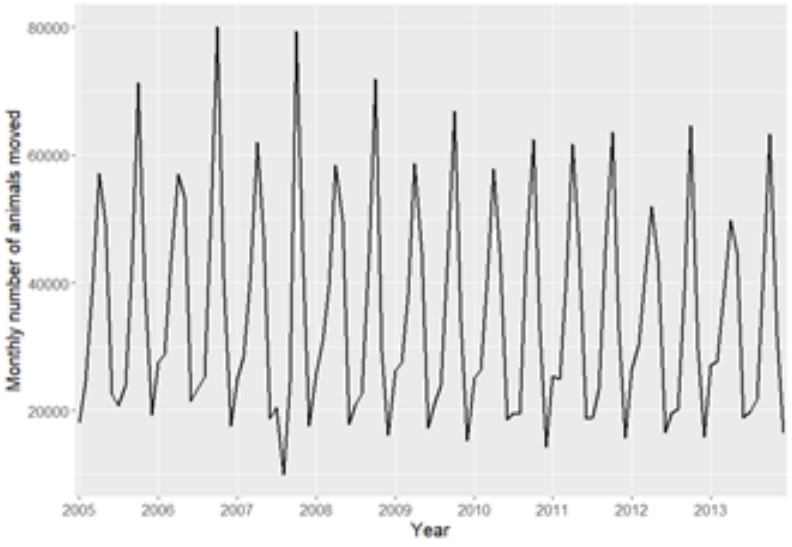

(b)

Figure 2.10: Monthly total number of animal movements (a) and number of animals moved (b). In general, animal movements and flows are consistent year-on-year, though there is a notable decline in 2007, corresponding to the small FMD outbreak that occurred.

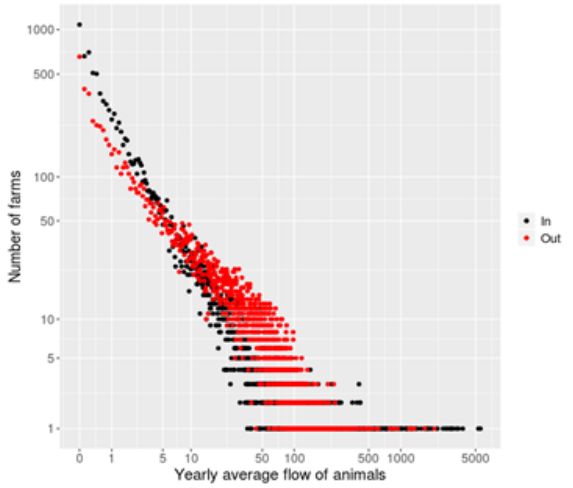

(a)

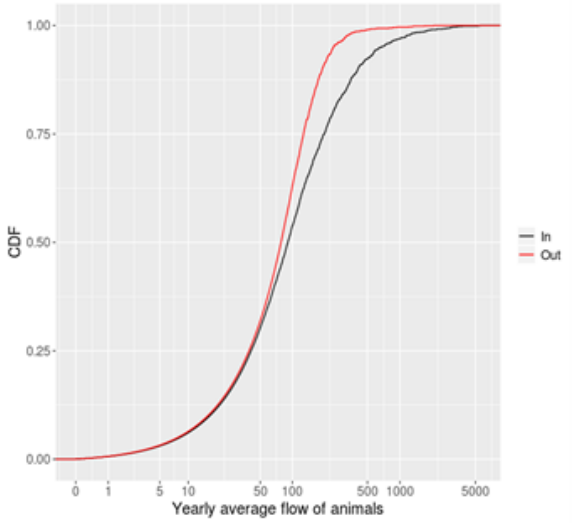

(b)

Figure 2.11: The distribution (a) and empirical cumulative distribution (b) of animal flows.

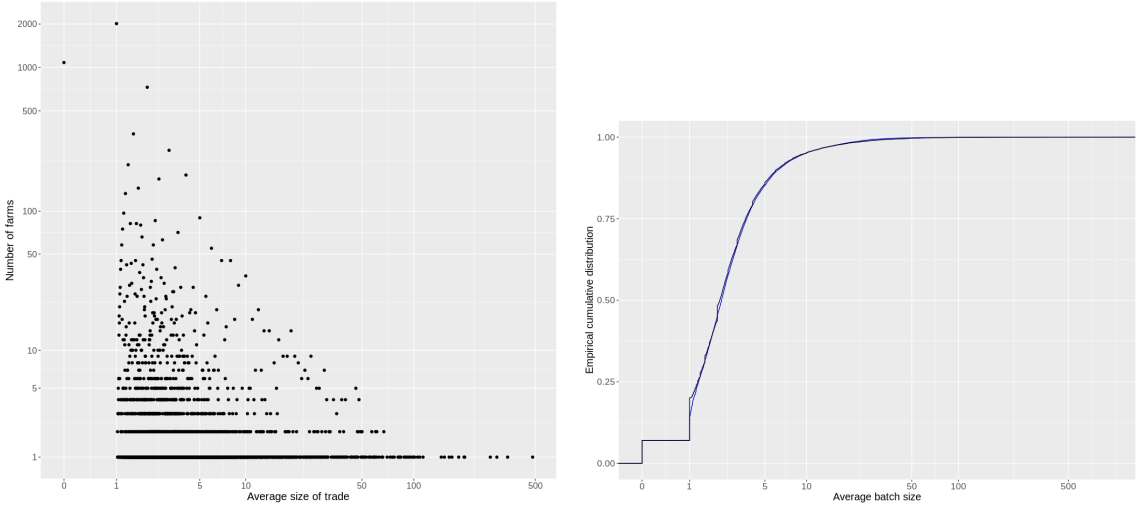

(a) (b)

Figure 2.14: The distribution (a) and empirical cumulative distribution (b) of the average batch size.

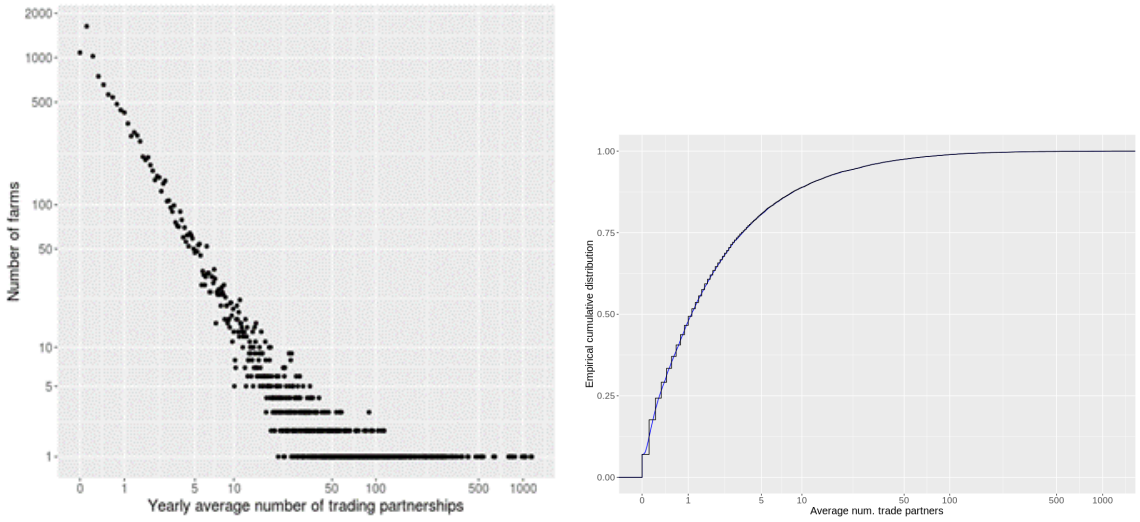

(a) (b)

Figure 2.12: The distribution (a) and empirical cumulative distribution (b) of the annual average number of trading partnerships.

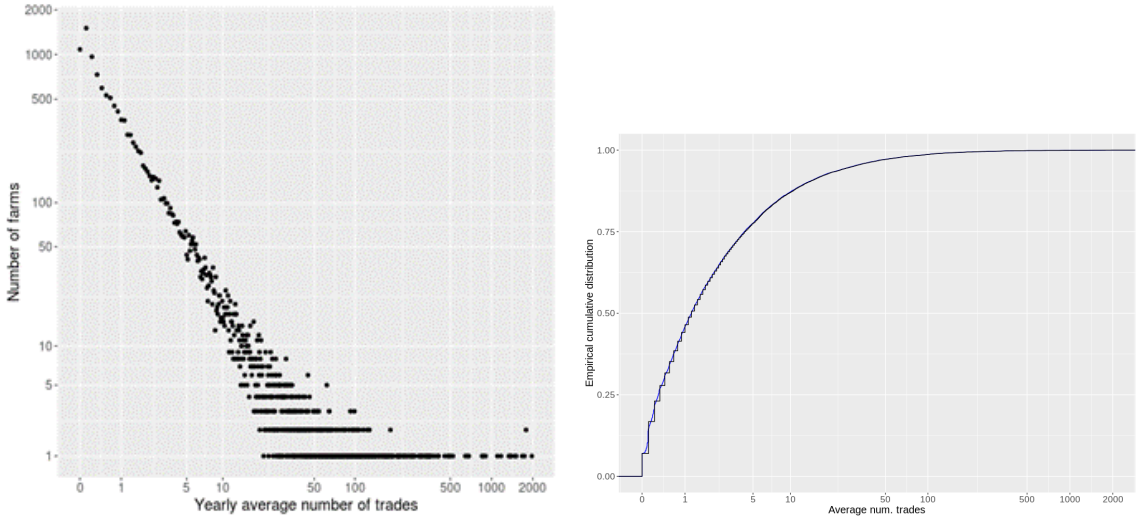

(a) (b)

Figure 2.13: The distribution (a) and empirical cumulative distribution (b) of the annual average number of trades.

2.6.13 Distribution of trading partners' out-flows and partnership duration before and after modification to formation and cessation rates

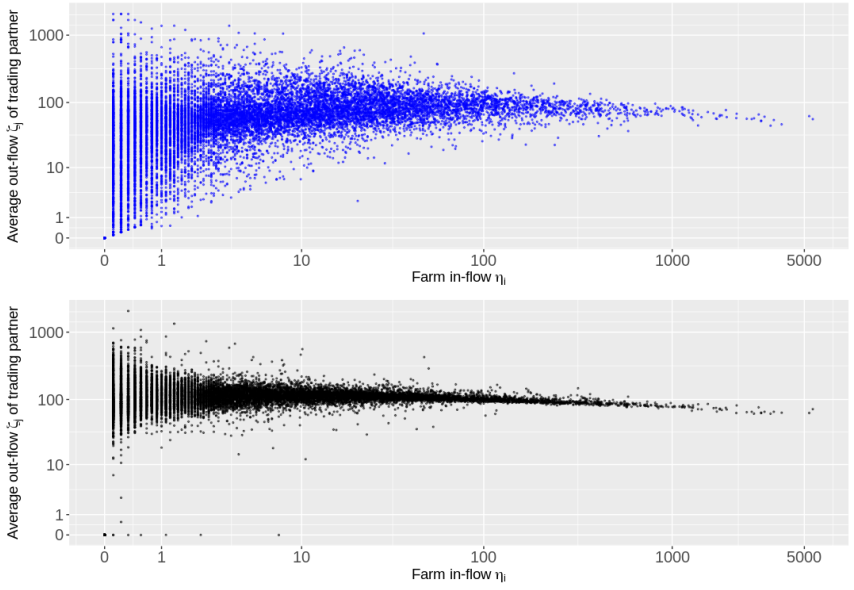

(a)

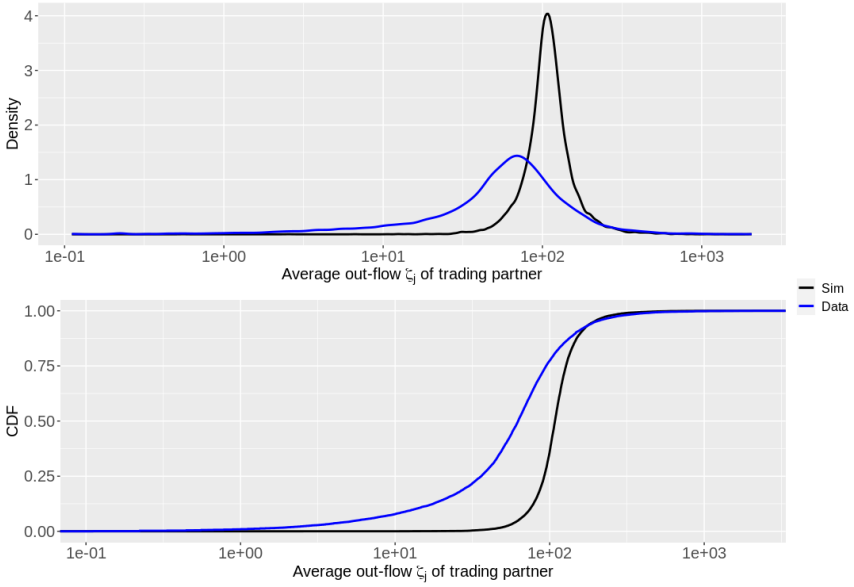

(b)

Figure 2.15: Simulation output and data for the distribution (a), and density and empirical cumulative distribution (b) of the average out-flow of farms' trading partners under original functional forms for the partnership formation and cessation rates.

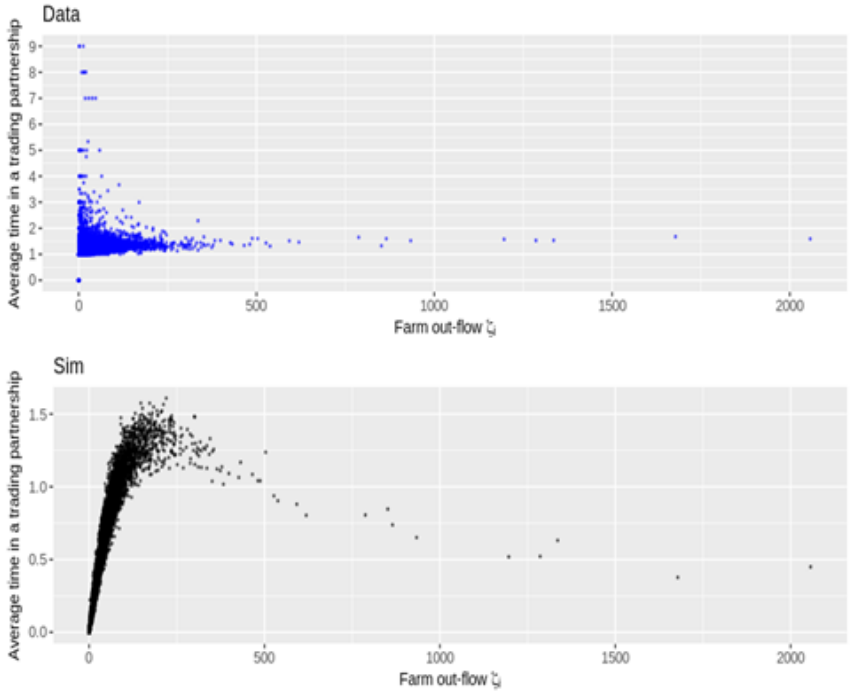

(a)

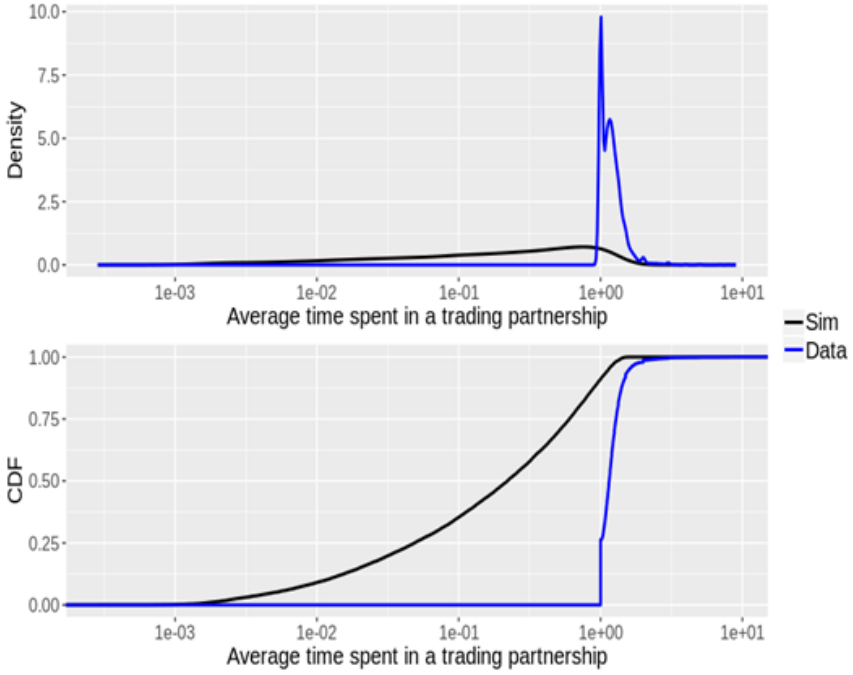

(b)

Figure 2.16: Simulation output and data for the distribution (a), and density and empirical cumulative distribution (b) of the average partnership duration of farms under original functional forms for the partnership formation and cessation rates.

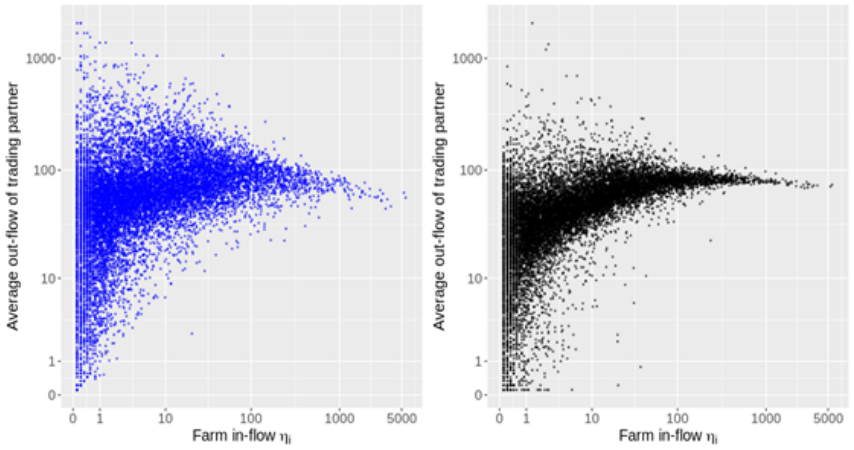

(a)

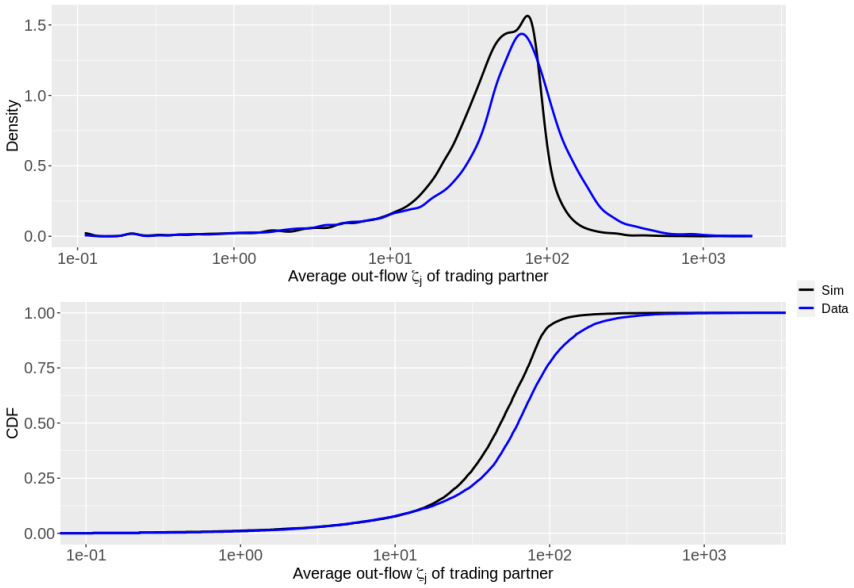

(b)

Figure 2.17: Simulation output and data for the distribution (a), and density and empirical cumulative distribution (b) of the average out-flow of farms' trading partners under modified functional forms for the partnership formation and cessation rates.

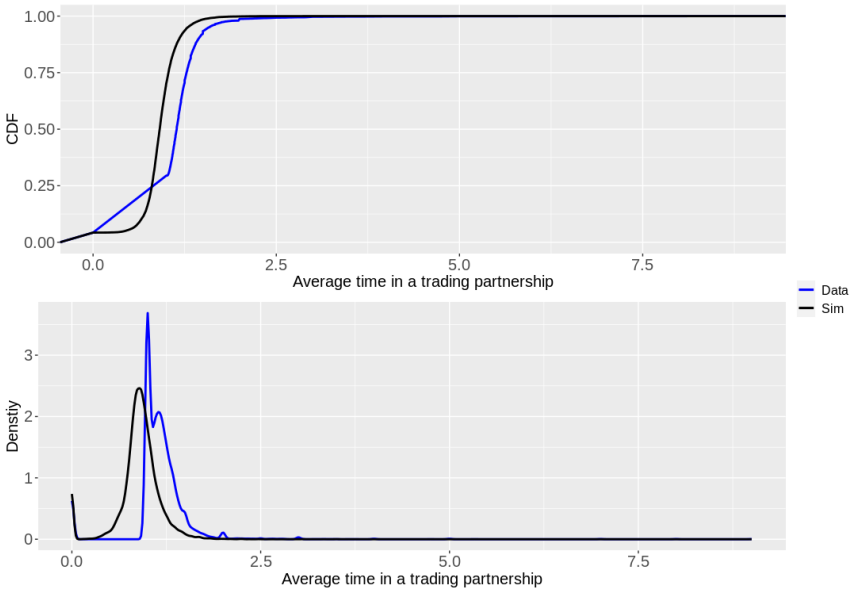

(a)

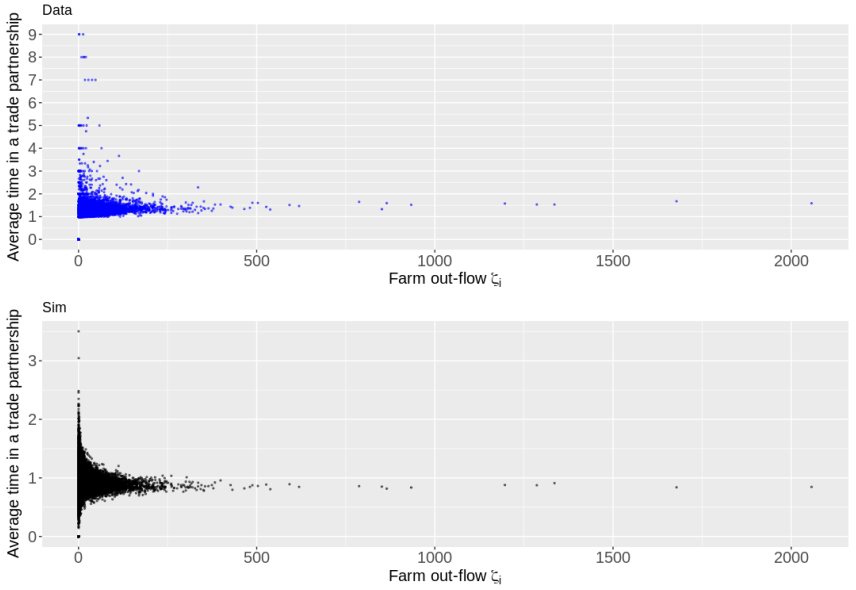

(b)

Figure 2.18: Simulation output and data for the distribution (a), and density and empirical cumulative distribution (b) of the average partnership duration of farms under modified functional forms for the partnership formation and cessation rates.

2.6.14 Values of R_0 for varying trade patterns

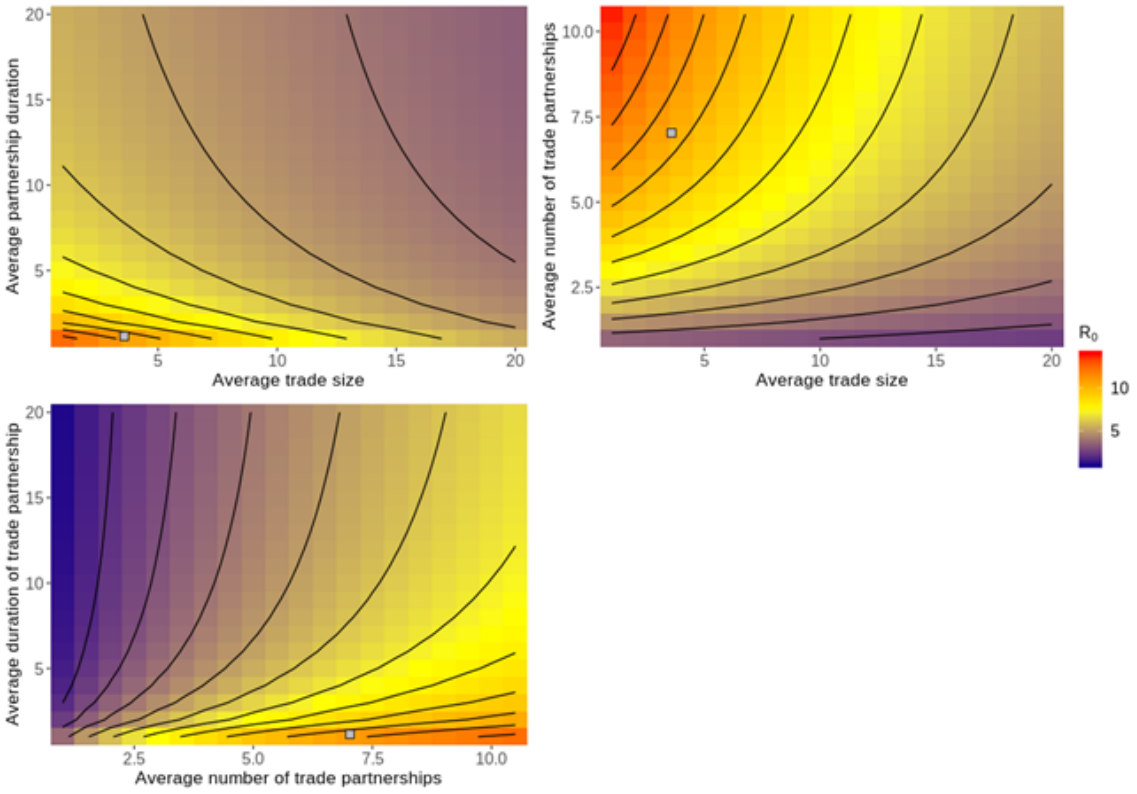

Figure 2.19: System average R_0 for varying values of average batch size, average partnership duration, and average number of concurrent trading partners. We consider changes to batch size and partnership duration (top left), batch size and number of concurrent trading partnerships (top right), and number of concurrent trading partnerships and partnership duration (bottom left). Grey squares represent the current trading patterns of the Scottish trade system. In all cases we set $\lambda = \gamma = 0.2$.

2.6.15 Values of R_0 for varying disease parameterisations

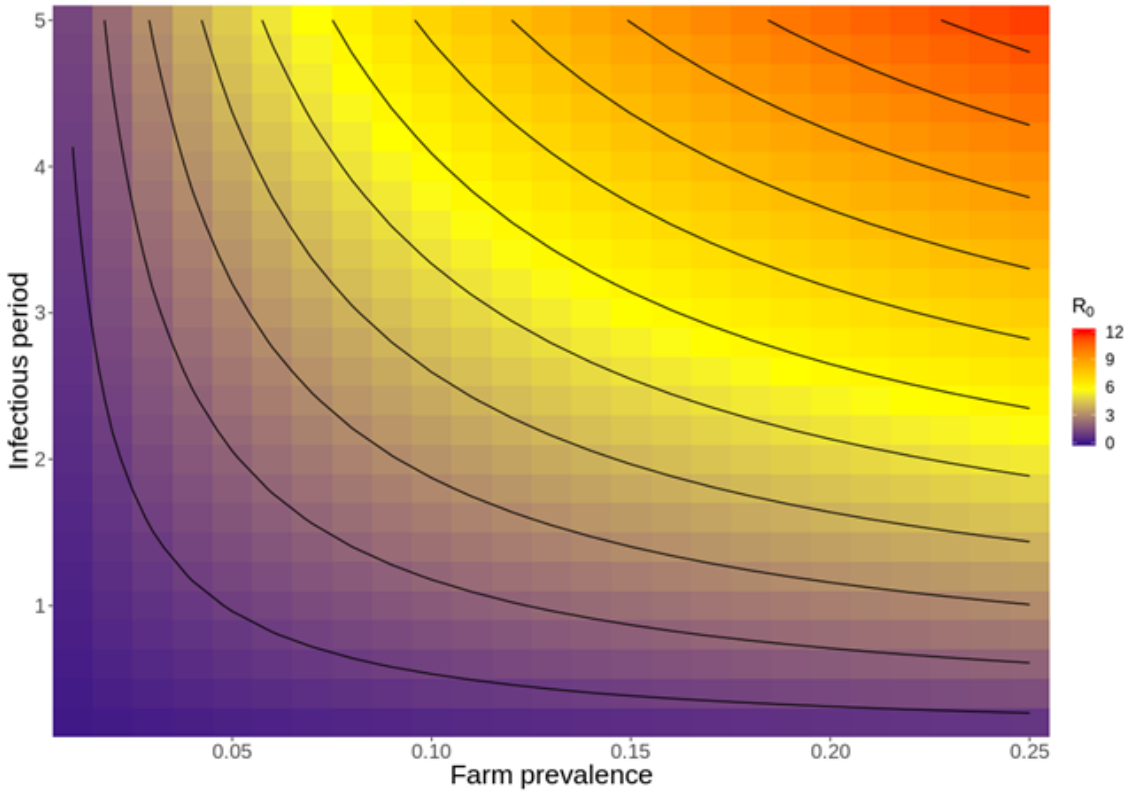

Figure 2.20: The predicted system average R_0 for a range of disease parameterisations under current observed trading patterns in the Scottish trade system.

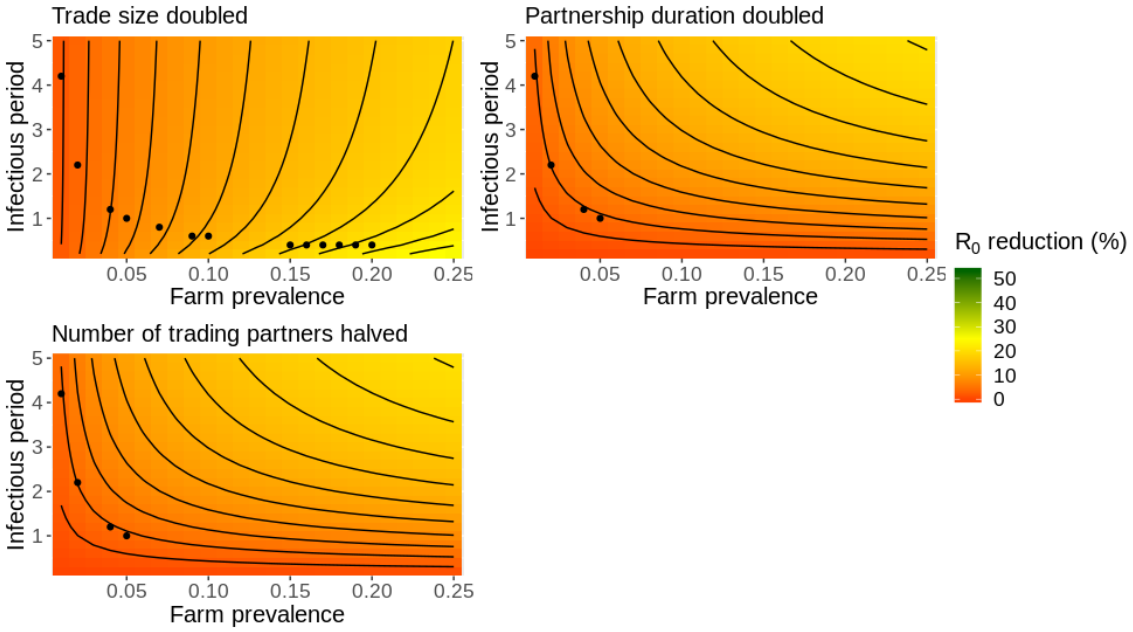

Figure 2.21: Percentage reduction in system average R_0 for singular changes to trade over a range of disease parameterisations. Changes considered are doubling the batch size, with an accompanying halving of the number of trades (top left), doubling the duration of trade partnerships (top right), and halving the number of concurrent trading partners (bottom left). Changes to the batch size are most effecitve for diseases characterised by high prevalence and short infectious periods, whereas changes to the duration and number of trading partnerships are most effective for diseases with high prevalence and long infectious periods.

Chapter 3

A stochastic, adaptive systems view of livestock trading

3.1 Introduction

In Chapter 2, we introduced a generative trade model that accounts for the stochastic formation and cessation of trade partnerships and the movement of animals that such partnerships permitted. The rates determining the formation and cessation of trade partnerships, α_{ij} and δ_i, and the rate of trade, φ_{ij}, were defined, respectively, as:

$$\alpha_{ij} = \frac{a_i}{N}\left(\eta_i \zeta_j^m + w\right), \tag{3.1}$$

$$\delta_i = \frac{d_i}{\eta_i}, \tag{3.2}$$

$$\varphi_{ij} = b_i \cdot \min(\eta_i, \zeta_j), \tag{3.3}$$

where η_i and ζ_j are the unit-time in- and out-flow of farms i and j, respectively, N is the system size, a_i, d_i, and b_i are rates defining the propensity for farm i to form and end partnerships, and trade, respectively, and m and w are constants. These rates are functions of static farm-level quantities, namely annual in- and out-flows of animals, and are thus invariant to changes and/or perturbations of the trading

system. However, trading patterns are generally not static, with seasonal trends clearly evident in the UK cattle trade system with the majority of animal movements occurring in springtime, corresponding to periods in which the majority of calves are born [46, 113]. Moreover, while farmer behaviour generally evolves with cultural changes, they can also be affected and disrupted by external pressures, including disease outbreaks, extreme weather events, and farm relocation [56]. In a network context, seasonal trading patterns are examples of "burstiness"; events occur in concentrated bursts, followed by a period of low activity [11]. The implications of bursty activity on disease spread has been studied previously, though its effect can be beneficial or deterimental to disease control based on correlations between the topological structure of the network and the frequency and timing of contacts [34].

The surges of trades in springtime represent periods in which supply and demand, or stock levels, are at their greatest and the drop in movements following the spring months suggests a level of satiation of demand. Our trading model outlined in Chapter 2 does not account for farm satiation; indeed, a farm is as likely to trade immediately following a previous trade as that farm is during a long inter-trade period. We therefore extend our model to account for farm-level time-varying stock quantities, measuring current farm-level supply and demand, which determine the rates at which farms form trading partnerships, make trades, and the size of trade batches. Our resulting model extends previous work in the literature which included similar time-varying stock quantities, however we go beyond the current state of the art by 1) explicitly accounting for trade partnerships, and 2) accounting for stock quantities in the rates of partnership formation and trade [58, 87].

In this chapter, we introduce an individual-based dynamic trading model in which time-varying farm-level stock quantities, defined as supply and demand, determine the rates at which farms form new trading partnerships and trade with current trade partners. We will explore the dynamics of this highly dynamic and adaptive system, initially in the absence of disease, and consider the response of individual farms in changes to trading propensities (such as increased trade friction) and how these individual-based responses alter the trading dynamics at the system level.

Moreover, we will analyse the sensitivity of the system to shocks in farm-level supply and demand. When disease is introduced, we will show that farm-level responses to changes in trading propensities alter the structure of the trading system in ways such that disease prevalence is largely unaltered, except in certain extreme cases. We introduce typical disease control strategies, such as on-movement animal testing, and evaluate the impact of animal and batch rejection on farms' ability to maintain their business needs, and also how such control strategies affect between-herd disease prevalence. Farm- and system-level information propagation, mediated through on-movement animal testing, indicating "high-risk" farms will be introduced, and the impact of farms' avoidance of high-risk farms on the trading system and disease prevalence will be explored. Our results will highlight the potential benefits of a global risk aversion strategy on significantly reducing disease prevalence.

3.2 An individual-based systems model of trade dynamics

3.2.1 Mechanisms of stock generation and a global pricing strategy

We assume a closed system of N farms in which farm i's propensity to form trading partnerships and make trades are determined by time-varying stock quantities, $\mathcal{D}_i(t)$ and $\mathcal{S}_i(t)$, which represent, respectively, the number of animals farm i wishes to purchase and has available to sell at time t. A full outline of model quantities and parameters is presented in Table 3.1. We herein use the terms *demand* and *supply* to refer to $\mathcal{D}_i(t)$ and $\mathcal{S}_i(t)$. The global supply and demand is thus defined as

$$D(t) = \sum_{i=1}^{N} \mathcal{D}_i(t), \tag{3.4}$$

$$S(t) = \sum_{i=1}^{N} \mathcal{S}_i(t). \tag{3.5}$$

Global stock levels determine a system-wide price of goods at a given time t, $P(t)$. We adopt the pricing model of [87] and assume that the rate of change of the logarithm of the price is proportional to the rate of change of the *net willingness to trade*, defined as $D(t) - S(t)$, i.e.

$$\frac{d}{dt}P(t) = \sigma P(t)\frac{d}{dt}\left(D(t) - S(t)\right), \tag{3.6}$$

$$\Rightarrow P(t) = P_0 \cdot \exp(\sigma(D(t) - S(t) - (D_0 - S_0)), \tag{3.7}$$

where P_0, D_0, and S_0 are, respectively, the price, global demand, and global supply at $t = 0$. The constant σ represents the price sensitivity of goods to the difference in global supply and demand. We assume that the system begins in a state with no stock, so that $D_0 = S_0 = 0$, meaning $P_0 = P^*$ can be interpreted as a steady-state price when supply and demand are balanced. Thus we have

$$P(t) = P^* e^{\sigma(D(t) - S(t))}. \tag{3.8}$$

Note that the price is determined not by absolute values of global stock quantities, rather by relative imbalances between supply and demand. The functional form for $P(t)$ is desirable as it does not permit negative prices, and replicates macroeconomic properties, namely that excess demand causes prices to increase, excess supply causes prices to decrease, and balanced supply and demand causes the price to equilibriate. Collectively, these form the so-called *law of supply and demand* [79].

Farms generate units of stock with a linear, per-farm, rate of $\eta_i(t)$ for demanded stock and $\zeta_i(t)$ for supply stock. This simple rate is intended to represent the fact that farms will accumulate supply and demand over time if no trades occur. The functional forms of $\eta_i(t)$ and $\zeta_i(t)$ are assumed to be

Quantity	**Definition**
N	Number of farms in the system
$\mathcal{D}_i(t)$	Demanded stock of farm i at time t
$\mathcal{S}_i(t)$	Available supply of farm i at time t
$D(t)$	Global demanded stock at time t
$S(t)$	Global available supply at time t
$P(t)$	Price of goods at time t
P^*	Price of goods when global stocks are equal
$\eta_i(t)$	Rate at which farm i generates new demand at time t
η_i^*	Rate at which farm i generate demand at price equilibrium
ε_D	Elasticity of demand. Measure of how demand generation changes due to changes in price
$\zeta_i(t)$	Rate at which farm i increases its available supply at time t
ζ_i^*	Rate at which farm i increases available supply at price equilibrium
ε_S	Elasticity of supply. Measure of how supply generation changes due to changes in price
$\alpha_{ij}(t)$	Rate at which i forms a trading partnership with j at time t
δ_i	Rate at which i ends a trading partnership
$\varphi_{ij}(t)$	Rate at which i trades with its trading partner j at time t
$\theta_{ij}(t)$	Size of trade following a trade between i and j at time t

Table 3.1: Table of quantities and parameters in the model

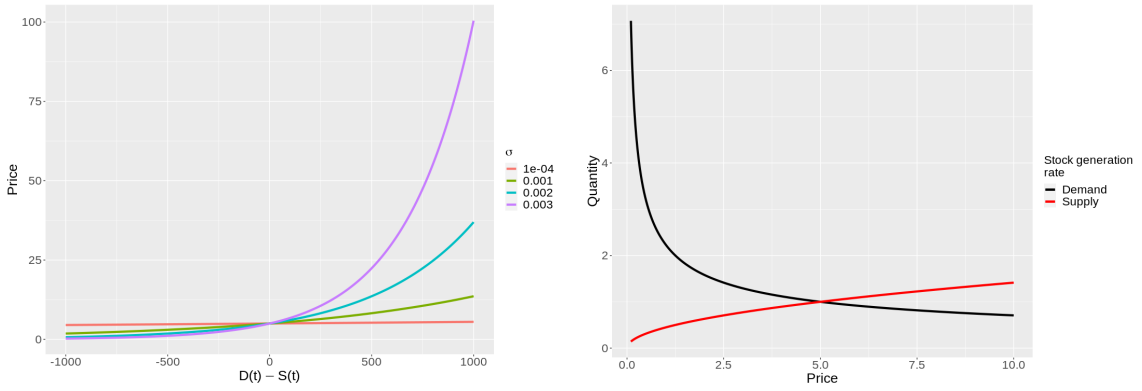

(a) (b)

Figure 3.1: **Sensitivity of price to stock imbalances** Price sensitivity to imbalances in global demand and supply (a) and stock generation rates for varying prices (b). In both cases we set $P^* = 5$, $\varepsilon_D = \varepsilon_S = 0.5$, and $\eta_i^* = \zeta_i^* = 1$. Each trajectory is obtained deterministically from Eqs. (3.8), (3.9), and (3.10)

.

$$\eta_i(t) = \eta_i^* \left(\frac{P(t)}{P^*} \right)^{-\varepsilon_D}, \tag{3.9}$$

$$\zeta_i(t) = \zeta_i^* \left(\frac{P(t)}{P^*} \right)^{\varepsilon_S}, \tag{3.10}$$

which are functionally similar to those used in [87], however we exclude stock losses, external flows, and explicit characterisation of farms as either strict buyers or sellers. The constants η_i^* and ζ_i^* represent stock generation rates at market equilibrium, i.e. when global stock levels are balanced and $P(t) = P^*$. We saw in Chapter 2 that these are readily determined from data on between-farm movements averaged over a suitable period. The constants ε_D and ε_S are, respectively, the price elasticities of demand and supply. Their values determine how sensitive stock generation is to perturbations of the price around the equilibrium price, and, for simplicity, we have assumed they are constant across farms.

Figure 3.1a shows the sensitivity of price to imbalances in demand and supply for varying values of the constant σ. As expected, a surplus in demand relative to supply yields exponential increases in price, particularly for larger values of the price sensitivitiy σ. Conversely, a surplus of supply causes the price to decrease,

approaching 0 as this surplus increases. We therefore have

$$\lim_{D(t)-S(t)\to\infty} P(t) = \infty,$$

$$\lim_{D(t)-S(t)\to-\infty} P(t) = 0,$$

$$\lim_{D(t)-S(t)\to 0} P(t) = P^*.$$

Figure 3.1b highlights the relationship between the stock generation rates and price as presented by Eqs. (3.9) and (3.10). Increases in price decrease the demand generation rate $\eta_i(t)$ and increases the supply generation rate $\zeta_i(t)$, whereas decreases in price increase $\eta_i(t)$ and decrease $\zeta_i(t)$. Thus farms generate more demand (and less supply) when prices are low, and less demand (and more supply) when prices are high. There is a feedback loop between the price of goods and stock levels: excess demand leads to increases in price, which cause the demand generation rate, $\eta_i(t)$, to decrease and the supply generation rate, $\zeta_i(t)$, to increase. This, in turn, causes the net willingness to trade, $D(t) - S(t)$, to decrease and thus the price to return to the equilibrium price P^*. As the price returns to the equilibrium price, the stock generation rates return to their equilibrium values. Therefore, the inclusion of a pricing model can act as a corrective mechanism in the model to prevent stock level divergences. Finally, we note that changes in price do not alter *current* supply and demand, altering only future generation of stock.

3.2.2 The dynamics of trade partnerships

The presence of trade partnerships explicitly distinct from trade events was a key extension to existing models in the model presented in Chapter 2. This innovation enabled representation of a dynamic network of trade partnerships on which trades occurred, also dynamically. This was a step forward compared with the static trade partnership networks with dynamic trades of earlier studies. However, the rates determining the dynamics of partnerships were constant, and unaffected by recent trade activity of farms. We extend these rates here by expressing them as functions of the farm-level stock quantities, so that the rate of partnership formation becomes:

$$\alpha_{ij}(t) = \frac{a_i}{N}\mathcal{D}_i(t)\mathcal{S}_j(t)^m. \tag{3.11}$$

We note here that further analysis of the length of partnership durations in the Scottish trading system revealed that farm in-flow is not a strongly determining factor in the duration of trade partnerships (correlation between farm-in flow and trade partnership duration length is $R^2 = 0.057$, $p << 0.01$). As such, and for simplicity, we herein keep the partnership cessation rate, δ_i for a given farm i, constant.

Eq. (3.11) describes how model farms' propensities for forming new trading partnerships are dictated by current stock levels, rather than average, long-term properties of farms as in Chapter 2, and new trade partners are chosen based on their current available supply stock. As demand now varies in the model, so does the partnership formation rate; periods of high demand will cause a surge of partnership formations, followed by the gradual removal of partnerships as demand is satisfied by trade so that new partnerships are formed less frequently. As in Chapter 2, we include the constant $m = 0.75$ to represent that farms' decision making process in the formation of trade partnerships is not influenced entirely by stock levels (though we do not explore such behaviour here) [56]. Our expression for $\alpha_{ij}(t)$ may lead to less discriminatory choices in trade partners as farms with small long-term supply rates are not precluded from having large instantaneous supply levels. We posit, however, that small ζ farms will have, on average, low supply so that the distribution of "sizes" (measured by farm out-flows ζ) of farms' trading partners will be similar to Figure 2.1 in Chapter 2.

3.2.3 The dynamics of trade

As with the partnership formation rate, we extend the rate of trade from Chapter 2 to be a function of current demand of a farm i and current supply of its trading partner j:

$$\varphi_{ij}(t) = b_i \cdot \min(\mathcal{D}_i(t), \mathcal{S}_j(t)), \tag{3.12}$$

where the constant b_i is intended to represent any impediment to efficient trade [87]. The trade rate presented in Chapter 2 was a function of the expected long-term average in- and out-flows of animals of a buying farm and its trading partner, and was intended to represent that large out-flow farms will generally have larger supply. As with Eq. (3.11), the key difference is that the rate at which farms purchase animals is driven entirely by current requirements for stock, rather than long-term trading trends. For a farm i, the min function in Eq. (3.12) allocates the highest trade rate to a trade partner j that can match or exceed i's demand. In other words

$$\varphi_{ij}(t) = b_i\mathcal{D}_i(t) \text{ if } \mathcal{D}_i(t) < \mathcal{S}_j(t), \tag{3.13}$$

$$\varphi_{ij}(t) = b_i\mathcal{D}_i(t) = b_i\mathcal{S}_j(t) \text{ if } \mathcal{D}_i(t) = \mathcal{S}_j(t), \tag{3.14}$$

$$\varphi_{ij}(t) = b_i\mathcal{S}_j(t) \text{ if } \mathcal{D}_i(t) > \mathcal{S}_j(t). \tag{3.15}$$

Thus, purchasing patterns of farms are driven by dynamical state variables, namely supply and demand. We neglect, therefore, more abstract and hard to quantify variables that are likely present in real-world trading systems, e.g. farmer reputation, details of the stock type that may make it more suitable, perceptions of disease risk, etc. The exploration of such behaviour is an avenue for future work and we consider some simple behavioural-trade feedback loops in the context of disease later in this chapter.

Trades initiate a batch movement of animals, the size of which is also determined by current demand $\mathcal{D}_i(t)$ of the purchasing farm and current supply $\mathcal{S}_j(t)$ of the selling farm:

$$\theta_{ij}(t) = \min(\mathcal{D}_i(t), \mathcal{S}_j(t)). \tag{3.16}$$

At most, farms will purchase enough animals to satisfy their demand at a given time, and sellers operate on a first come, first served basis, i.e. sellers will offload their entire supply in a single trade if demanded. Farms, therefore, buy and sell based on current market pressures, excluding any forecasting, allocation of stock, future agreements to sell, etc. Analysis in [58] found that Eq. (3.16) resulted in simulation output most closely resembling data, suggesting that farms do indeed purchase and sell animals in the most fluid way possible.

Interpreting Eq. (3.16) is straightforward: supply and demand are indivisible quantities in our model, representing animals available for sale and number of animals a farm wants to buy, respectively. As such, batches can take minimum size 1, i.e. a single animal moved. The maximum size, however, is determined by current stock quantities of the buying and selling farm, which can lead to excess demand and supply following a batch movement. Therefore, transactions are *imperfect* [87] in the sense that batch movements may not fully satisfy the buyer. Excess stock from a trade is carried over and influences future trades.

Finally, the cumulative in-flow of animals for a typical farm i at time t is given by

$$V_i^{in}(0,t) = \int_0^t \sum_{j \in k_i^{in}(\tau)}^{N} p_{ij}(\tau)\varphi_{ij}(\tau)\theta_{ij}(\tau)d\tau, \tag{3.17}$$

where $p_{ij}(t)$ is the probability that farm j is a seller to i, i.e. a trade partner, and $k_i^{in}(t)$ is the number of trade partners of farm i at time t. Eq. (3.17) accumulates the history of trade for farm i up to time t, however, unfortunately, is not analytically tractable as the functional forms of $\varphi_{ij}(t)$ and $\theta_{ij}(t)$ contain discontinuities and are themselves functions of $\mathcal{D}_i(t)$ and $\mathcal{S}_j(t)$ which cannot be expressed in closed-form.

To conclude, our model represents a free market, where agents (farms) buy and sell animals at a given price level, outside the influence of regulatory and governmental control. Nonetheless it is possible to add such externalities into future analyses based on modifications of the model presented here. It is possible that our model may be described as a *perfectly competitive* market, which must satisfy two conditions: 1)

goods are homogeneous, i.e. all the same, and 2) that there are sufficient numbers of buyers and sellers that no single individual can influence or dominate the market [79]. The first point is a simplifying assumption of our model (though is not a necessity; we could distinguish animals into type (beef and dairy, for example), or indeed quality). The second point is dependent on the trading system being analysed, and influenced by system size and the distributions of trading patterns of farms.

3.3 The adaptive system dynamics of trade

In this section we explore the behaviour of our trading model in the absence of disease dynamics for a simple, homogeneous system in which farms generate supply and demand with equal rates and have similar propensities to form and end trading partnerships, and to trade animals. In all cases we assume $N = 200$, $\eta_i^* = \zeta_i^* = 2.0$, $P^* = 1$, $a_i = 0.2$, $\delta_i = 1.0$, and $b = 2.0$ for all farms i. The price elasticities are set to $\varepsilon_D = 0.412$ and $\varepsilon_S = 0.821$ and are taken from the FAPRI-UK economic model documentation 2011 [36]. Stochastic simulations are performed using a standard Gillespie Stochastic Simulation Algorithm [47, 48].

3.3.1 Exclusion of a pricing model can lead to divergent stock levels

In Section 3.2.1 we highlighted that the presence of a pricing model introduces a feedback loop between imbalances in global supply and demand and the stock generation rates. Referring to Figures 3.2 and 3.3, variation in the price sensitivity parameter σ alters the sensitivity of the stock generation rates in response to changes in price, and the price itself is more sensitive to imbalances in global supply and demand for greater values of σ. The dynamic pricing model is effective at constraining stock levels so that stock imbalances are minimised, even for very small values of σ. The exception is the case when $\sigma = 0$, which is equivalent to the absence of a pricing model entirely. In this case, stock generation rates are equal to their equilibrium value at all times, and stochasticity of the simulation can lead to scenarios in which

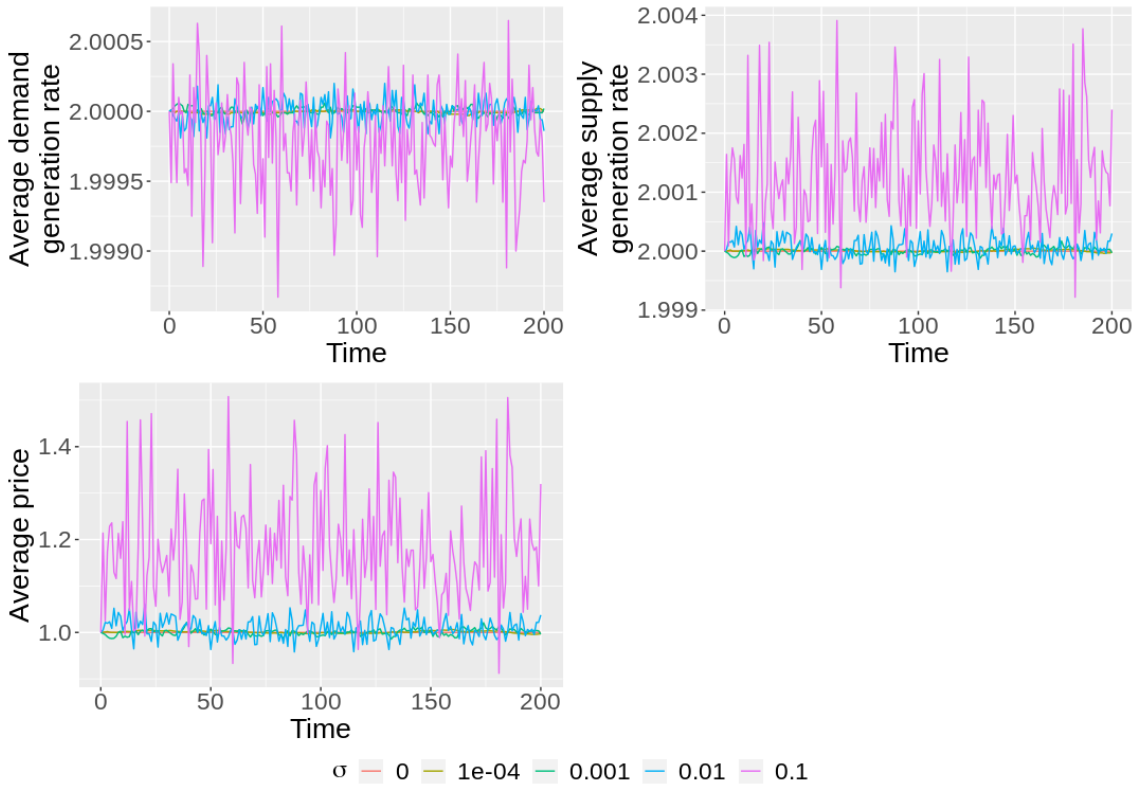

Figure 3.2: **Price sensitivity on stock generation** Average stock generation rates and average price over time for varying values of the price sensitivity parameter σ. The special case $\sigma = 0$ represents the absence of a pricing model. For each parameter value, output is generated by averaging 20 independent realisations of the stochastic simulation.

stock levels become imbalanced. Furthermore, in the absence of a pricing model, such imbalances are not corrected for by changes in the stock generation rates, leading to cascading imbalances and divergences in stock quantities. We note that in the output presented in Figure 3.3, a divergence in demand is evident, however divergences in supply are also possible (see Figure 3.4).

3.3.2 Shocks in stock quantities

We now explore the ability for the modelled trading system to adapt itself to shocks in global stock quantities when starting from equilibrium. We consider first shocks in global demand, namely the introduction of a fixed increase in demand for each farm at a specified point in time. Considering Figure 3.5, we see that shocks in demand cause rapid increases in excess demand and therefore price. However, these

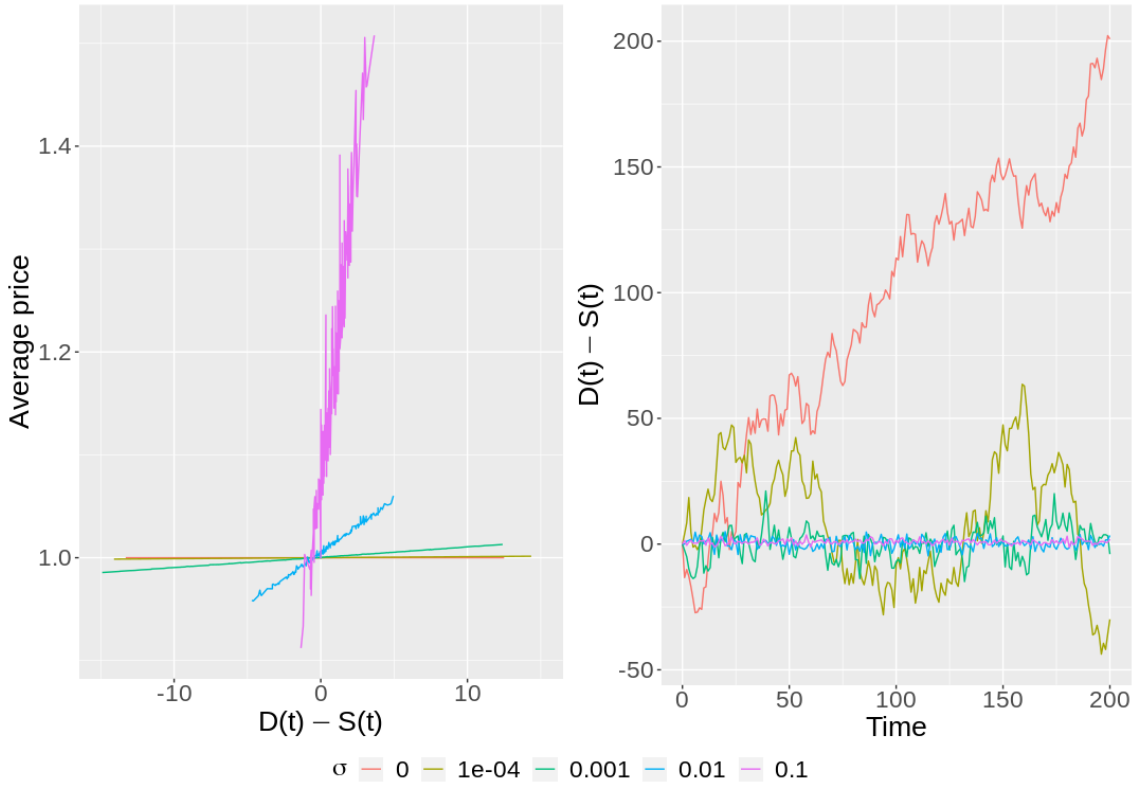

Figure 3.3: **Price sensitivity on supply and demand stability** Average price against excess demand (left) and excess demand over time (right) for varying values of the price sensitivity parameter σ. The special case $\sigma = 0$ represents the absence of a pricing model, i.e. no fluctuations in price caused by excess demand. For each parameter value, output is generated by averaging 20 independent realisations of the stochastic simulation.

spikes are temporary and the system rapidly adjusts by appropriate reductions in the demand generation rate $\eta(t)$ and increases in the supply generation rate $\zeta(t)$ so that excess demand and price return to pre-shock equilibrium values. Of note is the inability for the stock generation rates to return to pre-shock values, instead finding a new stable equilibrium (with larger shocks causing greater shifts away from pre-shock equilibria). Referring to Figure 3.6, shocks in demand bring about surges in the formation of new trade partnerships and trades as farms seek to satisfy their new demand. This leads to reductions in available supply, hence the increase in $\zeta(t)$. The surges in trade are temporary, quickly returning to pre-shock values, however average stock quantities do not return to pre-shock values, instead finding a new, slightly larger, equilibrium (this new equilibrium is approximately 25% larger for the largest demand shock).

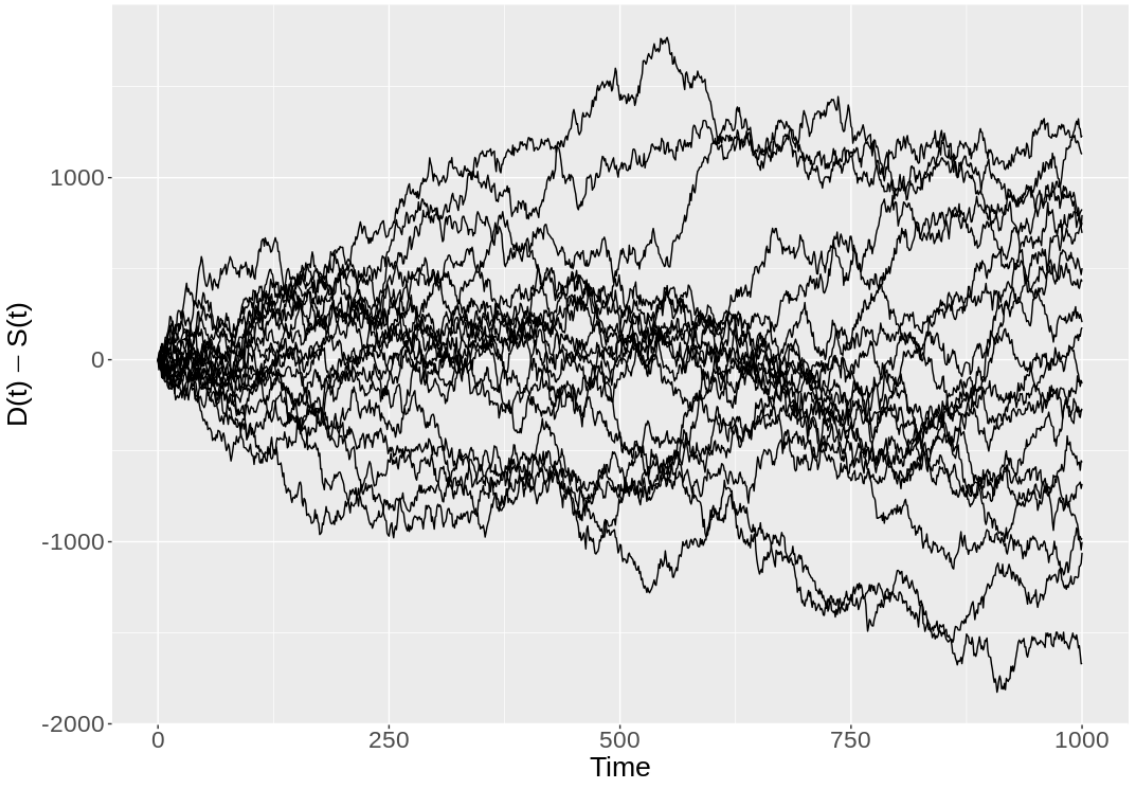

Figure 3.4: **Stock imbalances in the absence of price** Global excess demand for a number of independent stochastic simulations when a pricing model is absent ($\sigma = 0$).

Considering similar shocks to supply, Figures 3.7 and 3.8 show that the system response in terms of excess demand and price is similar, though mirrored compared to demand shocks, when the system exhibits supply shocks. The stock generation rates attain new equilibrium values in response to supply shocks, with farms generating more demand and less supply on average in the immediate aftermath than in pre-shock times. Interestingly, however, supply and demand levels do not deviate from pre-shock equilibrium values after the initial surge in trade following supply shocks, suggesting our trading system is more sensitive to shocks in demand than in supply. This may be explained by differences in our chosen supply and demand elasticities, as the supply generation rate $\zeta(t)$ is more elastic (sensitive to changes in price [79]) than is the demand generation rate $\eta(t)$. Moreover, the model itself responds differently to shocks in demand than supply because the partnership formation rate increases and decreases linearly with increasing and decreasing demand and fixed supply, and increases and decreases nonlinearly with increasing and decreasing supply and fixed

demand.

Finally, we explore the system response to complete removal of all stock, i.e. $\mathcal{D}_i(t) = \mathcal{S}_i(t) = 0$ for all farms i. Our stochastic simulations begin in a disconnected state, i.e. there are no trade partnerships, and farms have no stock quantities. As the simulation progresses, farms generate stock and begin to form partnerships until the system reaches an equilibrium where farms can match with appropriate sellers to satisfy their demand. In this shock scenario, we are investigating how the system in equilibrium responds to a sudden loss of all supply and demand. Considering Figures 3.9 and 3.10, we notice that removal of farm stocks has no discernible effect on the price of goods. This is to be expected, as the price is affected by imbalances in stock quantities rather than the individual availability of stock. As a result, stock generation rates are also unaffected by global stock removals. The removal of stock causes short-term out of equilibrium trade patterns, however the system rapidly returns to the pre-shock equilibrium as farms begin to re-accumulate stock. There is also negligible difference in the time taken for the system to return to the pre-shock equilibrium compared with the time taken to reach equilibrium beginning from the initial, disconnected state. We note that removal of all supply and demand is not equivalent to the real-world removal of all animals in the system, which would be catastrophic and prevent farms (in the short term, at least) to generate new supply.

3.3.3 Effects of trade and partnership friction on system dynamics

In this section we explore the impacts of *friction* on the rate of trade and partnership formation as given by Eqs (3.12) and (3.11), respectively. In economics, friction represents any impediment to efficient trade, for example distance, matching buyers and suppliers, and delivery times [27]. Friction is transposed onto our model in a similar manner as in [58, 87], but with a key difference; we treat the formation of trade partnerships as distinct from trade events. As such, the constant a_i in Eq (3.11) represents the frictional component to finding trade partners, and the constant b_i in Eq (3.12) represents the frictional component of all impediments to

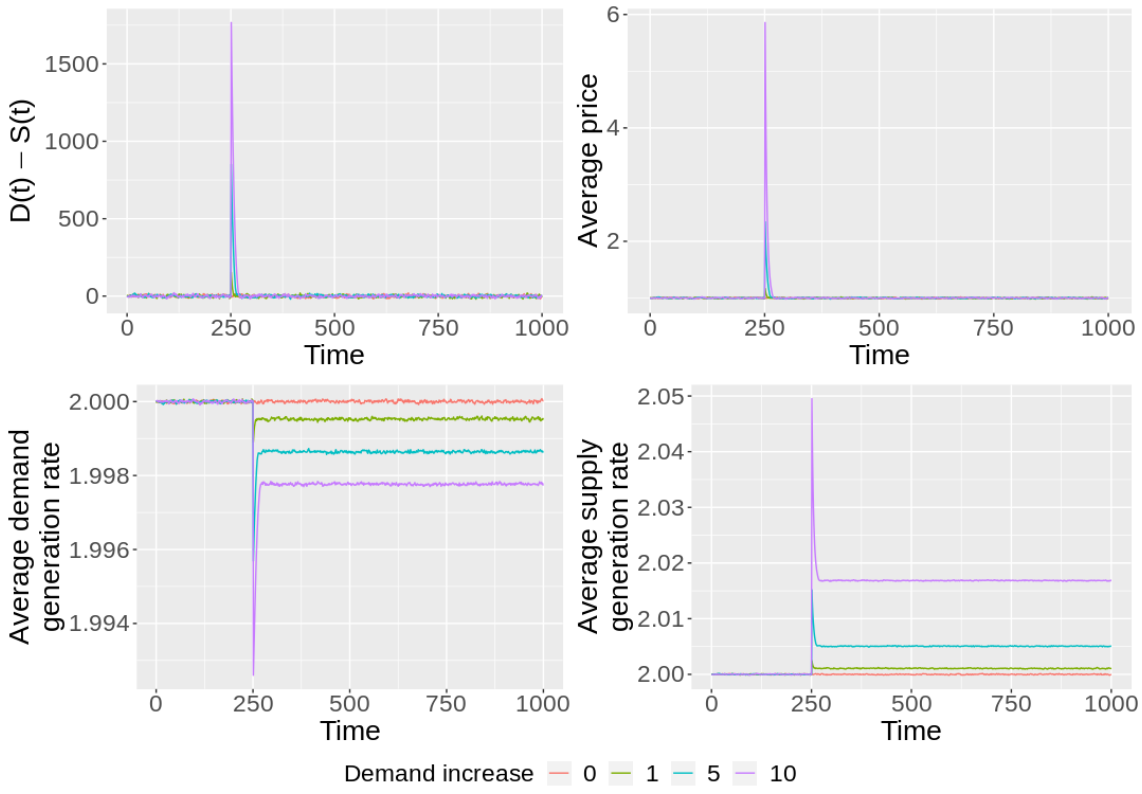

Figure 3.5: **Shocks in demand impact price and stock generation** Global excess demand (top left), average price (top right), average demand generation rate $\eta(t)$ (bottom left), and average supply generation rate $\zeta(t)$ (bottom right) for varying shocks to global demand. For a given demand shock s, for all farms i, farm-level demand is updated to $\mathcal{D}_i(t) \to \mathcal{D}_i(t) + s$. In all cases, shocks occur at $t = 250$.

trade between partners. Therefore, we can explore the role of friction in these two components of trade in isolation and together. In Chapter 2 we explored the role of friction in early-time disease spread, finding that manipulation of friction can lead to desirable reductions in R_0, but in this section we restrict our analysis solely to its impact on transient and long-term dynamics of trade.

Trade friction

We consider first changes to trade friction, via changes to the trade rate constant b, noting again that in this example system farms are homogeneous in their stock generation rates and trade and partnership rates (though farm stock levels will differ due to the stochasticity of the system and timing and sizes of trades). Increasing b decreases trade friction, so farms have a greater propensity to trade, whereas de-

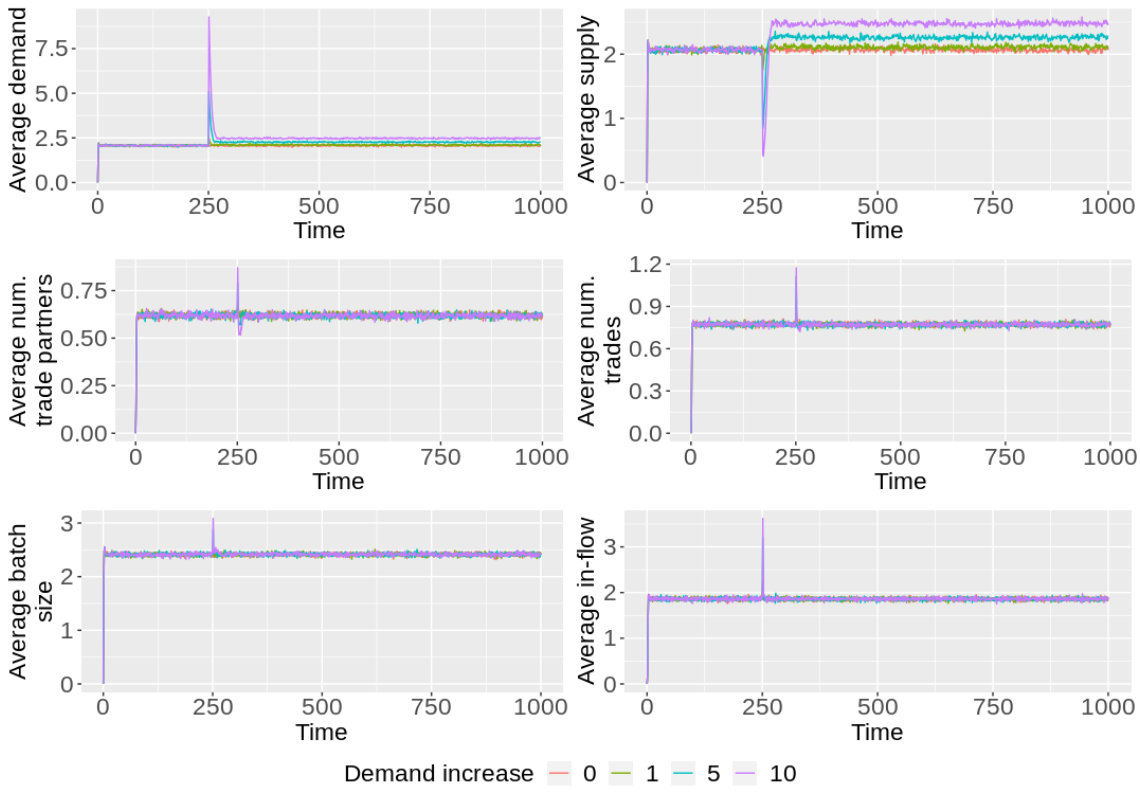

Figure 3.6: **Shocks in demand and response of trading system** Average per-farm demand (top left) and supply (top right), number of trading partners (middle left), number of trades (middle right), batch size (bottom left), and per unit-time animal in-flow (bottom right) for varying shocks to global demand. For a given demand shock s, for all farms i, farm-level demand is updated to $\mathcal{D}_i(t) \to \mathcal{D}_i(t) + s$. In all cases, shocks occur at $t = 250$.

creasing b increases trade friction and farms trade less frequently. For the model described in Chapter 2, and in the trading models presented in [58, 87], any change in the friction of trade is linearly reflected in the frequency of trade, e.g. a 50% reduction in b corresponds to 50% fewer trades, as conditional on b, the rates describing the frequency of trade are constant and are functions of farms' average long-term in- and out-flows. For the model described here, however, the rate of trade is a dynamic function, varying with farm stock levels. As such, a given change in b may not necessarily result in a correspondingly large change in the frequency of trade. Indeed, Figure 3.12 reveals that this is the case, and by considering $b = 1$ as a baseline, increasing b (less friction) does increase the frequency of trade, but not linearly. For example, setting $b = 100$ (2 orders of magnitude greater than $b = 1$) increases the number of trades per farm by approximately 55.68% (from an average of 0.67

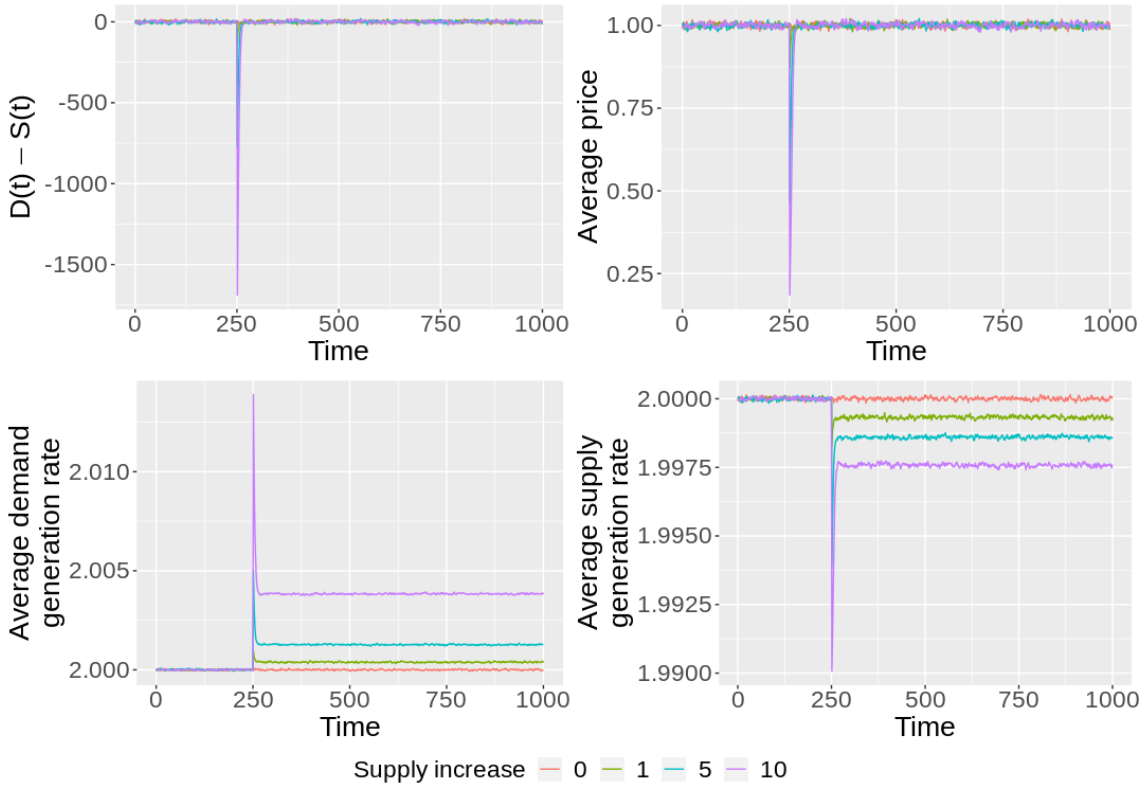

Figure 3.7: **Shocks in supply impact price and stock generation** Global excess demand (top left), average price (top right), average demand generation rate $\eta(t)$ (bottom left), and average supply generation rate $\zeta(t)$ (bottom right) for varying shocks to global supply. For a given supply shock s, for all farms i, farm-level supply is updated to $\mathcal{S}_i(t) \to \mathcal{S}_i(t) + s$. In all cases, shocks occur at $t = 250$.

trades when $b = 1$ to 1.05 when $b = 100$). This is due to the effect on stock levels as b is changed. For large b (low friction), farms begin by accumulating stock and forming trade partnerships. However, as friction is low, farms trade with their trade partners at high frequency leading to smaller batch sizes and lower levels of unmet demand and available supply. These depleted stock levels feed back into the rates of partnership formation and trade, so that farms require fewer trade partners, and the effect of increasing b on the trade rate is thus counteracted by smaller stock levels. The converse if true for reductions in b, as for small b there is greater friction in trade resulting in farms accumulating more stock before a trade occurs, resulting in large batches of animals. However, larger unmet demand and available supply leads to farms forming a greater number of trade partnerships in an attempt to satisfy their demand. When $b = 1$, average per-farm demand and supply is approximately

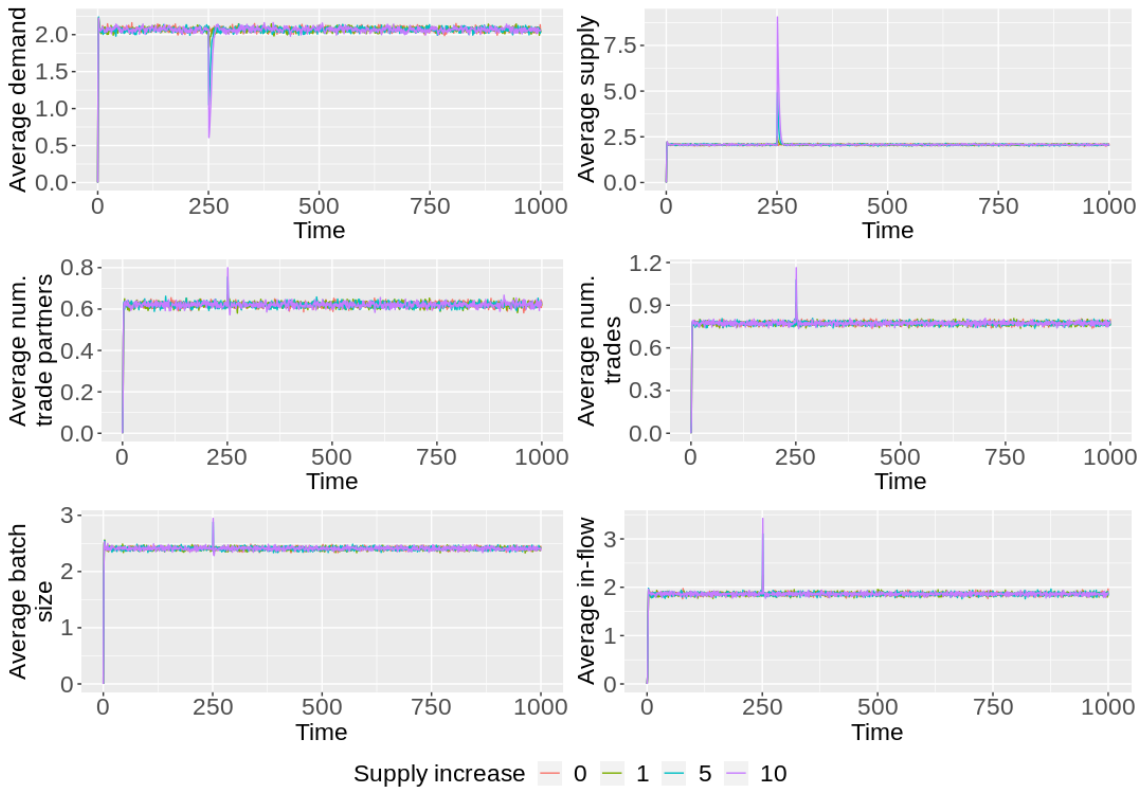

Figure 3.8: **Shocks in supply and response of trading system** Average per-farm demand (top left) and supply (top right), number of trading partners (middle left), number of trades (middle right), batch size (bottom left), and per unit-time animal in-flow (bottom right) for varying shocks to global supply. For a given supply shock s, for all farms i, farm-level supply is updated to $\mathcal{S}_i(t) \to \mathcal{S}_i(t) + s$. In all cases, shocks occur at $t = 250$.

2.26, when $b = 100$ the average is 1.74 (a reduction of 22.78%), and when $b = 0.01$ the average is 6.15 (an increase of 171.66%), hence the effect of friction on farms' ability to satisfy their demand is not symmetric, with a disproportionately larger impact when friction is high ($b = 0.01$) compared with when friction is low ($b = 100$). We note, however, that in all cases the system reaches an equilibrium, and farms maintain the same level of animal in-flow, though the time to reach equilibrium is greater when friction is high. Also, excess demand, price, and stock generation rates are largely unaffected by changes in trade friction.

Friction in partnership formation

We next consider changes to friction in the formation of trade partnerships by altering the formation rate constant a. Small values of a correspond to large amounts

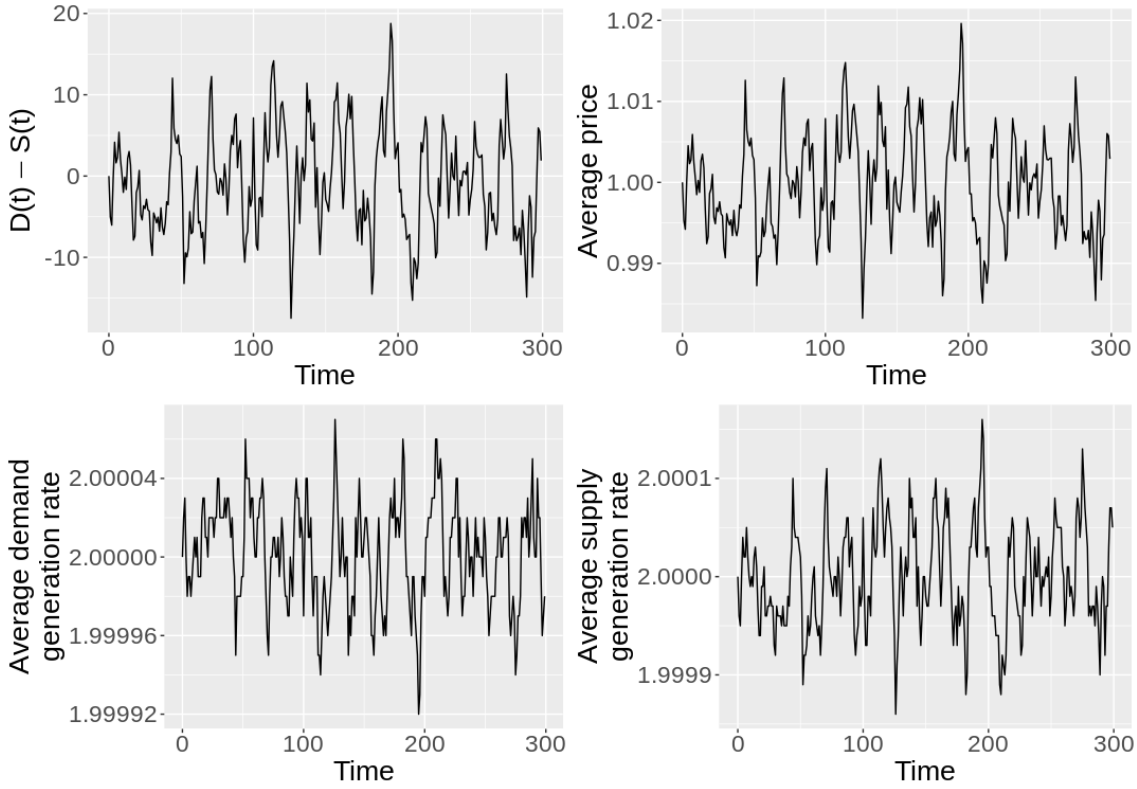

Figure 3.9: **Removal of all stock does not alter price and stock generation** Global excess demand (top left), average price (top right), average demand generation rate $\eta(t)$ (bottom left), and average supply generation rate $\zeta(t)$ (bottom right) when global supply and demand are removed. In all cases, shocks occur at $t = 250$.

of friction in forming trade partnerships, and large values of a correspond to small amounts of friction. To our knowledge, we are the first to consider friction in partnership formation, with current generative cattle trade models not distinguishing partnership dynamics with trade events [58, 87]. As with trade friction, changes to friction of partnership formation in the model of Chapter 2 resulted in corresponding changes in the number of trade partnerships. However as with changes to trade friction, Figure 3.13 shows that the responses to changes in a are nonlinear in the more complex model. Again using $a = 1$ as a baseline, setting $a = 100$ increases the equilibrium per-farm average number of trading partners from 1.12 to 7.07 (an increase of 528.98%). A correspondingly large reduction in a, setting $a = 0.01$, decreases the number of trading partners to 0.22 (a reduction of 80.02%). In terms of stock levels, setting $a = 100$ reduces average per-farm supply and demand to 0.29 from 1.18 (a

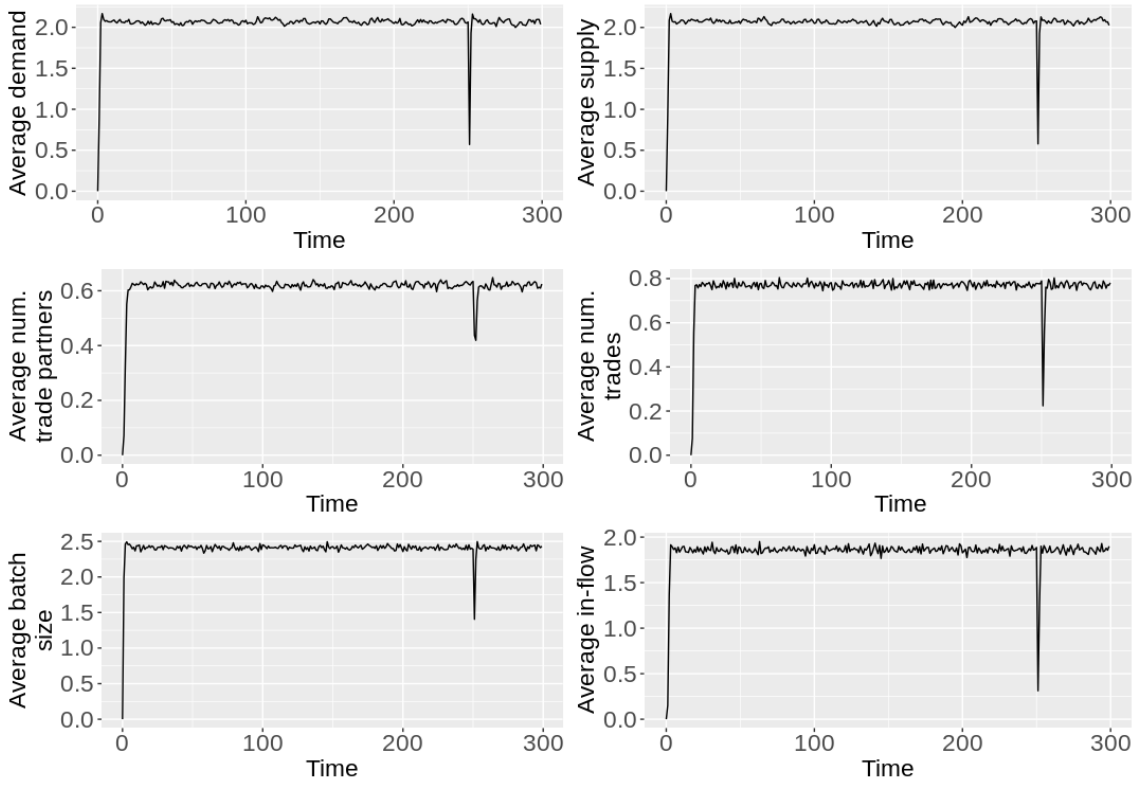

Figure 3.10: **Removal of all stock and response of trading system** Average per-farm demand (top left) and supply (top right), number of trading partners (middle left), number of trades (middle right), batch size (bottom left), and per unit-time animal in-flow (bottom right) when global supply and demand are removed. In all cases, shocks occur at $t = 250$.

reduction of 75.34%), whereas setting $a = 0.01$ increases these to 6.27 (an increase of 429.29%). Small values of a (large friction) result in farms having few trade partners at any given time, so that there are fewer farms from whom to purchase animals to satisfy demand. As such, average stock levels increase and animal batches during a trade increase. Conversely, large values of a (low friction) cause farms to form more partnerships, giving a greater number of farms from whom to purchase animals, so average stock levels decrease and batch sizes are small. As with changes to trade friction, greater friction in partnership formation (small a) increases the time for the system to reach equilibrium, however in all cases farms are able to maintain their required in-flow of animals.

Duration of trade partnerships

Finally, we consider changes to the propensity for farms to end trade partnerships, i.e. changes to the partnership cessation rate δ. Small values of δ result in longer lasting partnerships, and small values result in short duration partnerships. Considering Figure 3.14, small δ (long duration partnerships) result in a greater number of trading partners, more frequent trading (with smaller batches), and smaller levels of per-farm unmet demand and available supply. On the other hand, large δ values (short duration partnerships) result in very few trade partnerships and trades, larger batch sizes when trades do occur, and farms have, in general, larger unmet demand and available supply. It is impressive, however, that even in the case where $\delta = 100$, i.e. partnerships typically last 0.01 units of time, when farms have very few trade partners, the system is still able to adapt and reach a stable equilibrium, with farms maintaining their desired in-flow of animals. Of note is the transient dynamics of stock quantities and batch sizes for small δ, where stock levels initially increase, begin to level off, and then decrease to reach a stable equilibrium. The reason for this is that at these small δ values, the timescales of trade and partnership cessations are vastly different, with trade occurring more frequently than the removal of trade partners. This allows farms to more readily purchase animals from trade partners before the partnership ends, depleting supply levels and satisfying demand, causing the decrease in stock levels and approach to a stable equilibrium.

3.4 Disease control and trade in a complex adaptive system

In this section we extend our trading model to account for disease spread via trades. Previously in this chapter, we showed how alterations to the propensity for farms to form and end partnerships, and make trades do not necessarily result in predictable alterations to respective trade quantities, e.g. a reduction in the trade rate constant b_i does not yield a commensurate reduction in the number of trades. This was due to the resulting impact on stock quantities, increasing pressure for farms to

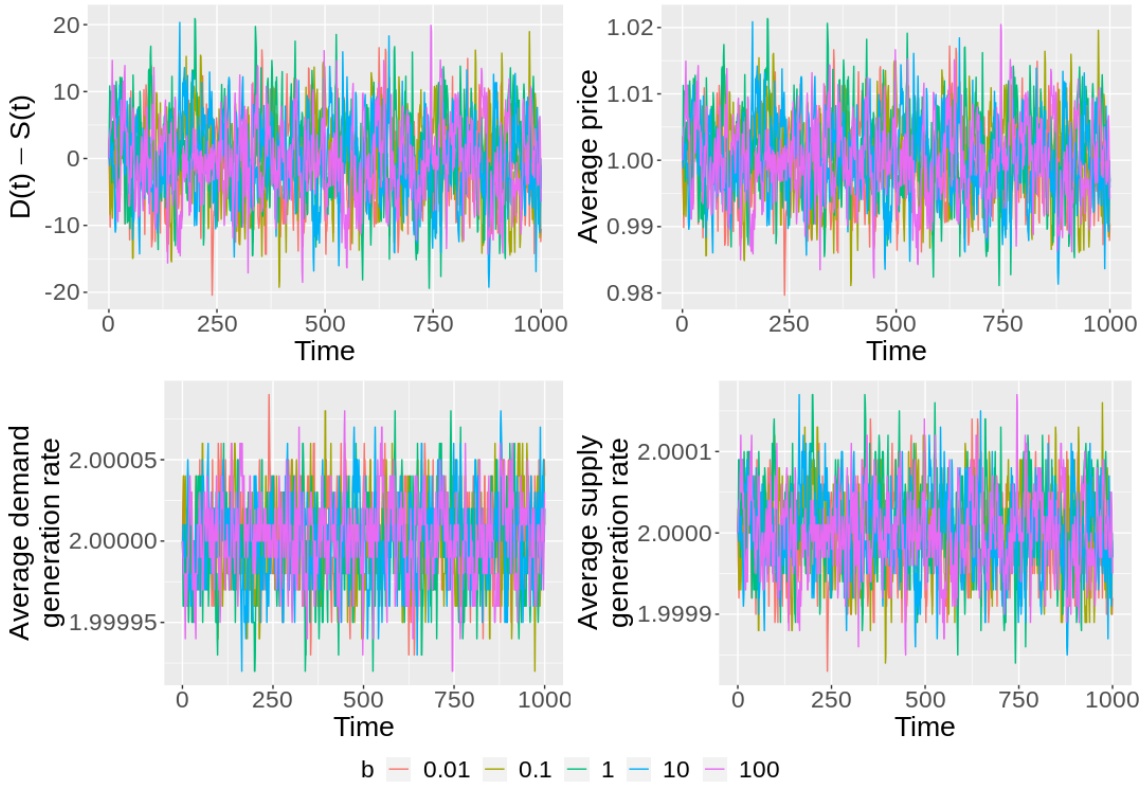

Figure 3.11: **Impact of trade friction on price and stock generation** Global excess demand (top left), average price (top right), average demand generation rate $\eta(t)$ (bottom left), and average supply generation rate $\zeta(t)$ (bottom right) for varying values of the trade rate constant b, representing varying levels of trade friction.

form partnerships and continue trading. Alterations to friction changed the trading structure of the system so that farms minimised their demand and maintain their in-flows of animals. Such effects on network structure in relation to cattle trade have not previously been explored, and the resulting implications for disease spread may contradict previous results highlighting the effect of restrictions and changes to network structure on disease spread [43, 85, 87].

We extend our trading model to include disease transmission in a similar manner as in Chapter 2. The dynamics of disease are coupled with partnership dynamics and trade by assuming disease is driven entirely by animal movements, neglecting indirect transmission such as from external wildlife sources. Disease status is categorised at farm level using a standard susceptible-infected-susceptible (SIS) model; susceptible farms become infected through trade with infected farms, and can themselves infect

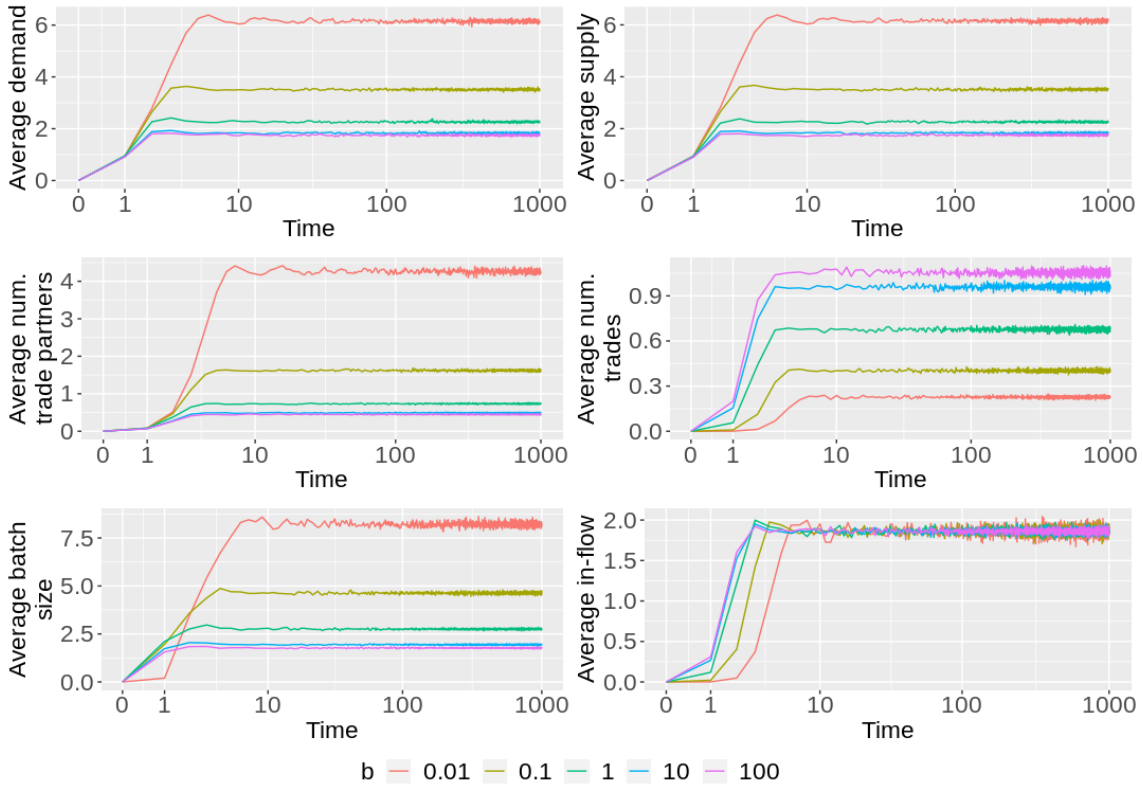

Figure 3.12: **Impact of trade friction on trading system equilibria** Average per-farm demand (top left) and supply (top right), number of trading partners (middle left), number of trades (middle right), batch size (bottom left), and per unit-time animal in-flow (bottom right) for varying values of the trade rate constant b, representing varying levels of trade friction.

others, and, after an exponentially distributed infectious period $1/\gamma$, recover to become susceptible once again [8]. In addition to the infectious period, a given disease is also characterised by an effective on-farm prevalence level λ, assumed constant across infected farms and time. We therefore take λ to be the average prevalence of an infected farm over its infectious lifetime. We assume each animal moved off an infected farm i has a constant probability λ of infecting the susceptible buying farm and that off-farm movements do not alter herd prevalence on the selling farm [106]. Our disease model differs from the one presented in Chapter 2 in one key element: batch sizes are not constant and thus the probability of infection varies over time and with farm-level stock quantities. If an infected farm j sells $\theta_{ij}(t)$ animals to a susceptible farm i at time t, the probability that that trade results in infection is $B(\theta_{ij}(t)) = 1 - (1 - \lambda)^{\theta_{ij}(t)}$, and the rate at which i receives infection

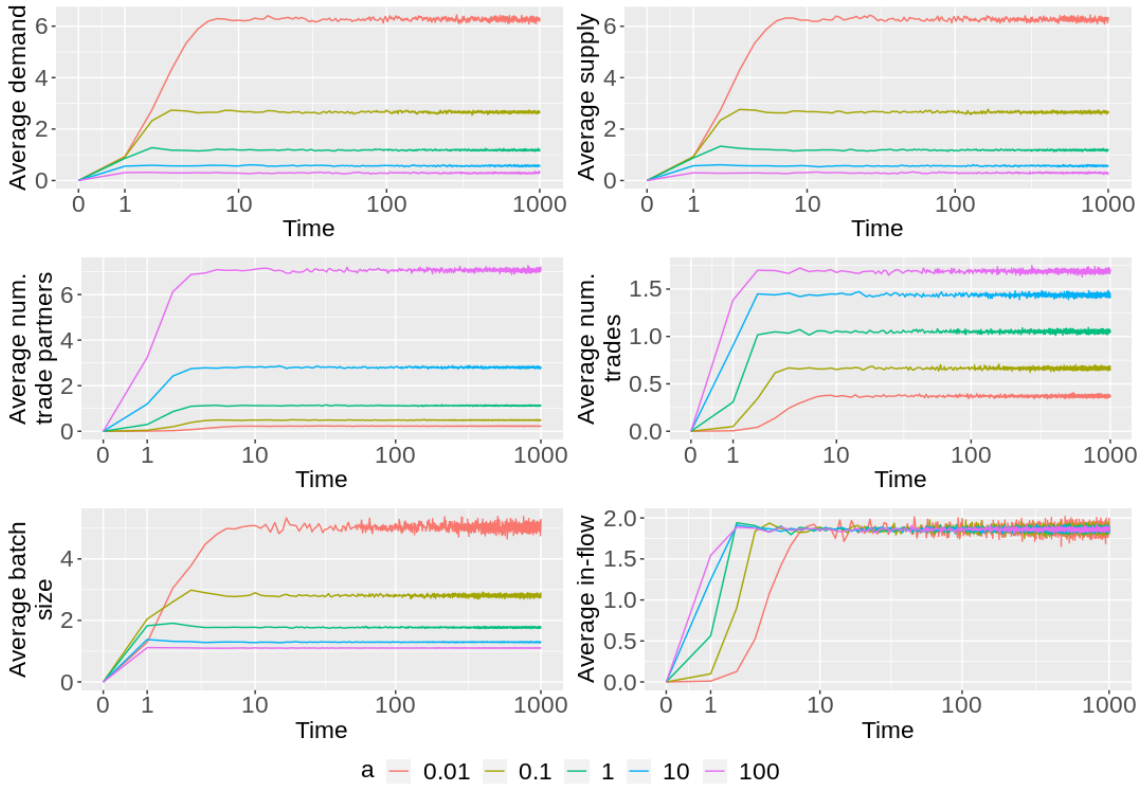

Figure 3.13: **Impact of partnership formation friction on trading system equilibria** Average per-farm demand (top left) and supply (top right), number of trading partners (middle left), number of trades (middle right), batch size (bottom left), and per unit-time animal in-flow (bottom right) for varying values of the partnership formation rate constant a, representing varying levels of friction in the formation of trade partnerships.

from j is $\beta_{ji}(t) = \varphi_{ij}B(\theta_{ij}(t))$, i.e. the rate at which i trades with j multiplied by the probability that the trade results in the transmission of disease. Thus, trading dynamics, and hence disease risks, change with the accumulation of stock and the satiation of demand.

Having explored the generic behaviour of adaptive trade dynamics in our individual-based systems model, we now explore a case study based on a simple representation of a real-world trading system. We simulate disease spread on our trading system for a network of $N = 200$ homogeneous farms (all farms share equal values for a, b, δ, η^*, and ζ^*), and parameterise the system so that equilibrium per-farm averages for number of trade partners, trades, batch size, and animal in-flow match those for the Scottish trading system. Average values for these trading quantities are presented

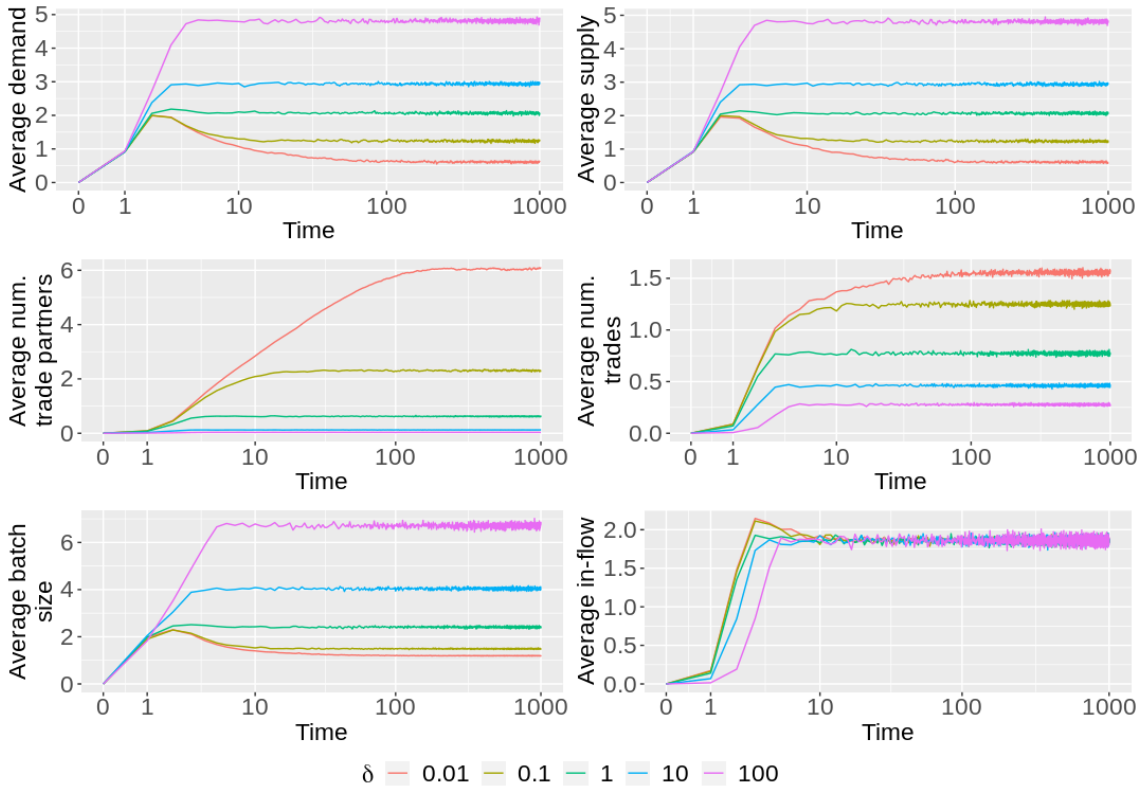

Figure 3.14: **Impact of partnership durations on trading system equilibria** Average per-farm demand (top left) and supply (top right), number of trading partners (middle left), number of trades (middle right), batch size (bottom left), and per unit-time animal in-flow (bottom right) for varying values of the partnership cessation rate δ, representing varying levels of propensities for farms to end trading partnerships.

in Table 3.2. In all scenarios presented below, we assume an initial burn-in period for the trading system to reach equilibrium and to allow disease to be introduced and reach an equilibrium prevalence level (we note that disease is introduced only after the trading system has reached equilibrium). Putative changes to trade are implemented at $t = 50$ in all cases. Disease parameters in all scenarios are $\lambda = 0.25$ (corresponding to 25% on-farm prevalence) and $1/\gamma = 3$ (farms remain infectious for an average of 3 time units). We will refer to this as the baseline disease scenario throughout. All figures presented below are replicated in the Appendix for two further disease scenarios: 1) $\lambda = 0.05$, $\gamma = 1/3$, representing a low farm prevalence, long infectious period disease, and 2) $\lambda = 0.25$, $\gamma = 1.5$, representing a high farm prevalence, short infectious period disease. In all three disease scenarios, trading patterns using the chosen parameterisation predict high system-level prevalence, suggesting

that the trading system operates in a way that permits widespread prevalence across a range of different diseases.

Quantity	**Data average**
Trade partners	7.0
Trades	7.7
Batch size	3.58
In-flow (and out-flow)	27.1

Table 3.2: Table of system-level averages for trading quantities obtained from the Scottish trading system.

3.4.1 The effect of friction on disease spread and control

To explore the role of friction on disease spread, we use a similar strategy as in Chapter 2 by scaling the frictional components of partnership formations and trade, a and b, and the partnership cessation rate δ, by constants ε_a, ε_b, and ε_δ, i.e.

$$a \to \varepsilon_a a,$$
$$b \to \varepsilon_b b,$$
$$\delta \to \varepsilon_\delta \delta.$$

Recall from Chapter 2 that these scalings were used to alter farm-level trading propensities to desired levels.

Trade friction

Considering first alterations to trade via changes to ε_b, Figures 3.15 and 3.16 show, respectively, the impact of changes to trade friction on trade quantities and prevalence levels over time, and at equilibrium. As expected, increases in trade friction (small values of ε_b) result in significant alterations to the trade network, with farms having more trade partners, overall greater demand and available supply, and with

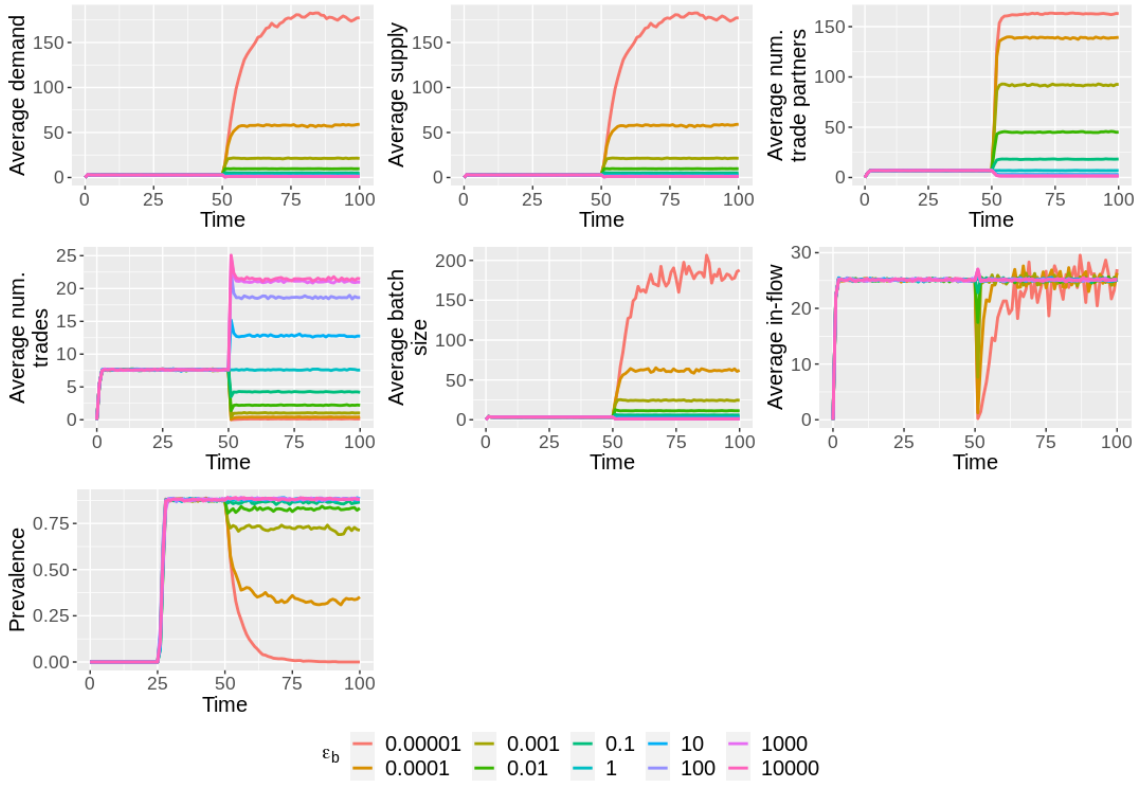

Figure 3.15: **Impact of trade friction on trade and disease prevalence** Average per-farm demand (top left) and supply (top middle), number of trading partners (top right), number of trades (middle left), batch size (middle middle), per unit-time animal in-flow (middle right), and system disease prevalence (bottom left) for varying values of ε_b, the scaling factor to the frictional component of trade, b. In all cases, disease is introduced at $t = 25$ and changes to trade at $t = 50$.

trades occurring much less frequently and with much larger size. We note, however, that for all values of ε_b considered, the system is able to adapt so that farm in-flows are maintained, though there is a transitory period in which farm flows are not maintained as the system adjusts to the alterations in the trade rate and farms search for new trade partners. The resulting network still permits stable disease persistence except in the case of very high friction when $\varepsilon_b = 10^{-5}$, as in this case trades occur infrequently enough to allow infected farms to recover before they are traded with, even though these trades are highly likely to spread disease if the source farm is infected, due to the very large batch sizes of these trades. Considering Appendix Figure 3.30 for the low farm prevalence, long infectious period scenario, we see that the impact of ε_b on disease prevalence is similar, with disease eradication possible only in the extreme cases where trades become very infrequent. However,

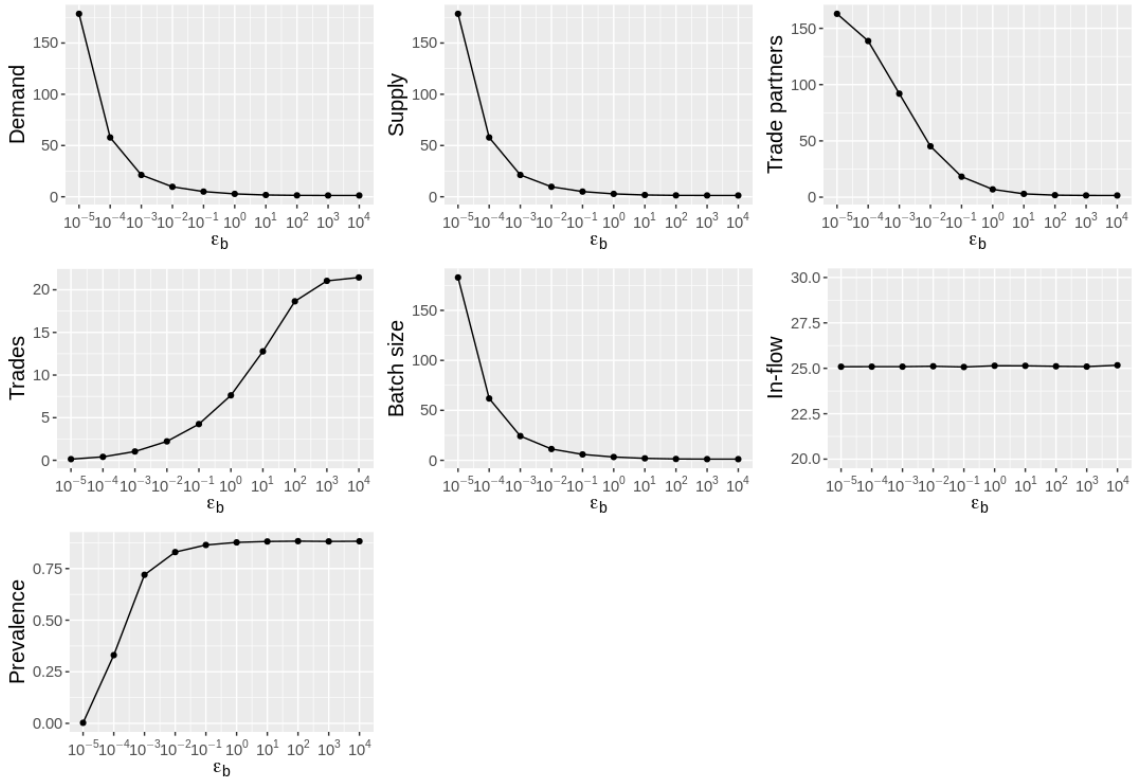

Figure 3.16: **Impact of trade friction on equilibrium values of trading system and disease prevalence** Average equilibrium per-farm demand (top left) and supply (top middle), number of trading partners (top right), number of trades (middle left), batch size (middle middle), per unit-time animal in-flow (middle right), and system disease prevalence (bottom left) for varying values of ε_b, the scaling factor to the frictional component of trade, b.

Appendix Figure 3.44 for the high farm prevalence, short infectious period scenario shows that alterations to trade via ε_b are more effective, with complete removal of disease achievable at smaller ε_b ($\varepsilon_b \leq 0.001$). As prevalence is high under the baseline trading network, this suggests that the recovery rate determines the efficacy of alterations to trading patterns, highlighting the potential for on-farm biosecurity to play a significant role in disease control.

Friction in partnership formation

Similar qualitative behaviour is observed when alterations are made to the frictional component of partnership formation via ε_a as shown in Figures 3.17 and 3.18, with disease persisting except at very small values of ε_a, which corresponds to a sparse network in which few trade partnerships are present. In those scenarios farms are

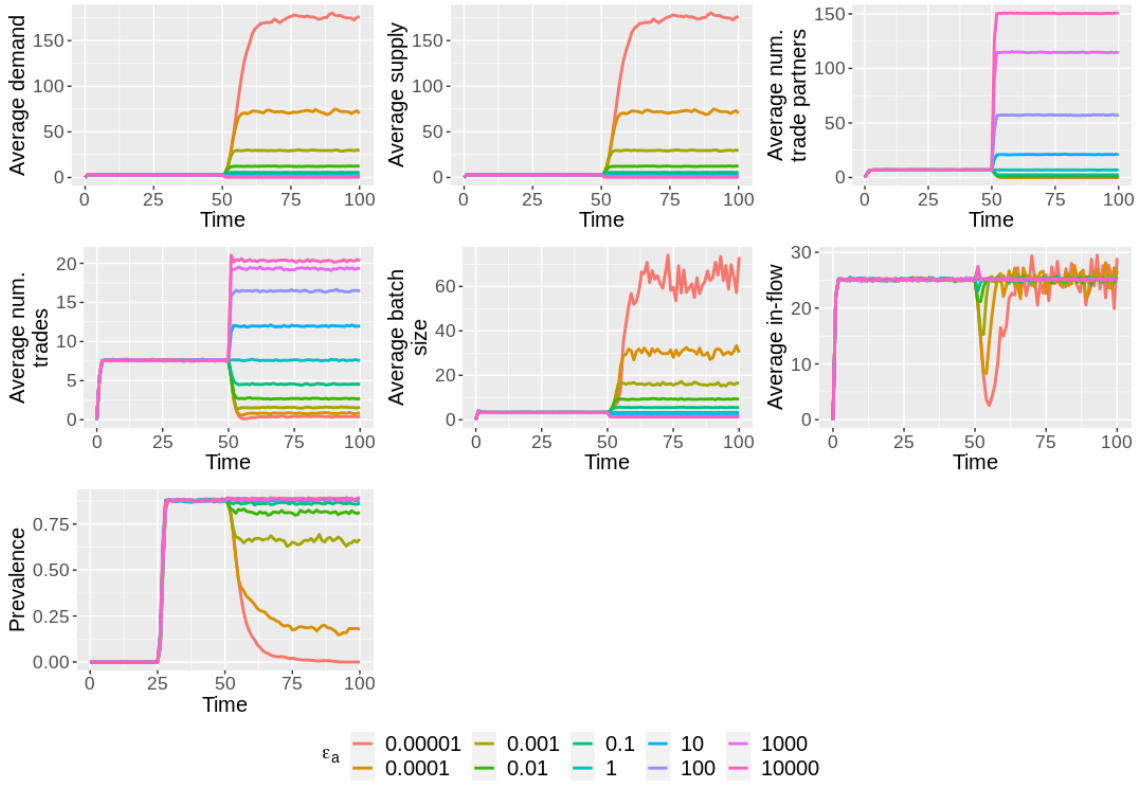

Figure 3.17: **Impact of partnership formation friction on trade and disease prevalence** Average per-farm demand (top left) and supply (top middle), number of trading partners (top right), number of trades (middle left), batch size (middle middle), per unit-time animal in-flow (middle right), and system disease prevalence (bottom left) for varying values of ε_a, the scaling factor to the frictional component of trade, a. In all cases, disease is introduced at $t = 25$ and changes to trade at $t = 50$.

characterised by similar stock quantities as was observed for small ε_b, and few trades occur but take large size. Again, however, the system adapts itself so that farm flows are maintained. Interestingly, for very large values of ε_a, disease prevalence is largely unaffected, despite the system tending towards a highly connected, highly frequent trading regime in which farms are more readily able to satisfy their demand and maintain animal flows. This is in direct contradiction of the results presented in Chapter 2, which predicted that increasing network connectivity and trade frequency would increase R_0^i, leading to greater disease persistence. This result clearly highlights the important role of accounting for farm-level stock quantities, and the nontrivial effect satiation has on mitigating the potential role of trade on disease spread. As with ε_b, the efficacy of alterations to partnership formation via ε_a is

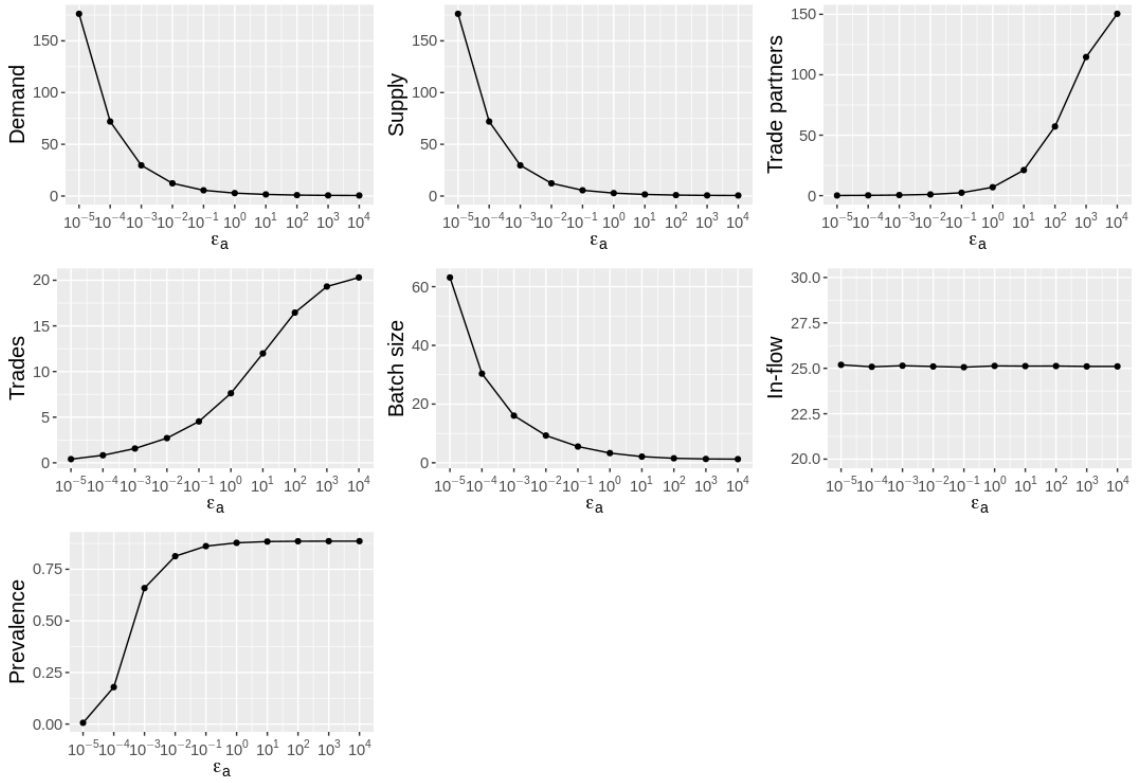

Figure 3.18: **Impact of partnership formation friction on equilibrium values of trading system and disease prevalence** Average equilibrium per-farm demand (top left) and supply (top middle), number of trading partners (top right), number of trades (middle left), batch size (middle middle), per unit-time animal in-flow (middle right), and system disease prevalence (bottom left) for varying values of ε_a, the scaling factor to the frictional component of trade, a.

determined by the disease parameters. For the low farm prevalence, long infectious period scenario, Appendix Figure 3.32 shows that disease can only be eradicated in the extreme cases when ε_a is very small. In the high farm prevalence, short infectious period, scenario, Appendix Figure 3.46 shows that, as with ε_b, disease can be eradicated at larger values of ε_a, so smaller alterations to the trading system are required to reduce disease prevalence.

Duration of trade partnerships

Finally, we consider alterations to the trade partnership duration, $1/\delta$, through changes in ε_δ. Larger values of ε_δ correspond to reductions in partnership duration, and vice versa. Referring to Figures 3.19 and 3.20, we see that encouraging longer lasting trade partnerships (small ε_δ) does not alter equilibrium prevalence signifi-

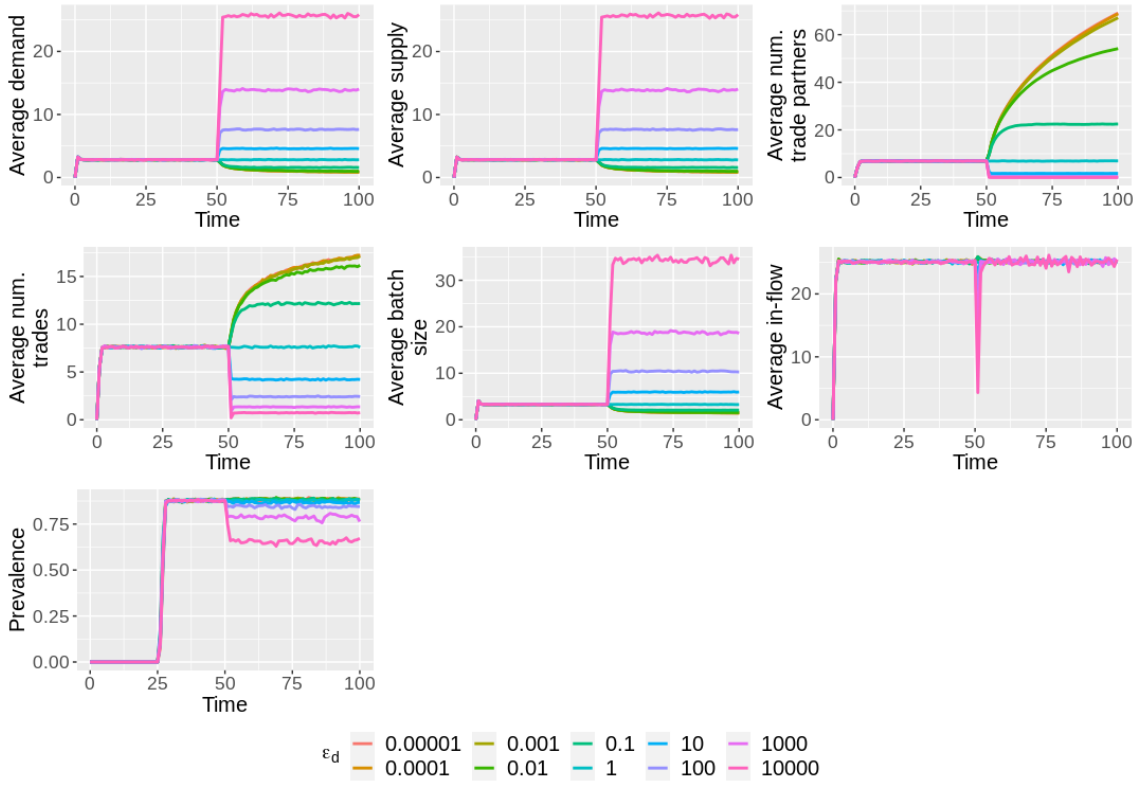

Figure 3.19: **Impact of partnership durations on trade and disease prevalence** Average per-farm demand (top left) and supply (top middle), number of trading partners (top right), number of trades (middle left), batch size (middle middle), per unit-time animal in-flow (middle right), and system disease prevalence (bottom left) for varying values of ε_δ, the scaling factor to the partnership cessation rate, δ. In all cases, disease is introduced at $t = 25$ and changes to trade at $t = 50$.

cantly, however it does lead to greater satiation of farm-level demand, due to the greater average number of trade partnerships. Our results of Chapter 2 showed that encouraging longer lasting partnerships could reduce disease persistence to non-zero levels, but not completely eradicate disease. On the other hand, significantly reducing the duration of partnerships (large ε_δ) does reduce disease prevalence but even for extreme values of ε_δ, eradication is not possible and the disease is able to persist at a lower equilibrium prevalence. Appendix Figure 3.34 shows that for the low farm prevalence, long infectious period scenario, the impact of ε_δ on disease prevalence is similar to the baseline disease scenario, and complete eradication is not possible for the values of ε_δ considered here. Indeed, only small reductions are achievable relative to the magnitude of change to the trading system. Encouragingly, in the high

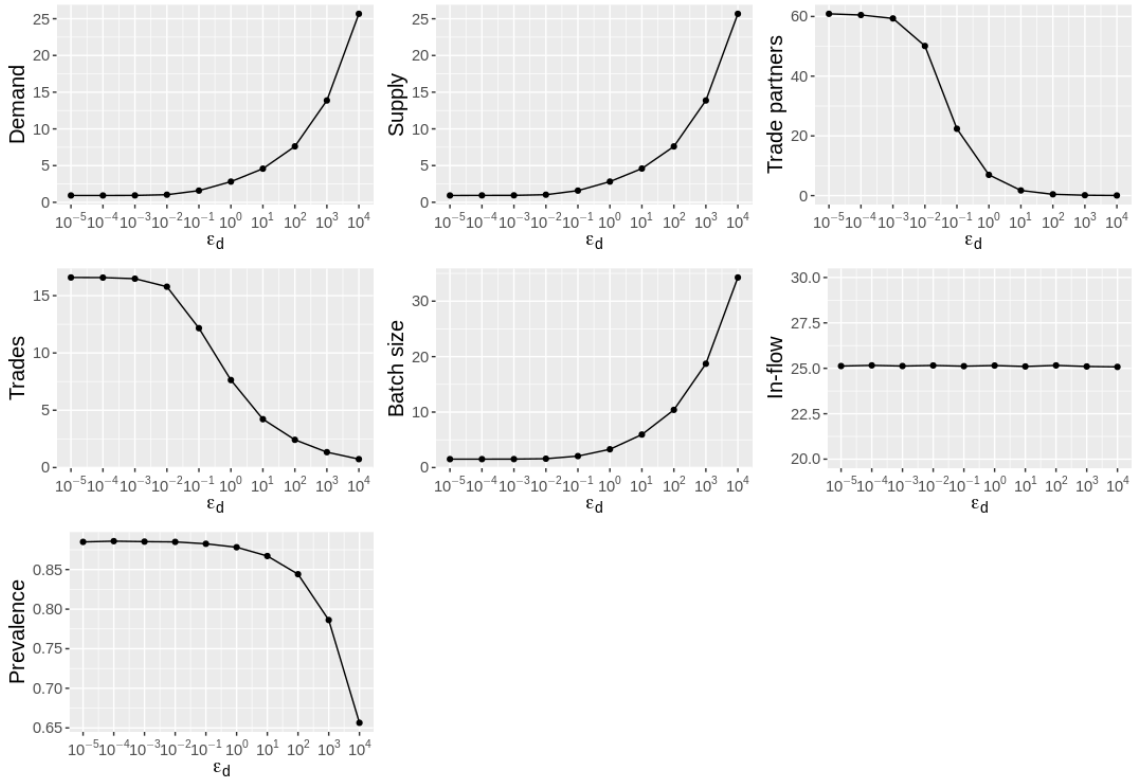

Figure 3.20: **Impact of partnership durations on equilibrium values of trading system and disease prevalence** Average equilibrium per-farm demand (top left) and supply (top middle), number of trading partners (top right), number of trades (middle left), batch size (middle middle), per unit-time animal in-flow (middle right), and system disease prevalence (bottom left) for varying values of ε_δ, the scaling factor to the partnership cessation rate, δ.

prevalence, short infectious period scenario, complete eradication of disease is possible when trade partnerships last for increasingly short durations, again highlighting that the impact of changes to trade on disease prevalence is largely determined by the infectious period, rather than the farm-level prevalence, possibly due to the baseline structure of the trading system permitting widespread between-herd prevalence even for low farm-level prevalences.

3.4.2 Movement testing: impact on trading patterns and prevalence

Animal testing and culling is a common approach to control livestock diseases [59, 73, 123], however these result in financial burdens on farms due to production losses.

In this section we explore the ability for post-movement animal testing to control and eradicate disease globally across a trading system for variable test sensitivities and under two on-movement testing regimes: 1) test-and-cull individual animals, and 2) test-and-cull whole animal batches. In contrast to existing models, a critical issue we are able to address here is the system-wide response of the trading dynamics to the impacts of such on-movement testing. That is, testing may cause long-term changes to trading patterns due to the creation of imbalances in stock levels; if a trade results in the detection of infected animals, the removal of these animals will result in different levels of depletion of supply and demand for the selling and buying farm, respectively, as the selling farm reduces its supply by the batch size of the trade, but the buying farm's demand is reduced only by the number of animals in the batch that were not rejected. For example, assume a susceptible farm i makes a trade with its infectious trade partner j. If the trade takes size θ, and the test sensitivity is τ, i.e. infected animals test positive with probability τ, then the *expected number of detected animals* in the batch is $\tau\lambda\theta$, i.e. the probability of detecting an infected animal given a herd-level prevalence of λ multiplied by the batch size. Thus for individual animal testing and rejecting, the expected number of infected animals entering the buying farm is $\lambda\theta(1-\tau)$ and the stock levels of the buying and selling farm are updated to, respectively,

$$\begin{aligned}\mathcal{D}_i(t) &\to \mathcal{D}_i(t) - \theta(1-\tau\lambda)\\ \mathcal{S}_j(t) &\to \mathcal{S}_j(t) - \theta.\end{aligned}$$

In the case of testing and rejecting the entire batch, batches can only enter the buying farm if all animals test negative, which occurs with probability $(1-\tau)^\theta$, so the expected number of infected animals to enter the buying farm is $\lambda\theta(1-\tau)^\theta$. In this scenario, the *expected update to stocks* of the buying and selling farm is

$$\begin{aligned}\mathcal{D}_i(t) &\to \mathcal{D}_i(t) - \theta\left(1-\lambda(1-\tau)^\theta\right)\\ \mathcal{S}_j(t) &\to \mathcal{S}_j(t) - \theta.\end{aligned}$$

The two testing strategies are equivalent when $\tau = 0$, in which case no animals are detected to be infected so there are no imbalances to stock depletion, and when $\tau = 1$, in which case all infected animals are detected and removed. In this scenario, the effect of testing is expected to produce the greatest disturbance to trading patterns, though is guaranteed to eradicate disease as batches from infected farms will always be rejected, preventing any disease spread between farms. To measure the potential financial burden of such on-movement controls, i.e. the costs of rejecting animals, we calculate a simple measure of farms' income, defined as the number of animals each supplying farm sells (regardless of whether they are rejected due to testing positive for infection) multiplied by the price at the time of the trade, and farms' lost income, defined as the number of animals that are rejected due to testing positive for infection multiplied by the price at the time of the trade. We then define the net income as the difference between these two quantities. We assume that detection of infected animals does not alter farms' propensities to trade in the future with the selling farm, except through the typical changes due to depletion of stock following a trade.

Rejection of individual animals

Considering first testing-and-rejecting of individual animals, Figure 3.21 shows the long-term evolution of the trading system when animal testing is introduced for a range of selected test sensitivities. In general, we find that implementation of a testing regime causes long-term changes to trading patterns (except when testing eradicates disease). For example, at $\tau = 0.5$, testing causes long-term increases in farm-level demand and reductions in supply, causing long-term increases in price and reductions in the net income of farms. Moreover, due to rejection of animals, farms are unable to maintain their desired in-flow of animals. These long-term changes in the system are due to testing being insufficient in fully removing disease, with very small observed reductions in prevalence. When $\tau = 1$, however, disease is guaranteed to be eradicated as every infected animal tests positive for infection. In this scenario, the system still exhibits a temporary shock to trading patterns following the introduction of on-movement testing as animals are rejected during trades, however this

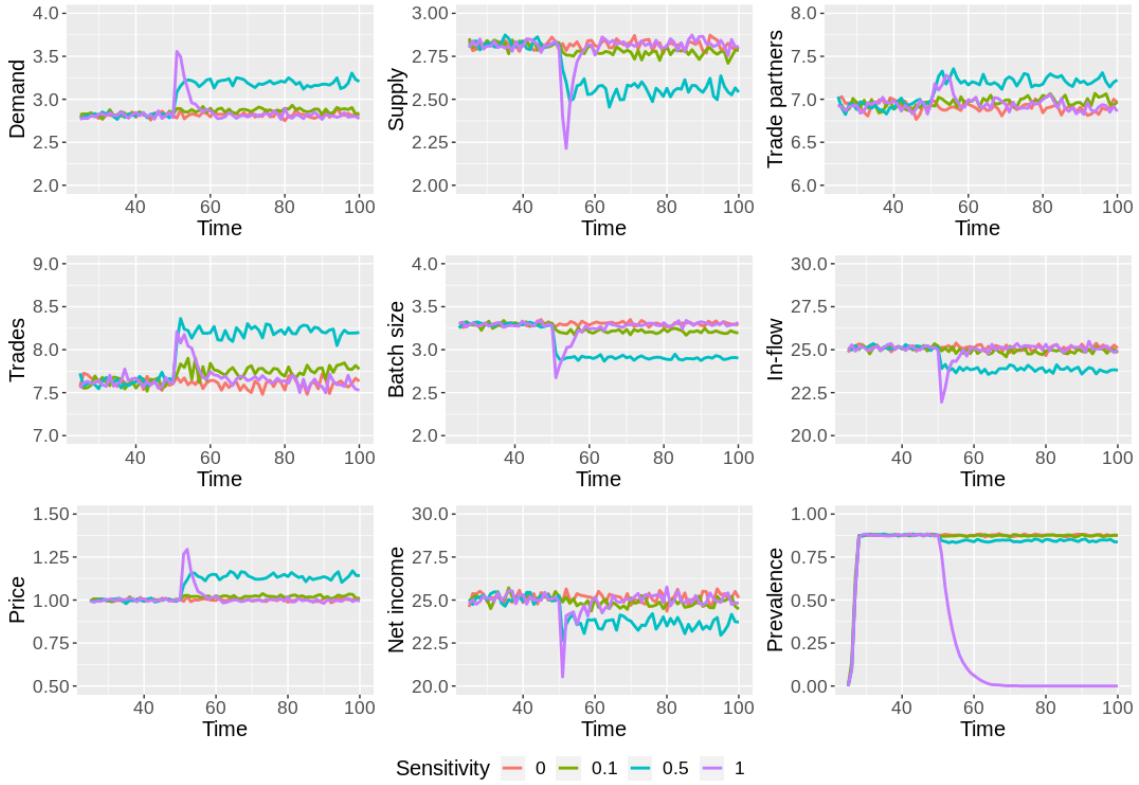

Figure 3.21: **Impact of individual animal rejection on trading system and disease prevalence** Average per-farm demand (top left) and supply (top middle), number of trading partners (top right), number of trades (middle left), batch size (middle middle), per unit-time animal inflow (middle right), price (bottom left), net income (bottom middle) and system disease prevalence (bottom right) for various test sensitivities under the test-and-reject individual animal regime.

leads to rapid reduction in system-wide disease prevalence and trading patterns return to pre-testing equilibrium values. Assessing the effect of testing across a larger range of sensitivities, Figure 3.23 shows that complete elimination of disease is possible only at very high test sensitivities, i.e. $\tau > 0.95$, with prevalence being reduced by only 3.45% at $\tau = 0.5$ and 12.71% at $\tau = 0.75$, though at $\tau = 0.95$ prevalence is reduced by approximately 87%, suggesting significant reductions in prevalence are still possible at high, but not perfect, test sensitivities. From Appendix Figure 3.35, for the low farm prevalence high infectious period scenario, individual animal rejection appears more effective at reducing prevalence, even for test sensitivities in which eradication is not possible. This may be due to the fact that at low farm prevalences λ, the number of infected animals in a batch is expected to be small. As such, successful detection and removal of infected animals essentially clear infection

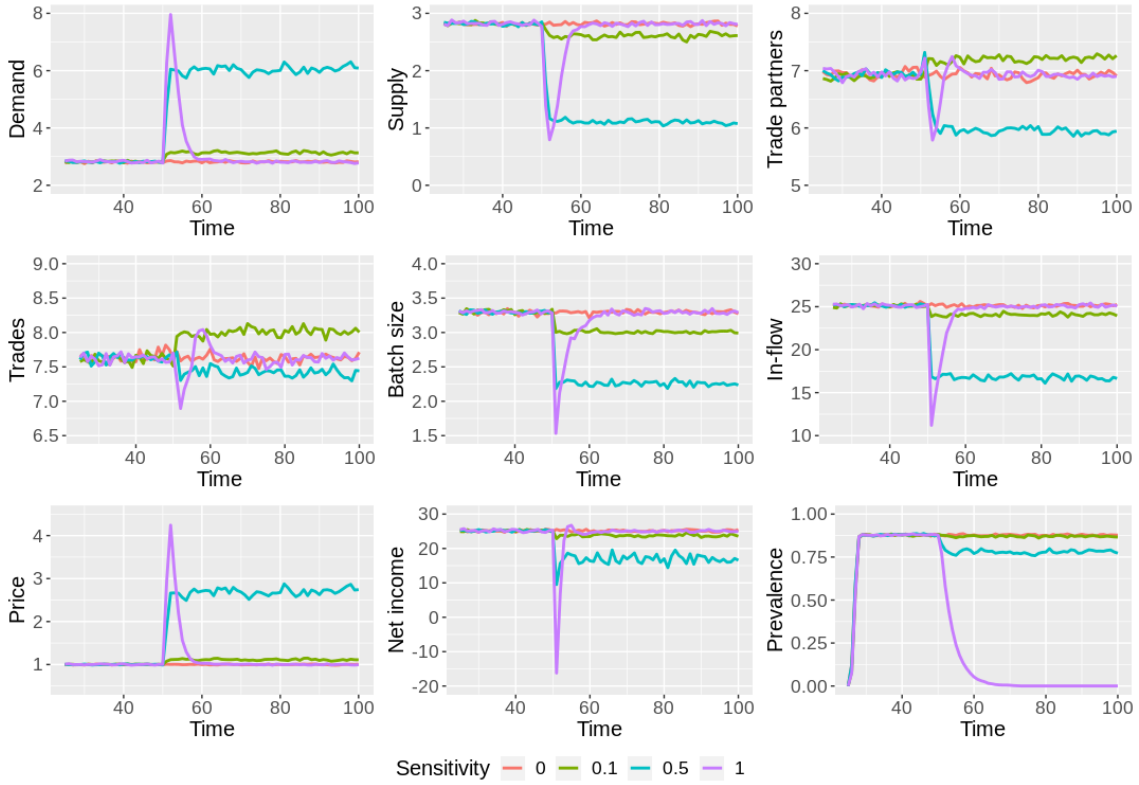

Figure 3.22: **Impact of whole batch rejection on trading system and disease prevalence** Average per-farm demand (top left) and supply (top middle), number of trading partners (top right), number of trades (middle left), batch size (middle middle), per unit-time animal in-flow (middle right), price (bottom left), net income (bottom middle) and system disease prevalence (bottom right) for various test sensitivities under the test-and-reject whole batch regime.

from the batch, leading to fewer infectious trades. This results in smaller disturbances to trade, as fewer animals in a batch are rejected, minimising imbalances in stock quantities. For the high farm prevalence, short infectious period scenario (see Appendix Figure 3.49), testing and rejection of individual animals is also more effective than in the baseline disease scenario. In this case, however, animal rejection is more effective because infected farms recover more quickly, so the number of potentially infectious contacts is smaller. As such, if sufficient numbers of animals are rejected so that disease spread is prevented, infected farms are more likely to recover before they are traded with again and therefore are denied the chance to infect their buyers.

Rejection of animal batches

We now consider the testing-and-rejecting of batches. As explained above, under this regime entire batches are rejected if a single infected animal is detected, which is expected to cause greater long-term disturbances to trade for test sensitivities that fail to fully eradicate disease, and even for sensitivities in which eradication is possible, we expect the temporary shocks to be significantly greater than the individual animal test-and-reject regime. From Figure 3.22 we see that this is indeed true. At $\tau = 0.5$, rejecting batches leads to greater long-term increases in demand and reductions in supply, larger increases in price, greater reductions in net income, and a greater inability for farms to maintain their in-flows. Moreover, at this sensitivity disease prevalence is reduced by 11.17%, compared with 3.45% for the individual rejection scheme. At $\tau = 1$, we see again that complete eradication of disease is possible, though the temporary shocks to the trading system are significantly greater than in the individual animal rejection regime. Of note is the temporary net loss exhibited under this regime when $\tau = 1$, as all batches from infected farms are temporarily removed while disease is cleared from the system. Referring to Figure 3.23, we see that for all test sensitivities, batch rejection leads to larger reductions of disease prevalence than individual animal rejection, though the long-term disturbances to trade are significantly greater for test sensitivities $\tau \leq 0.85$. For sensitivities greater than this, the differences in disturbance to trade are small between the two regimes, while the batch removal regime provides greater reduction in disease prevalence. Sensitivities of the single intradermal comparative cervical tuberculin test for bTB have been estimated to have median values of between 87-90% [96, 111], and the ELISA test to detect paratuberculosis is highly variable with sensitivities ranging from 13.5% to 75% for high shedding animals [60, 120]. Referring to Appendix Figure 3.37, in the low farm prevalence, long infectious period scenario, the differences in testing regimes is small for disease prevalence, though the whole batch rejection strategy causes greater disturbances to trade at lower test sensitivities. However, testing is more effective at reducing disease prevalence compared to the baseline disease scenario, with lower disease prevalence at all test sensitivities and eradication

possible at $\tau \approx 0.8$, compared with $\tau = 0.95$ in the baseline disease scenario. The reasons for the small differences in prevalence reduction are due to the fact that at small λ, batches are more likely to contain only a single infected animal, so the detection of an infected animal in the individual rejection scheme has a similar effect to the detection of an infected animal in the batch rejection scheme. In this case, however, individual animal rejection is preferable as it is unlikely there are more infected animals in the batch, whereas rejection of the entire batch overestimates the risk of infection and leads to unnecessary disturbances on the trading system. For the high farm prevalence, short infectious period scenario, Appendix Figure 3.51 shows that both individual and whole batch rejection is more effective compared to the baseline disease scenario for all test sensitivities, highlighting the ability of testing to prevent disease spread between farms before infected farms recover. We observe that complete eradication is possible at $\tau = 0.75$ for the individual rejection scenario, and $\tau \approx 0.6$ for the whole batch rejection scenario. As in the baseline disease scenario, whole batch rejection leads to greater reduction in prevalence, due to batches containing, in general, a larger number of infected animals. At lower test sensitivities, where infected animals are more likely to avoid detection, rejecting the batch requires only a single detection, minimising the likelihood that infected batches will avoid detection, and reducing onwards transmission.

3.4.3 Networked versus global information to inform risk aversion

In the previous section we explored animal testing via trade, with successful detection of infected animals resulting in either individual animal or whole batch removal, and showed that this can lead to disease eradication for high sensitivity tests, but leads to long-term trade disturbances when testing is unable to eradicate disease. However, detection of infected animals from a given supplier did not alter the likelihood of the buying farm purchasing animals again from the still potentially infected farm (beyond the typical effect due to the depletion of stock). Risk aversion, whereby individuals avoid high-risk individuals, has been an observed behaviour of farmers in

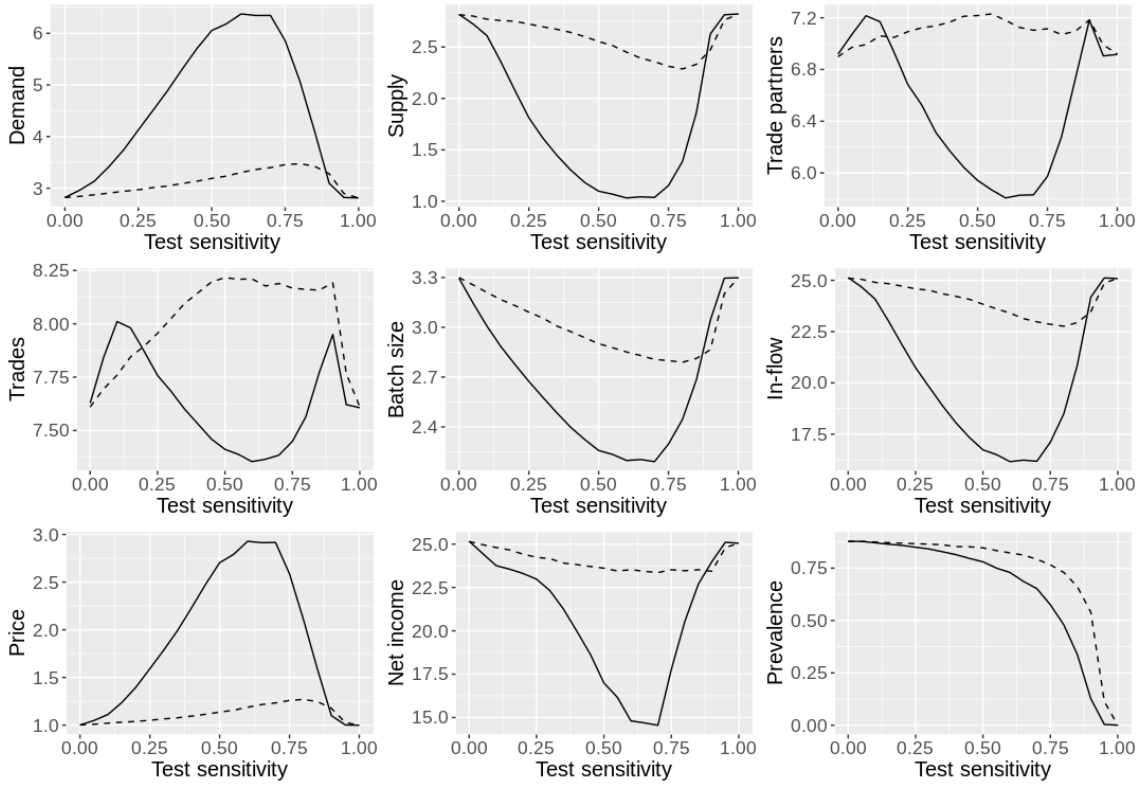

Figure 3.23: **Equilibrium values of trading system and prevalence for both testing regimes** Equilibrium average per-farm demand (top left) and supply (top middle), number of trading partners (top right), number of trades (middle left), batch size (middle middle), per unit-time animal in-flow (middle right), price (bottom left), net income (bottom middle) and system disease prevalence (bottom right) for various test sensitivities under the test-and-reject individual animal regime (dashed lines) and test-and-reject batch regime (solid lines).

an attempt to control bTB [21, 35] and is generally know to impact the spread and stability of disease [41]. Here we implement risk aversion through animal testing, by altering the propensities for farms to form and maintain partnerships, and trade with farms that are deemed high-risk, i.e. farms for which there is past evidence that they are infected. We assume throughout that trade operates under a test-and-reject batch scheme, i.e. farms reject the entire batch if a single animal tests positive.

We first implement risk aversion at a farm level, where buyers perceive suppliers to be high-risk based on their previous trades with them and thus develop a perceived prevalence of disease based on information from their individual trade network. Farms maintain a vector of weights, W_i for farm i, that determine the propensity

to form and end partnerships, and trade with each farm within the system. As such we modify trade partnership formation, rate of trade with trade partners, and dissolution of trade partnerships as follows:

$$\begin{aligned}\alpha_{ij}(t) &\to W_{ij}\alpha_{ij}(t),\\ \varphi_{ij}(t) &\to W_{ij}\varphi_{ij}(t),\\ \delta_i &\to (W_{ij})^{-1}\,\delta_i,\end{aligned}$$

where W_{ij} is the j-th element of farm i's vector of weights, i.e. the weight assigned by farm i to farm j, and we take $(W_{ij})^{-1}$ to be the inverse of the j-th element of W_{ij}. Weights initially take value 1, with successful detection of infected animals assigning a new weight $\omega < 1$. Further trades that do not result in the detection of infected animals incrementally increase weights in steps of ω until they return to 1, and further trades in which detection occurs returns weight W_{ij} to ω. We note that this aversion strategy may lead to unnecessary long-term disturbances to trade even when disease is eradicated, as farms only update their weights with each specific supplier farm during trades, which the risk aversion strategy itself hinders.

Information propagation on local networks

Figure 3.24 shows the effect of individual risk aversion, with a chosen aversion parameter $\omega = 0.1$ in all cases. At test sensitivity $\tau = 0.5$, risk aversion causes long-term perturbations to trade within the system, as test sensitivity is high enough for farms to begin detecting infection and rejecting batches. This causes initial reductions in farm-level supply, however risk aversion causes farms to avoid farms that are deemed high-risk, resulting in these high-risk farms accumulating supply, causing system-average supply levels to increase. When testing was performed in isolation (Figure 3.22), we observed only long-term reductions in supply. We also observe greater long-term increases in demand as a result of risk aversion, as farms avoid trade with high-risk farms, reducing the number of farms that can be traded with. In terms of disease prevalence, however, individual based risk aversion has a positive

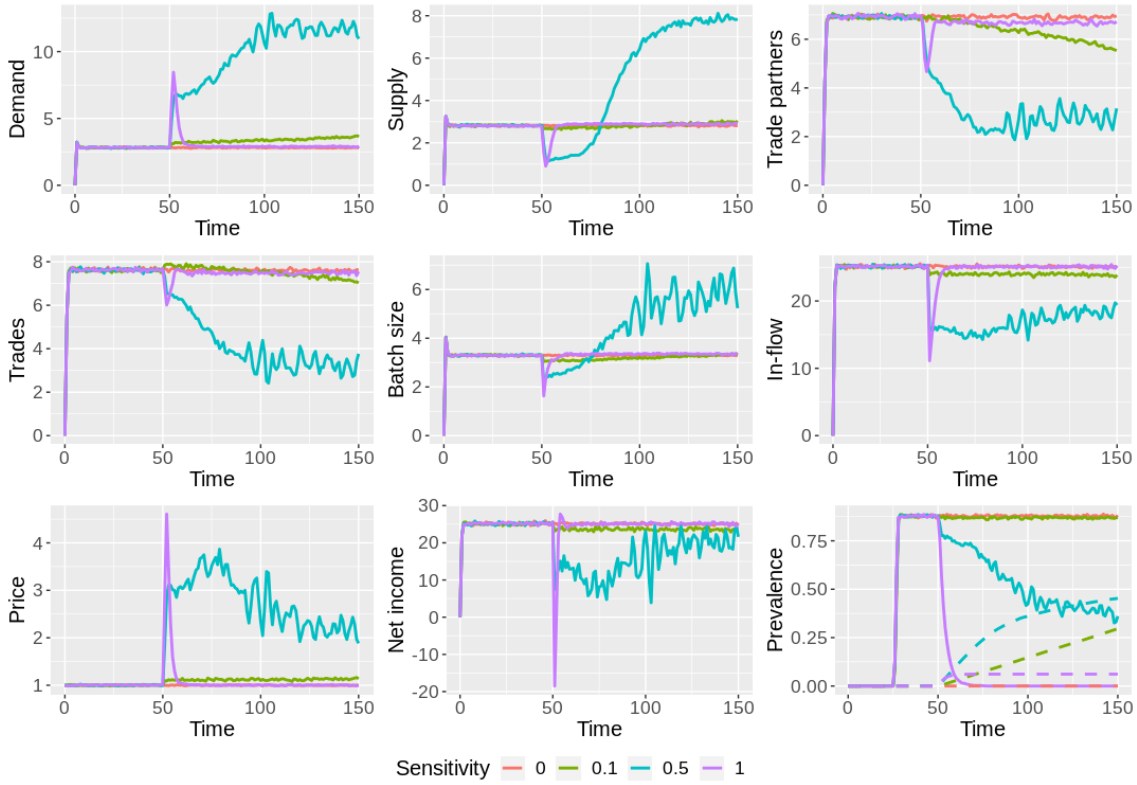

Figure 3.24: **Impact of individual-based risk aversion on trading system and disease prevalence** Average per-farm demand (top left) and supply (top middle), number of trading partners (top right), number of trades (middle left), batch size (middle middle), per unit-time animal in-flow (middle right), price (bottom left), net income (bottom middle) and system disease prevalence (bottom right) for various test sensitivities combining batch testing and removal with farm-level risk aversion, where we set the aversion parameter $\omega = 0.1$. Dashed lines in the disease prevalence plot represent the average per-farm perceived level of prevalence, defined as the fraction of the network with $\omega \neq 1$.

effect in reducing prevalence for $\tau = 0.5$, a sensitivity that did not permit removal of disease when only testing was performed, with further reductions in disease prevalence compared with only testing. This reduction in prevalence reduces the number of batches rejected, so that the price, net income, and in-flow of animals begin to return to pre-testing equilibrium values, though we note that this return is slow (and we do not follow the trajectory long enough to see complete convergence). We see that weights that are updated solely through individual trades cause unnecessary system-wide "distrust" for test sensitivities that complete remove disease, e.g. $\tau = 1$. While disease is fully removed in this scenario, the average per-farm perceived

prevalence (the fraction of farms that have a weight $\omega < 1$) does not return to zero, leading to long-term avoidance of farms deemed high-risk. Figure 3.26 shows that over a range of test sensitivities, an individual based risk aversion strategy leads to greater reductions in disease prevalence compared to the test-and-reject only strategy for all test sensitivities $\tau > 0.15$. Qualitatively, including individual based risk aversion alters the impact of testing on farm-level supply and batch size, with both quantities increasing with individual risk aversion, compared with decreasing with test-and-reject only. Individual based risk aversion is not as effective in the low farm prevalence, long infectious period scenario (see Appendix Figure 3.40), as risk aversion is tied to successful detections of infected batches, which at low farm prevalences are less likely than in the baseline disease scenario. As such, farm-level perceived prevalences are lower and the actual disease prevalence is reduced by similar magnitudes compared to simply testing, i.e. with no risk aversion. Similarly, in the high farm prevalence, short infectious period scenario (see Appendix Figure 3.54), individual based risk aversion does not significantly alter the ability for disease to spread and persist. In this case, however, the small differences are due to the short infectious periods, meaning farms are unlikely to repeat trade with infected farms even without risk aversion. Thus, for short infectious period diseases, an individual based risk aversion strategy is unnecessary compared to simply testing and rejecting animal batches.

System-wide propagation of information

We now consider a system-wide aversion strategy, which we define as global risk aversion. This aversion strategy differs from the individual based aversion strategy in that farms no longer possess an individual vector of weights, rather all farms share and contribute to information on high-risk suppliers through a single global vector of weights. Thus, all farms adjust their behaviour towards individual farms when any farm detects infection from a selling farm during a trade. We expect, therefore, for a greater degree of risk aversion (at least initially) due to farms combining their weights into a single, system-wide, aversion strategy. Considering Figure 3.25, we indeed see that a global aversion strategy causes greater initial shocks in stock levels

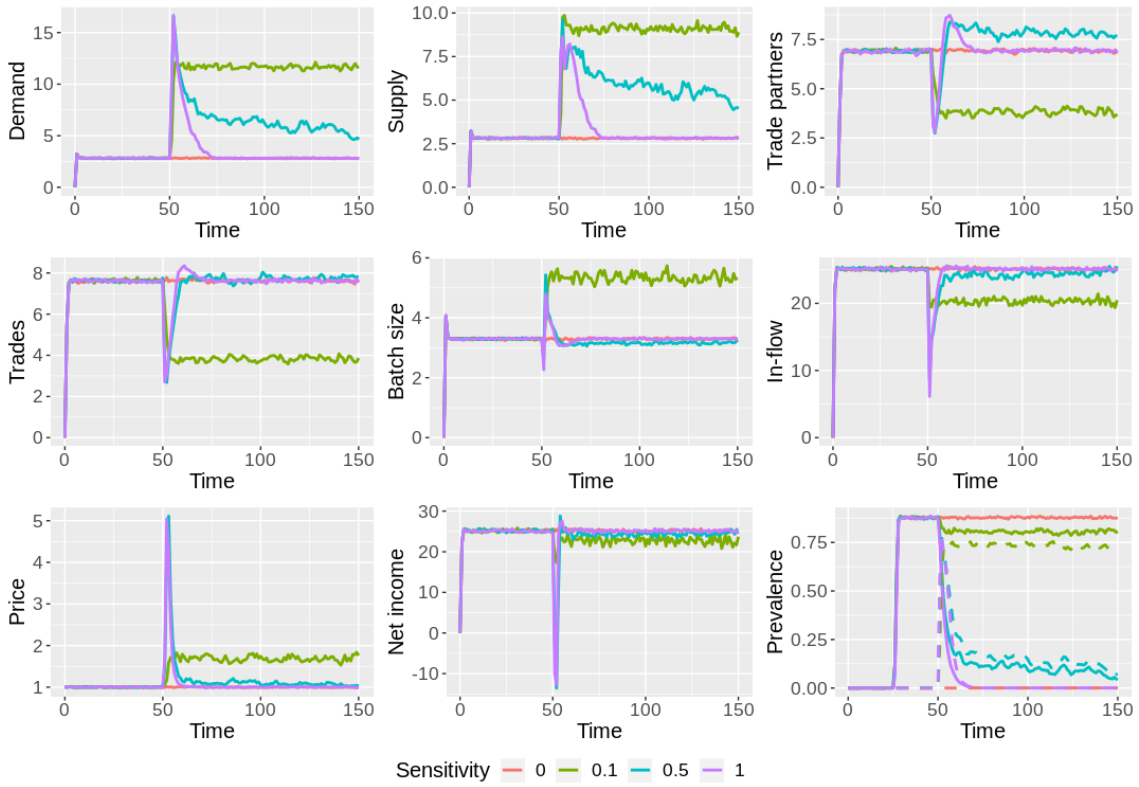

Figure 3.25: **Impact of global risk aversion on trading system and disease prevalence** Average per-farm demand (top left) and supply (top middle), number of trading partners (top right), number of trades (middle left), batch size (middle middle), per unit-time animal in-flow (middle right), price (bottom left), net income (bottom middle) and system disease prevalence (bottom right) for various test sensitivities combining batch testing and removal with global (system-wide) risk aversion, where we set the aversion parameter $\omega = 0.1$. Dashed lines in the disease prevalence plot represent the average per-farm perceived level of prevalence, defined as the fraction of the network with $\omega \neq 1$.

than individual based aversion, however for $\tau = 0.5$ and $\tau = 1$, these shocks are temporary and farms begin to return to pre-testing equilibrium values. We notice that for $\tau = 0.1$, a global aversion strategy is still unable to eradicate disease, though does lead to larger reductions in prevalence than in the individual based aversion strategy. Long-term perturbations to the system are greater for this sensitivity than for the individual based aversion strategy, due to a greater system-wide perceived prevalence. For the global aversion strategy, we note that perceived prevalences generally follow the trend of actual disease prevalence, which was not observed in the individual based aversion strategy. For the individual based aversion strategy,

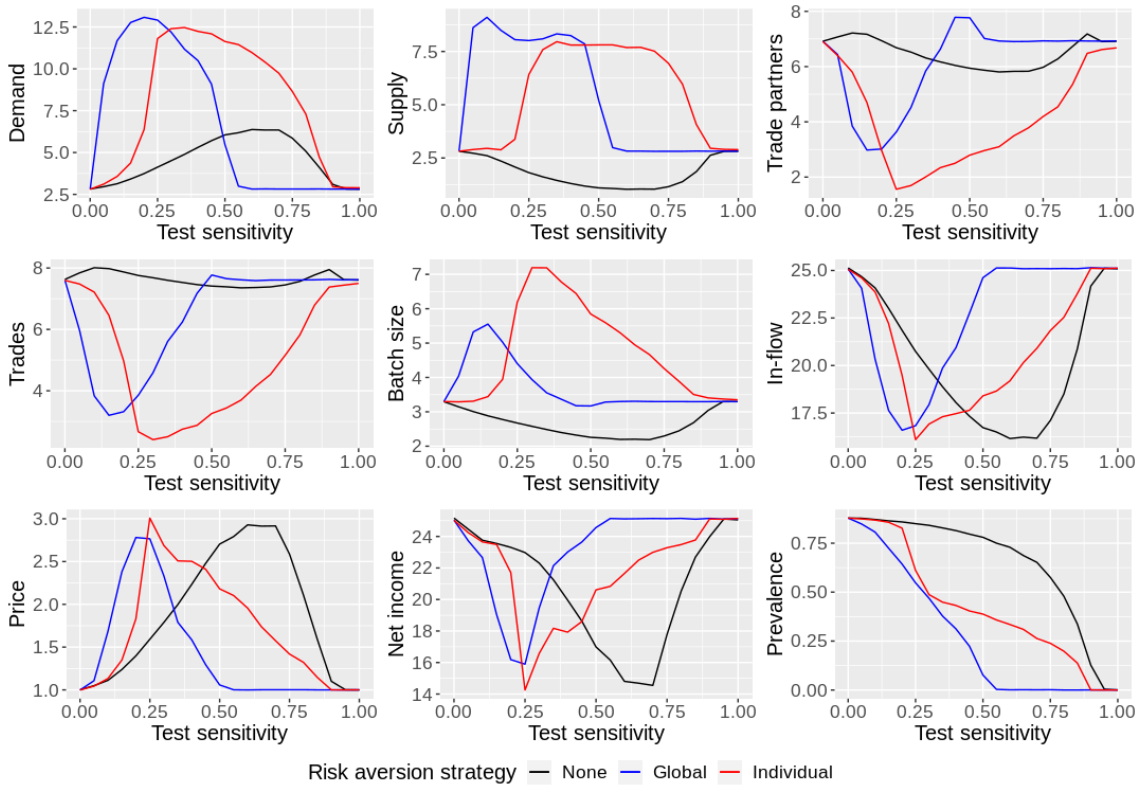

Figure 3.26: **Equilibrium values of trading system and prevalence for both risk aversion strategies** Equilibrium average per-farm demand (top left) and supply (top middle), number of trading partners (top right), number of trades (middle left), batch size (middle middle), per unit-time animal in-flow (middle right), price (bottom left), net income (bottom middle) and system disease prevalence (bottom right) for various test sensitivities under a test-and-reject batch regime only (black line), test-and-reject batch with individual risk aversion (red line), and test-and-reject batch with a global aversion strategy (blue line). In both aversion strategies we set the aversion parameter $\omega = 0.1$.

farms updated their weights based on their trades with farms, resulting in perceived prevalences that did not track actual prevalence levels. However, for the global aversion strategy, farms collectively contribute to system-levels weights, so that trades with high-risk farms are more likely to occur, resulting in updates to weights and perceived prevalences that more closely resemble actual prevalence levels. Referring to Figure 3.26, we observe that a global risk aversion strategy removes disease for a much larger range of test sensitivities ($\tau \geq 0.55$). Furthermore, for sensitivities that do not result in complete removal of disease, system-wide prevalence is still significantly reduced compared to both an individual based aversion strategy and

no aversion strategy at all (the latter corresponding to simply testing and rejecting batches). As mentioned above, a global aversion strategy causes greater long-terms disturbances to trade than an individual based and no aversion strategy at low test sensitivities ($\tau \leq 0.25$), but is less intrusive than individual based risk aversion at larger sensitivities. For the low farm prevalence, long infectious period scenario (see Appendix Figure 3.54), global aversion does further reduce disease prevalence, but not as significantly as in the baseline disease scenario. As with individual based risk aversion, farms deem suppliers high-risk based on successful detections of infected batches, which are less likely when the farm-level prevalence is low. As farm weights increase based on subsequent trades that do not result in detected animals, this reduced likelihood of detecting infected animals results in farm weights that are generally higher than in the baseline disease scenario, so that farms are less risk averse towards infected farms. In the high farm prevalence, short infectious period scenario (see Appendix Figure 3.54), a global risk aversion strategy is highly effective for all test sensitivities, significantly reducing disease prevalence compared with individual risk aversion and only testing, and can eradicate disease at test sensitivities as low as $\tau = 0.25$. As the global risk aversion strategy allows farms to preemptively avoid high-risk farms (in the individual risk aversion regime farms must trade at least once to determine whether a farm is high-risk), due to information on risk being shared across the system, high-risk farms are avoided to such an extent that they recover from infection before they are traded with and have the potential to spread disease.

Discounting risk information

We conclude this section by including a natural incremental increase to weights after some fixed period of time, as well as via trade. This is intended to represent a regaining of trust of farms that are deemed high-risk. For a given aversion parameter ω, we assume that farms incrementally increase weights of high-risk farms (whether at an individual farm level or globally depending on the risk aversion strategy) by ω if, after some fixed period, a positive test has not occurred with that high-risk farm, until the weight returns to 1. We assume that this is in addition to

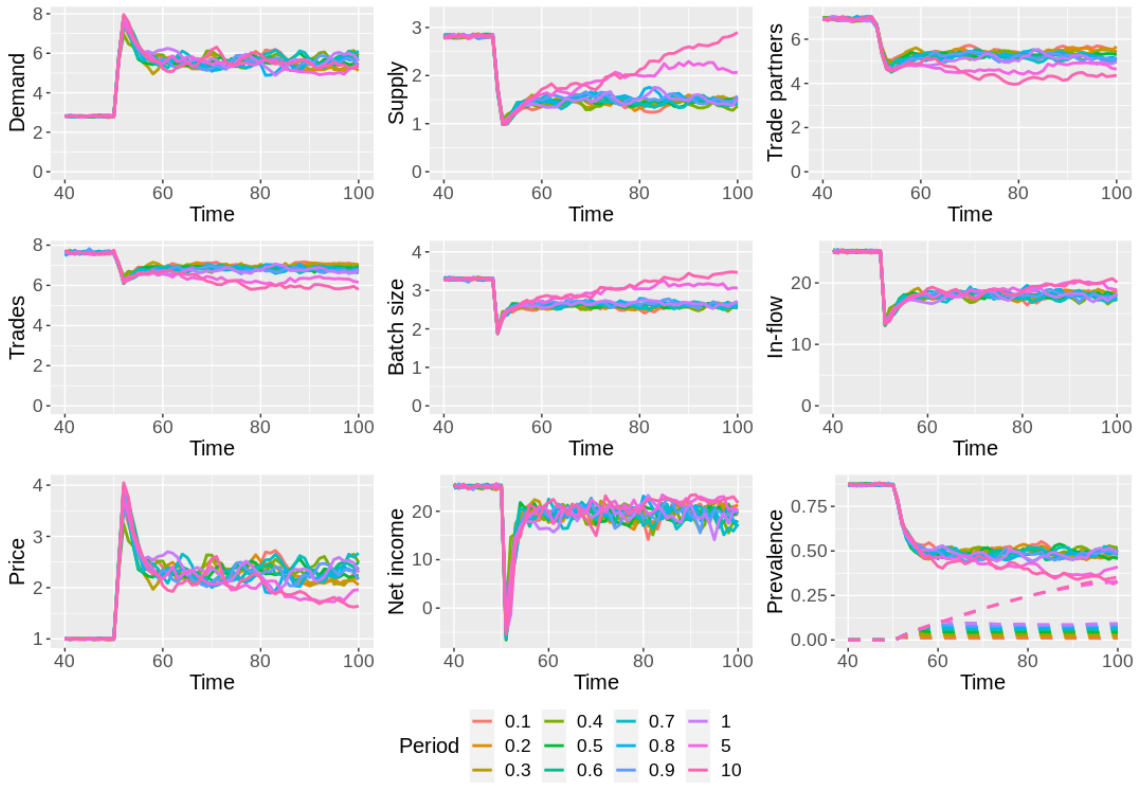

Figure 3.27: **Impact of discounting of risk for individual-based risk aversion on trading system and prevalence** Average per-farm demand (top left) and supply (top middle), number of trading partners (top right), number of trades (middle left), batch size (middle middle), per unit-time animal in-flow (middle right), price (bottom left), net income (bottom middle) and system disease prevalence (bottom right) for test sensitivity $\tau = 0.75$ combining batch testing and removal with individual risk aversion and an incremental increase in weights after various periods of no trades with a detected batch, where we set the aversion parameter $\omega = 0.1$ and weights increase in increments of ω. Dashed lines in the disease prevalence plot represent the average per-farm perceived level of prevalence, defined as the fraction of the network with $\omega \neq 1$.

the incremental increases to weights that occur if trades with high-risk farms do not result in the testing and rejection of animal batches. We test the impact of these natural incremental increases to weights for both the individual based aversion strategy and the global aversion strategy. In all cases presented below we assume a test sensitivity $\tau = 0.75$, a sensitivity that allowed for complete removal of disease in the global aversion regime, and significant (though not complete) reduction in prevalence in the individual based aversion regime, and that farms operate under a test-and-reject whole batch regime.

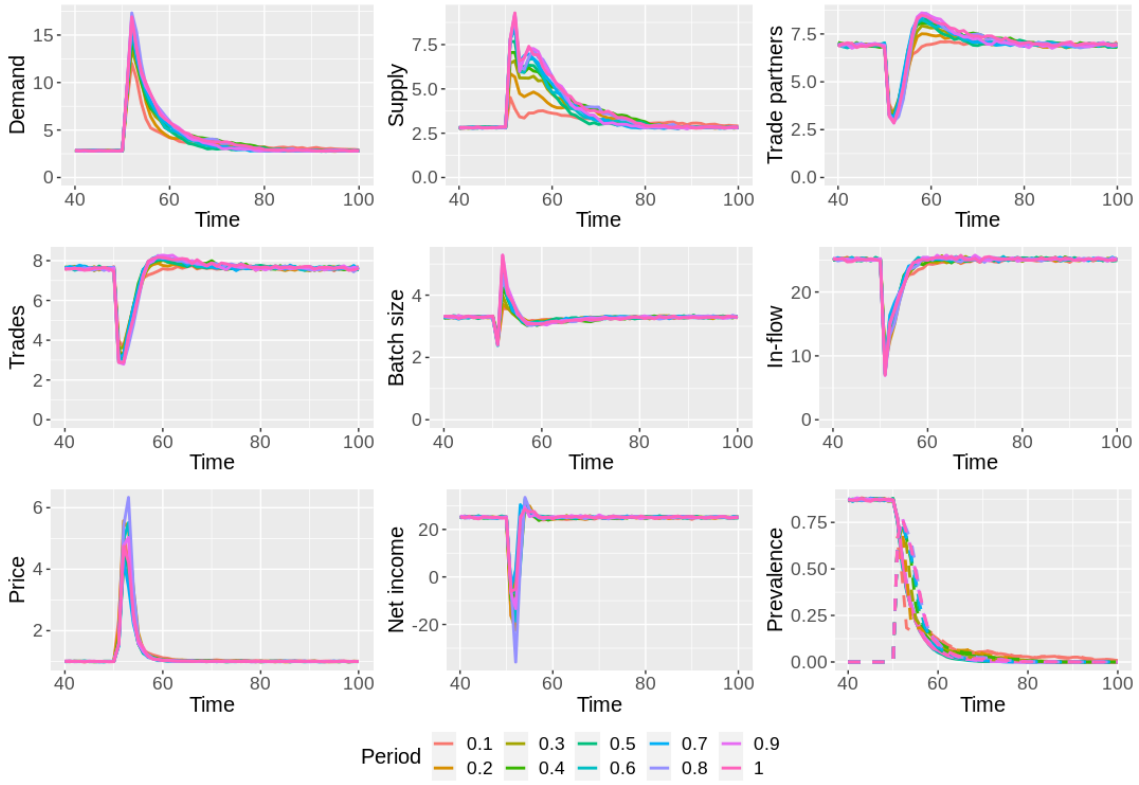

Figure 3.28: **Impact of discounting of risk for global risk aversion on trading system and prevalence** Average per-farm demand (top left) and supply (top middle), number of trading partners (top right), number of trades (middle left), batch size (middle middle), per unit-time animal in-flow (middle right), price (bottom left), net income (bottom middle) and system disease prevalence (bottom right) for test sensitivity $\tau = 0.75$ combining batch testing and removal with global risk aversion and an incremental increase in weights after various periods of no trades with a detected batch, where we set the aversion parameter $\omega = 0.1$ and weights increase in increments of ω. Dashed lines in the disease prevalence plot represent the average per-farm perceived level of prevalence, defined as the fraction of the network with $\omega \neq 1$.

Considering first the individual risk aversion scenario, Figure 3.27 shows that a natural weight increase is detrimental to the ability for risk aversion to reduce disease prevalence, with a short period between weight increments resulting in higher disease prevalence compared with no natural weight increases. This is because weights return to 1 more quickly, resulting in a perceived prevalence that is markedly lower than the actual prevalence. Even when the period between increments is long, disease prevalence is generally larger, suggesting that for the chosen test sensitivity, long-term "distrust" is beneficial in controlling disease. There are positive benefits

of a natural weight increase, however, with farms more readily able to satisfy their demand, but farm flows, price, and net income remain depressed compared with no on-movement testing. In the case of small farm-level prevalence and long infectious period Appendix Figure 3.42 shows that a natural weight increase does not significantly alter the ability for risk aversion to remove disease, with similar qualitative reductions in disease prevalence regardless of the time period in which weights are updated. This is also the case for the high prevalence, short infectious period scenario (see Appendix Figure 3.56), with rapid eradication of disease possible for all weight increment periods.

For the global risk aversion scenario, Figure 3.28 shows that for all weight increment periods, global risk aversion is still able to fully remove disease for our chosen test sensitivity. There are clear benefits to including a natural weight increment in this case, however, with smaller initial disturbances to trading patterns for smaller weight increment periods (increased discounting of historic information on risk), and no significant impact on the time for the trading system to return to pre-testing equilibrium values once disease has been removed. This behaviour is also observed in the low farm prevalence, long infectious period case (Appendix Figure 3.41) and the high farm prevalence, short infectious period case (Appendix Figure 3.55), suggesting a natural weight increment may be effective in minimising disruption to trade while not impacting the ability for risk aversion to remove disease from the system for a global risk aversion strategy and test sensitivity that is capable of removing disease.

3.5 Discussion

In this chapter, a highly dynamic generative trading model was introduced in which farms' propensities to form partnerships and trade with their trade partners are determined by farm-level time-varying stock quantities, defined as supply and demand. These stock quantities vary over time due to a constant rate at which farms increase them in unitary amounts, and they are depleted via trade with farms' trade partners. Thus here we add the dynamics of farm-level supply and demand to the dynamics of the trade partnership network modelled in Chapter 2. This ensures that trading

and partnership formation behaviours of any given farm reflect livestock levels and in particular satiation of demand due to trade can lead to long inter-trade times in which farms accumulate stock before they trade again, a dynamic not systematically accounted for in the model of Chapter 2. As real-world trading patterns vary over time in the UK cattle trade network, with peaks in springtime, for example, [46, 113], incorporating a simple time-varying trading mechanism into our generative models allows for more realistic trading dynamics.

However, these additional features come at the cost of analytical tractability, as our model rates contain discontinuities (in the trade rate and batch size, for instance), and we thus rely heavily on stochastic simulation of our system. Our model in Chapter 2 was designed in such a way that analytical tractability was maintained, and we were able to obtain disease relevant expressions for R_0 that informed potentially effective control strategies. An ongoing challenge is the development of a theoretical framework allowing for analysis of our dynamic trading model. Our generative trading model introduced in this chapter goes beyond currently developed generative trading models by 1) explicitly including time-varying trade partnerships, an element of trade that is conspicuously lacking in the literature (except for our model outlined in Chapter 2 [72]) and 2) all of our rates are functions of supply and demand (current generative models assume constants rates of trade, for example) [58, 87].

By altering the propensities for farms to form and end partnerships, and make trades with their trade partners, we showed that our dynamic trading model reflects the emergent adaptive nature of real-world trading amongst intelligent actors all seeking to meet their business needs, and will adapt itself in response to these changes in such a way that the structure of the network changes. This adaptive systems behaviour is fundamentally different from the model introduced in Chapter 2. The network adaptation is due to the pressure of accumulation of farm-level stock quantities that these changes bring about, and enables farms to maintain their animal inflows. This network adaptation clearly shows the potential of generative trading models, as typical data-driven network-based models of livestock trade have not, to

our knowledge, explored how the network adapts to changes in trading propensities, restrictions, or shocks. Our model shows that simple changes to trading propensities do not result in predictable changes in farm trading patterns, as seen in the model in Chapter 2. In response to shocks in stock quantities, our model rapidly adjusts, leading to surges in trade as these shocks are mitigated, and quickly return to pre-shock equilibrium values except in the extreme cases where farm-level demand is perturbed by a significant amount, in which the system maintains an equilibrium in which farm-level supply and demand are very slightly greater than pre-shock equilibrium values.

We introduced disease spread via trade on a simple homogeneous system of $N = 200$ farms, parameterised in such a way that system-average properties, such as the number of trade partners, trading frequency, batch size, and animal flows, matched system-averages obtained from the Scottish subset of the CTS data. To our knowledge, our analysis of trade, and changes in trade, on disease spread represents the first in-depth attempt at exploring the role of trade on such a dynamic trading model. We assumed a baseline disease parameterisation characterised by farm-level prevalence $\lambda = 0.25$, and recovery rate $\gamma = 1/3$, representing a highly prevalence and persistent disease, but also considered the effect of trade on two other diseases: 1) $\lambda = 0.05$ and $\gamma = 1/3$, a low prevalence, highly persistent disease, and 2) $\lambda = 0.25$ and $\gamma = 1.5$, a high prevalence, short duration disease. We first explored the potential of changes to trading propensities on disease persistence, because the model of Chapter 2 suggested these may be effective in reducing disease and reducing trade frequency has also been shown to be potentially effective in a generative modelling framework [87]. Under our dynamic trading model, we find that simple changes to trading propensities do not reduce disease prevalence by significant amounts, except in extreme cases where trade essentially stops, the network dissolves, or trade partnerships last for vanishingly small durations (even in this latter case, disease is not completely eradicated). This resilience of disease to changes in trading propensities is due to the adaptation of the trading system in response, with farms finding new avenues of minimising their demand and maintaining animal flows that also allowed

for the persistence of disease. The UK cattle trade network has been previously shown to adapt in response to changes in trade aimed at reducing disease spread, resulting in network structures that permit greater disease spread [44, 109, 115]. An interesting observation is that changes in trading propensities so that trades occur more frequently leads to farms having a greater number of trade partners, and partnerships that last longer, do not result in noticeable increases in disease prevalence, as might be expected. As our homogeneous model is parameterised to match system-average properties of the Scottish trading system, this may suggest that farms currently trade in a very low frictional trading system, and significant alterations to trading patterns may be required to reduce disease persistence.

Introducing testing of traded animals showed the potential for routine batch testing on disease prevalence. For our baseline disease scenario, testing animals through trade was shown to reduce disease prevalence, but could only eradicate disease in high test sensitivity scenarios for both individual animal rejection, and whole batch rejection. There were significant alterations to network structure in response to the introduction of testing, with both individual and whole batch rejection resulting in imbalances in farm-level stock quantities that disrupted animal flows, increased prices, and reduced farms' net incomes. We supplemented our testing strategies by linking animal detections to different risk aversion strategies, in which farms change their trading patterns towards farms deemed high-risk. Farm risk aversion is an observed behaviour in an attempt to avoid infected of bTB [21, 35] and more generally risk aversion has been shown to be effective in controlling disease (such as COVID-19) [41]. We proposed two risk aversion strategies: an individual-based risk aversion, whereby farms avoid farms from whom they have detected an infected animal, and a global risk aversion, whereby farms share a common source of information and avoid farms that have been deemed high-risk (by supplying an animal detected as infected) either by them or by other farms in the system. Risk aversion was shown to be an effective supplemental control strategy and significantly reduced disease prevalence compared with only testing. In particular, a global risk aversion strategy was shown to be able to eradicate disease even for low sensitivity tests, and

resulted in lower disease prevalence for all test sensitivities. In the cases where risk aversion could not completely remove disease, there were further disturbances to the trading system as farms began avoiding high-risk farms, leading to greater unmet demand. Moreover, individual level risk aversion lead to inaccurate perceptions of prevalence. We attempted to prevent this by incorporating a natural increment to farm weights, so that farms would regain "trust" in high-risk farms over time. For the individual-based risk aversion strategy, this was shown to be detrimental to prevalence reduction, as farms would more readily trade with high-risk farms, resulting in greater prevalence than without this natural weight increment. For the global aversion strategy, however, there were no significant impacts on disease prevalence, with eradication still possible at the chosen test sensitivities. In addition, the transitory disturbances to the trading system were smaller when farms rapidly regained their trust in high-risk farms, further augmenting the positive benefits of risk aversion.

While our parameterisation was intended to match observed Scottish trading patterns, we assumed for simplicity that the system was homogeneous, i.e. that all farms traded in similar manners (on average). However, the Scottish and UK cattle trading system is known to be highly heterogeneous, displaying scale-free behaviour [22, 84, 113], and, more generally, network structure is known to have an impact on disease spread [89, 100]. Moreover, we assumed a small system of $N = 200$ farms, so factors that may influence disease spread such as network density are unexpected to match the Scottish trading system. The results of this chapter, therefore, should be interpreted with care, as they may not necessarily be indicative of the effect of our explored control measures on real-world networks, but they do present a first attempt at exploring such control measures using a complex adaptive systems model of trading behaviour. In the next chapter we address the challenges of parameterising our dynamic trading model for the Scottish trading system. In addition, we will explore the potential for the control measures outlined here to be successful in a real-world system, and the magnitude of disturbances to the trading system.

3.6 Appendix

3.6.1 Plots for $\lambda = 0.05$, $\gamma = 1/3$

Effect of friction

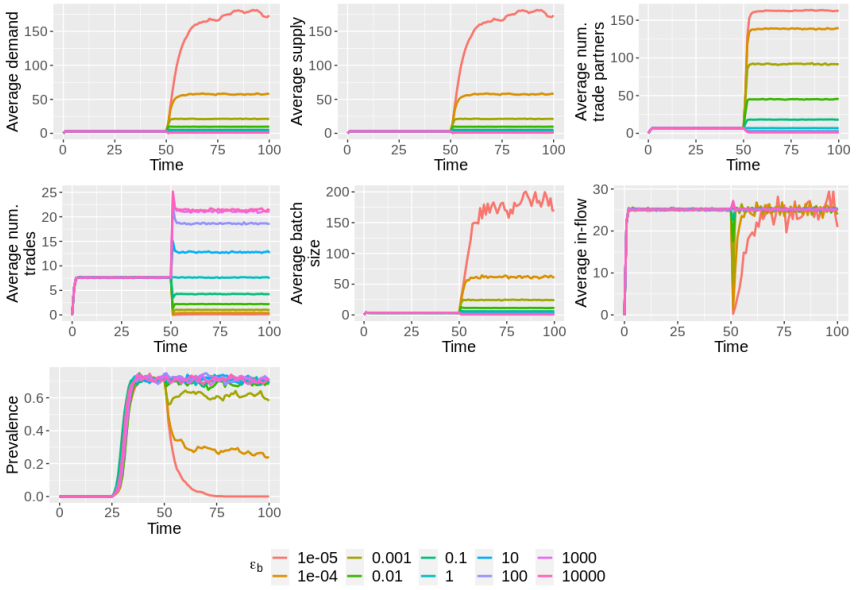

Figure 3.29: Average trade quantities and disease prevalence for varying values of ε_b, the scaling factor to the frictional component of trade, b, when $\lambda = 0.05$ and $\gamma = 1/3$.

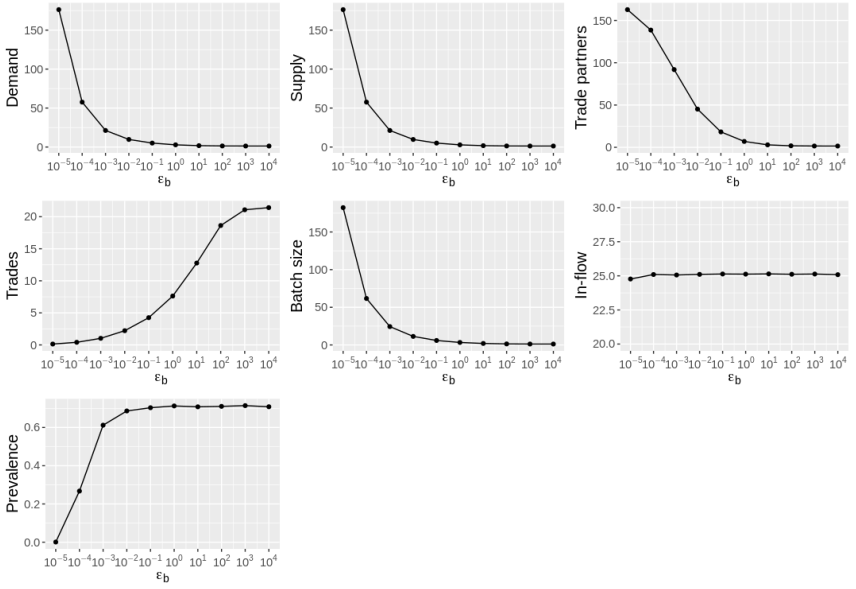

Figure 3.30: Average equilibrium trade quantities and disease prevalence for varying values of ε_b, the scaling factor to the frictional component of trade, b, when $\lambda = 0.05$ and $\gamma = 1/3$.

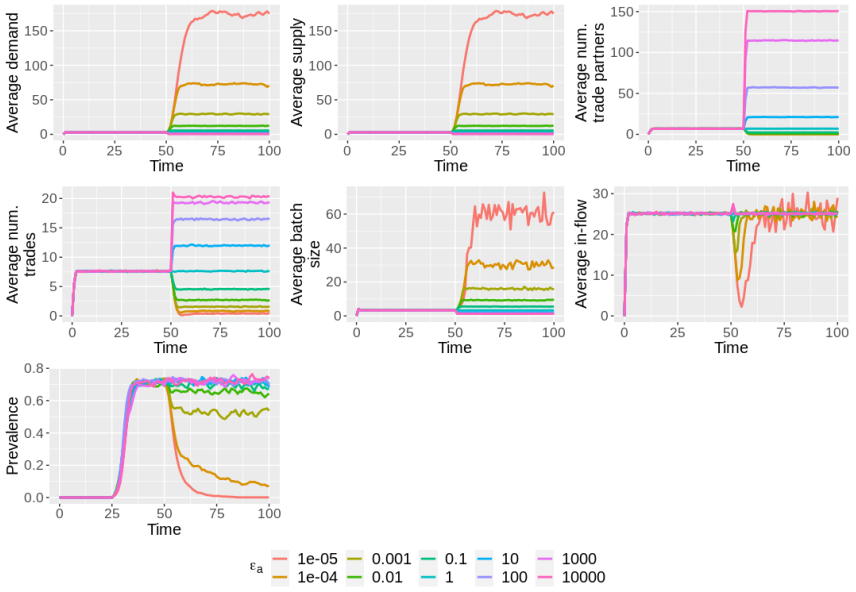

Figure 3.31: Average trade quantities and disease prevalence for varying values of ε_a, the scaling factor to the frictional component of trade, a, when $\lambda = 0.05$ and $\gamma = 1/3$.

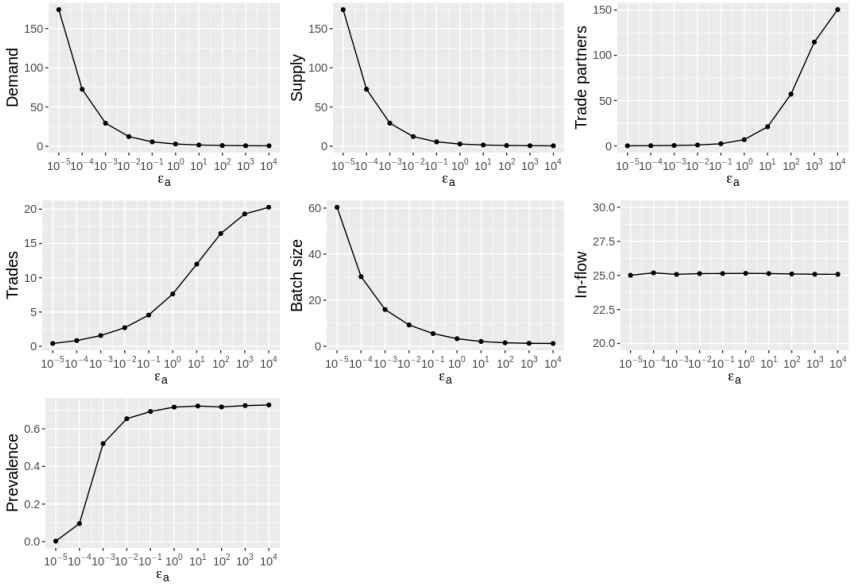

Figure 3.32: Average equilibrium trade quantities and disease prevalence for varying values of ε_a, the scaling factor to the frictional component of trade, a, when $\lambda = 0.05$ and $\gamma = 1/3$.

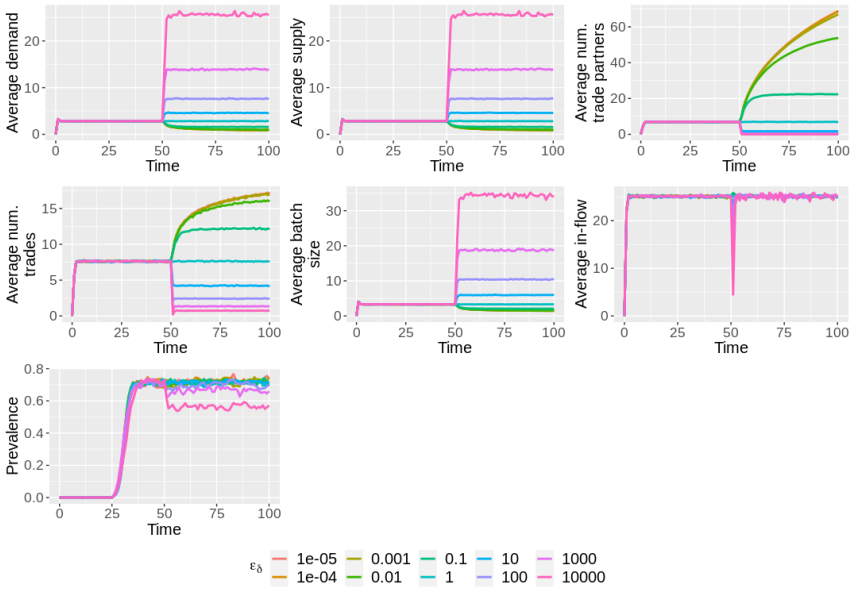

Figure 3.33: Average trade quantities and disease prevalence for varying values of ε_δ, the scaling factor to the partnership cessation rate, δ, when $\lambda = 0.05$ and $\gamma = 1/3$.

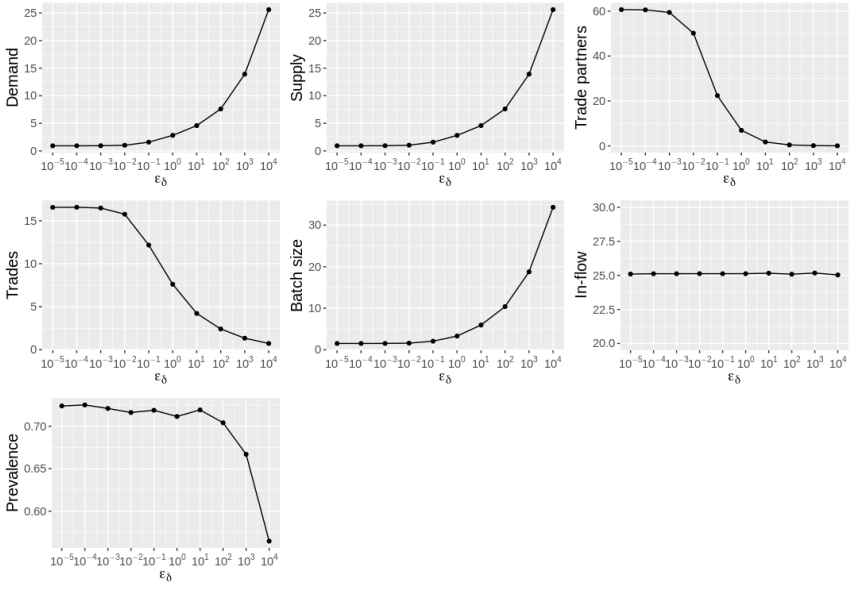

Figure 3.34: Average equilibrium trade quantities and disease prevalence for varying values of ε_δ, the scaling factor to the partnership cessation rate, δ, when $\lambda = 0.05$ and $\gamma = 1/3$.

Batch testing

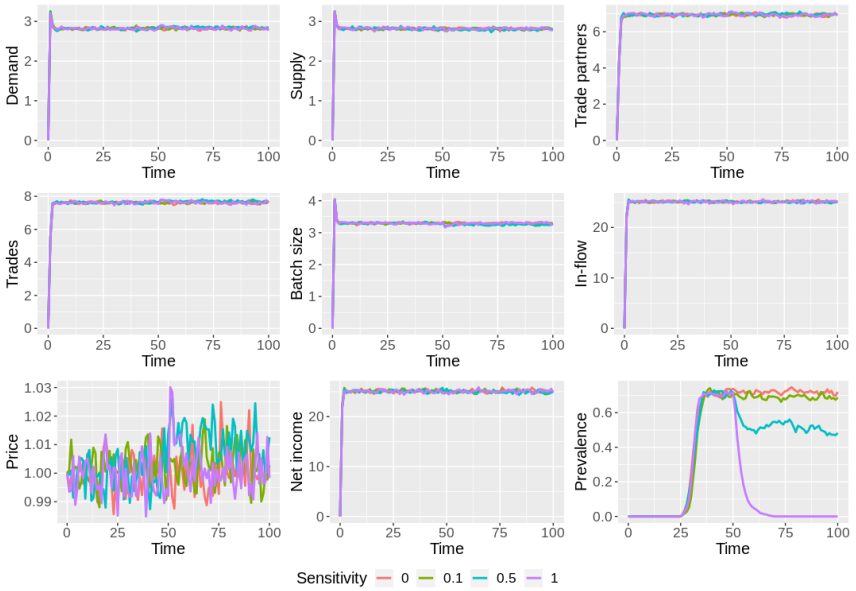

Figure 3.35: Average trade quantities and disease prevalence for various test sensitivities under the test-and-reject individual animal regime, and when $\lambda = 0.05$ and $\gamma = 1/3$.

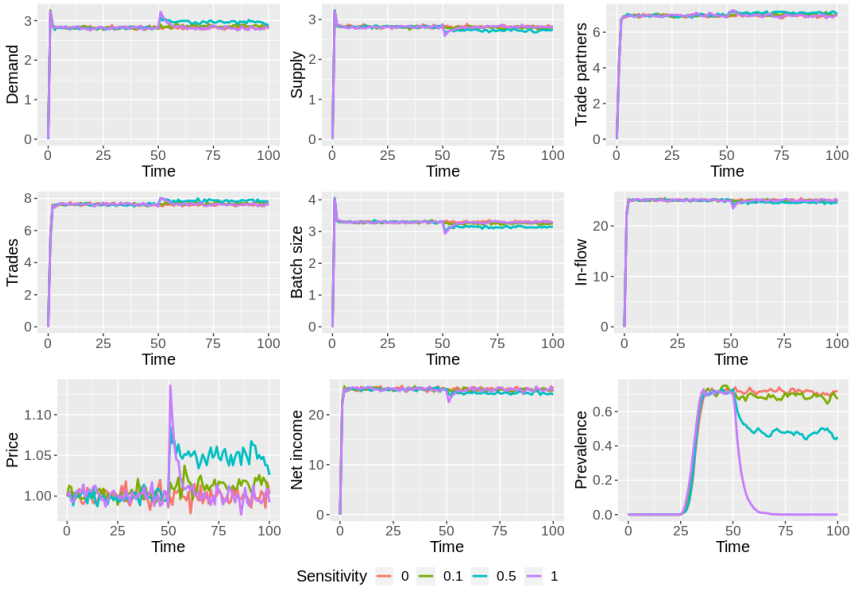

Figure 3.36: Average trade quantities and disease prevalence for various test sensitivities under the test-and-reject whole batch regime, and when $\lambda = 0.05$ and $\gamma = 1/3$.

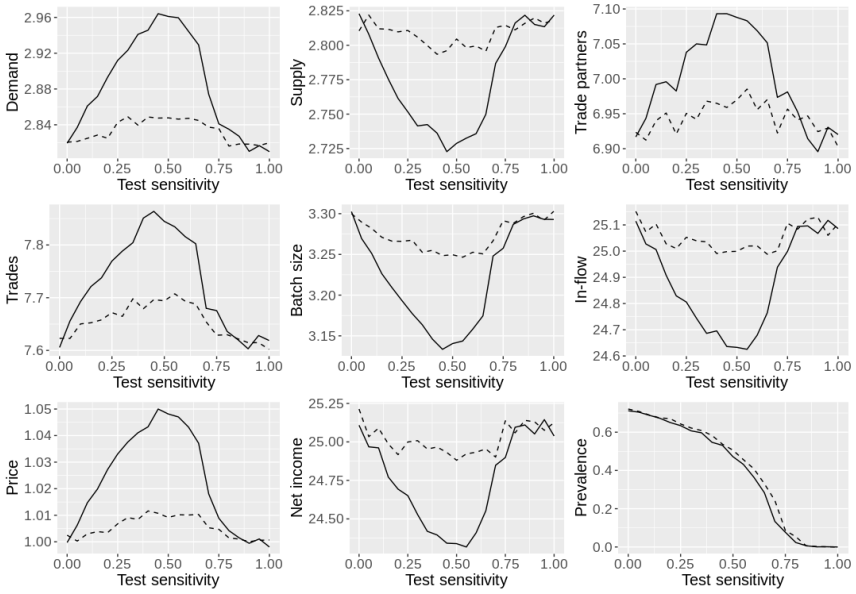

Figure 3.37: Equilibrium average trade quantities and disease prevalence for various test sensitivities under the test-and-reject individual animal regime (dashed lines) and test-and-reject batch regime (solid lines), and when $\lambda = 0.05$ and $\gamma = 1/3$.

Risk aversion

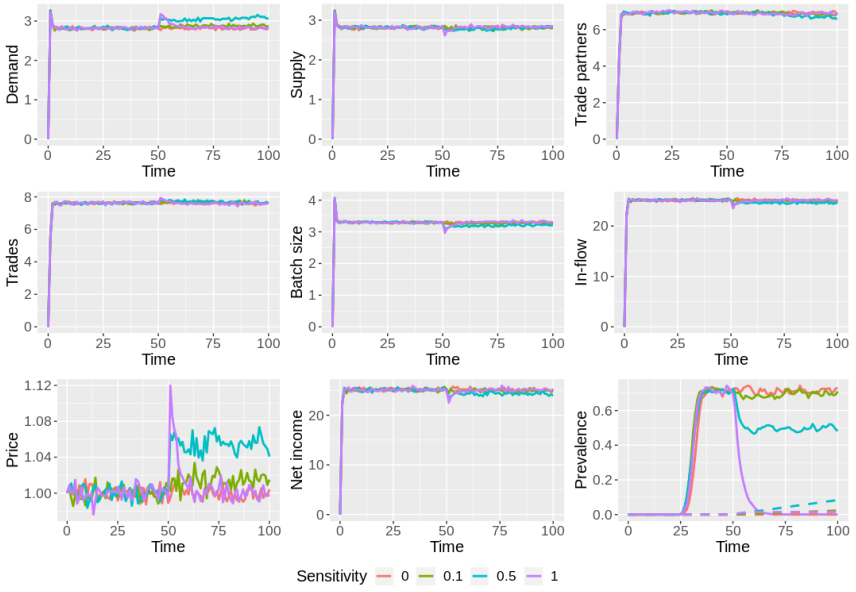

Figure 3.38: Average trade quantities and disease prevalence for various test sensitivities combining batch testing and removal with farm-level risk aversion, where we set the aversion parameter $\omega = 0.1$, and $\lambda = 0.05$ and $\gamma = 1/3$. Dashed lines in the disease prevalence plot represent the average per-farm perceived level of prevalence, defined as the fraction of the network with $\omega \neq 1$.

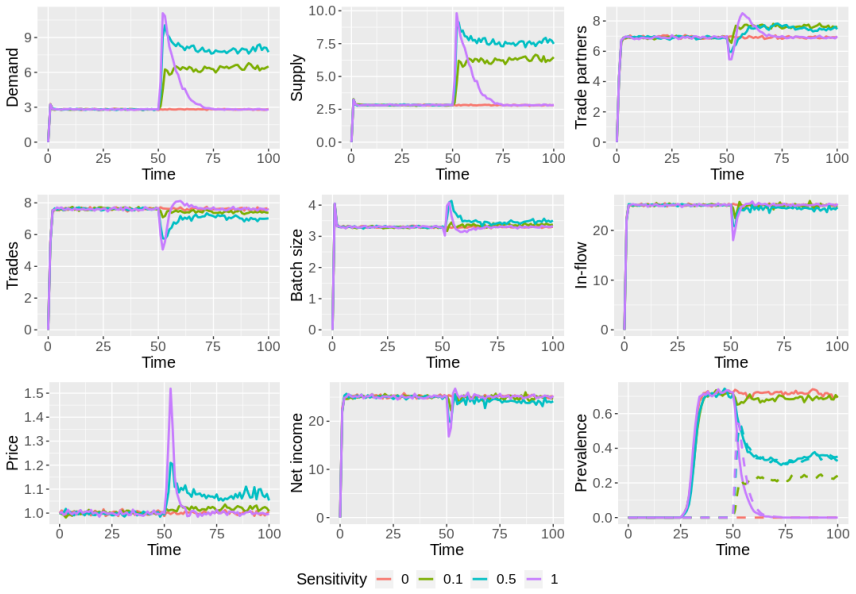

Figure 3.39: Average trade quantities and disease prevalence for various test sensitivities combining batch testing and removal with global (system-wide) risk aversion, where we set the aversion parameter $\omega = 0.1$, and $\lambda = 0.05$ and $\gamma = 1/3$. Dashed lines in the disease prevalence plot represent the average per-farm perceived level of prevalence, defined as the fraction of the network with $\omega \neq 1$.

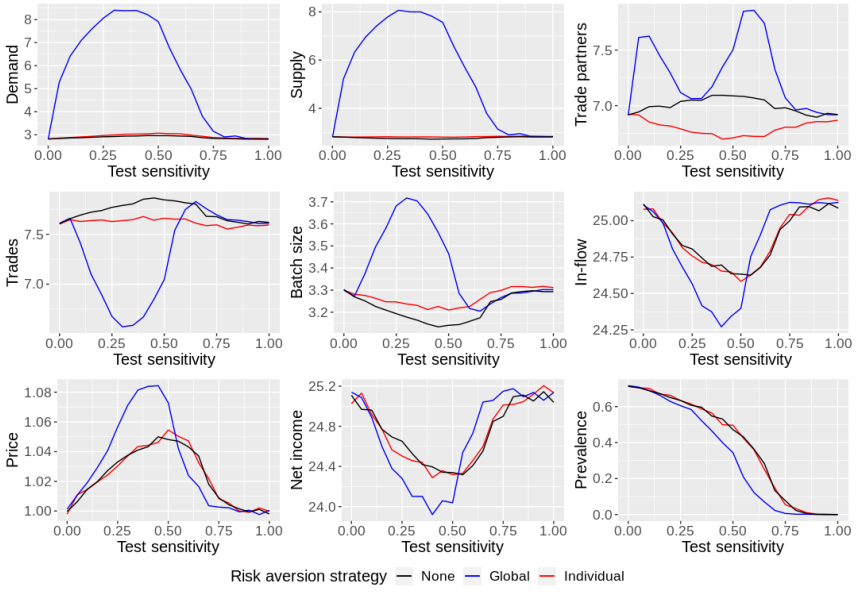

Figure 3.40: Average equilibrium trade quantities and disease prevalence for various test sensitivities combining batch testing and removal with global (system-wide) risk aversion, where we set the aversion parameter $\omega = 0.1$, and $\lambda = 0.05$ and $\gamma = 1/3$. Dashed lines in the disease prevalence plot represent the average per-farm perceived level of prevalence, defined as the fraction of the network with $\omega \neq 1$.

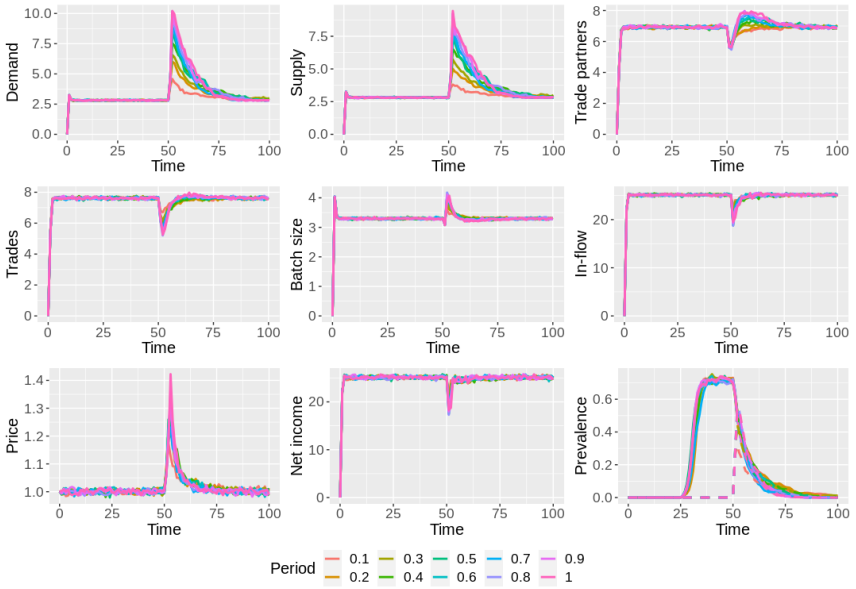

Figure 3.41: Average trade quantities and disease prevalence for various test sensitivities combining batch testing and removal with global (system-wide) risk aversion and natural incremental increase to weights, where we set the aversion parameter $\omega = 0.1$, and $\lambda = 0.05$ and $\gamma = 1/3$. Dashed lines in the disease prevalence plot represent the average per-farm perceived level of prevalence, defined as the fraction of the network with $\omega \neq 1$.

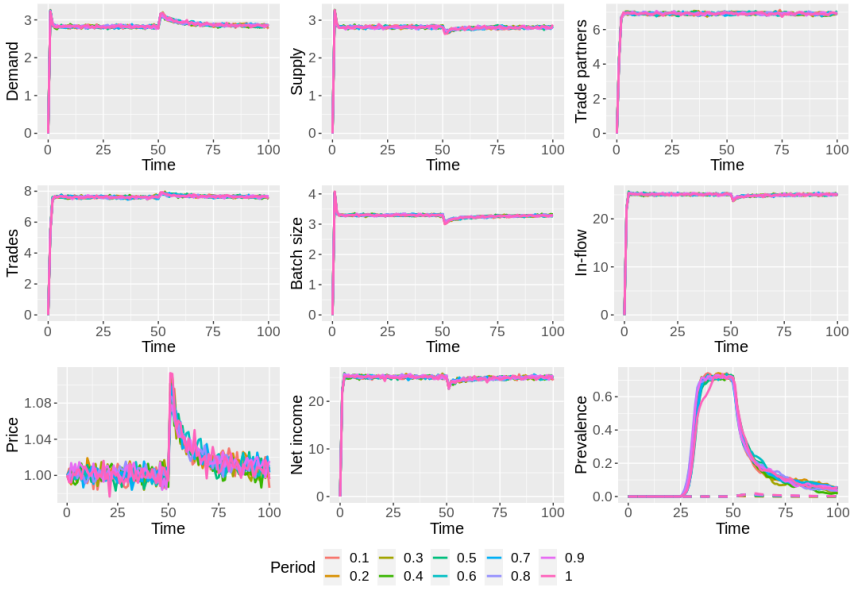

Figure 3.42: Average trade quantities and disease prevalence for various test sensitivities combining batch testing and removal with individual risk aversion and natural incremental increase to weights, where we set the aversion parameter $\omega = 0.1$, and $\lambda = 0.05$ and $\gamma = 1/3$. Dashed lines in the disease prevalence plot represent the average per-farm perceived level of prevalence, defined as the fraction of the network with $\omega \neq 1$.

3.6.2 Plots for $\lambda = 0.25$, $\gamma = 1.5$

Effect of friction

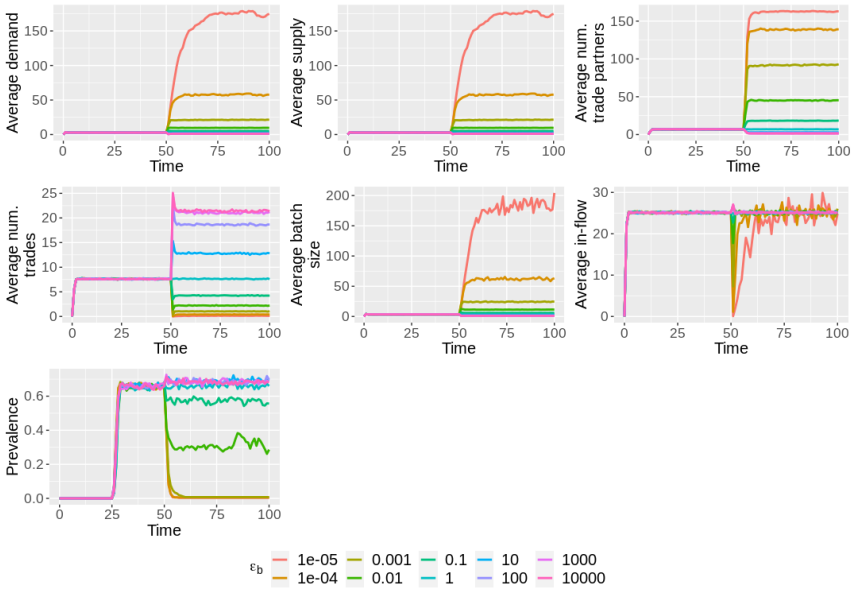

Figure 3.43: Average trade quantities and disease prevalence for varying values of ε_b, the scaling factor to the frictional component of trade, b, when $\lambda = 0.25$ and $\gamma = 1.5$.

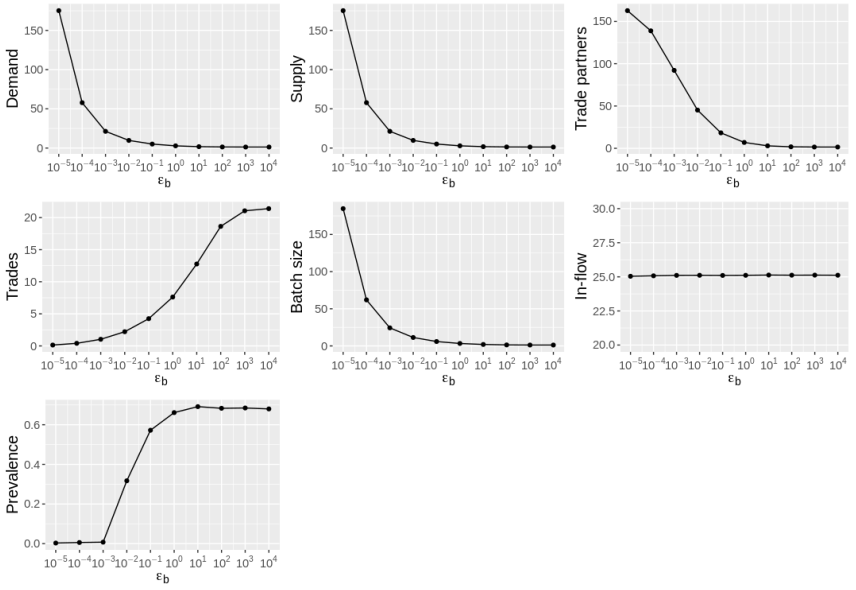

Figure 3.44: Average equilibrium trade quantities and disease prevalence for varying values of ε_b, the scaling factor to the frictional component of trade, b, when $\lambda = 0.25$ and $\gamma = 1.5$.

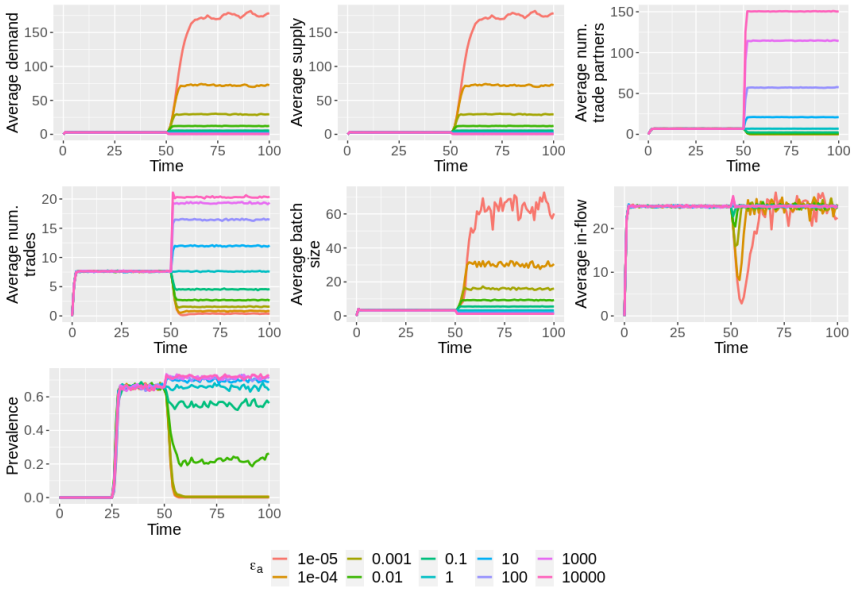

Figure 3.45: Average trade quantities and disease prevalence for varying values of ε_a, the scaling factor to the frictional component of trade, a, when $\lambda = 0.25$ and $\gamma = 1.5$.

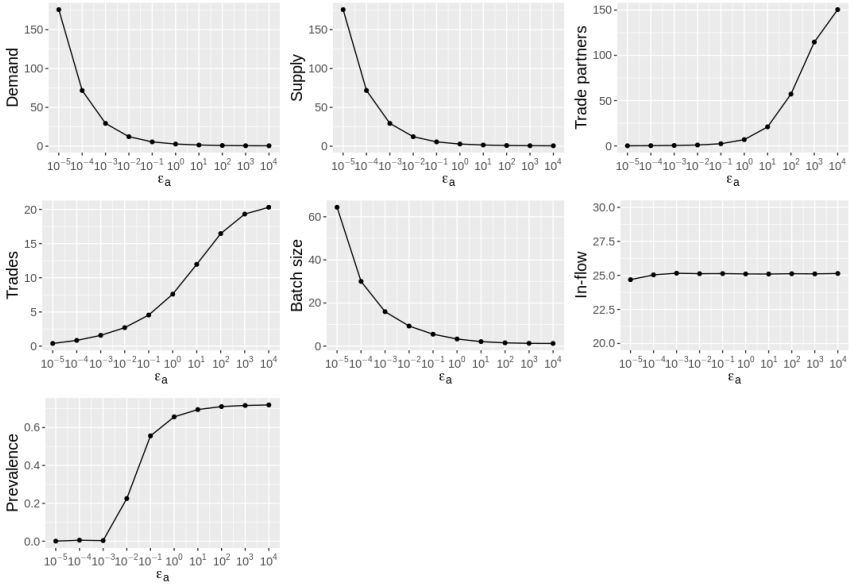

Figure 3.46: Average equilibrium trade quantities and disease prevalence for varying values of ε_a, the scaling factor to the frictional component of trade, a, when $\lambda = 0.25$ and $\gamma = 1.5$.

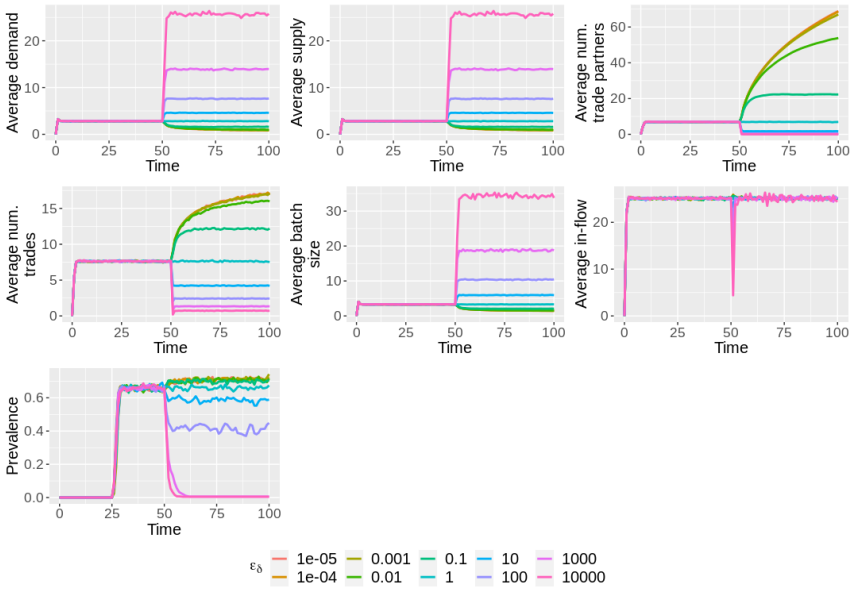

Figure 3.47: Average trade quantities and disease prevalence for varying values of ε_δ, the scaling factor to the partnership cessation rate, δ, when $\lambda = 0.25$ and $\gamma = 1.5$.

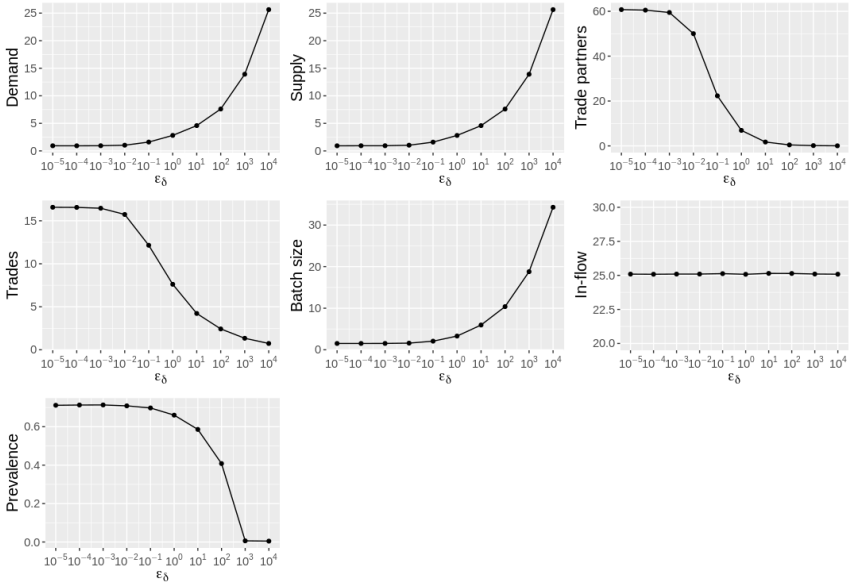

Figure 3.48: Average equilibrium trade quantities and disease prevalence for varying values of ε_δ, the scaling factor to the partnership cessation rate, δ, when $\lambda = 0.25$ and $\gamma = 1.5$.

Batch testing

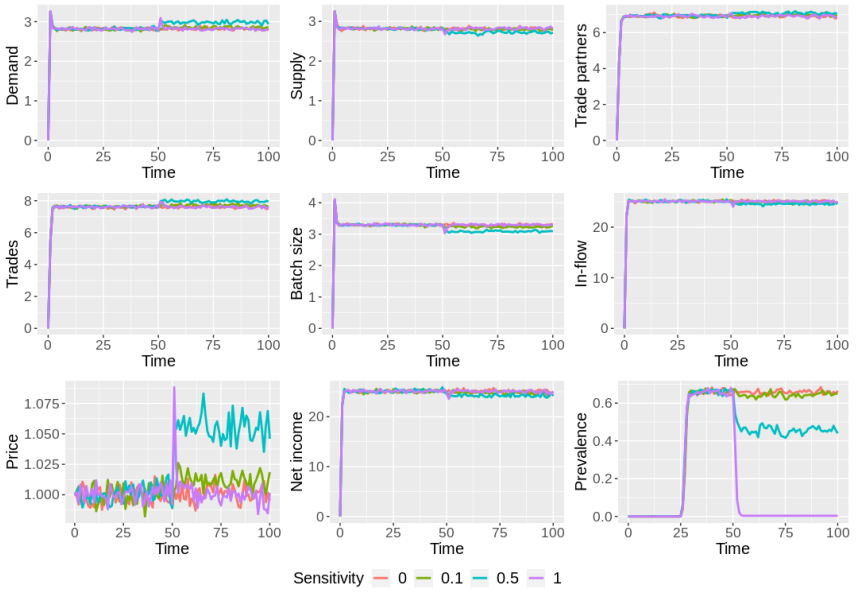

Figure 3.49: Average trade quantities and disease prevalence for various test sensitivities under the test-and-reject individual animal regime, and when $\lambda = 0.25$ and $\gamma = 1.5$.

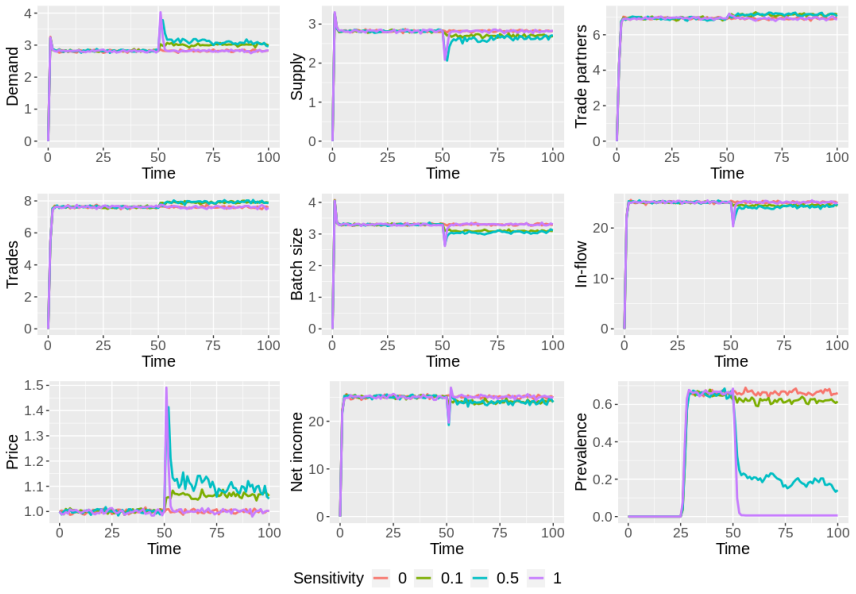

Figure 3.50: Average trade quantities and disease prevalence for various test sensitivities under the test-and-reject whole batch regime, and when $\lambda = 0.25$ and $\gamma = 1.5$.

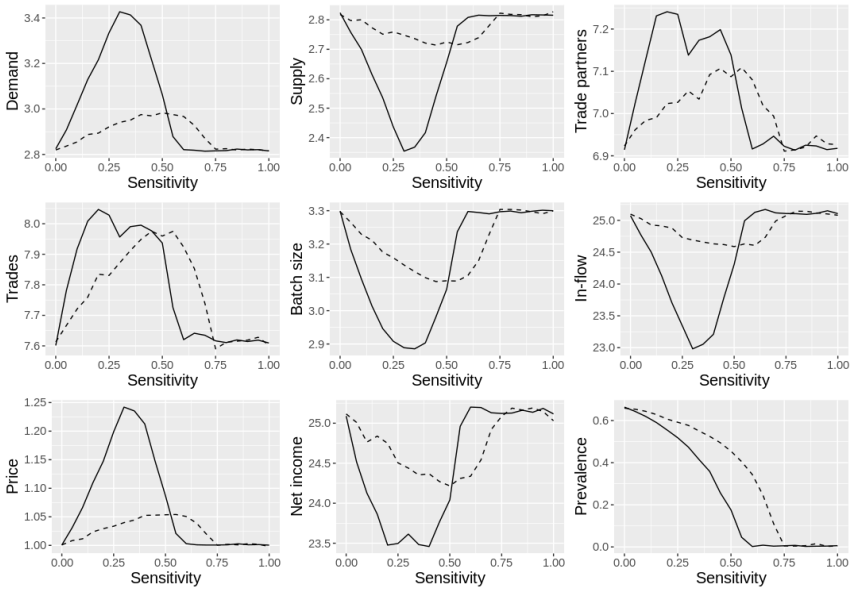

Figure 3.51: Equilibrium average trade quantities and disease prevalence for various test sensitivities under the test-and-reject individual animal regime (dashed lines) and test-and-reject batch regime (solid lines), and when $\lambda = 0.25$ and $\gamma = 1.5$.

Risk aversion

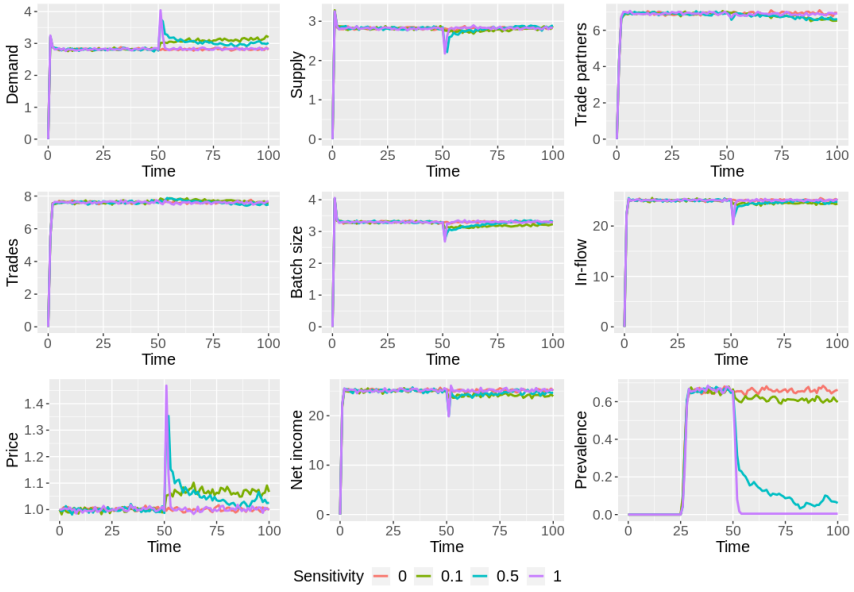

Figure 3.52: Average trade quantities and disease prevalence for various test sensitivities combining batch testing and removal with farm-level risk aversion, where we set the aversion parameter $\omega = 0.1$, and $\lambda = 0.25$ and $\gamma = 1.5$. Dashed lines in the disease prevalence plot represent the average per-farm perceived level of prevalence, defined as the fraction of the network with $\omega \neq 1$.

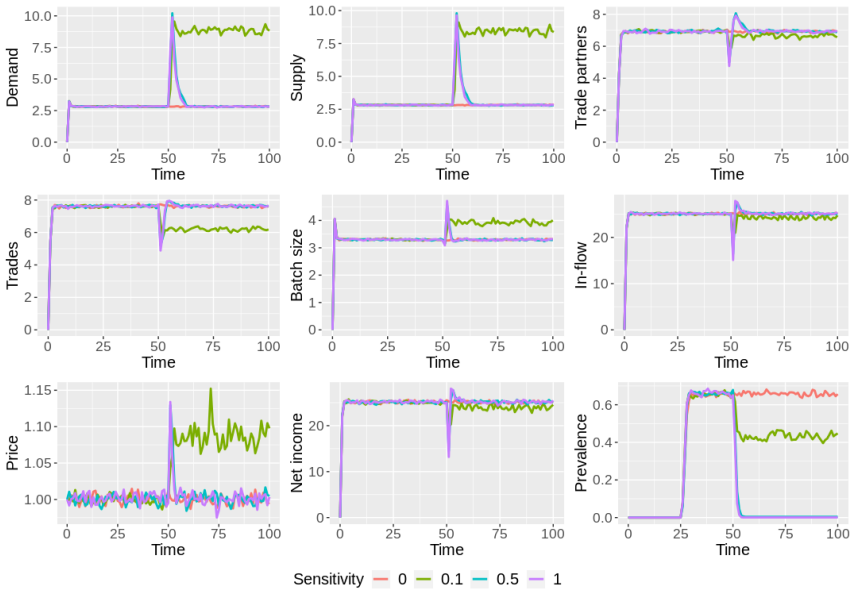

Figure 3.53: Average trade quantities and disease prevalence for various test sensitivities combining batch testing and removal with global (system-wide) risk aversion, where we set the aversion parameter $\omega = 0.1$, and $\lambda = 0.25$ and $\gamma = 1.5$. Dashed lines in the disease prevalence plot represent the average per-farm perceived level of prevalence, defined as the fraction of the network with $\omega \neq 1$.

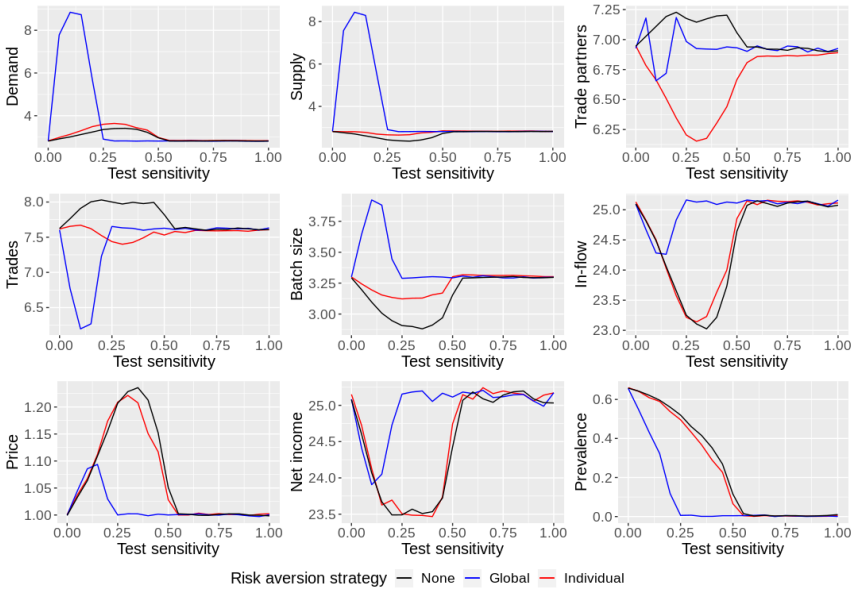

Figure 3.54: Average equilibrium trade quantities and disease prevalence for various test sensitivities combining batch testing and removal with global (system-wide) risk aversion, where we set the aversion parameter $\omega = 0.1$, and $\lambda = 0.25$ and $\gamma = 1.5$. Dashed lines in the disease prevalence plot represent the average per-farm perceived level of prevalence, defined as the fraction of the network with $\omega \neq 1$.

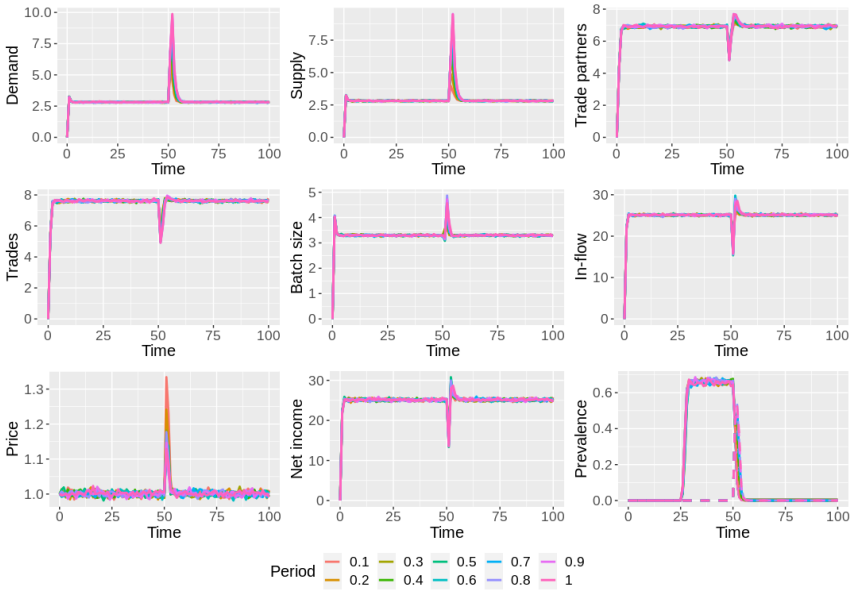

Figure 3.55: Average trade quantities and disease prevalence for various test sensitivities combining batch testing and removal with global (system-wide) risk aversion and natural incremental increase to weights, where we set the aversion parameter $\omega = 0.1$, and $\lambda = 0.25$ and $\gamma = 1.5$. Dashed lines in the disease prevalence plot represent the average per-farm perceived level of prevalence, defined as the fraction of the network with $\omega \neq 1$.

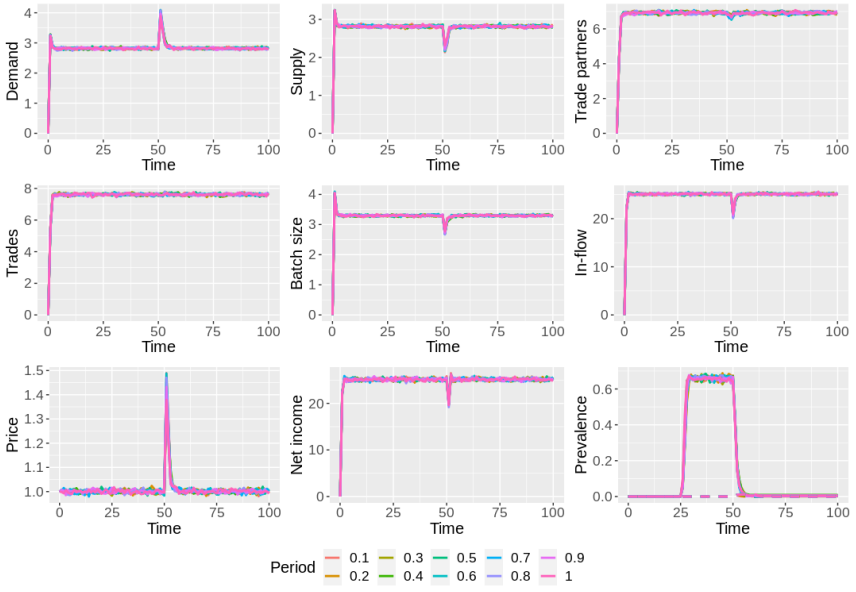

Figure 3.56: Average trade quantities and disease prevalence for various test sensitivities combining batch testing and removal with individual risk aversion and natural incremental increase to weights, where we set the aversion parameter $\omega = 0.1$, and $\lambda = 0.25$ and $\gamma = 1.5$. Dashed lines in the disease prevalence plot represent the average per-farm perceived level of prevalence, defined as the fraction of the network with $\omega \neq 1$.

Chapter 4

National-scale parameterisation of generative systems model for livestock trade and implications for disease control

4.1 Introduction

It is well understood that trade plays a role in the spread of livestock diseases, though a complete understanding of the mechanisms through which trade influences disease spread are not fully understood. It is vital, therefore, that models of livestock trade that can capture much of the complexity of the systems they represent are developed so that a thorough understanding of trade can be obtained and used to develop truly effective disease control strategies. Attempts to model livestock trade and disease have largely consisted of constructing static and temporal networks of observed trades from a dataset and subsequent simulation of disease spread through those movements [43, 71, 76, 98, 117]. These models, while illustrative, cannot necessarily be generalised to ask "what if..." questions, as they are necessarily constrained by past movements observed in data. For example, such approaches are

not suited to address questions that relate to how the trade system might adapt in the face of shocks or under the imposition of regulations or control policies; precisely the kind of questions of most interest to policy makers. Generative models in which a system is parameterised according to data that capture individual-level properties while not being constrained to specific movements may be an invaluable tool in exploring the role of trade in disease spread and there is a pressing need for the development of such models [57]. Cattle trading networks, with more or less complete observation of a dynamic network process in realtime, represent an ideal case-study for the development of such tools. However, there have been few such attempts to develop generative network models for cattle trading networks, and these have generally made simplifying assumptions such as parameterising assuming a homogeneous system or treating trading dynamics as static [58, 87].

In Chapter 3, a generative model of livestock trade dynamics was developed that included farm-level time-varying quantities, representing available supply and demand for a given farm and time. The model was designed so that these stock quantities determined the rates at which farms sought out trading partners and initiated trades. It was shown that altering the propensities for farms to form or end partnerships, or initiate trades would ultimately change the structure of the network as farms sought to minimise their unmet demand and maintain animal flows. When disease spread was introduced through trade, it was shown that these manipulations may not be as effective in reducing disease prevalence as had been shown in Chapter 2, due to this adaptation of the system and resulting restructuring of the network, however disease could be eliminated in some extreme cases, such as when trades occurred very infrequently, or the network was essentially dissolved. Alternative control strategies, such as batch testing and risk aversion, were considered and shown to be potentially effective, but would lead to transitory disturbances to the trading system in the cases when widespread disease could be eradicated, and ongoing disturbances when disease could not be eradicated.

While the analysis of Chapter 3 was informative on the potential dynamics of disease spread in our modelled dynamic trading system, homogeneity was assumed and the

system size was small ($N = 200$). The model was parameterised in such a way that system-average properties, such as average unit-time trades, trade partners, and batch size were similar to those observed in the Scottish cattle trading system, however the network structure ultimately differed markedly from the real-world system as the Scottish system is highly heterogeneous and exhibits scale-free behaviour, i.e. a small fraction of farms trade in ways and frequencies vastly different to the majority of the system [22, 84, 113]. Network structure is known to have an impact on disease spread [89, 100], so applying the model of Chapter 3 to the Scottish trading system is vital in truly understanding the impact of proposed trading and control strategies on disease spread.

The highly dynamic nature of the our trading model introduces challenges in terms of parameterisation for the Scottish trading system, namely due to the fact that farm-level stock quantities are unobservable in the data. In this chapter, therefore, a method for using the CTS data to parameterise our dynamic trading model is outlined in Section 4.2 and an analysis of the resulting parameterised system is explored to ensure that system- and farm-level properties are well characterised in our dynamic trading model. It will be shown that the parameterised system represents farms' trading properties to a very high degree of success, and accurately characterises qualitative and quantitative distributional properties at system-level. Disease spread via trade is introduced in Section 4.3 and alterations to trade and control strategies similar to those explored in Chapter 3 will be applied to the Scottish system, highlighting potential effective avenues for disease control on this real-world system.

4.2 Parameterising systems model of trade dynamics using farm-to-farm movement data

In this section we describe the challenges and our method for parameterising the trading model outlined in Chapter 3 Section 3.2 to the Scottish cattle trade system using the Cattle Tracing System (CTS) data. We show that an accurate parameter-

isation is possible and that farm-level properties can be captured by our dynamic model.

The fundamental challenge of parameterising our model is that the rates of partnership formation and trade are functions of dynamic, time-varying stock quantities, $\mathcal{D}_i(t)$ and $\mathcal{S}_i(t)$, which are not recorded in available data. While animal flows are readily observable in the data, farm-level demanded and available stock are hidden and the relationship between farm-level supply and demand and animal flows may be difficult to discover (preventing a simple mapping of the farm-level parameterisation from Chapter 2 to our supply and demand based trading model used here), as in the data farms maintain their animal flows in different ways, e.g. by purchasing from multiple farms, making frequent small batch trades, infrequent large batch trades, etc. In Chapter 2, parameterisation was more straightforward as rates were constant functions of farms' average annual in- and out-flows, so we had only to obtain values of a_i, δ_i, and b_i that replicated the frequency of partnership formations, cessations, and trades, respectively.

To parameterise our dynamic trading model, we take the parameterisation from Chapter 2 as an initial state, so we assume that farm-level equilibrium demand and supply is, on average, equivalent to their respective equilibrium stock generation rates, η_i^* and ζ_i^*. This assumption is likely to overestimate stock levels for farms that trade frequently, but underestimate stock levels for farms that do not trade frequently. Farms that trade frequently, e.g. more than once per year, accumulate less demand before it is satisfied (at least partially) via trade so that typically $\mathcal{D}_i(t) \leq \eta_i^*$), whereas farms that trade infrequently (less than once per year), will accumulate more demand before it is satisfied via trade so typically $\mathcal{D}_i(t) \geq \eta_i^*$. Nonetheless, using this initial state, we simulate our trading system to obtain per unit-time averages (for each farm) for the number of trading partnerships and number of trades. We then use these values to inform necessary adjustments to a_i and b_i (the parameters η_i^*, ζ_i^*, and δ_i are invariant to changes in farm-level supply and demand and so their values are readily observed from data as described in Chapter 2) in the following way:

$$a_i(s+1) = a_i(s)\frac{k_i^{in,data}}{k_i^{in}(s)}, \tag{4.1}$$

$$b_i(s+1) = b_i(s)\frac{\Phi_i^{data}}{\Phi_i(s)}, \tag{4.2}$$

where s is the s^{th} simulation (equivalently the s^{th} step in the fitting algorithm), $k_i^{in}(s)$ is the average number of trading partners for farm i in simulation s, $\Phi_i(s)$ is the average number of trades for farm i in simulation s, and $k_i^{in,data}$ and Φ_i^{data} are the number of trading partners and trades for farm i from the data, respectively. The ratios $k_i^{in,data}/k_i^{in}(s)$ and $\Phi_i^{data}/\Phi_i(s)$ are the factors quantifying the difference between the data and simulation for number of trading partners and number of trades for farm i in simulation s, respectively. We implicitly assume, therefore, that the number of trading partners and number of trades are monotonic functions of a_i and b_i, respectively (our method may still be applicable for non-monotonic functions if the initial values of a_i and b_i are sufficiently close to the true values). We then use the updated values for a_i and b_i and iteratively re-simulate the system and update a_i and b_i. These simulations are run to simulate trade dynamics in the modelled system for the period of time spanned by the observations so that numbers of trades and trade partners can be compared as described above. In addition, it is important to note that simulations are allowed to equilibriate before recording these measures since, as noted in Chapters 2 and 3 we assume that the observed data is representative of a system in equilibrium. We note here that we assume that the generation of stock is deterministic, so in an abritrary time interval $[t, t+\Delta t]$, farm i will generate $\eta_i(t)\Delta t$ demand and $\zeta_i(t)\Delta t$ supply. We choose Δt to be the largest time interval that allows for the farms with the largest η_i^* and ζ_i^* to generate one unit of demand and supply in this time interval, respectively. This was done due to the computational complexity of simulating our trading system, but does lead to predictable fluctuations in price and excess demand that operate on 9 year cycles, reflecting the duration of observations in the CTS used here.

Our iterative method for obtaining parameter values is somewhat analogous to an Expectation-Maximisation algorithm (EM algorithm). The EM algorithm calculates

an expectation for the log-likelihood given current parameter estimates, followed by computation of parameter values that maximise the expectation of the calculated log-likelihood. The two steps are then iteratively repeated until suitable parameter values are obtained [28]. Starting from an initial reasonable best guess, our method proceeds by calculating a discrepancy measure between simulations based on current parameter values (which plays the role of the log-likelihood here), and then uses this to make an adjustment to the parameter values. This process is iterated until convergence. Our method is able to parameterise farms in such a way that per-farm trading quantities are replicated in stochastic simulation, though we note that it does not explain the relationship between farm-level supply and demand and their respective animal flows. For farms that trade infrequently, in particular farms that only make one observed trade in the nine year period we consider from the CTS data, the above method requires multiple iterations to obtain suitable parameterisations. This is because these farms are susceptible to inherent stochasticity in simulation and long inter-event times, resulting in unit-time averages obtained from only a small number of observed events.

4.2.1 Assessing model fit at global and farm level

Figure 4.1 shows per-farm fits after a sequence of parameter iterations using the method outlined above. In general, simulation output is able to replicate desired trading behaviour for individual farms as described in the data. Correlations between data and simulated output of trade quantities for individual farms are given in Table 4.1, highlighting that in general our parameterisation replicates, at farm level, trading behaviour exhibited in the data extremely well. The area of poorest performance is that farm batch sizes are generally not as well represented by simulation. However there is still a statistically significant positive correlation between simulation and data (see Table 4.1). In particular it is farms that trade with large batch sizes that are not as accurately represented. However, such farms are generally those that make a small number of trades (typically 1 or 2) over the 9 year period of the observations, and as such are those farms that are challenging to parameterise.

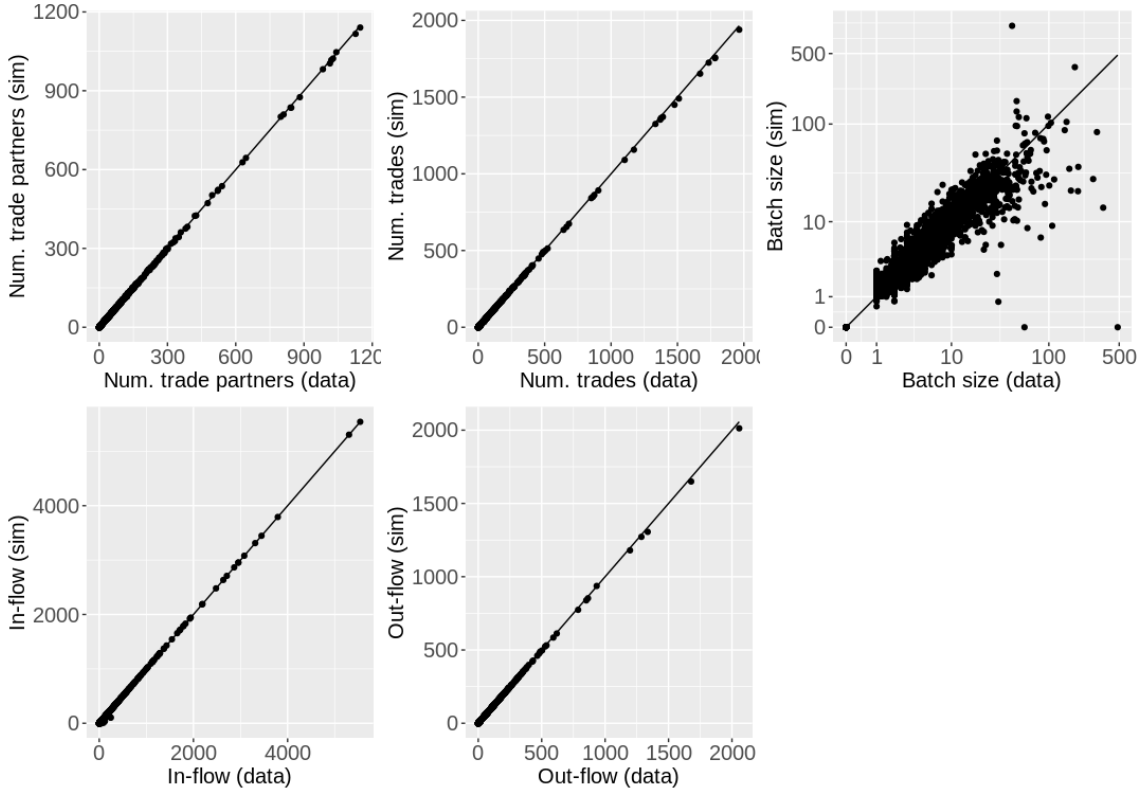

Figure 4.1: **Model fits to data** The average number of trade partners (top left), number of trades (top middle), batch size (top right), animal in-flow (bottom left), and animal out-flow (bottom middle) comparing respective values obtained from data against average values from stochastic simulation, where each point represents a farm in the system.

Quantity	**Correlation**	**p-value**
Trade partners	0.9999	$< 2.2 \times 10^{-16}$
Trades	0.9999	$< 2.2 \times 10^{-16}$
Batch size	0.4261	$< 2.2 \times 10^{-16}$
In-flow	0.9998	$< 2.2 \times 10^{-16}$
Out-flow	0.9999	$< 2.2 \times 10^{-16}$

Table 4.1: Table of correlation coefficients of trade quantities from simulation and data output for individual farms.

Figure 4.2 shows simulation output over time (of a single realisation) for our current optimal parameterisation, starting from an initial condition in which no trade partnerships are present but must be formed through parnership formations and ces-

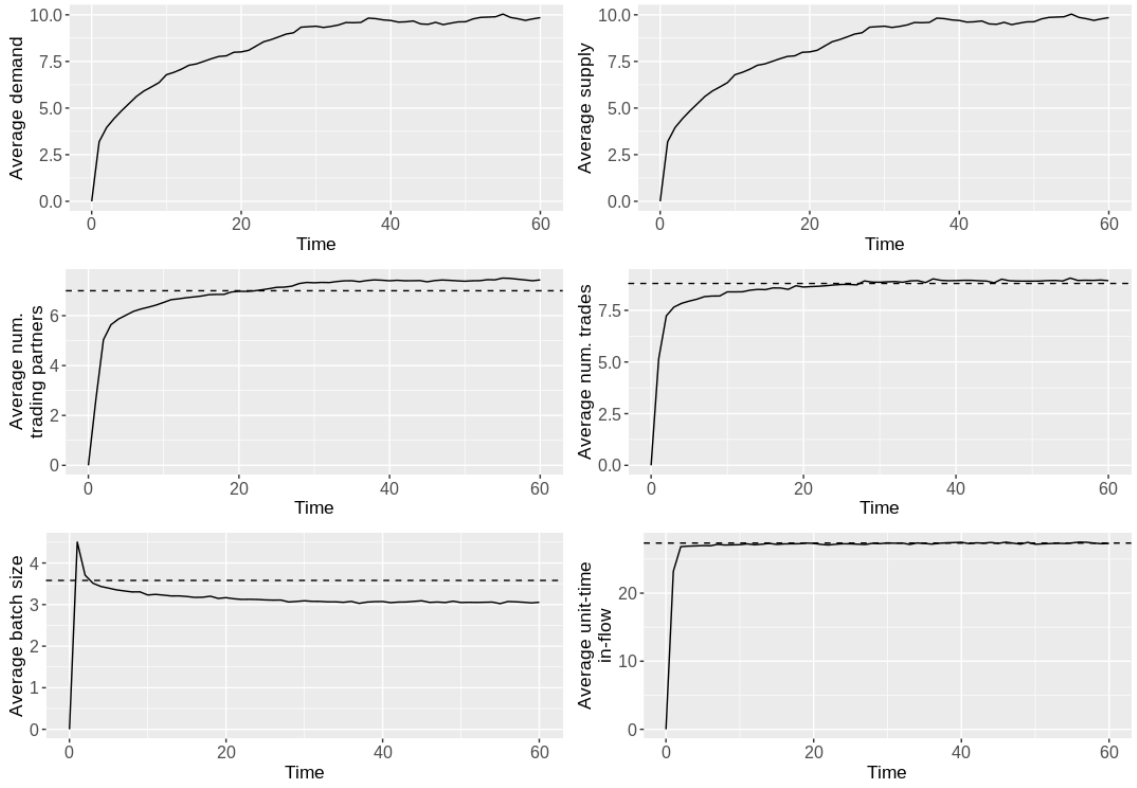

Figure 4.2: **Time evolution of trading system** System average per-farm demand (top left), supply (top right), number of trade partners (middle left), trades (middle right), batch size (bottom left), and animal in-flow (bottom right). In all cases dashed horizontal lines represent system averages obtained from data.

sations. After an initial burn-in period, where the system rapidly evolves to satisfy demand and ensure farm flows are maintained, the system reaches a stable equilibrium. We note that the equilibria differ slightly for number of trade partners and average batch size, so that in general in simulation farms have a greater number of trade partners and trade batches of smaller size than the data. To explore the properties of this equilibrium, we use the autocorrelation function as a measurement of the correlation between successive time points for each of our trading quantities. Figure 4.3 shows that for all trade quantities, autocorrelations show a general trend of tending towards zero, which is typically the case in stochastic dynamic systems [81]. Perhaps unsurprisingly, the dynamics of supply and demand operate on similar timescales (likewise for the dynamics of trades and partnership formation). Furthermore, it is interesting to note that the dynamics of supply and demand appear to

operate on longer timescales than those of trade partnership and trade dynamics, with the former having an autocorrelation length (time over which the ACF falls to 0.5) of around half a decade, whereas the autocorrelation lengths of partnership and trade dynamics are less than a year. However, whilst the form of these autocorrelations are informative of the dynamical properties of the trading system, their further analysis remains the subject of future work.

Considering distributional properties of the trading system (again noting that values are obtained once the simulations have reached equilibrium), Figure 4.4 highlights that our stochastic model is also able to replicate the distributions of trade quantities to a very high degree. More rigorously, we use the Kolmogorov-Smirnov test (K-S test) to measure the extent to which our simulation deviates from the data. To do so, the K-S test calculates the empirical cumulative distribution function (CDF) of each trade quantity from the data and from simulation output, and obtains the absolute maximum difference D between the simulation CDF and the data CDF. Table 4.2 shows the values of D for various trade quantities, and we conclude that there is no significant difference between the distribution of simulation output and data output.

Quantity	D	**p-value**
Trade partners	0.0541	$< 2.2 \times 10^{-16}$
Trades	0.0767	$< 2.2 \times 10^{-16}$
Batch size	0.0574	$< 2.2 \times 10^{-16}$
In-flow	0.0433	5.548×10^{-13}
Out-flow	0.0258	7.121×10^{-5}

Table 4.2: Table of K-S test maximum absolute difference between stochastic simulation output and data.

On a more granular scale, we consider the per-farm ratio of simulation output to data output for each of our trading quantities, i.e. we calculate

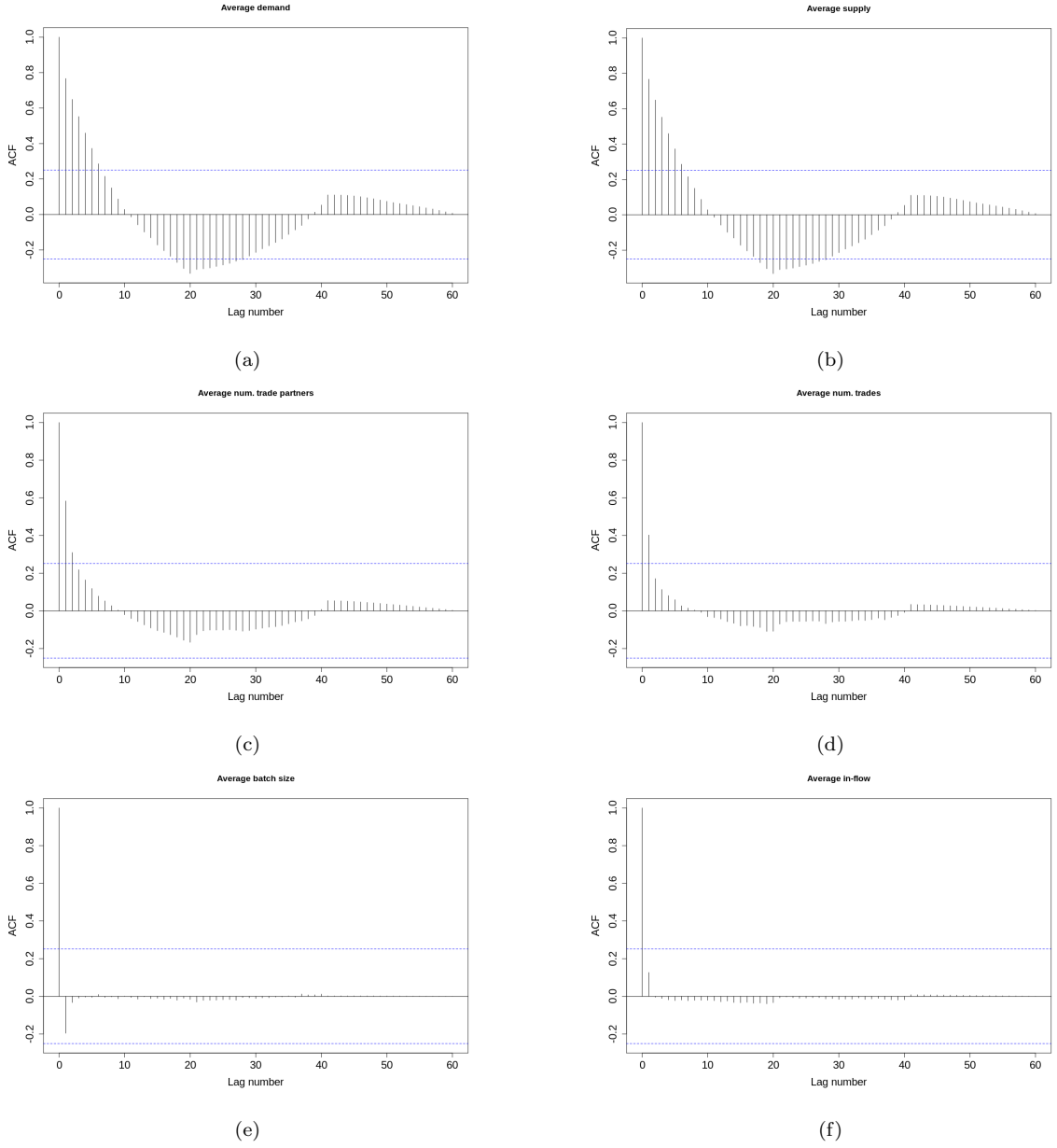

Figure 4.3: **Autocorrelations of trading system** Autocorrelation function plots for simulation output of trade quantities as presented in Figure 4.2. Blue lines represent a 95% confidence interval centered at 0.

$$\text{ratio} = \frac{x^{\text{sim}}}{x^{\text{data}}}.$$

If the simulation value matches the data value, then this ratio will be equal to 1, if it is smaller then the ratio will be smaller than 1, and if it is larger then the ratio will be greater than 1. From Figure 4.5, we see that, for all trade quantities,

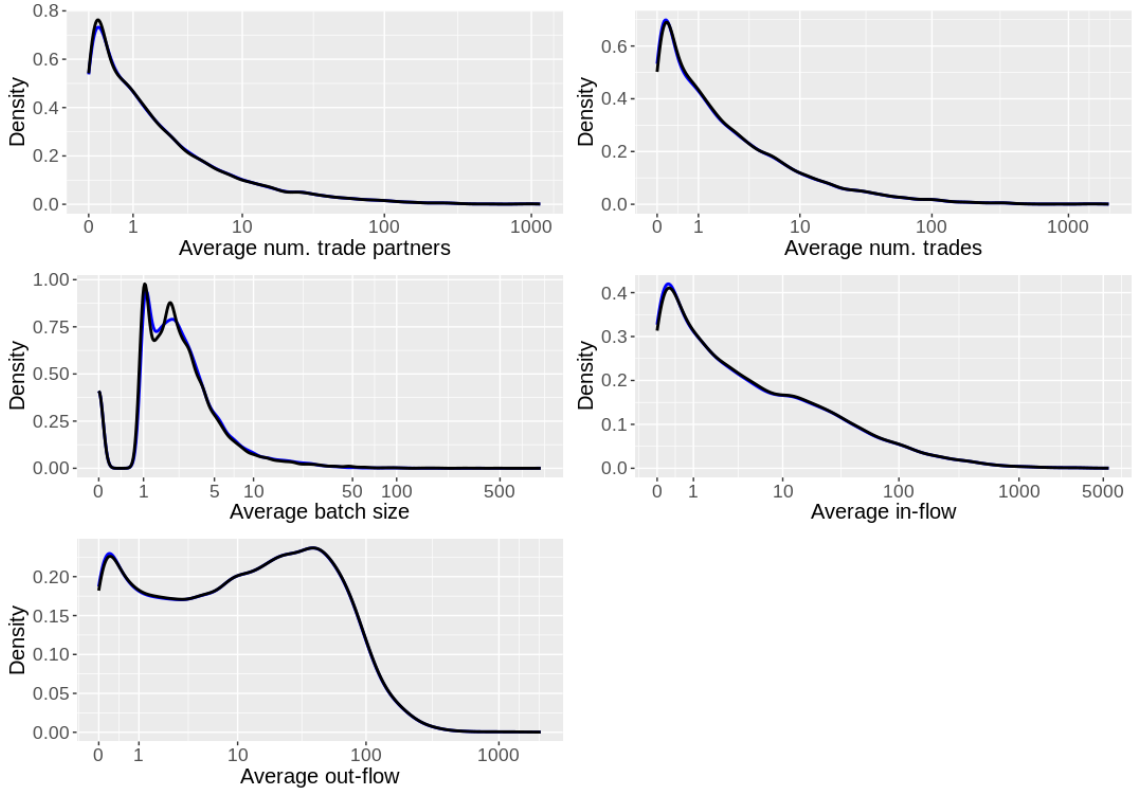

Figure 4.4: **Model distributions of trade quantities** Density distributions of average number of trade partners (top left), trades (top right), average batch size (middle left), average animal in-flow (middle right), and out-flow (bottom left). In all cases blue lines represent out from stochastic simulation, and black lines are obtained from the data.

farms generally operate in the simulation similarly to their observed behaviour in the data. Table 4.3 shows that there are some farm-level differences between the simulation and data, with not insignificant values for the Mean Absolute Percentage Error (MAPE), defined as,

$$MAPE = \frac{1}{N}\sum_{i=1}^{N}\frac{D_i - S_i}{D_i},$$

where N is the system size, and D_i and S_i are the data and simulation output for farm i for a given trade quantity, e.g. number of trade partners. Table 4.4 also highlights that the percentage of farms whose simulations outputs deviate greatly from the data are relatively small, with the number of trading partners being the most variable. Encouragingly, however, we see that farm in- and out-flows are very

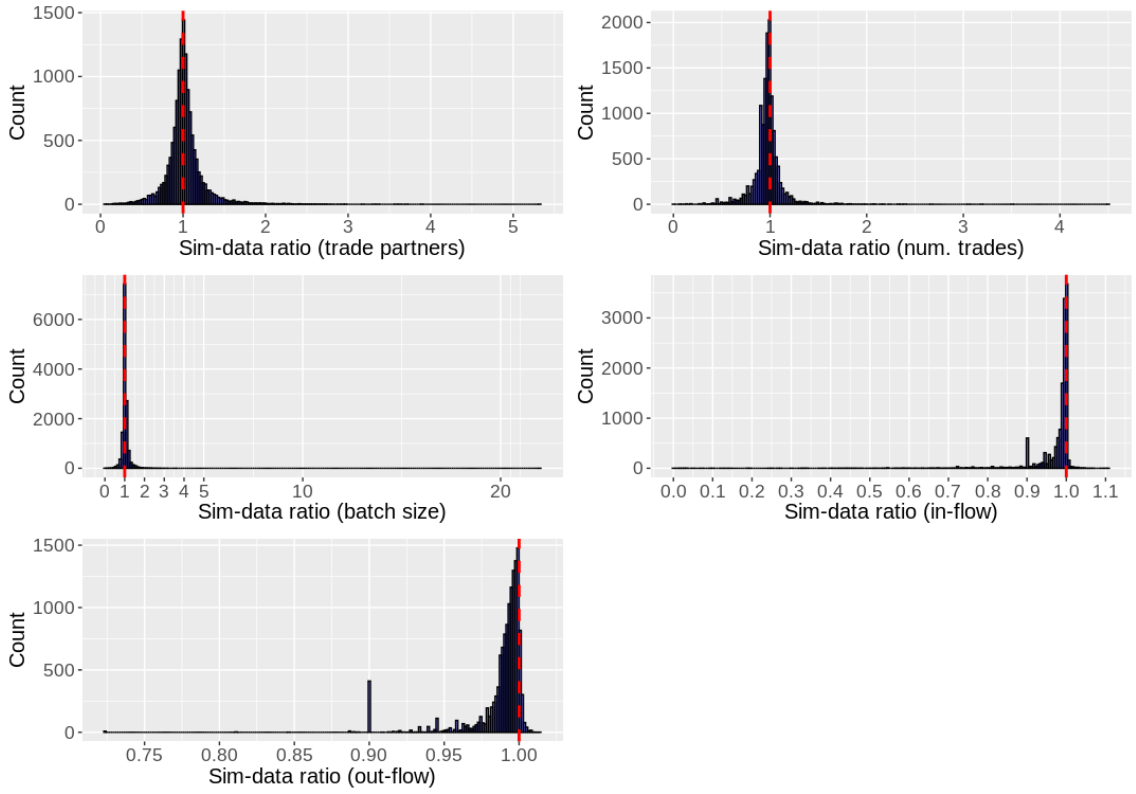

Figure 4.5: **Assessing farm-level differences in model compared to data** Distributions of the per-farm ratios between simulation output and data for the average number of trade partners (top left), number of trades (top right), the average batch size (middle left), and the animal in- and out-flows (middle right and bottom left, respectively). In all cases, red dashed lines represent a ratio of 1, indicating the simulation perfectly represents the data. Note the scales of x-axes differ between panels, emphasising small differences in farm flows.

well represented by simulation, clearly showing that our model is able to accurately match buyers and sellers so that farm flows are maintained.

Sim-data ratio	**Mean**	**S.D**	**MAPE**
Batch size	1.03	0.24	9.06
Num. trades	0.97	0.15	8.95
Num. trade partners	1.02	0.24	13.72
In-flow	0.97	0.07	2.77
Out-flow	0.99	0.02	1.32

Table 4.3: Table of sim-data ratios of trade quantities with their respective system-wide means, standard deviations, and MAPE, the mean absolute percentage error.

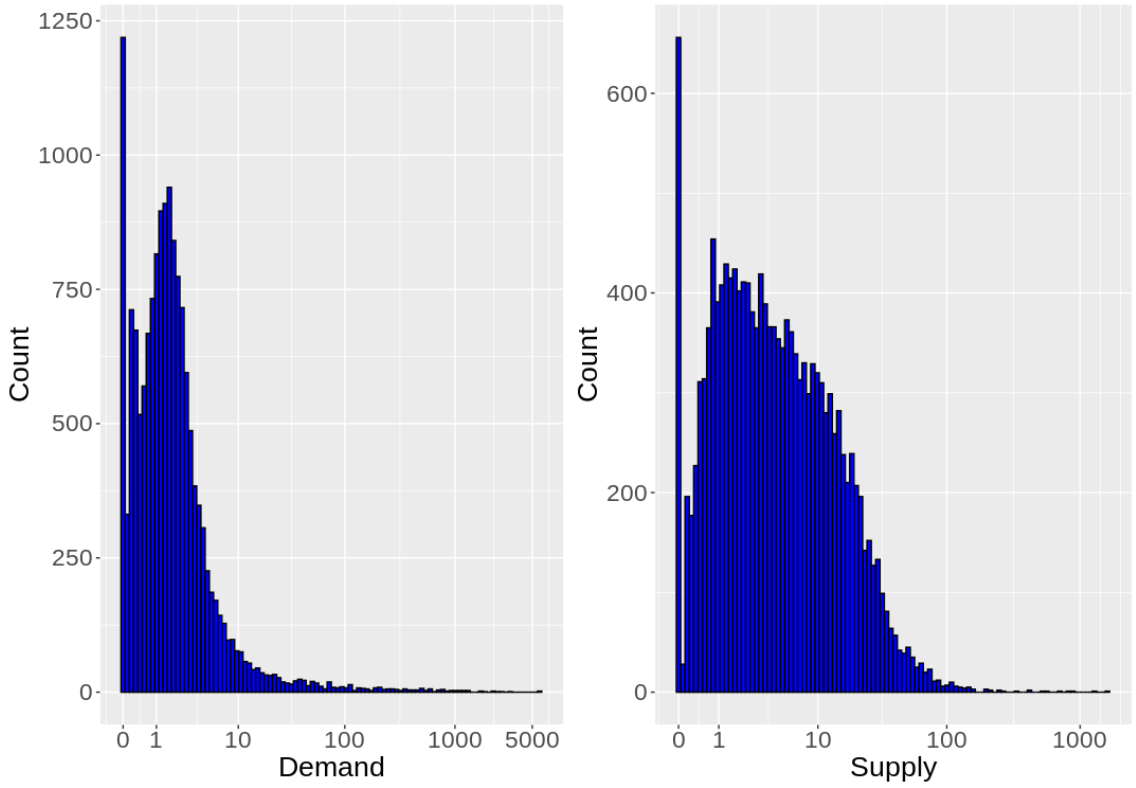

Figure 4.6: **Model distributions of supply and demand** Histogram of average farm-level demand (left) and supply (right) obtained from stochastic simulation of our trading system.

Sim-data ratio	**Num (%) $\leq$ 0.8**	**Num (%) $\geq$ 1.2**
Batch size	580 (3.77)	1162 (7.55)
Num. trades	1169 (7.60)	598 (3.89)
Num. trade partners	1436 (9.33)	1777 (11.55)
In-flow	362 (2.35)	0 (0)
Out-flow	13 (0.08)	0 (0)

Table 4.4: Table of the number (and percentages) of farms with sim-data ratios smaller than 0.8 and greater than 1.2.

4.2.2 Measuring farm stock quantities

It was highlighted in Section 4.2 that the fundamental challenge of paramterisation of our trading model was the inability to explicitly relate farm flows, that were used to parameterise the model in Chapter 2, to time-varying, farm-level stock quantities,

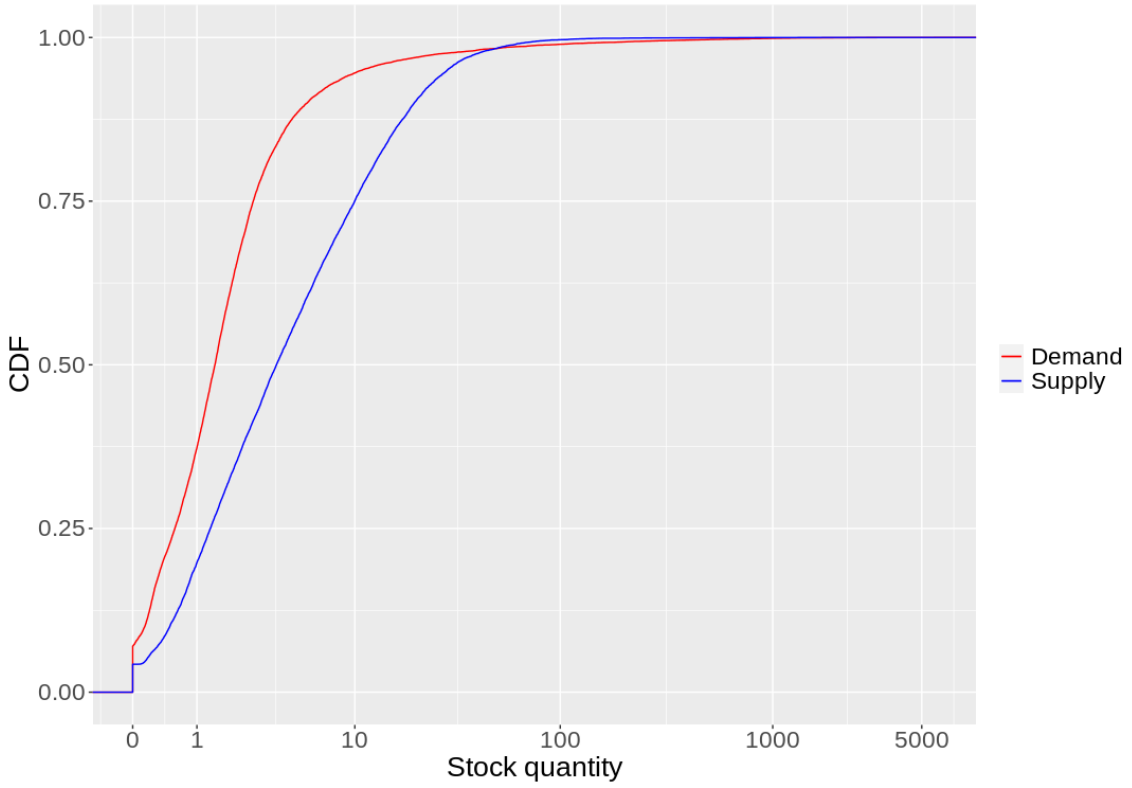

Figure 4.7: **Model cumulative distributions of supply and demand** Cumulative distribution of farm-level supply and demand stock, obtained from stochastic simulation of our trading system.

namely supply and demand. Our iterative method for parameterising the system, however, allowed us to achieve accurate, per-farm values for a_i and b_i, the frictional components of partnership formation and trade, respectively, without requiring us to define this relationship explicitly (the resulting simulations define an implicit relationship). We dedicate this section, therefore, to exploring potential relationships between farm-level stock quantities and trade behaviour. Referring to Figure 4.6, we see that the majority of farms have small unmet demand and available supply at any given time; indeed 94.58% and 75.04% of farms have, on average, demand and supply smaller than 10, respectively. Figure 4.7 shows that farms have, in general, smaller available supply than demand, suggesting that waiting times between trades are due primarily to the requirement for farms to accumulate supply, and also shows that our model is efficient in matching buyers and sellers so that available supply is minimised by efficient trade.

Exploring the relationship between farm-level trading patterns and stock quantities

(noting that our calculations are based on simulation output), we find there is little correlation between a farm's demand generation rate η_i^* and its average demand ($R^2 = 0.0303$), but there is a strong, significant, positive relationship between a farm's average batch size and its average demand ($R^2 = 0.4375$), indicating that farms with large demand generally trade in large batches. Conversely, there is a very strong relationship between a farm's supply generation rate ζ_i^* and its available supply ($R^2 = 0.9203$). This may be due to the fact that in our model farms have no agency in offloading supply, with trades and the formation of partnerships being initiated by the buying farm. Moreover, the partnership formation rate $\alpha_{ij}(t)$ nonlinearly increases with supply, so large supply farms are not disproportionately chosen as trade partners. This does not lead to divergences in excess demand, however, as is evident from Figure 4.8, showing that global excess demand is small and any imbalances in stock levels are quickly accounted for by appropriate alterations to price and stock generation rates. In addition, the average ratio of demand to supply, another measurement for imbalances in stock quantities, is very tightly constrained around 1.

Exploring whether high farm-level demand can be explained by an inability for farms to maintain their in-flow, we find that farms that do not maintain their in-flow relative to their expected in-flow from the data (the number of such farms is very small, see Table 4.4) generally have larger demand ($R^2 = -0.3453$) suggesting that unmet demand may be reduced for these farms if they were able to maintain their in-flows. Conversely, there is very little correlation between farm-level supply and the difference in out-flow from simulation compared to the data ($R^2 = 0.0976$) (see Figure 4.9).

4.3 Disease spread on Scottish cattle trading system

We now use the parameterised model to explore the dynamics of potential disease control in the Scottish cattle trading system. Disease is introduced and spreads via

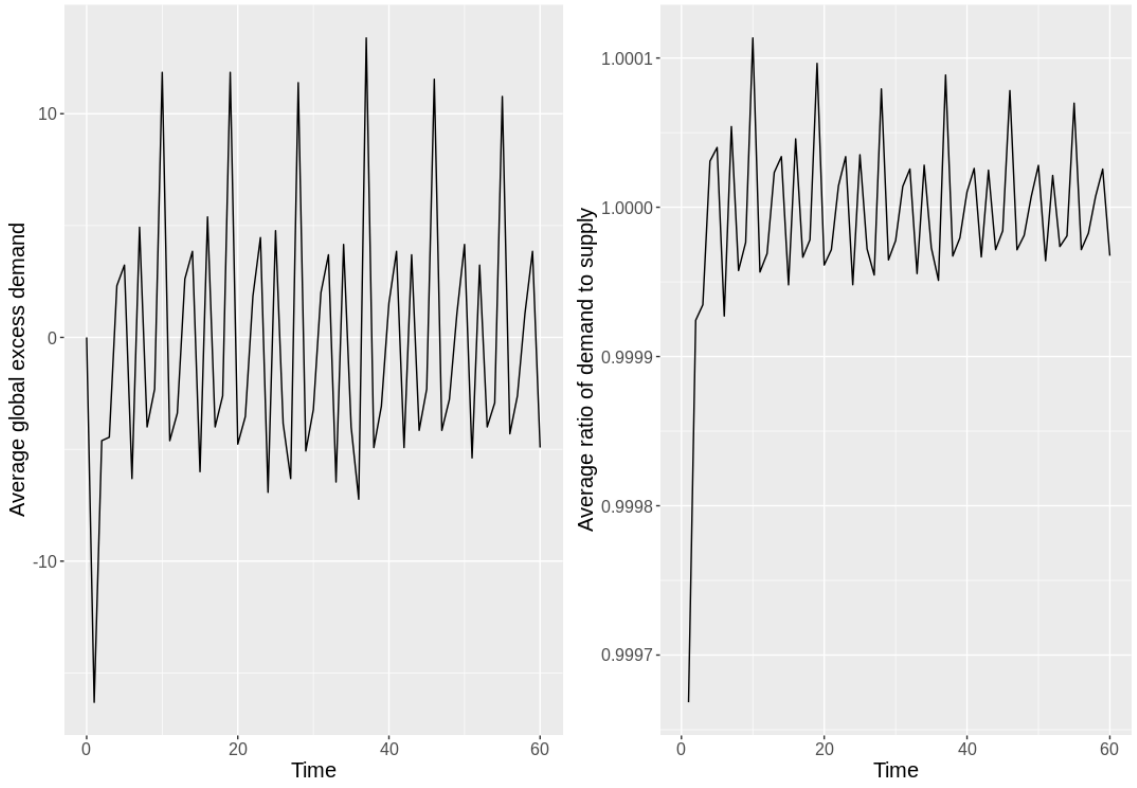

Figure 4.8: **Measuring model imbalances in supply and demand** The average system-wide excess demand (left) and the average ratio of demand to supply (right), obtained from stochastic simulation of our trading system.

trade in a way similar as in Chapter 3. We assume infected farms have a constant farm-level prevalence λ and recover with rate γ so that infected farms are infected for an exponentially distributed period with mean $1/\gamma$. If a susceptible farm i makes a trade with its infectious trade partner j of batch size θ, the probability that i becomes infected is simply the probability that at least one infected animal from j is chosen in the batch, which occurs with probability $1-(1-\lambda)^{\theta}$. Thus, larger batches have a greater probability of transmitting disease. In the scenarios presented below we assume $\lambda = 0.25$, and $\gamma = 1/3$, intended to represent a high prevalence disease that is highly persistent. Under current trading patterns of the Scottish trading system, our model predicts an equilibrium between-herd prevalence of approximately 55%, as opposed to approximately 88% for the homogeneous system studied in Chapter 3. This disparity highlights a number of important network characteristics that should be taken into account. Firstly, we assumed a system size of $N = 200$ in

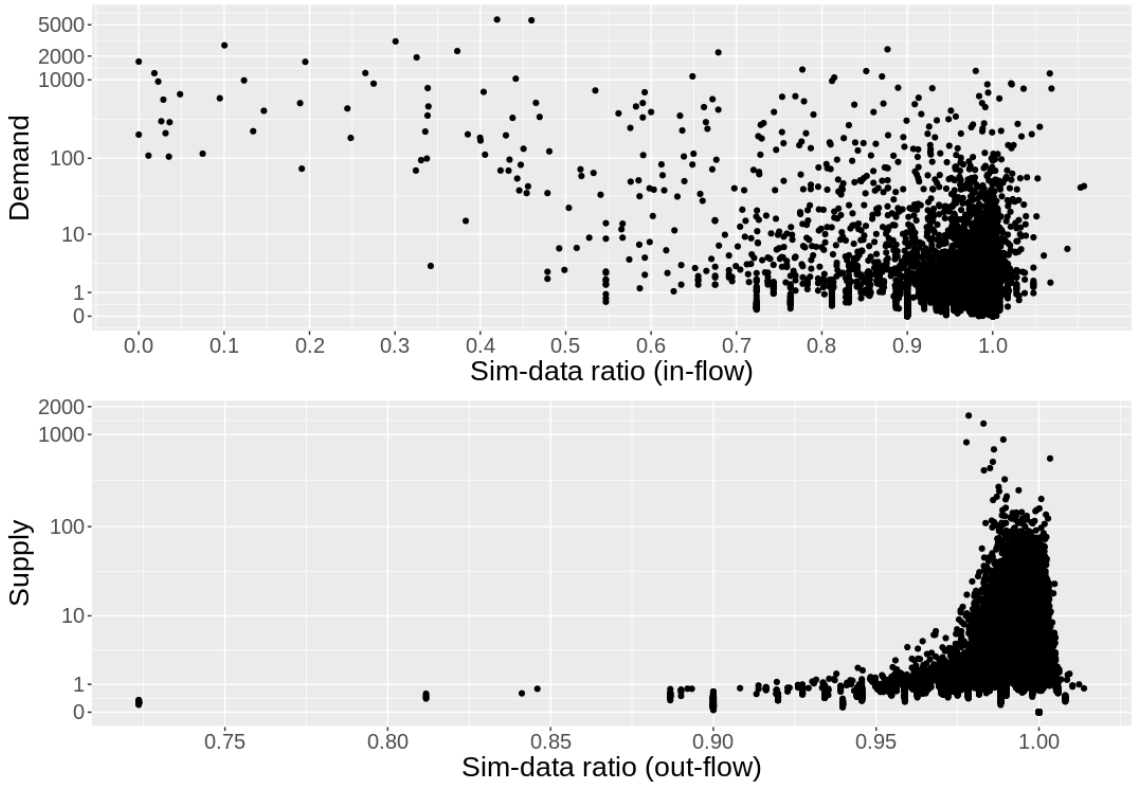

Figure 4.9: **Impact of model and data differences on farm-level supply and demand** Per-farm average animal in-flow against demand and out-flow against supply averaged over a 45 year period.

Chapter 3, as opposed to $N = 15386$ in the real-world system, and while the model was parameterised so that system-average properties of the Scottish system were replicated, this lead to a more densely connected network, allowing disease to spread more easily between farms. Secondly, the homogeneous structure of the network itself played a role, as all farms exhibited average system-level properties of the Scottish system. However, the Scottish system is highly heterogeneous, displaying scale-free properties, which are known to skew the mean. As such, trading patterns of farms in the homogeneous system are different from those of "typical" farms in the Scottish system.

4.3.1 Impact of changes to propensities of trade

In Chapter 3, we showed that simple changes to the propensitities for farms to form and end partnerships, and initiate trades by scaling the partnership formation rate

constant a_i, the cessation rate δ_i and the trade frictional constant b_i by, respectively, ε_a, ε_δ, and ε_b were insufficient in significantly reducing disease prevalence. The exceptions were in extreme scenarios where trading patterns were disturbed sufficiently to effectively halt trade in the case of ε_b, alter network structure so that farms have very few trade partners in the case of ε_a, and cause partnerships to last vanishingly small time periods in the case of ε_δ. This was in contrast of the results of Chapter 2 which suggested these changes could be highly effective. These differences are a result of the adaptive capacities of the trade system as represented in the model developed in Chapter 3. This flexibility is mediated by the dynamic nature of individual farm-level supply and demand levels which rise in response to restrictions represented by the above mentioned scalings of trade rate and partnership formation and duration. Since the relevant rates depend on both the intrinsic rate parameters and dynamically adjusted supply and demand, this allows the farm-level animal flows to be maintained, with potential prevalence reducing benefits of alterations to trade patterns being limited or nullified.

We now explore the potential for impacts on the structure of the Scottish trading system, and disease prevalence, resulting from such changes, i.e. to changes in friction associated with trading and the formation of trade partnerships, as well as to the duration of such partnerships. In particular, we consider two alterations: halving current rate constants for each individual farm, i.e. we set $\varepsilon = 0.5$, and doubling current rate constants for each individual farm, i.e. we set $\varepsilon = 2$. Considering first alterations to trading frequency via ε_b, we observe from Figure 4.10 that setting $\varepsilon_b = 0.5$ results in a noticeable decrease in trade frequency, however these trades occur with larger batch sizes, and farms have, in general, a larger number of trade partners. The opposite holds true when $\varepsilon_b = 2$, with farms trading more frequently and in smaller batches, and have fewer trade partners in general. In both scenarios, we note that farms flows are not disturbed, highlighting the ability for the modelled system to adapt and find new structures that enable farm flows to be maintained. Figure 4.11 shows that the effect on prevalence of changes to ε_b are small, with slight reductions in prevalence when $\varepsilon_b = 0.5$, and little to no increase when $\varepsilon_b = 2$. Recall

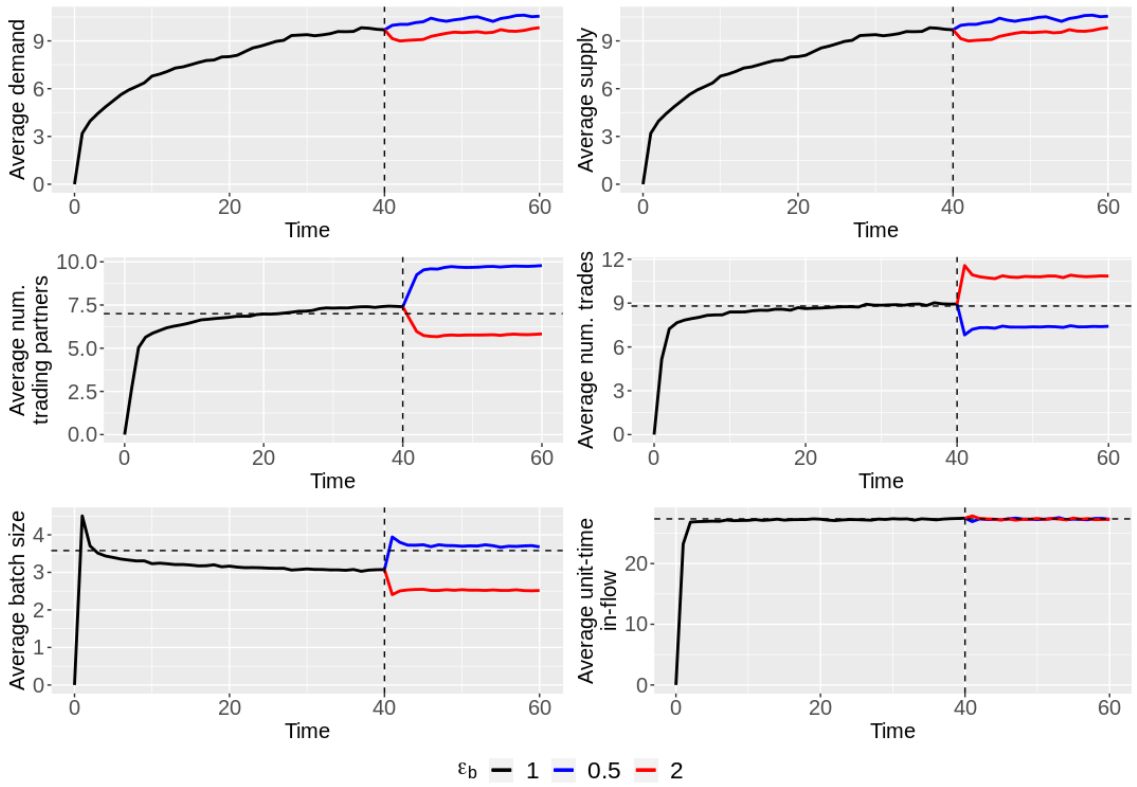

Figure 4.10: **Impact of trade friction on Scottish trading system** System-averages for various trade quantities when each farm's trade rate constant b_i is scaled by various values of ε_b. Vertical dashed lines represent the point at which ε_b is changed, and horizontal dashed lines represent respective system-wide averages for various trade quantities as obtained from the CTS data.

that this was also observed in the homogeneous adaptive systems model of Chapter 3. The fact that prevalence is largely unaltered suggests that simple interventions designed to impact one aspect of trade behaviour, e.g. to increase trade friction, can result in complex changes to trade networks and unpredictable changes in prevalence, due to farms finding new avenues to maintain animal flows. It may also suggest that the Scottish trading system is currently operating in a very low frictional trading regime in the sense that changes to trade friction make little difference to overall outcome in terms of net flows of animals. This implies that the system dynamic (the market) is sufficiently flexible to overcome the effect of increased friction in one or other constituent activity, in this case trade. This may also be inferred from Figure 4.4, when considering batch sizes. Most farms buy animals in batches of 1, i.e. a single animal is bought per observed trade, whereas if trade friction was very high,

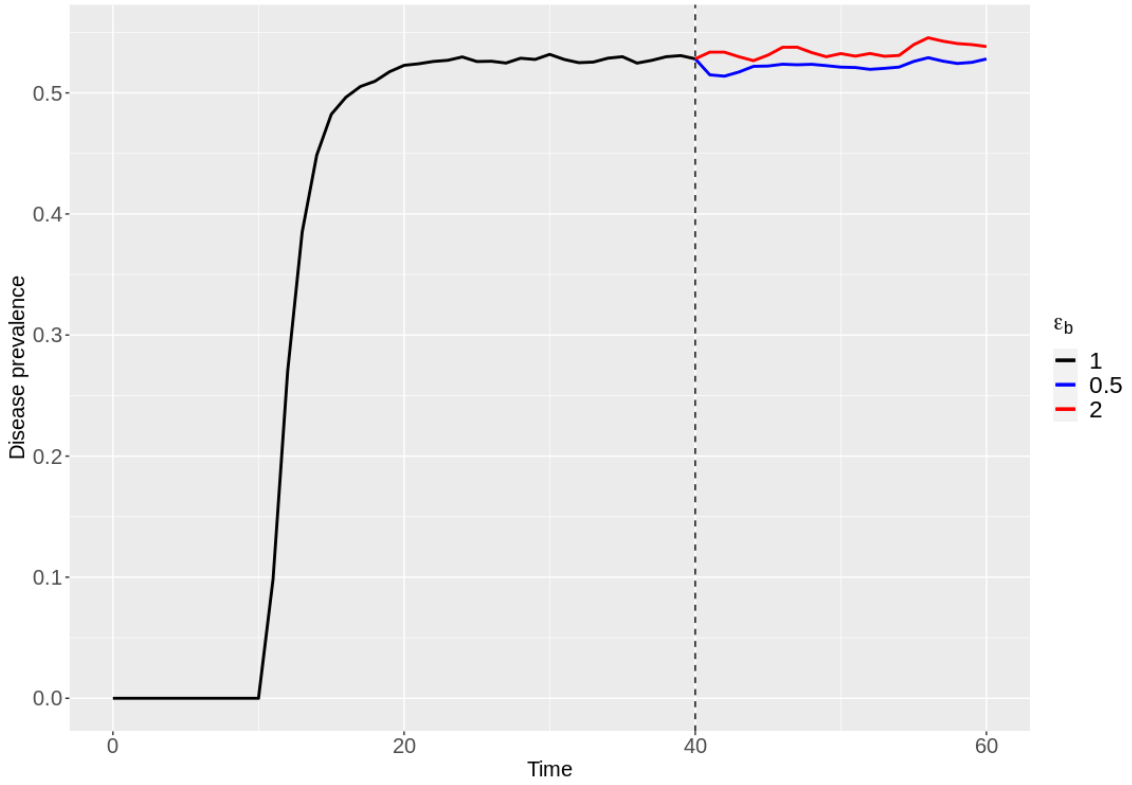

Figure 4.11: **Impact of trade friction on disease prevalence** System-wide disease prevalence when each farm's trade rate constant b_i is scaled by various values of ε_b. Vertical dashed lines represent the point at which ε_b is changed.

it might be expected that farms would generally purchase larger batches.

Considering now alterations to the propensity for farms to form trading partnerships via ε_a, we again consider scenarios where $\varepsilon_a = 0.5$, so that farms generally form fewer partnerships, and $\varepsilon = 2$ so that farms form more partnerships. From Figure 4.12, when $\varepsilon_a = 0.5$ the trading system shifts to one which the methods of Chapter 2 would suggest is highly favourable for reducing disease prevalence; farms have fewer trade partners, and trade less frequently with larger batches. Conversely, when $\varepsilon_a = 2$, the system shifts to an unfavourable structure, with farms having a larger number of trade partners, and trade more frequently in smaller batches. Figure 4.13 shows, however, that while disease prevalence is reduced and increased when $\varepsilon = 0.5$ and $\varepsilon = 2$, respectively, the magnitude of these changes are small. Again, this result was highlighted in Chapter 3, with significant alterations to ε_a required to reduce disease prevalence. We note that in the case of $\varepsilon_a = 2$, farm-level stock

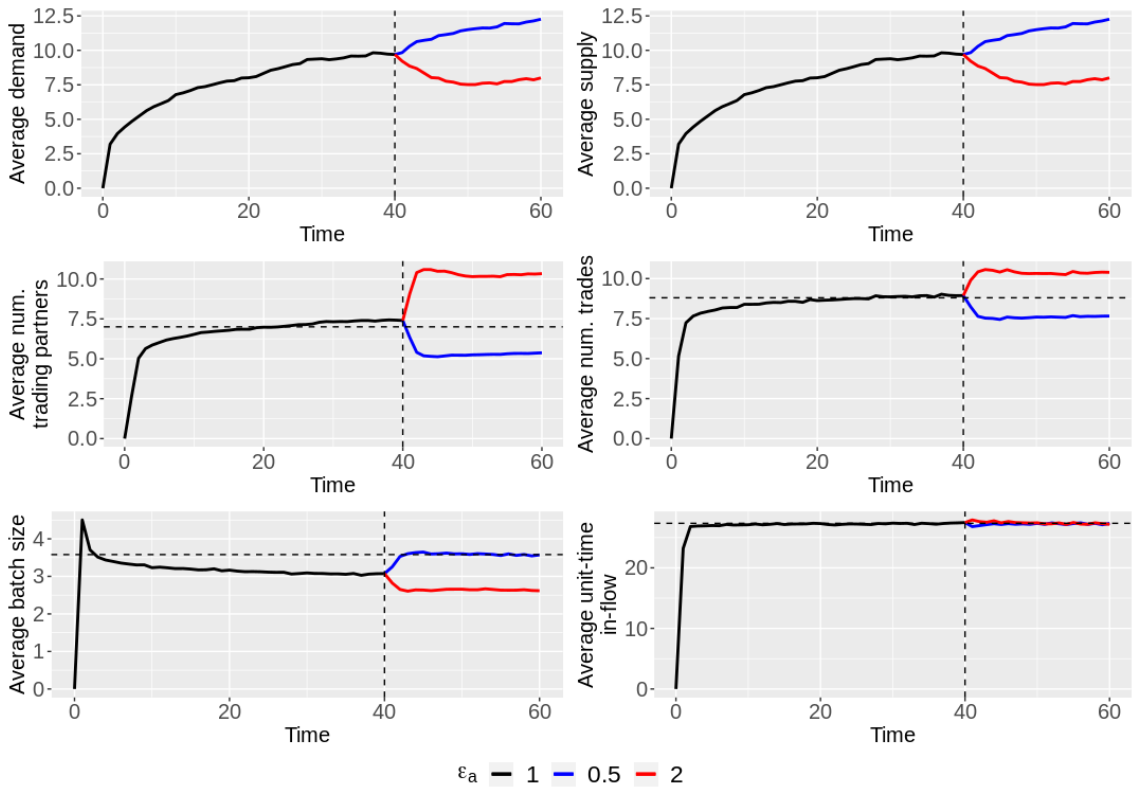

Figure 4.12: **Impact of partnership formation friction on Scottish trading system** System-averages for various trade quantities when each farm's partnership formation rate constant a_i is scaled by various values of ε_a. Vertical dashed lines represent the point at which ε_a is changed, and horizontal dashed lines represent respective system-wide averages for various trade quantities as obtained from the CTS data.

quantities are reduced significantly, as farms have a greater number of available suppliers from whom to purchase stock. Our model, therefore, suggests there may be scope for changes to the Scottish cattle trading system, allowing farms to form a greater number of trade partnerships, as this appears to have only small implications for disease prevalence.

Finally, we consider alterations to the duration of partnerships via ε_δ, and again assume two scenarios: $\varepsilon_\delta = 0.5$ so farms maintain trade partners for twice as long, and $\varepsilon_\delta = 2$ so partnerships last half as long as they currently do. Figure 4.14 shows that in the case where $\varepsilon_\delta = 0.5$, farms possess a larger number of trade partners, trade more frequently and in smaller batches. This leads to reductions in farm-level stock quantities as farms have a larger number of trade partners and those partners

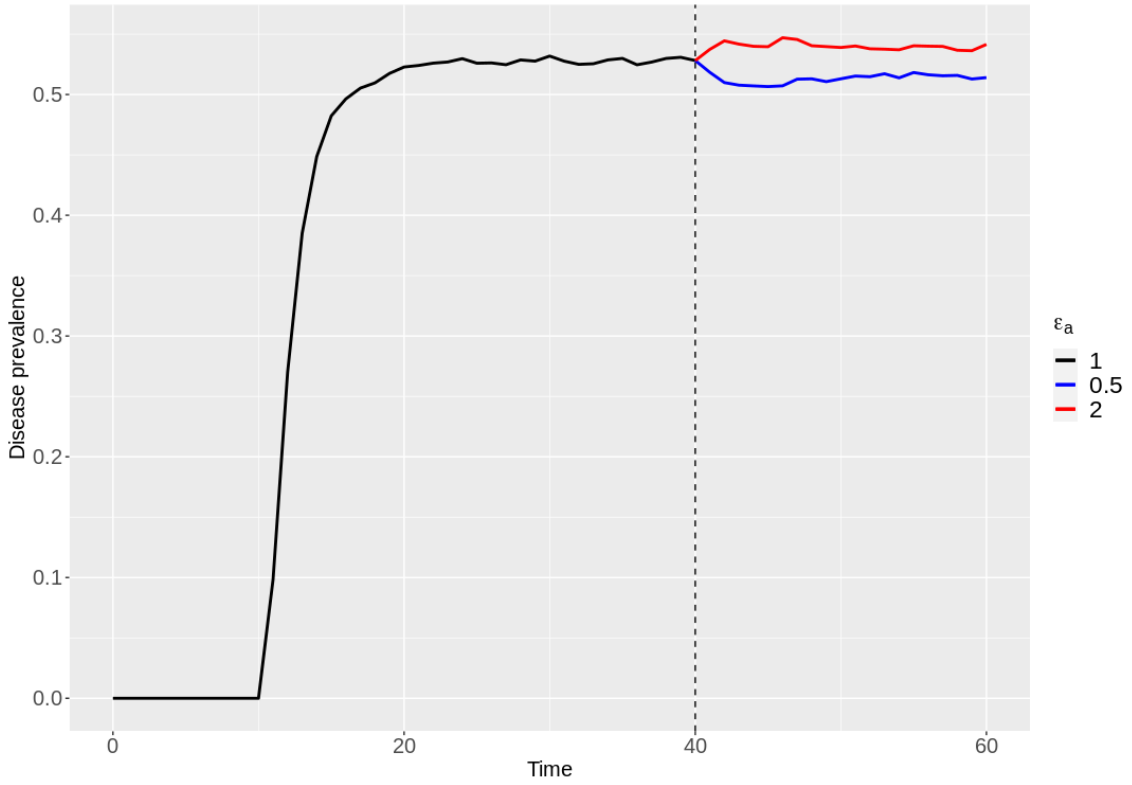

Figure 4.13: **Impact of partnership formation friction on disease prevalence** System-wide disease prevalence when each farm's partnership formation rate constant a_i is scaled by various values of ε_a. Vertical dashed lines represent the point at which ε_a is changed.

remain as partners for a longer period of time, allowing a greater level of supply depletion before the partnership ends. When partnerships last smaller durations, i.e. when $\varepsilon_\delta = 2$, farms have fewer trade partners, trades occur less frequently and are of larger batch size. This results in greater available supply and unmet demand, as farms wait longer before trades occurs, leading to greater accumulation of stock. The effect on prevalence is, again, small and considering Figure 4.15, longer lasting partnerships result in a small increase in disease prevalence, and shorter duration partnerships resulting in a small decrease in prevalence.

To conclude, it appears the Scottish trading system is resistant to simple changes in farm propensities to alter trading patterns, with even substantial alterations in network structure resulting in little to no significant changes in disease prevalence. This is because a simple change in the frequency of trade, for example, results in changes to farm-level stock quantities, and the system adapts itself and finds a new

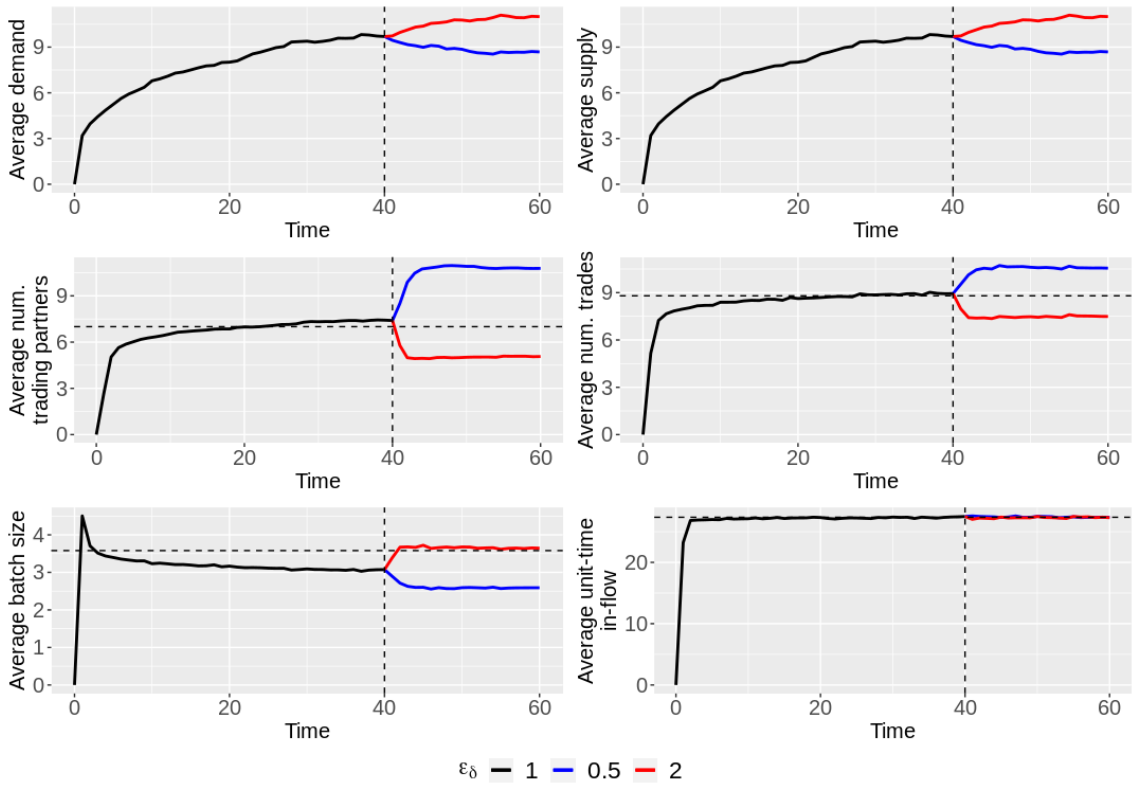

Figure 4.14: **Impact of partnership durations on Scottish trading system** System-averages for various trade quantities when each farm's partnership cessation rate constant δ_i is scaled by various values of ε_δ. Vertical dashed lines represent the point at which ε_δ is changed, and horizontal dashed lines represent respective system-wide averages for various trade quantities as obtained from the CTS data.

network structure that mitigates the effects of these changes to trade. Such changes to network structure in response to legislative changes to trade, and the implications they have on disease spread, have been observed for the UK cattle trading network, finding these changes to network structure have increased the susceptibility for disease spread on the UK network [44, 109, 115].

4.3.2 Whole batch testing and rejecting

In Chapter 3, we showed that animal batch testing through trade may be an effective strategy, though its effectiveness was dependent on both test sensitivity (the probability that an infected animal tests positive), and the batch rejection strategy employed. We found that whole batch rejection, whereby farms reject entire batches

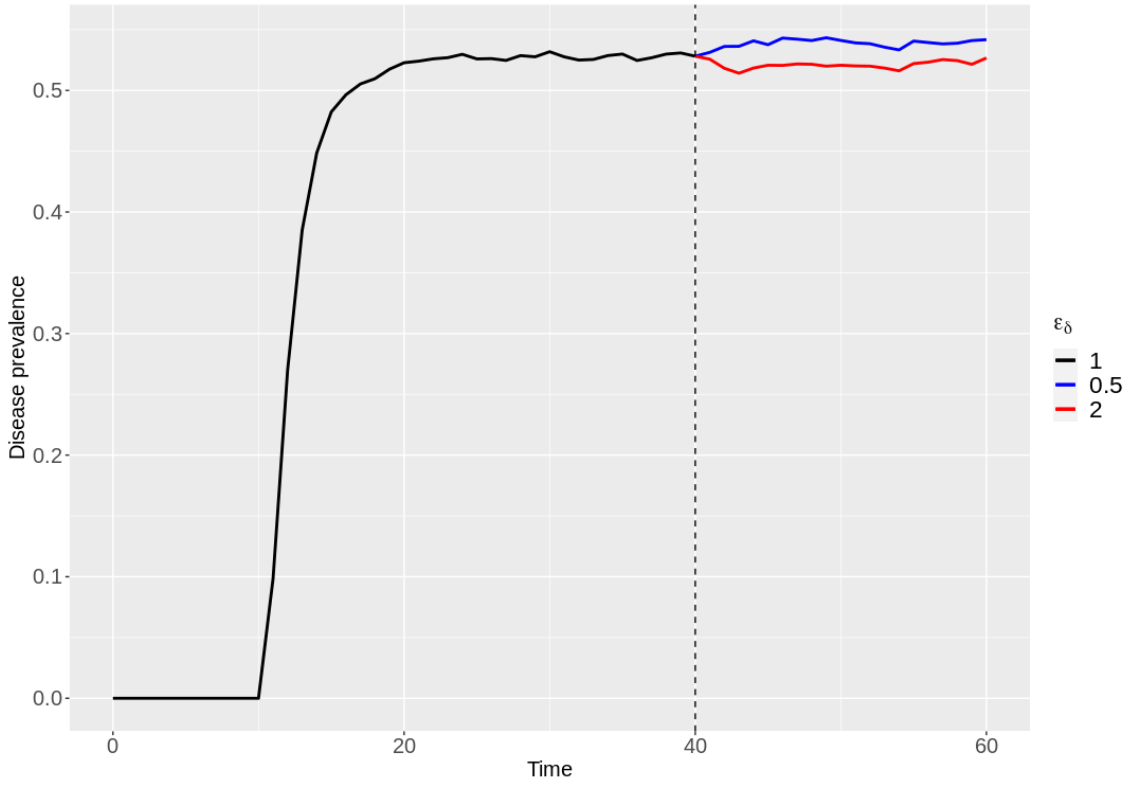

Figure 4.15: **Impact of partnership durations on disease prevalence** System-wide disease prevalence when each farm's partnership cessation rate constant δ_i is scaled by various values of ε_δ. Vertical dashed lines represent the point at which ε_δ is changed.

if a single animal tests positive, was more effective than individual animal rejection, whereby farms reject single animals if they test positive, in reducing disease prevalence for all test sensitivities, and could eradicate disease for smaller test sensitivities. We now explore the potential for whole batch rejection to reduce disease prevalence on the Scottish system for various selected test sensitivities.

Figure 4.16 shows the impact of whole batch rejection on system-wide trade quantities, with larger test sensitivities causing larger shocks to the system. In particular, at sensitivity $\tau = 1$, testing causes price to more than double initially, and farms report net losses, though these shocks are temporary due to the detection of infected animals and consequent rejection of batches, and trading patterns return to pre-testing equilibrium values. Qualitatively similar behaviour is observed when $\tau = 0.9$, though under this sensitivity the trading system does not return to pre-testing values as quickly. When $\tau = 0.5$ and $\tau = 0.1$, the trading system exhibits

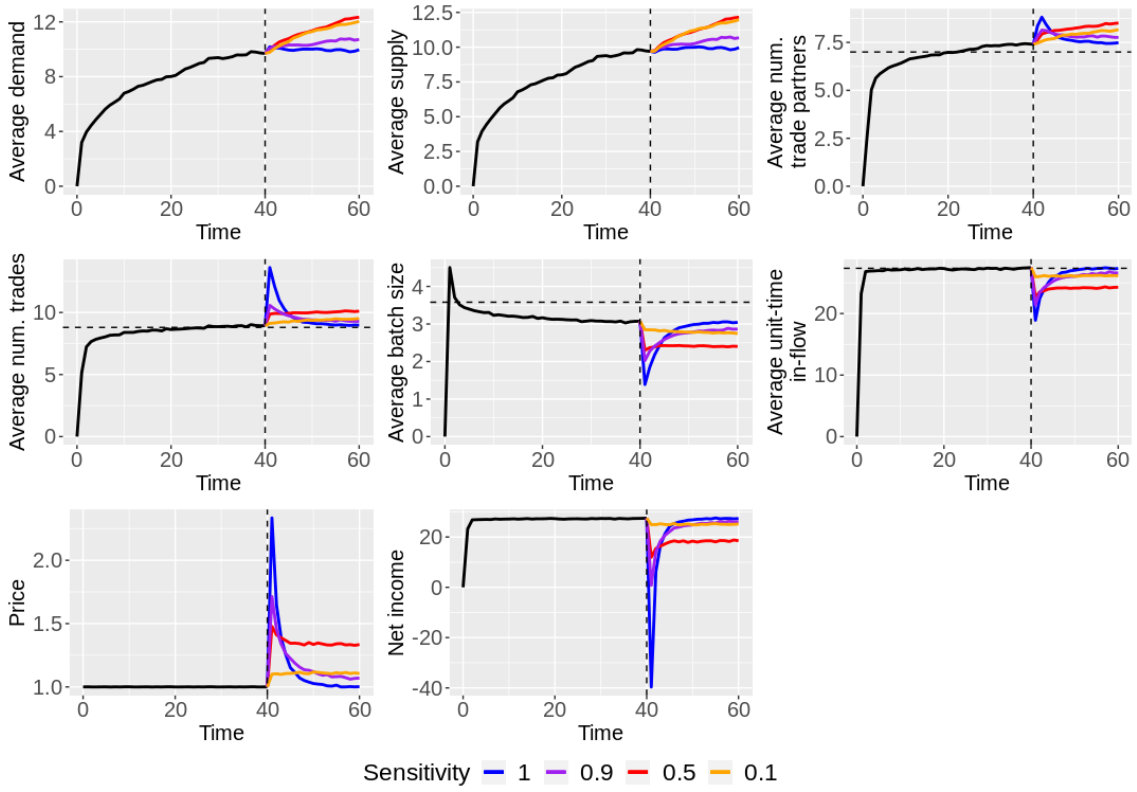

Figure 4.16: **Impact of whole batch rejection on Scottish trading system** System-averages for various trade quantities when whole batch testing and rejecting is enforced, for various test sensitivities.

long-term disturbances, with farms unable to maintain their in-flow, and increased prices and less net income observed. Figure 4.18 shows that testing causes significant transitory imbalances in stock levels for $\tau = 1$ and $\tau = 0.9$, due to the initial rejection of batches leading to varying levels of stock depletion at farm level following a trade. For $\tau = 0.5$ and $\tau = 0.1$, these imbalances are longer lasting, with large persistent excess demand observed, though the magnitude of the disturbances are smaller for $\tau = 0.1$ than $\tau = 0.5$. These different system-level responses to testing are due to the ability for testing to remove disease. When $\tau = 1$, all trades with infected farms result in the batch being rejected, and infected farms cannot spread infection. This results in rapid reduction in disease prevalence, and eventually eradication, so that trading patterns return to pre-testing values. When $\tau = 0.9$, we observe similar rapid reduction in disease prevalence, however complete eradication is not possible in the time period considered. While disease could not be fully eradicated, preva-

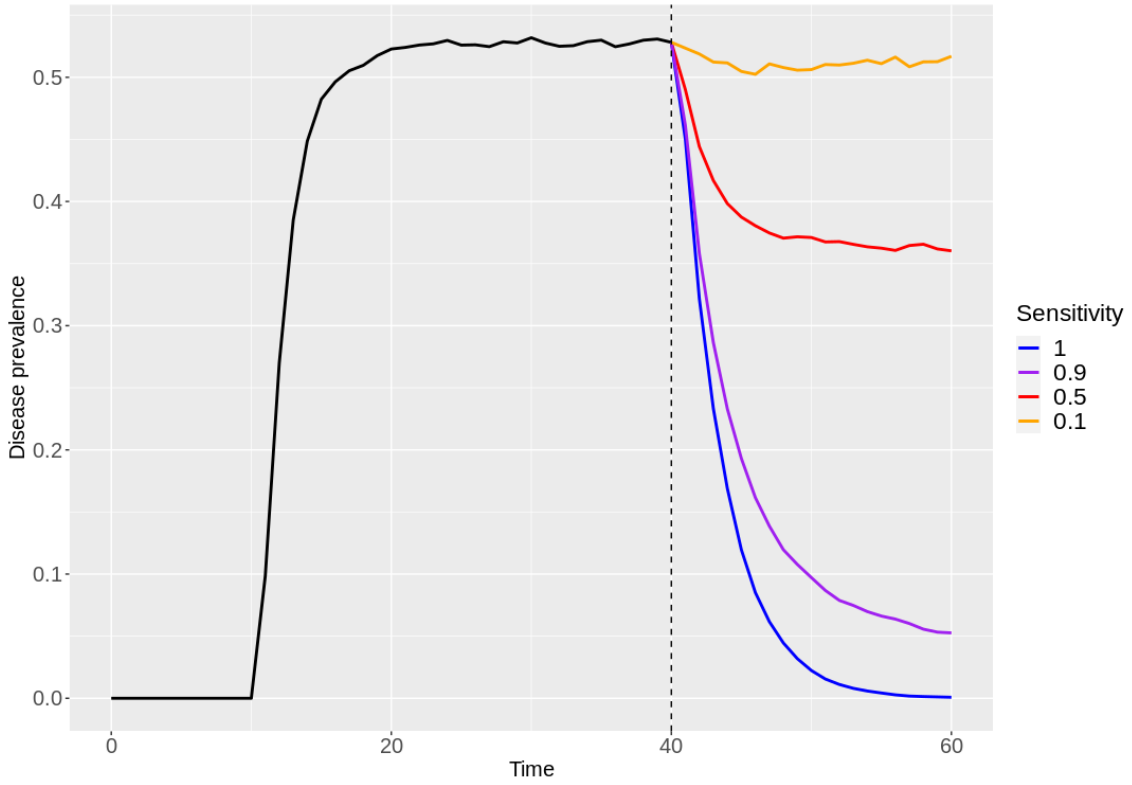

Figure 4.17: **Impact of whole batch rejection on disease prevalence** Effect of whole batch testing and rejecting on system-wide disease prevalence for various test sensitivities.

lence is reduced to sufficiently low levels that batch rejections become increasingly rare and trading properties return to near pre-testing equilibrium values. In the case where $\tau = 0.5$ or $\tau = 0.1$, testing still reduces disease prevalence, however testing alone is insufficient in eradicating disease due to a sufficient number of infected batches avoiding detection and allowing disease spread. This inability to eradicate disease results in permanent disturbances to trading patterns and associated costs.

The testing and rejection of animal batches may therefore be an effective control strategy for the Scottish cattle trade system, though only when animal tests are of high sensitivity. For low sensitivities, disease cannot be eradicated through testing alone and leads to long-term disturbances to the trading system, in particular increased prices and lower farm net income.

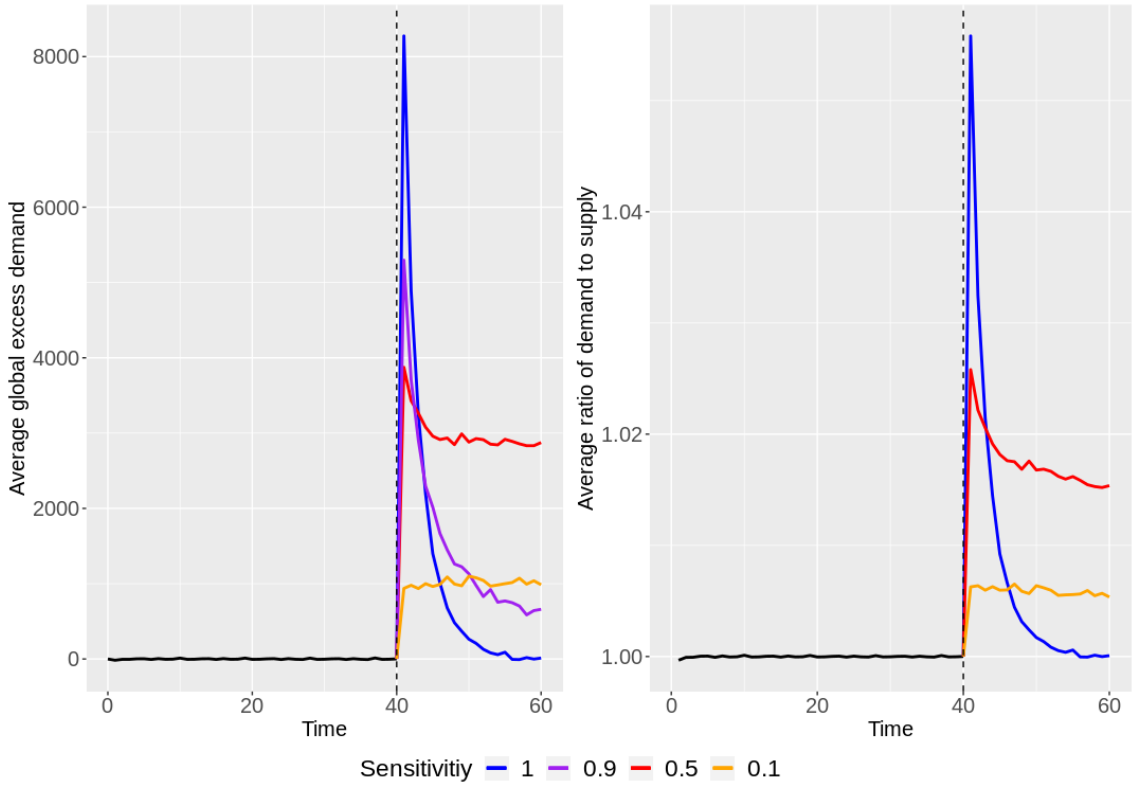

Figure 4.18: **Impact of whole batch rejection on stock imbalances** Impact of batch testing and rejection for various test sensitivities on imbalances in stock quantities (left) and the ratio of system-average demand to supply (right).

4.3.3 Whole batch testing and rejecting with a global risk aversion strategy

Recall from Chapter 3 that risk aversion, where farms avoid farms deemed high-risk, modulated through batch testing, was an effective combination control strategy that could further reduce disease prevalence compared to testing alone. We now explore the potential for a global risk aversion strategy to further reduce disease prevalence within the Scottish cattle trade system (we omit individual-based risk aversion due to computational limitations for a system of $N = 15386$ farms, and due to the fact that the results of Chapter 3 showed global sharing of information was more effective in reducing prevalence).

In the global aversion regime, there is a system-wide vector of weights $\mathbf{W}$ that represents knowledge of the empirically determined risk level associated with each

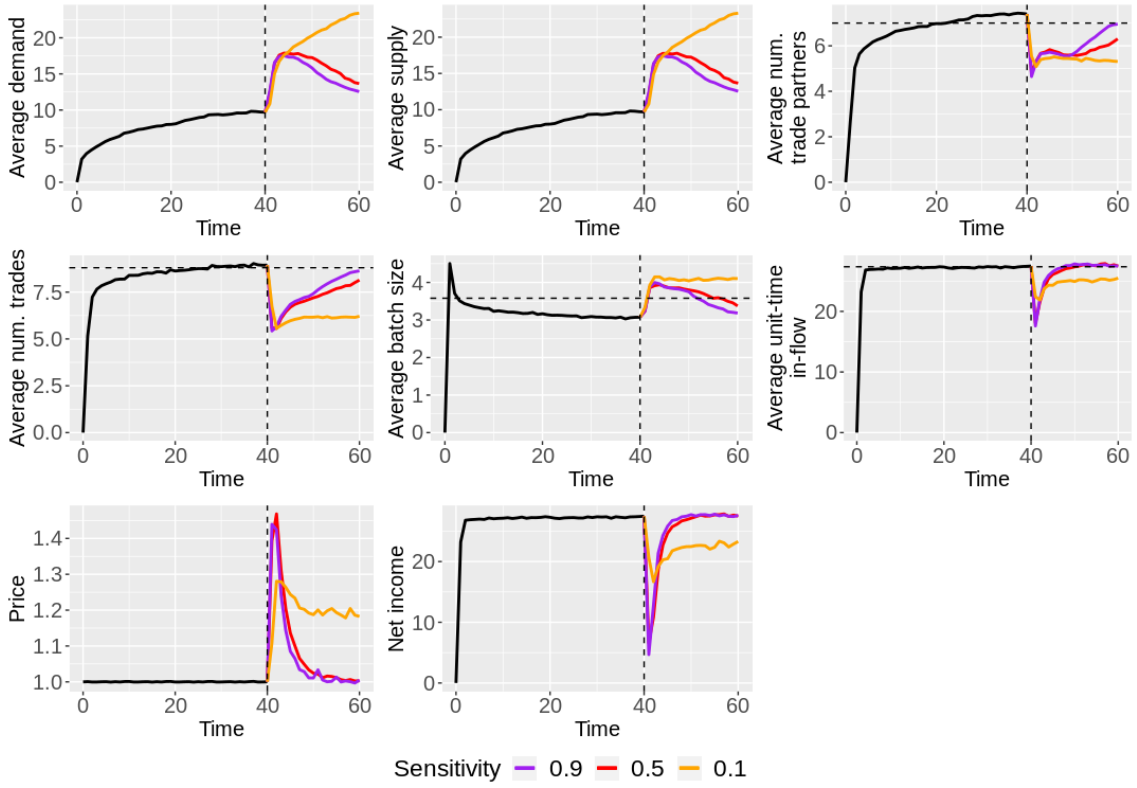

Figure 4.19: **Impact of global risk aversion on Scottish trading system** System-averages for various trade quantities when whole batch testing and rejecting is enforced which informs a global risk aversion strategy, for various test sensitivities.

selling farm. In this model we assume that this information is used to determine alterations for farms to form and end trade partnerships, and to trade with a given farm. By default the elements of $\mathbf{W}$ take value 1, however trades with a farm, j, that result in detection of infected animals alter the value of weights to some value ω (we use $\omega = 0.1$ in all cases here to represent a large level of risk aversion). When this occurs, the rate of partnership formation, cessation, and trade become

$$\alpha_{ij}(t) \to \omega\alpha_{ij}(t),$$
$$\delta_{ij} \to \omega^{-1}\delta_{ij},$$
$$\varphi_{ij}(t) \to \omega\varphi_{ij}(t),$$

respectively, for all farms i. Thus, information on high-risk farms is shared throughout the system, and all farms have a tendency to avoid such high-risk farms in

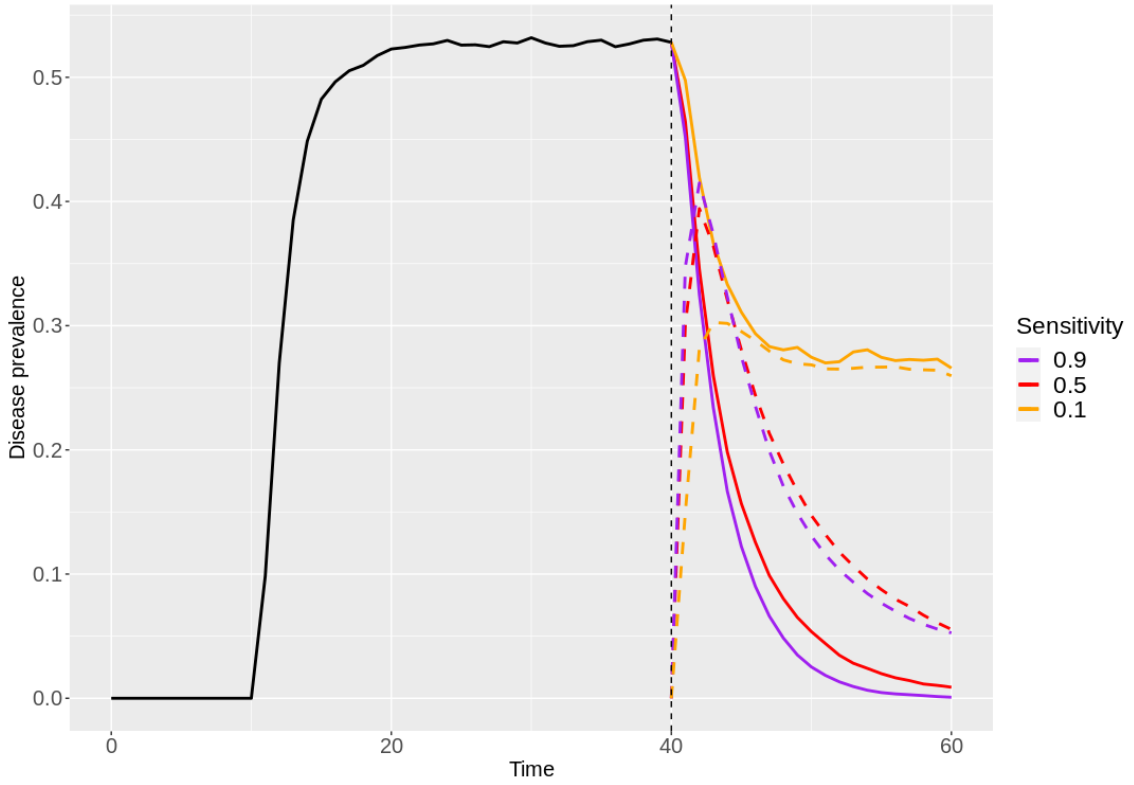

Figure 4.20: **Impact of global risk aversion on disease prevalence** System-wide disease prevalence when whole batch testing and rejecting is enforced which informs a global risk aversion strategy, for various test sensitivities. Dashed lines represent system-wide perceived prevalence, the fraction of the system with weight $\omega < 1$.

similar ways. In the global aversion regime, farms are able to preemptively avoid high-risk farms due to the sharing of information on risk, which differs from the individual-based aversion regime, as in that case farms necessarily must directly trade and detect an infected batch before they would deem a supplier high-risk and alter their trading patterns. As in Chapter 3, we assume that repeat trades with high-risk farms increase their weight in steps of ω, until the weight of the high-risk farm returns to 1.

Introducing global risk aversion alters trading behaviour compared with testing alone, regardless of test sensitivity. Considering Figure 4.19, global risk aversion perturbs farm-level stock quantities to a greater degree than testing alone, with a general increase in supply and demand, especially for test sensitivity $\tau = 0.1$, in which long-term consistent increases in stock are observed. This is because test-

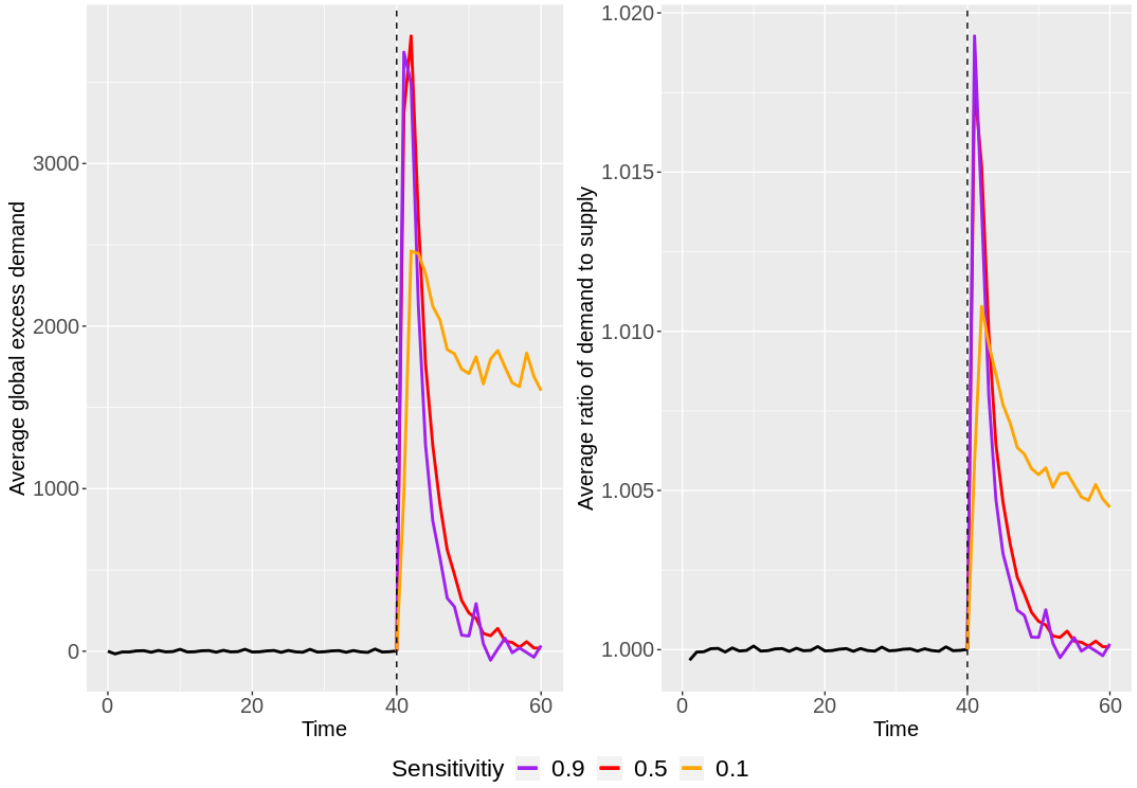

Figure 4.21: **Impact of global risk aversion on stock imbalances** Impact of batch testing and rejection, and global risk aversion for various test sensitivities on imbalances in stock quantities (left) and the ratio of system-average demand to supply (right).

ing creates imbalances in supply and demand, and risk aversion leads to long-term avoidance of farms, leading to the accumulation of supply for farms deemed high-risk and the accumulation of demand because there are fewer suppliers that buyers are willing to trade with. The avoidance of farms is also reflected by the fact that the introduction of testing and risk aversion cause farms to reduce their number of trade partners, whereas an increase in the number of trade partners was observed when testing only was introduced. As positive tests cause farms to increase the cessation rate and decrease the formation rate of the farm from whom the batch originated, it is not surprising that risk aversion leads to a thinning of network structure. This is further observed in the frequency of trade, with risk aversion causing a decrease in the number of trades, whereas testing alone caused increases in trade frequency. Trades that do occur take larger batch sizes in the risk aversion regime than when testing alone, and we observe similar shocks to animal flows, price, and net income

in both regimes.

There is a noticeable effect of risk aversion on between-herd prevalence, with disease eradicated for $\tau = 0.9$ more quickly than through testing alone, and for $\tau = 0.5$ disease is almost completely eradicated, highlighting the significant role risk aversion could have on controlling diseases for low test sensitivities. For $\tau = 0.1$, the disease cannot be eradicated with the inclusion of risk aversion, but prevalence is significantly reduced to a new equilibrium. We observe, however, that the perceived disease prevalence, defined as the fraction of the network with a weight smaller than 1, is generally overestimated compared with actual prevalence, except when $\tau = 0.1$ due to the poor sensitivity of testing, suggesting that our mechanism through which weights are updated (trade) contains a lag and thus may result in altered trading patterns for longer than is necessary. Nonetheless, a global risk aversion strategy is clearly effective in reducing disease prevalence, and for test sensitivities for which testing alone could not eradicate disease, there is potential for risk aversion to alter trading patterns such that disease can be eradicated or prevalence significantly reduced. This would allow the trading system to return to pre-testing (and risk aversion) equilibrium values that is not possible through testing alone when risk aversion allows for eradication of disease, but we note that long-term disturbances to trade are observed when disease cannot be eradicated.

4.3.4 Whole batch testing and rejecting with a global risk aversion strategy and discounting of risk

We attempt to reduce the lag between actual prevalence and perceived prevalence that was observed for the global risk aversion strategy by introducing a natural, incremental, increase to farm weights after a specified and fixed time period in which no detected batches from a high-risk farm were detected. That is we discount information about supplier risk levels. In Chapter 3, this was shown to not alter disease prevalence for the global risk aversion strategy for a test sensitivity in which disease was eradicated without this incremental weight updating, however it did reduce the transitory perturbations of the trading system when farms regained trust

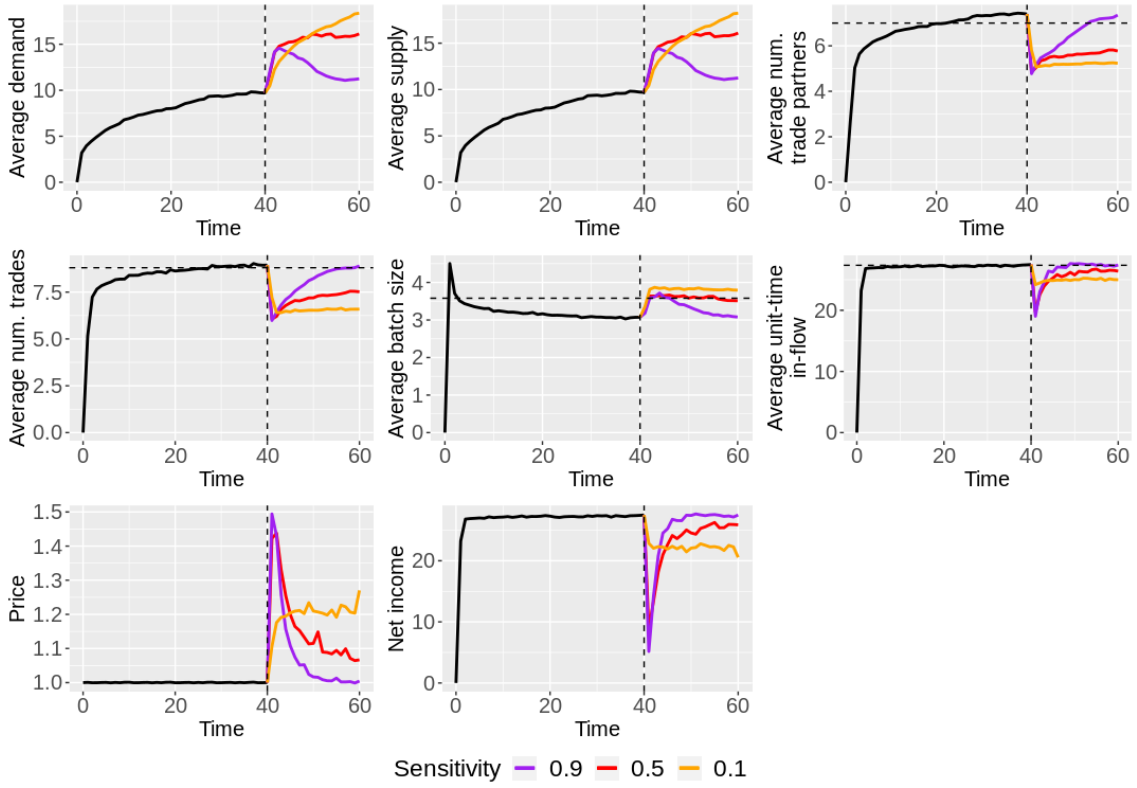

Figure 4.22: **Impact of discounting of risk on Scottish trading system** System-averages for various trade quantities when whole batch testing and rejecting is enforced which informs a global risk aversion strategy, for various test sensitivities. High-risk farms have their weights incrementally increased in steps of ω after a period, $\Delta t = 0.1$, in which no batches were detected to contain an infected animal.

quickly. We apply this to the Scottish trading system and assume $\omega = 0.1$ and weights update in steps of ω after a chosen time period $\Delta t = 0.1$ (corresponding to roughly one month) in which no batch was detected positive. Weights continue to be incremented (globally) through trade as before.

Considering Figure 4.22, qualitatively similar behaviour is observed for $\tau = 0.9$ when natural weight increments are introduced, though the initial shocks to supply and demand are less severe, as farm weights update more quickly. Generally, the system returns to pre-testing equilibrium values more quickly than in the scenario where there is no discounting of information on supplier risk, which may be understood by considering Figure 4.23, noting that the perceived prevalence for $\tau = 0.9$ matches the actual prevalence to a greater degree than in the case without risk discounting

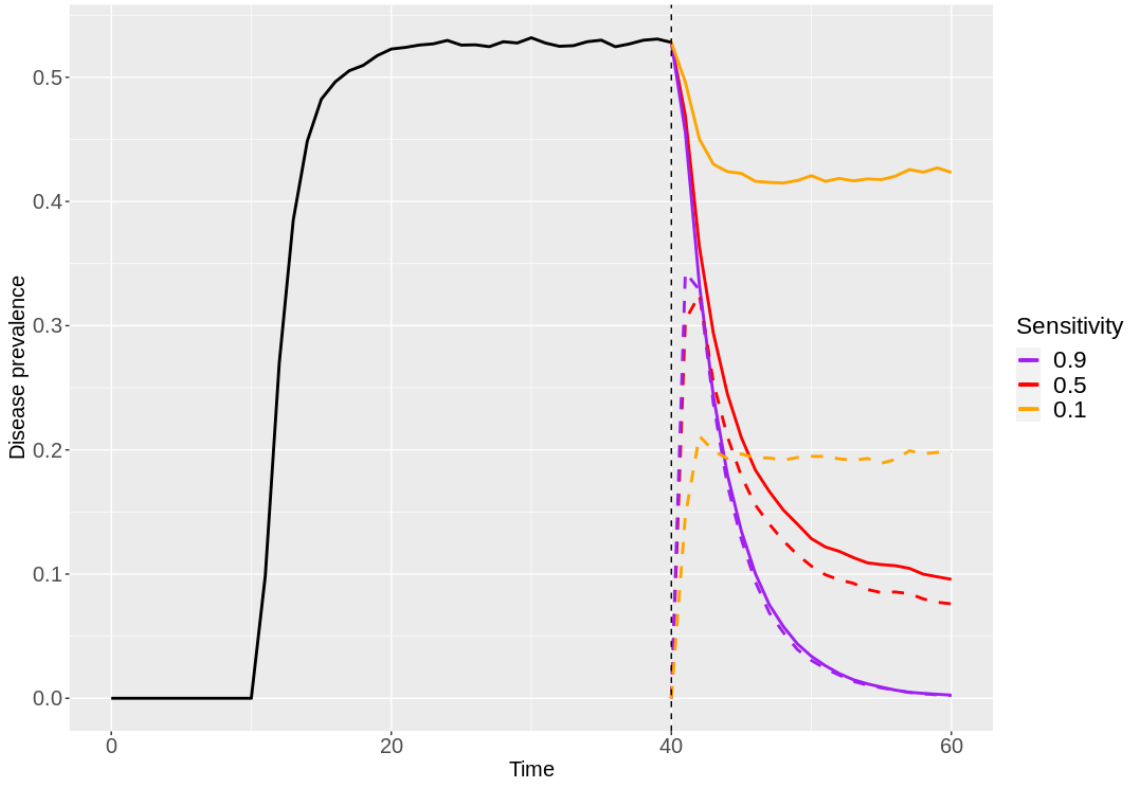

Figure 4.23: **Impact of discounting of risk on disease prevalence** System-wide disease prevalence when whole batch testing and rejecting is enforced which informs a global risk aversion strategy, for various test sensitivities. High-risk farms have their weights incrementally increased in steps of ω after a period, $\Delta t = 0.1$, in which no batches were detected to contain an infected animal.

(see Figure 4.20). For $\tau = 0.5$ and $\tau = 0.1$, natural increments to weights appear to negatively impact the effect of risk aversion, with the system once again exhibiting long-term disturbances to trading patterns. This is because of the increased disease prevalence compared with no discounting of risk. In addition, in this case the perceived prevalence is now underestimated, so farms are less risk averse than they should be. Thus incorporating a natural regaining of trust via time-dependent increments to weights can be effective in reducing unnecessary burden on the trading system for test sensitivities that permit eradication of disease, however care must be taken for lower test sensitivities, as this regaining of trust may detrimentally impact the success of risk aversion and cause longer-run persistence of disease and strain on the trading system.

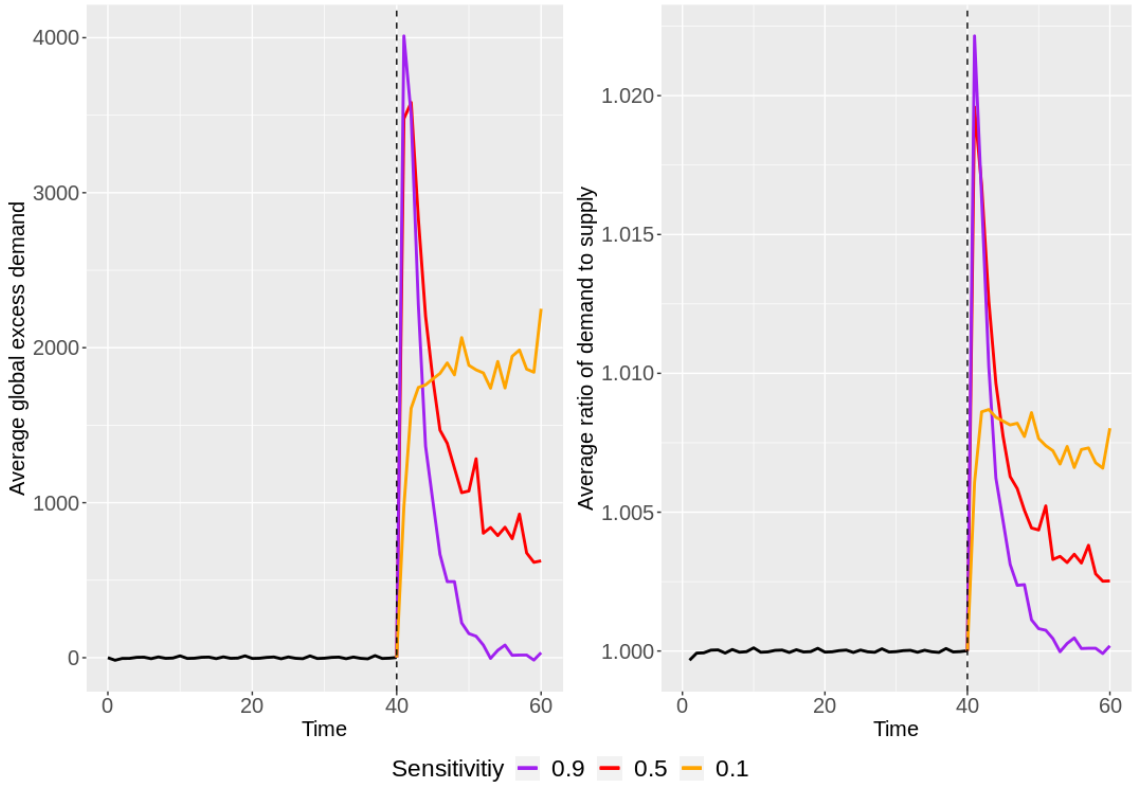

Figure 4.24: **Impact of discounting of risk on stock imbalances** Impact of batch testing and rejection, and global risk aversion with natural increments to weights for various test sensitivities on imbalances in stock quantities (left) and the ratio of system-average demand to supply (right).

4.4 Discussion

In this chapter, we outlined the challenges of parameterising our highly dynamic generative trading model to the Scottish cattle trading system, owing to the presence of time-varying farm-level stock quantities in our model that are not observable in the data. By initiating the parameterisation from an assumed starting point taken from the parameterisation of the model described in Chapter 2, we showed our method for obtaining farm-level parameters for a_i and b_i, the frictional components of partnership formation and trade, respectively, can lead to parameterisations that represent distributional properties of the Scottish trading system, as well as capturing farm-level trading dynamics to a remarkable level of accuracy, especially considering the relative simplicity of the model. This method, however, is computationally intensive as it requires simulation of the system, followed by a reevaluation of a_i and b_i for each farm, followed by subsequent simulations using these updated values. More-

over, it does not define an explicit relationship between farm-level trading patterns and farm-level supply and demand. To our knowledge this model represents the first attempt at developing and parameterising a highly dynamic generative trading model. With the parameterisation developed here it has been shown that it is possible to explore the dynamics of trade in ways that have, up to now, not been possible using current modelling approaches, such as the conceptually simple approach of representing observed cattle movements as a snapshotted temporal network. Current approaches to modelling livestock trading dynamics are limited to generation of trade events on existing trade partnership networks. However, our generative model goes beyond current models by including dynamic trading partnerships, and parameterising at farm-level [58, 87] and can be used to explore the response of the trading system to a wide range of proposed disease control measures, including those studied here.

Extending our parameterised trading model to account for disease spread via trade for a disease characterised by farm-level prevalence $\lambda = 0.25$ and recovery rate $\gamma = 1/3$, representing a high prevalence, highly persistent disease, we showed that under current Scottish trading patterns, the disease is expected to persist at a between-herd prevalence of approximately 55%. We first explored the potential for changes to the propensities for farms to form and end partnerships, and to make trades and showed that our model under the Scottish parameterisations predicts similar qualitative behaviour as the homogeneous model in Chapter 3, with the trading system adapting to increased (or reduced) frictions such that the network structure changes to maintain farm flows. As a result, disease prevalence is largely unaltered by such changes to trade propensities. This is in direct contradiction of the results of the model of Chapter 2, which suggested such changes could be highly effective, and also of current generative trading models, which have suggested reductions to trade (and compensatory increased batch sizes) could reduce disease prevalence [87]. Our results highlight that trade is complex and dynamic, and farm response to alterations to trade can have unexpected consequences for disease spread. This has been observed previously, with legislative changes to trade following the 2001 FMD

outbreak altering the UK cattle trade network in such a way that it has been shown the UK network is now more susceptible to disease spread [44, 109, 115], further emphasising the need for trading models that can accurately explore the role of trade on disease spread.

Including animal batch testing and rejection was shown to be an effective control measure against persistent endemic disease spread, with eradication or near eradication for high test sensitivities, and significant reductions possible for lower test sensitivities. The impact of such tests on the trading system, however, was clearly visible, with large, short-term, disturbances to trade for sensitivities in which disease could be eradicated, and long-term persistent alterations to trade for sensitivities that did not eradicate disease. Thus testing alone through traded animal batches may be insufficient in eradicating diseases such as paraTB, a disease for which the commonly used ELISA test has notoriously variable test sensitivities [60, 120]. We also note that for paraTB, it has been shown on a dataset of animal movements in France that typical control measures such as animal testing of trade animals may be insufficient in eradicating the disease [13].

We extended our testing regime by linking it to a global risk aversion strategy, where farms share a common pool of information regarding high-risk farms. Farm risk aversion, where farmers avoid high-risk farms is observed as a behaviour related to avoidance of bTB infection [21, 35] and more generally risk aversion has been shown to be effective in controlling disease [41]. We incorporated risk aversion through changes to farms' propensities to form and end partnerships, and make trades, with farms deemed high-risk by scaling the appropriate rates by a weight, ω. Risk aversion employed in this manner was shown to be highly effective at eradicating disease, and near complete removal of disease was possible for test sensitivities for which testing alone could not eradicate disease. However, it generally resulted in an overestimated perceived prevalence, leading to unnecessarily long disturbances to trade. In an attempt to mitigate this, we introduced a natural regaining of "trust", or discounting of risk, in which weights incrementally increased after some period of time in which no infected batches were detected. For high test sensitivities, this was shown to be an

effective supplement to risk aversion, allowing for complete eradication of disease. In addition perceived disease prevalence matched actual disease prevalence, minimising the duration of disturbances to trade. For lower test sensitivities, however, the same rate of discounting of risk was shown to detrimentally impact risk aversion, preventing disease eradication and causing ongoing disturbances to trading patterns.

While this dynamic model represents the first attempt at developing a parameterimised model of the Scottish cattle trade, there is scope for extension. We chose not to include animal markets, though animal flows through these premises are maintained in our parameterisation as we treat farm-to-market movements as transitory, and replace them with the resultant farm-to-farm movements. As markets generally do not operate permanently, including them in our model is challenging as their presence must be accounted for in our parameterisation. Moreover, it is unclear whether our supply and demand based trading model can accurately account for market dynamics, an issue highlighted in previous generative trade models [58]. Finally, while we generally assume that we are modelling endemic diseases, for which markets may not be as influential, for epidemic diseases such as FMD, markets are known to play a significant role [45]. In terms of our method of parameterisation, while we showed that our parameterisation could capture farm-level dynamics to a very high degree, it was less successful for farms that trade very infrequently, and in general simulation of our parameterised system predicted smaller batch sizes than is observed in the data. The limited number of observed trading events for such farms is likely to make and parameterisation challenging. Nonetheless, development of a more rigorous method for parameterising the system at farm-level is a natural next step, as this may allow for a deeper understanding of the nature of farms' trading patterns and the accumulated stock levels that are observed in simulation.

Chapter 5

Discussion

5.1 Aims of the thesis

The general aim of this thesis was to expand and develop generative trading models of cattle trade, an area of research currently lacking, and explore the role of trade on disease spread. These generative models are an attempt to extend current modelling approaches of livestock trade, in which large-scale datasets are employed to replay a network of animal movements as either a static or temporally snapshotted network, and simulation of a simulated disease process modulated by the observed animal movements.

The thesis aimed to answer the following questions: 1) can analytically tractable generative models of livestock trade be developed that capture farm-level properties? Yes, in Chapter 2 we presented such a model that was amenable to theoretical analysis, and parameterisation to the Scottish cattle trade system was achieved using the Cattle Tracing System (CTS) dataset; 2) can the dynamics of trade be exploited in such a way that disease persistence is reduced while maintaining farm-level animal flows? Yes, the trade properties of farms in the model of Chapter 2 could be manipulated to conserve farm-flows, and it was shown that this could reduce R_0, the basic reproductive number, across a range of diseases; 3) can these models be expanded to account for time-varying farm-level stock quantities, dictating trading

patterns? Yes, the model of Chapters 3 and 4 were an extension of the model of Chapter 2 and incorporated farm-level supply and demand, altering the rates at which farms formed new trade partnerships and trade at a given time, though at the loss of analytical tractability; 4) do changes to trade affect stock quantities to such an extent that the trading system fundamentally changes? Yes, the model of Chapters 3 and 4 were highly dynamic, and changes to farm trading patterns lead to network adaptation as farms attempted to minimise their demand and maintain animal flows; 5) under such scenarios, how does network adaptation impact disease spread? It was found in Chapters 3 and 4 that network adaptation nullifies the potential disease reducing benefits of changes to trading patterns, except in extreme scenarios where trade is essentially halted; 6) how do traditional disease control measures, such as animal testing, impact the trading network, and how does that affect disease spread? Testing of trade animal batches was shown to be effective in reducing disease prevalence for certain test sensitivities. Test-and-slaughter strategies caused transitory disturbances to system-wide trading patterns when testing could remove disease, and permanent disturbances when testing could not fully remove disease. Risk aversion strategies were shown to be an effective supplemental behavioural change in response to detection of infected animals, further reducing disease prevalence. A global aversion strategy was found to be more effective than an individual-based aversion strategy; 7) when applied to the Scottish cattle trade industry, do these results hold, and if so can effective disease control strategies be proposed? Yes, simple changes to trading propensities alter the Scottish trading system but do not yield significant reductions in disease prevalence. Control measures such as batch testing and risk aversion can significantly reduce (or eradicate) disease even for low test sensitivities, though cause disturbances to system-wide trading patterns.

For complex systems and intractable problems, there is often no one approach to best suggest solutions. However, understanding the dynamics of the system, including how key factors interact enable proposed interventions to be designed, tested for unexpected outcomes, and combined in ways that may yield significant insight to be

made in addressing challenging problems. In this thesis we have developed an approach to modelling complex trading patterns and shown that the resulting models provide a good representation of the highly complex Scottish cattle trading system. Application of our models to putative disease control measures provide useful understanding of their potential impacts, including unintended outcomes that mitigate against desired goal of disease prevalence reduction. These models therefore confirm that control of endemic disease is a complex problem, but provide tools that may enable more intelligent design and combinations of interventions to address it.

We now discuss the results of each chapter in more detail.

5.1.1 Chapter 2

In Chapter 2 a heterogeneous trading model was introduced in which farms possessed a dynamic list of trading partners from whom they exclusively purchase animals. This model was analytically tractable and applying the methods of [6] we were able to derive a per-farm expression for the diseases basic reproductive number, defined as R_0^i. This expression highlighted the role of the dynamic nature of trade partnerships and trade on disease spread that does not appear to have been considered previously. Using the expression, it was shown that manipulation of farm-level trading propensities while maintaining animal in-flows were an effective method of reducing R_0^i, with sufficient changes to trade patterns capable of bringing R_0^i below 1, the critical threshold value that destabilises the endemic disease equilibrium. We applied our methods to the Scottish subset of the CTS dataset over the years 2005-2013, and showed that per-farm parameterisations could be obtained such that farm-level trading properties were matched, along with system-level distributional properties. Analysis of changes to trading patterns on this parameterised system via R_0^i were shown to significantly reduce R_0^i. In particular, encouraging fewer, longer lasting trade partnerships, with fewer trades of larger batch size could reduce R_0^i significantly, especially for high farm prevalence, highly persistent diseases; the diseases that are typically challenging to control. Moreover, targeted trading changes to the largest farms were shown to be highly effective in reducing disease persistence,

more so than traditional biosecurity control measures.

5.1.2 Chapter 3

The model of Chapter 2 assumed that a farm's trading behaviour was not altered by the effects of trade events, i.e. it did not account for fluctuations in farm-level supply and demand. However, this is not realistic for the real-world Scottish cattle trading system as time-varying trading patterns are readily observable, e.g. burstiness of trade events. We therefore extended the model of Chapter 2 by including farm-level stock quantities, defined as supply and demand, that accumulated at constant rate and were depleted via trades. We incorporated demand satiation and supply depletion at a farm-level by modelling rates of trade partnership formation and trade as functions of farms' dynamically varying demand and the selling farms' supplies. Thus, farms trade and form trade partnerships more frequently when demand is high, but demand is satisfied through trade, leading to demand satiation resulting in farms' trading behaviour (tendency to form trade partnerships and trade) altering. Our generative models go beyond current state-of-the-art by dynamically modelling stock levels and allowing these to influence event rates by incorporating farm stock levels into our model rates [58, 87]. However we lost analytical tractability due to discontinuities in model rates and farm-level stock quantities at a given time could not be expressed in a closed-form expression. A simple pricing model (similar to the pricing model of [87]) was included into our model, that satisfied simple macroeconomic supply-demand principles, as a mechanism for controlling global stock imbalances, finding that without a pricing model, small imbalances in global stock levels could lead to cascading and long-term imbalances. The inclusion of a pricing model was also desirable to measure the potential financial impact on the system of changes to trade.

The dynamic nature of our model was explored by manipulating farm-level trading propensities. We found that the trading system would adapt itself in response to these alterations, and network structure would change so that new avenues of trade were found which minimised the effect of changes to trading propensities such

that farm-level unmet demand was minimised and farm flows were maintained. The robustness of the trading system to instantaneous shocks to stock levels was investigated, finding the model would rapidly adjust to these shocks, leading to temporary surges in trade, but with the system quickly returning to pre-shock equilibrium values. The exception was when demand was perturbed significantly, with the system finding a new equilibrium in which farm-level demand was slightly larger than pre-shock equilibrium values.

Disease spread via trade was included in the model, and similar changes to trade propensities as in Chapter 2 were made to explore the impact of the dynamic adaptation of the model on disease spread. Changing the propensities for farms to form and end partnerships, and make trades was found to be largely ineffective in reducing disease prevalence, except in extreme cases where either trade effectively halted, or the network dissolved. These findings were in direct contradiction of the results of Chapter 2, which showed these changes to trade were highly effective, and highlight the dynamic nature of trade and the challenges of effectively modelling livestock trading systems.

We introduced animal batch testing, a common control strategy for diseases such as bTB and paraTB [4, 123], and considered two animal rejection strategies: removing individual animals that test positive, and removing entire batches if a single infected animal is detected. Testing in this way is similar to post-movement testing, and while we did not consider pre-movement testing, this can be incorporated into the model. As expected, the greater the test sensitivity, the more effective both testing strategies were in reducing disease prevalence, however whole batch rejection always leads to greater reductions in prevalence and could eradicate disease at lower test sensitivities. Animal rejection naturally leads to imbalances in global stock levels, as buyers accept only animals that do not test positive for disease in a batch, and our dynamic model allowed us to explore the effect on trade that these imbalances cause; an analysis that, to our knowledge, has not been performed before using standard livestock trade modelling approaches. Both individual and whole batch rejection lead to disturbances to trading patterns, and the magnitude of these disturbances were,

in general, larger for whole batch rejection. These disturbances were permanent for test sensitivities for which post-movement testing was unable to eradicate disease, and transitory when testing could eradicate disease.

An adaptive risk aversion strategy was incorporated that was influenced by animal testing; farms would adjust their trading propensities towards farms that were deemed high-risk. We explored two risk aversion strategies, an individual-based strategy, whereby farms possessed a list of farms that they identified as high-risk, i.e. from whom they had detected infected animals, and a global strategy whereby the trading system shared and contributed towards a global list of farms that were deemed high-risk. High-risk farms were assigned a weight that altered the rates at which farms would form and end partnerships, and make trades, and risk aversion was shown to be an effective supplemental control strategy that further reduced disease prevalence compared with testing alone. Risk aversion altered the disturbances to the trading system compared with only testing, as testing alone did not alter the propensities for farms to trade with high-risk farms (except due to stock depletion), whereas risk aversion caused farms to avoid these high-risk farms, leading to a reduction in network connectivity. Both aversion strategies lead to disease eradication at lower test sensitivities than testing alone, however a global aversion strategy was shown to be more effective than individual-based aversion allowing for disease eradication at even lower test sensitivities. This was due to farms being able to preemptively avoid high-risk farms, whereas for the individual-based aversion farms necessarily had to trade with farms before they could be deemed high-risk. While risk aversion was effective at reducing prevalence, farms generally overestimated their "perceived" prevalences, i.e. the fraction of the system that were deemed high-risk, which lead to unnecessarily long disturbances to trading patterns. To mitigate this, we incorporated a natural regaining of "trust", or discounting of risk, allowing for weights of high-risk farms to incrementally increase after some period in which no animal or batch were detected to have infection. We evaluated this for a test prevalence in which global aversion allowed for complete removal of disease, and for which individual aversion lead to near eradication. For the global aversion strategy,

natural increments to weights were found to not alter long-run disease prevalence, but did cause smaller disturbances to trading patterns, especially when weights were updated quickly. On the other hand, for individual-based aversion, the same rate of discounting of risk was shown to be detrimental and lead to increased disease prevalence. Both aversion strategies have the potential for reducing prevalence, however a system-wide aversion scheme appears to be a highly effective surveillance system supplementing animal testing that could reduce disease prevalence, even for low test sensitivities.

5.1.3 Chapter 4

The model analysed in Chapter 3 was parameterised for a small homogeneous system of farms. However, real-world trade networks display a large degree of heterogeneity, including scale-free like distributions across farms int he case of livestock trading systems [22, 84, 113]. The challenges of parametersing our dynamic trading model for the Scottish trading system via the CTS data was presented, the main challenge being that the model rates were functions of farm-level supply and demand, which are unobserved in the data. We chose to use an iterative method to parameterise our model, where each farm is parameterised by an iterative method starting from an initial parameterisation (we chose to use the parameterisation used for the model in Chapter 2). The system was then simulated, and average values for per-farm trading quantities were compared with their values in the data. The factor differences between simulation and data for each farm were used to inform a new parameterisation, the system was re-simulated and the process repeated. This method was computationally intensive, requiring multiple iterations to obtain appropriate parameterisations. In addition, our method was inefficient in obtaining parameterisations for farms that trade very infrequently, as these farms are sensitive to stochasticity in the simulation. However, it should also be noted that the data contain relatively few events and by implication limited data for such farms. Further refinement of this parameterisation method is an avenue for future work. Nevertheless, we were able to obtain a parameterisation that represented the trading patterns of the Scottish system to a very high degree, both at system-level and farm-level.

Introducing disease spread via trade into our parameterised system, we explored the effects of similar changes to trading propensities on prevalence as in Chapter 3. Our results conformed to the results of Chapter 3, finding that the system adapted to changes in trading propensity so that animal flows were maintained, which lead to minimal reductions in disease prevalence. Even for trading patterns that the model of Chapter 2 predicted would lead to increased incidence, for example increased network connectivity, more frequent trades, and smaller batch sizes, there were only very small increases in disease prevalence. We posit that the Scottish trading system is currently operating with very low friction, and fundamental alterations to the system would be required to reduce disease prevalence without other disease control strategies. However, as with many complex systems it may be that multiple interventions could yield useful benefits.

Whole batch testing and rejection was included and shown to be an effective control strategy at reducing disease prevalence, but could not eradicate disease except for high test sensitivities. For all test sensitivities, the introduction of batch testing resulted in disturbances to the trading system caused by imbalances in farm stock levels that testing resulted in (in a trade, the buying farm accepts either the whole batch if all animals test negative for infection, or the batch is rejected if a single animal tests positive, but the supply of the selling farm depletes by the batch size regardless of whether the batch is accepted or rejected by the buying farm). For test sensitivities in which disease was eradicated (or very close to eradication), these disturbances were temporary and the trading system would return to pre-testing equilibrium values. When testing could not eradicate disease, these disturbances were permanent and the trading system would find a new stable trading equilibrium. We linked animal testing to a behavioural response by introducing the global risk aversion strategy outlined in Chapter 3. As in Chapter 3, the introduction of risk aversion altered the trading patterns of farms compared to testing alone, and was again highly effective in reducing disease prevalence, with disease eradication possible for test sensitivities that did not permit eradication through testing alone, and substantial reductions for very low test sensitivities (though eradication was

still not possible in these cases). As with animal testing, when risk aversion could not eradicate disease, there were permanent disturbances to trading patterns, such as increased prices, lower farm net income, and farms were not able to fully meet their in-flow requirements. For test sensitivities in which testing combined with risk aversion could eradicate disease, farms generally overestimated the risk of disease, and perceived prevalences were generally higher than the actual prevalence. The discounting of risk as in Chapter 3 was included, and similar behaviour was observed for the parameterised system. For high test sensitivities, disease could still be eradicated and perceived prevalence more closely matched the actual prevalence, minimising the disruption to the trading system that testing and risk aversion caused. For lower test sensitivities, there was a detrimental impact on prevalence reduction, with disease no longer able to be eradicated for middling test sensitivities, and the effect of risk aversion was largely mitigated for low test sensitivities, resulting in further disruptions to the trading system.

5.2 The role of trade in disease spread

The models presented in this thesis are the first attempt at developing new tools in analysing the role and effect of trade on livestock diseases, with case studies applied to the Scottish cattle trading system by parameterising our models to the Scottish subset of the CTS dataset. With the recent development of network theory and the increasing availability of large, rich datasets of animal movements, typical models of livestock trade have consisted of replicating observed animal movements and observing a simulated process modulated through these movements, finding that trade (specifically the movement of infected animals between herds) is a significant risk factor to the spread and maintenance of livestock diseases [13, 37, 39, 46, 51, 71, 97, 98]. These modelling approaches have identified potential avenues for exploiting the highly heterogeneous nature of trade, with targeted rewiring of network connections based on network-level properties such as centrality measures, or by rewiring movements away from particular holdings shown to be reduce disease prevalence [43, 85, 117]. In addition, effectively removing certain connections in the network has been

shown to alter the structure of the network and the size of the giant component in a way that may be effective in reducing disease persistence [62, 63]. However, assessing the impact of these alterations to trade on farm-level properties, such as maintaining animal flows or minimising demand, or on system-level properties such as price, is challenging using these modelling approaches as they are typically constrained by the models designed around fixed observed animal movements. It has previously been shown that alterations to farm trading patterns in response to legislative changes intended to control disease or in response to a disease outbreak (for example the 2001 UK FMD outbreak) can have unintended consequences on the structure of the trading network, leading to increased susceptibility to disease spread [44, 109, 115], highlighting the need for the development of trading models that can incorporate business considerations of farms that may influence trading behaviour.

We have developed novel generative trading models, in which the trading system grows and develops based on farm-level trading characteristics, for which there is a pressing need in general [57], and when parameterised to the Scottish cattle trading system represent, to our knowledge, the first attempt at analysing trade and its effect on disease spread on a national scale for a highly heterogeneous system using a systems modelling approach. There have been very few attempts at developing generative models within livestock trading, and none applied to Scotland, and these models have focused primarily on trading dynamics, with small consideration to disease spread. Moreover, simplifying assumptions such as constant trade networks, rates of trade, and homogeneity cannot capture the complexity and time-varying nature of livestock movement patterns [58, 87]. The generative model outlined in Chapter 3, and parameterised for the Scottish trading system in Chapter 4, was effective in showing the potential for a generative modelling framework, yielding new insight into how farms may adapt their trading behaviour in response to alterations in trading propensities. Our generative models are effective in capturing the complexities and nuance of livestock trade, and show that simple alterations to trading patterns may not yield expected changes to disease prevalence, as farms dynamically alter their trading behaviour, a phenomena that may not be easily understood using

typical network-based approaches. In addition, the effect of typical disease control measures, such as post-movement testing, and the response of the trading system to such measures can be analysed using our generative modelling approach, to inform potential intervention strategies that reduce prevalence while minimising farm- and system-level disturbances to trade.

5.3 Extensions and future work

Our generative modelling framework is a flexible tool allowing for the modelling of trade and disease spread, and the effect of control strategies and alterations to trade can be incorporated into the model. There are a number of elements of real-world trading systems that we have not included in our models, and the inclusion of some of these will be the focus of future work. Firstly, we have neglected any spatial component to our trading models, for example farms preferentially buying/selling to nearby farms, with farms' decisions on who to farm trade partnerships and trade with dictated entirely by current stock quantities. While the presence of markets facilitates long-range animal movements, it has been observed that cattle in the UK, for example, generally travel short distances via movements in their lifetime [113]. The comparison between the dynamic model presented in Chapters 3 and 4 and an amended model in which distance influenced trades between farms would be informative, both when considering the differences in disease prevalence and how distance-based movements impact the dynamics of the trading system. The 2001 UK FMD epidemic is an example of a disease outbreak in which long- and short-range animal movements contributed to the magnitude of the outbreak; long-range movements via animal markets were primarily responsible for the initial nationwide spread, with subsequent local movements considered responsible for the maintenance of the disease [45].

External sources of infection, such as wildlife reservoirs, is a natural future inclusion to our models, as we have considered the spread of disease solely through trade throughout this thesis. For example, the presence of infected badgers, which can act as environmental reservoirs of bTB [103], is suspected of increasing herd-levels

risk of infection of bTB [82], with the UK having higher badger densities than mainland Europe [18], although Scotland does have lower densities than the rest of the UK [61]. The impact of persistent external sources of infection into herds on the control measures outlined in this thesis is a promising area for future work, and one that can be facilitated within our modelling framework. In particular, while we showed in Chapters 3 and 4 that simple changes to farm trading propensities was unsuccessful in eradicating disease except in extreme cases where the system fundamentally changes, it would be interesting to explore how such changes, when combined with distance-based trading as above, may effect the ability for local high-risk areas of infection from wildlife to spread disease to low-risk areas of infection from wildlife.

A simplifying assumption of our models is to treat farms as a unit, that is to say we do not track individual animals. As the CTS dataset contains the identification and movement records of individual animals, there is scope to extend our model to incorporate individual animals. As we treats as a single unit, we assume that infected farms maintain a constant herd-level prevalence throughout its infectious lifetime, however herd demographics (such as births and deaths) and animal movements (infected animals may be introduced or leave the farm) may cause prevalence to fluctuate. Our disease model could be considered a "worst-case" scenario, due to farms maintaining their herd-level prevalence regardless of the frequency and size animal movements. An individual-based trading model has previously shown that increasing animal movements could be beneficial to reducing disease persistence, if combined with constant animal tests during these movements [106]. As we neglect herd demographics such as herd size, interpreting farm-level supply and demand can be challenging, and we have considered these quantities as a measure of inefficiency in farms' abilities to completely satisfy their demand, and also to measure the potential impact on farms caused by changes to trading patterns and disease control strategies. Our analysis and parameterisation of the Scottish cattle trade system further highlighted that these stock quantities should not be taken as representative of herd demographics, with some farms having extremely large supply and demand

at any given time, and their values were more a consequence of farm-level trading patterns rather than an indicator of herd size.

We have considered the impacts of disease control measures both on disease prevalence and also on the trading system, however there are a number of intervention strategies that we have not considered but can be analysed using our generative modelling framework. While alterations to trading propensities were explored as a potential alternative to movement restrictions, movement restrictions are a common control strategy in response to the detection of disease. For example, in the 2001 and 2007 UK FMD outbreaks, nationwide movement restrictions were imposed to minimise the spread of disease causing widespread disruption to farms and incurring large economic costs [7, 45, 116]. Moreover, following the relaxation of these restrictions, animal movements were atypical as farms attempted to offload larger amounts of stock and to recuperate losses due to slaughter [19, 116]. Movement restrictions can be incorporated into our generative trading model, and the inclusion of farm-level stock quantities allow for both a measurement on the stress of these restrictions on farms, but will also influence short- and perhaps long-term trading behaviour following the relaxation of restrictions. Initial exploration (not shown in the thesis) of simple movement restrictions have suggested that the success of system-wide restrictions depends entirely on whether disease can be eradicated during the time period of restrictions. If the disease is not eradicated before restrictions are lifted, large surges of trade due to accumulation of stock result in prevalence rapidly returning to pre-restriction levels. More work is required on behavioural changes of farms in response to restrictions, e.g. less generation of supply and demand, to fully understand the effect of restrictions on disease spread, but is a potentially economically important area of study due to the large disruptions nationwide restrictions create.

We explored risk-based trading through an adaptive risk-aversion strategy, modulated through the testing of traded animals. A natural extension of such approaches is to model so-called risk-based trading schemes. There has been little modelling of such schemes, however the introduction of trading schemes based on bTB score cards has been shown to potentially reduce the number of infected animals purchased from

high-risk farms [3]. Our generative modelling framework is well suited to exploration the potential of similar trading schemes on control of disease, but also on the financial burden on farms and their ability to maintain animal flows and meet demand. Considerations such as minimum scheme size necessary to maintain farm-level demand, critical scheme sizes at which disease can be maintained within the scheme, and the development of "smart" schemes in which trading schemes partition at critical sizes so that potential disease persistence within the scheme is prevented are all future areas of work that may help inform the effectiveness of trading schemes and inform potential future policy when applied to real-world cattle trading systems.

Our dynamic models of Chapters 3 and 4 were analytically intractable and required extensive use of simulation. A challenge, and area of future work, is developing a theoretical framework to allow for similar theoretical analyses of the model as was presented in Chapter 2.

We conclude by noting that while we have focused on cattle trading systems, our generative models are not confined to such systems, and can potentially be adapted to other dynamic systems, for example computer networks and the spread of viruses in data packets. The current COVID-19 pandemic has shed light on the devastating impact diseases can have on human health and national economies, and the role of control strategies that minimise contacts between individuals on preventing disease spread. Our model has the potential to be adapted to human contact networks and could be an invaluable tool in quantifying the risks of certain contact patterns and the economic and financial impacts to individuals on typical control strategies, and in also investigating potentially effective control strategies that minimise disruption to daily life.

Chapter 6

References

[1] Jessica M. Abbate et al. "Prevalence of Bovine Tuberculosis in Slaughtered Cattle in Sicily, Southern Italy". In: *Animals* 10.9 (2020), p. 1473. DOI: 10.3390/ani10091473.

[2] D. A. Abernethy et al. "Bovine tuberculosis trends in the UK and the Republic of Ireland, 1995-2010". In: *Veterinary Record* 172.12 (2013), pp. 312–312. DOI: 10.1136/vr.100969.

[3] A. Adkin et al. "Assessing the impact of a cattle risk-based trading scheme on the movement of bovine tuberculosis infected animals in England and Wales". In: *Preventive Veterinary Medicine* 123 (2016), pp. 23–31. DOI: 10.1016/j.prevetmed.2015.11.021.

[4] A. R. Allen, R. A. Skuce, and A. W. Byrne. "Bovine Tuberculosis in Britain and Ireland – A Perfect Storm? the Confluence of Potential Ecological and Epidemiological Impediments to Controlling a Chronic Infectious Disease". In: *Frontiers in Veterinary Science* 5 (2018). DOI: 10.3389/fvets.2018.00109.

[5] Linda J.S. Allen. "A primer on stochastic epidemic models: Formulation, numerical simulation, and analysis". In: *Infectious Disease Modelling* 2.2 (2017), pp. 128–142. DOI: 10.1016/j.idm.2017.03.001.

[6] M. Altmann. "Susceptible-infected-removed epidemic models with dynamic partnerships". In: *Journal of Mathematical Biology* 33.6 (1995), pp. 661–675. DOI: 10.1007/bf00298647.

[7] Iain Anderson. *Foot and mouth disease 2007: a review and lessons learned*. The Stationery Office, 2008.

[8] Roy M. Anderson and Robert M. May. *Infectious diseases of humans: dynamics and control*. Oxford University Press, 1992.

[9] Paolo Bajardi et al. "Dynamical Patterns of Cattle Trade Movements". In: *PLoS ONE* 6.5 (2011). DOI: 10.1371/journal.pone.0019869.

[10] Shweta Bansal et al. "The dynamic nature of contact networks in infectious disease epidemiology". In: *Journal of Biological Dynamics* 4.5 (2010), pp. 478–489. DOI: 10.1080/17513758.2010.503376.

[11] Albert-László Barabási. "The origin of bursts and heavy tails in human dynamics". In: *Nature* 435.7039 (2005), pp. 207–211. DOI: 10.1038/nature03459.

[12] Andrew Bates et al. "The effect of sub-clinical infection with Mycobacterium avium subsp. paratuberculosis on milk production in a New Zealand dairy herd". In: *BMC Veterinary Research* 14.1 (2018). DOI: 10.1186/s12917-018-1421-4.

[13] Gaël Beaunée et al. "Controlling bovine paratuberculosis at a regional scale: Towards a decision modelling tool". In: *Journal of Theoretical Biology* 435 (2017), pp. 157–183. DOI: 10.1016/j.jtbi.2017.09.012.

[14] Richard Bennett and Jos Ijpelaar. "Updated Estimates of the Costs Associated with Thirty Four Endemic Livestock Diseases in Great Britain: A Note". In: *Journal of Agricultural Economics* 56.1 (2005), pp. 135–144. DOI: 10.1111/j.1477-9552.2005.tb00126.x.

[15] Richard E. Booth and Joe Brownlie. "Comparison of bulk milk antibody and youngstock serology screens for determining herd status for Bovine Viral Diarrhoea Virus". In: *BMC Veterinary Research* 12.1 (2016). DOI: 10.1186/s12917-016-0797-2.

[16] J. M. Broughan et al. “A review of risk factors for bovine tuberculosis infection in cattle in the UK and Ireland”. In: *Epidemiology and Infection* 144.14 (2016), pp. 2899–2926. DOI: 10.1017/s095026881600131x.

[17] Allan J. Butler, Matt Lobley, and Michael Winter. *Economic Impact Assessment of Bovine Tuberculosis in the South West of England*. Tech. rep. Sept. 2010. DOI: 10.22004/ag.econ.94718.

[18] Andrew W. Byrne et al. “The ecology of the European badger (Meles meles) in Ireland: a review”. In: *Biology & Environment: Proceedings of the Royal Irish Academy* 112.1 (2012), pp. 105–132. DOI: 10.3318/bioe.2012.02.

[19] J.J. Carrique-Mas, G.F. Medley, and L.E. Green. “Risks for bovine tuberculosis in British cattle farms restocked after the foot and mouth disease epidemic of 2001”. In: *Preventive Veterinary Medicine* 84.1-2 (2008), pp. 85–93. DOI: 10.1016/j.prevetmed.2007.11.001.

[20] T. Carta et al. “Wildlife and paratuberculosis: A review”. In: *Research in Veterinary Science* 94.2 (2013), pp. 191–197. DOI: 10.1016/j.rvsc.2012.11.002.

[21] R.M. Christley et al. “Responses of farmers to introduction in England and Wales of pre-movement testing for bovine tuberculosis”. In: *Preventive Veterinary Medicine* 100.2 (2011), pp. 126–133. DOI: 10.1016/j.prevetmed.2011.02.005.

[22] Rob Christley et al. “Network Analysis of Cattle Movements in Great Britain”. In: *Proceedings of a meeting held at Nairn, Inverness, Scotland* (Jan. 2005).

[23] M. J. Daniels et al. “The potential role of wild rabbits Oryctolagus cuniculus in the epidemiology of paratuberculosis in domestic ruminants”. In: *Epidemiology and Infection* 130.3 (2003), pp. 553–559. DOI: 10.1017/s0950268803008471.

[24] Mike J. Daniels et al. “Do Non-Ruminant Wildlife Pose A Risk Of Paratuberculosis To Domestic Livestock And Vice Versa In Scotland?” In: *Journal of Wildlife Diseases* 39.1 (2003), pp. 10–15. DOI: 10.7589/0090-3558-39.1.10.

[25] Leon Danon et al. “Networks and the Epidemiology of Infectious Disease”. In: *Interdisciplinary Perspectives on Infectious Diseases* 2011 (2011), pp. 1–28. DOI: 10.1155/2011/284909.

[26] R. S. Davidson et al. “Use of host population reduction to control wildlife infection: rabbits and paratuberculosis”. In: *Epidemiology and Infection* 137.1 (2008), pp. 131–138. DOI: 10.1017/s0950268808000642.

[27] Ramon P. DeGennaro and Cesare Robotti. “Financial market frictions”. In: *Economic Review* 92.Q 3 (2007), pp. 1–16.

[28] A. P. Dempster, N. M. Laird, and D. B. Rubin. “Maximum Likelihood from Incomplete Data via the EM Algorithm”. In: *Journal of the Royal Statistical Society. Series B (Methodological)* 39.1 (1977), pp. 1–38.

[29] O. Diekmann, J.A.P. Heesterbeek, and J.A.J. Metz. “On the definition and the computation of the basic reproduction ratio R 0 in models for infectious diseases in heterogeneous populations”. In: *Journal of Mathematical Biology* 28.4 (1990). DOI: 10.1007/bf00178324.

[30] Christl A. Donnelly et al. “Impact of localized badger culling on tuberculosis incidence in British cattle”. In: *Nature* 426.6968 (2003), pp. 834–837. DOI: 10.1038/nature02192.

[31] Christl A. Donnelly et al. “Impacts of widespread badger culling on cattle tuberculosis: concluding analyses from a large-scale field trial”. In: *International Journal of Infectious Diseases* 11.4 (2007), pp. 300–308. DOI: 10.1016/j.ijid.2007.04.001.

[32] Christl A. Donnelly et al. “Positive and negative effects of widespread badger culling on tuberculosis in cattle”. In: *Nature* 439.7078 (2005), pp. 843–846. DOI: 10.1038/nature04454.

[33] Rick Durrett. “Random Graph Dynamics”. In: (2006). DOI: 10.1017/cbo9780511546594.

[34] Jessica Enright and Rowland Raymond Kao. “Epidemics on dynamic networks”. In: *Epidemics* 24 (2018), pp. 88–97. DOI: 10.1016/j.epidem.2018.04.003.

[35] G. Enticott et al. “Farming on the edge: farmer attitudes to bovine tuberculosis in newly endemic areas”. In: *Veterinary Record* 177.17 (2015), pp. 439–439. DOI: 10.1136/vr.103187.

[36] *FAPRI-UK model documentation*. June 2011. URL: https://www.afbini.gov.uk/publications/fapri-uk-model-documentation.

[37] Eric M. Fèvre et al. “Animal movements and the spread of infectious diseases”. In: *Trends in Microbiology* 14.3 (2006), pp. 125–131. DOI: 10.1016/j.tim.2006.01.004.

[38] Helen R. Fielding et al. “Contact chains of cattle farms in Great Britain”. In: *Royal Society Open Science* 6.2 (2019), p. 180719. DOI: 10.1098/rsos.180719.

[39] Helen R. Fielding et al. “Effects of trading networks on the risk of bovine tuberculosis incidents on cattle farms in Great Britain”. In: *Royal Society Open Science* 7.4 (2020), p. 191806. DOI: 10.1098/rsos.191806.

[40] Babak Fotouhi and Michael Rabbat. “Temporal evolution of the degree distribution of alters in growing networks”. In: *Network Science* 6.1 (2018), pp. 97–155. DOI: 10.1017/nws.2017.19.

[41] S. Funk et al. “The spread of awareness and its impact on epidemic outbreaks”. In: *Proceedings of the National Academy of Sciences* 106.16 (2009), pp. 6872–6877. DOI: 10.1073/pnas.0810762106.

[42] M Carolyn Gates et al. “Not all cows are epidemiologically equal: quantifying the risks of bovine viral diarrhoea virus (BVDV) transmission through cattle movements”. In: *Veterinary Research* 45.1 (2014). DOI: 10.1186/s13567-014-0110-y.

[43] M. Carolyn Gates and Mark E.J. Woolhouse. “Controlling infectious disease through the targeted manipulation of contact network structure”. In: *Epidemics* 12 (2015), pp. 11–19. DOI: 10.1016/j.epidem.2015.02.008.

[44] M.C. Gates, V.V. Volkova, and M.E.J. Woolhouse. “Impact of changes in cattle movement regulations on the risks of bovine tuberculosis for Scottish farms”. In: *Preventive Veterinary Medicine* 108.2-3 (2013), pp. 125–136. DOI: 10.1016/j.prevetmed.2012.07.016.

[45] J. C. Gibbens et al. “Descriptive epidemiology of the 2001 foot-and-mouth disease epidemic in Great Britain: the first five months”. In: *Veterinary Record* 149.24 (2001), pp. 729–743. DOI: 10.1136/vr.149.24.729.

[46] M. Gilbert et al. “Cattle movements and bovine tuberculosis in Great Britain”. In: *Nature* 435.7041 (2005), pp. 491–496. DOI: 10.1038/nature03548.

[47] Daniel T Gillespie. "A general method for numerically simulating the stochastic time evolution of coupled chemical reactions". In: *Journal of Computational Physics* 22.4 (1976), pp. 403–434. DOI: 10.1016/0021-9991(76)90041-3.

[48] Daniel T. Gillespie. "Exact stochastic simulation of coupled chemical reactions". In: *The Journal of Physical Chemistry* 81.25 (1977), pp. 2340–2361. DOI: 10.1021/j100540a008.

[49] F.J. Reviriego Gordejo and J.P. Vermeersch. "Towards eradication of bovine tuberculosis in the European Union". In: *Veterinary Microbiology* 112.2-4 (2006), pp. 101–109. DOI: 10.1016/j.vetmic.2005.11.034.

[50] Felipe Grando, Diego Noble, and Luis C. Lamb. "An Analysis of Centrality Measures for Complex and Social Networks". In: *2016 IEEE Global Communications Conference (GLOBECOM)* (2016). DOI: 10.1109/glocom.2016.7841580.

[51] D.M Green, I.Z Kiss, and R.R Kao. "Modelling the initial spread of foot-and-mouth disease through animal movements". In: *Proceedings of the Royal Society B: Biological Sciences* 273.1602 (2006), pp. 2729–2735. DOI: 10.1098/rspb.2006.3648.

[52] J.M. Griffin et al. "The impact of badger removal on the control of tuberculosis in cattle herds in Ireland". In: *Preventive Veterinary Medicine* 67.4 (2005), pp. 237–266. DOI: 10.1016/j.prevetmed.2004.10.009.

[53] GJ Gunn, Roger Humphry, and Alistair Stott. "Comparison of the modelled effects and consequential losses due to Johne's disease outbreaks for beef and dairy herds in Great Britain". In: *Cattle Practice* 12 (Feb. 2004), pp. 1–1.

[54] Daniel T. Haydon, Rowland R. Kao, and R. Paul Kitching. "The UK foot-and-mouth disease outbreak — the aftermath". In: *Nature Reviews Microbiology* 2.8 (2004), pp. 675–681. DOI: 10.1038/nrmicro960.

[55] J.M Heffernan, R.J Smith, and L.M Wahl. "Perspectives on the basic reproductive ratio". In: *Journal of The Royal Society Interface* 2.4 (2005), pp. 281–293. DOI: 10.1098/rsif.2005.0042.

[56] Arata Hidano, M. Carolyn Gates, and Gareth Enticott. "Farmers Decision Making on Livestock Trading Practices: Cowshed Culture and Behavioral Triggers Amongst New Zealand Dairy Farmers". In: *Frontiers in Veterinary Science* 6 (2019). DOI: 10.3389/fvets.2019.00320.

[57] Petter Holme. "Temporal Networks". In: *Encyclopedia of Social Network Analysis and Mining* (2018), pp. 3053–3062. DOI: 10.1007/978-1-4939-7131-2_42.

[58] Patrick Hoscheit et al. "Dynamical network models for cattle trade: towards economy-based epidemic risk assessment". In: *Journal of Complex Networks* 5.4 (2016), pp. 604–624. DOI: 10.1093/comnet/cnw026.

[59] H. Houe, A. Lindberg, and V. Moennig. "Test Strategies in Bovine Viral Diarrhea Virus Control and Eradication Campaigns in Europe". In: *Journal of Veterinary Diagnostic Investigation* 18.5 (2006), pp. 427–436. DOI: 10.1177/104063870601800501.

[60] T F Jubb et al. "Estimate of the sensitivity of an ELISA used to detect Johnes disease in Victorian dairy cattle herds". In: *Australian Veterinary Journal* 82.9 (2004), pp. 569–573. DOI: 10.1111/j.1751-0813.2004.tb11206.x.

[61] Johanna Judge et al. "Abundance of badgers (Meles meles) in England and Wales". In: *Scientific Reports* 7.1 (2017). DOI: 10.1038/s41598-017-00378-3.

[62] R.R Kao et al. "Demographic structure and pathogen dynamics on the network of livestock movements in Great Britain". In: *Proceedings of the Royal Society B: Biological Sciences* 273.1597 (2006), pp. 1999–2007. DOI: 10.1098/rspb.2006.3505.

[63] Rowland R Kao et al. "Disease dynamics over very different time-scales: foot-and-mouth disease and scrapie on the network of livestock movements in the UK". In: *Journal of The Royal Society Interface* 4.16 (2007), pp. 907–916. DOI: 10.1098/rsif.2007.1129.

[64] Rowland R. Kao. "The impact of local heterogeneity on alternative control strategies for foot-and-mouth disease". In: *Proceedings of the Royal Society of*

London. Series B: Biological Sciences 270.1533 (2003), pp. 2557–2564. DOI: 10.1098/rspb.2003.2546.

[65] M. J. Keeling and L. Danon. "Mathematical modelling of infectious diseases". In: *British Medical Bulletin* 92.1 (2009), pp. 33–42. DOI: 10.1093/bmb/ldp038.

[66] M. J. Keeling et al. "Modelling vaccination strategies against foot-and-mouth disease". In: *Nature* 421.6919 (2002), pp. 136–142. DOI: 10.1038/nature01343.

[67] Matt J Keeling. "Models of foot-and-mouth disease". In: *Proceedings of the Royal Society B: Biological Sciences* 272.1569 (2005), pp. 1195–1202. DOI: 10.1098/rspb.2004.3046.

[68] A. Khodakaram-Tafti and G. H. Farjanikish. "Persistent bovine viral diarrhea virus (BVDV) infection in cattle herds". In: *Iran J Vet Res* 18.3 (2017), pp. 154–163.

[69] Hyoungshick Kim and Ross Anderson. "Temporal node centrality in complex networks". In: *Physical Review E* 85.2 (2012). DOI: 10.1103/physreve.85.026107.

[70] Joern Klein. "Understanding the molecular epidemiology of foot-and-mouth-disease virus". In: *Infection, Genetics and Evolution* 9.2 (2009), pp. 153–161. DOI: 10.1016/j.meegid.2008.11.005.

[71] Tanja Knific et al. "Implications of Cattle Trade for the Spread and Control of Infectious Diseases in Slovenia". In: *Frontiers in Veterinary Science* 6 (2020). DOI: 10.3389/fvets.2019.00454.

[72] Martin A. Knight et al. "Generative models of network dynamics provide insight into the effects of trade on endemic livestock disease". In: *Royal Society Open Science* 8.3 (2021), p. 201715. DOI: 10.1098/rsos.201715.

[73] J Krebs et al. *Bovine Tuberculosis in Cattle and Badgers*. MAFF, 1997.

[74] I Krishnarajah et al. "Novel moment closure approximations in stochastic epidemics". In: *Bulletin of Mathematical Biology* 67.4 (2005), pp. 855–873. DOI: 10.1016/j.bulm.2004.11.002.

[75] A.B. Kudahl and S.S. Nielsen. "Effect of paratuberculosis on slaughter weight and slaughter value of dairy cows". In: *Journal of Dairy Science* 92.9 (2009), pp. 4340–4346. DOI: 10.3168/jds.2009-2039.

[76] Hartmut H. K. Lentz et al. "Disease Spread through Animal Movements: A Static and Temporal Network Analysis of Pig Trade in Germany". In: *Plos One* 11.5 (2016). DOI: 10.1371/journal.pone.0155196.

[77] Cong Li, Huijuan Wang, and Piet Van Mieghem. "Epidemic threshold in directed networks". In: *Physical Review E* 88.6 (2013). DOI: 10.1103/physreve.88.062802.

[78] Marco Mancastroppa et al. "Burstiness in activity-driven networks and the epidemic threshold". In: *Journal of Statistical Mechanics: Theory and Experiment* 2019.5 (2019), p. 053502. DOI: 10.1088/1742-5468/ab16c4.

[79] N. Gregory Mankiw and Mark P. Taylor. *Economics*. Cengage Learning EMEA, 2020.

[80] L. M. Mansley et al. "Early dissemination of foot-and-mouth disease virus through sheep marketing in February 2001". In: *Veterinary Record* 153.2 (2003), pp. 43–50. DOI: 10.1136/vr.153.2.43.

[81] Glenn Marion, Eric Renshaw, and Gavin Gibson. "Stochastic Modelling of Environmental Variation for Biological Populations". In: *Theoretical Population Biology* 57.3 (2000), pp. 197–217. DOI: 10.1006/tpbi.2000.1450.

[82] S.W Martin et al. "The association between the bovine tuberculosis status of herds in the East Offaly Project Area, and the distance to badger setts, 1988–1993". In: *Preventive Veterinary Medicine* 31.1-2 (1997), pp. 113–125. DOI: 10.1016/s0167-5877(96)01111-7.

[83] Lauren Ancel Meyers, M.E.J. Newman, and Babak Pourbohloul. "Predicting epidemics on directed contact networks". In: *Journal of Theoretical Biology* 240.3 (2006), pp. 400–418. DOI: 10.1016/j.jtbi.2005.10.004.

[84] A. Mitchell et al. "Characteristics of cattle movements in Britain – an analysis of records from the Cattle Tracing System". In: *Animal Science* 80.3 (2005), pp. 265–273. DOI: 10.1079/asc50020265.

[85] Sibylle Mohr et al. “Manipulation of contact network structure and the impact on foot-and-mouth disease transmission”. In: *Preventive Veterinary Medicine* 157 (2018), pp. 8–18. DOI: 10.1016/j.prevetmed.2018.05.006.

[86] Maggie Mort et al. “Psychosocial effects of the 2001 UK foot and mouth disease epidemic in a rural population: qualitative diary based study”. In: *Bmj* 331.7527 (2005), p. 1234. DOI: 10.1136/bmj.38603.375856.68.

[87] Mathieu Moslonka-Lefebvre et al. “Epidemics in markets with trade friction and imperfect transactions”. In: *Journal of Theoretical Biology* 374 (2015), pp. 165–178. DOI: 10.1016/j.jtbi.2015.02.025.

[88] Mathieu Moslonka-Lefebvre et al. “Market analyses of livestock trade networks to inform the prevention of joint economic and epidemiological risks”. In: *Journal of The Royal Society Interface* 13.116 (2016), p. 20151099. DOI: 10.1098/rsif.2015.1099.

[89] M. E. J. Newman. “Spread of epidemic disease on networks”. In: *Physical Review E* 66.1 (2002). DOI: 10.1103/physreve.66.016128.

[90] Mark E. J. Newman. *Networks an introduction*. Oxford University Press, 2018.

[91] MEJ Newman. “Power laws, Pareto distributions and Zipfs law”. In: *Contemporary Physics* 46.5 (2005), pp. 323–351. DOI: 10.1080/00107510500052444.

[92] Vincenzo Nicosia et al. “Components in time-varying graphs”. In: *Chaos: An Interdisciplinary Journal of Nonlinear Science* 22.2 (2012), p. 023101. DOI: 10.1063/1.3697996.

[93] S.S. Nielsen and N. Toft. “Ante mortem diagnosis of paratuberculosis: A review of accuracies of ELISA, interferon-γ assay and faecal culture techniques”. In: *Veterinary Microbiology* 129.3-4 (2008), pp. 217–235. DOI: 10.1016/j.vetmic.2007.12.011.

[94] S.S. Nielsen and N. Toft. “Effect of management practices on paratuberculosis prevalence in Danish dairy herds”. In: *Journal of Dairy Science* 94.4 (2011), pp. 1849–1857. DOI: 10.3168/jds.2010-3817.

[95] Javier Nuñez-Garcia et al. “Meta-analyses of the sensitivity and specificity of ante-mortem and post-mortem diagnostic tests for bovine tuberculosis in the

UK and Ireland". In: *Preventive Veterinary Medicine* 153 (2018), pp. 94–107. DOI: 10.1016/j.prevetmed.2017.02.017.

[96] M. J. H. Ohagan et al. "Test characteristics of the tuberculin skin test and post-mortem examination for bovine tuberculosis diagnosis in cattle in Northern Ireland estimated by Bayesian latent class analysis with adjustments for covariates". In: *Epidemiology and Infection* 147 (2019). DOI: 10.1017/s0950268819000888.

[97] A. Ortiz-Pelaez et al. "Use of social network analysis to characterize the pattern of animal movements in the initial phases of the 2001 foot and mouth disease (FMD) epidemic in the UK". In: *Preventive Veterinary Medicine* 76.1-2 (2006), pp. 40–55. DOI: 10.1016/j.prevetmed.2006.04.007.

[98] Aurore Palisson, Aurélie Courcoul, and Benoit Durand. "Role of Cattle Movements in Bovine Tuberculosis Spread in France between 2005 and 2014". In: *Plos One* 11.3 (2016). DOI: 10.1371/journal.pone.0152578.

[99] Romualdo Pastor-Satorras and Alessandro Vespignani. "Epidemics and immunization in scale-free networks". In: *Handbook of Graphs and Networks* (2004), pp. 111–130. DOI: 10.1002/3527602755.ch5.

[100] Romualdo Pastor-Satorras et al. "Epidemic processes in complex networks". In: *Reviews of Modern Physics* 87.3 (Aug. 2015), pp. 925–979. ISSN: 1539-0756. DOI: 10.1103/revmodphys.87.925. URL: http://dx.doi.org/10.1103/RevModPhys.87.925.

[101] Aurore Payen, Lionel Tabourier, and Matthieu Latapy. "Spreading dynamics in a cattle trade network: Size, speed, typical profile and consequences on epidemic control strategies". In: *Plos One* 14.6 (2019). DOI: 10.1371/journal.pone.0217972.

[102] Rosario Pérez-Morote et al. "Quantifying the Economic Impact of Bovine Tuberculosis on Livestock Farms in South-Western Spain". In: *Animals* 10.12 (2020), p. 2433. DOI: 10.3390/ani10122433.

[103] C.J.C Phillips et al. "The transmission of Mycobacterium bovis infection to cattle". In: *Research in Veterinary Science* 74.1 (2003), pp. 1–15. DOI: 10.1016/s0034-5288(02)00145-5.

[104] J.M. Pollock and S.D. Neill. "Mycobacterium boviss Infection and Tuberculosis in Cattle". In: *The Veterinary Journal* 163.2 (Mar. 2002), pp. 115–127. DOI: 10.1053/tvjl.2001.0655. URL: https://doi.org/10.1053/tvjl.2001.0655.

[105] Wouter Poortinga et al. "The British 2001 Foot and Mouth crisis: a comparative study of public risk perceptions, trust and beliefs about government policy in two communities". In: *Journal of Risk Research* 7.1 (2004), pp. 73–90. DOI: 10.1080/1366987042000151205.

[106] Jamie C. Prentice et al. "Complex responses to movement-based disease control: when livestock trading helps". In: *Journal of The Royal Society Interface* 14.126 (2017), p. 20160531. DOI: 10.1098/rsif.2016.0531.

[107] Tracey C. Pritchard et al. "Phenotypic effects of subclinical paratuberculosis (Johne's disease) in dairy cattle". In: *Journal of Dairy Science* 100.1 (2017), pp. 679–690. DOI: 10.3168/jds.2016-11323.

[108] S. J. Rangel et al. "A systematic review of risk factors associated with the introduction of Mycobacterium avium spp. paratuberculosis (MAP) into dairy herds". In: *Can Vet J* 56.2 (2015), pp. 169–177.

[109] S.E Robinson, M.G Everett, and R.M Christley. "Recent network evolution increases the potential for large epidemics in the British cattle population". In: *Journal of The Royal Society Interface* 4.15 (2007), pp. 669–674. DOI: 10.1098/rsif.2007.0214.

[110] Gianluigi Rossi et al. "Epidemiological modelling for the assessment of bovine tuberculosis surveillance in the dairy farm network in Emilia-Romagna (Italy)". In: *Epidemics* 11 (2015), pp. 62–70. DOI: 10.1016/j.epidem.2015.02.007.

[111] Tawatchai Singhla et al. "Determination of the sensitivity and specificity of bovine tuberculosis screening tests in dairy herds in Thailand using a Bayesian approach". In: *BMC Veterinary Research* 15.1 (2019). DOI: 10.1186/s12917-019-1905-x.

[112] Martina Velasova et al. "Herd-level prevalence of selected endemic infectious diseases of dairy cows in Great Britain". In: *Journal of Dairy Science* 100.11 (2017), pp. 9215–9233. DOI: 10.3168/jds.2016-11863.

[113] Matthew C Vernon. "Demographics of cattle movements in the United Kingdom". In: *BMC Veterinary Research* 7.1 (2011), p. 31. DOI: 10.1186/1746-6148-7-31.

[114] Matthew C Vernon and Matt J Keeling. "Representing the UKs cattle herd as static and dynamic networks". In: *Proceedings of the Royal Society B: Biological Sciences* 276.1656 (2008), pp. 469–476. DOI: 10.1098/rspb.2008.1009.

[115] Matthew C. Vernon and Matt J. Keeling. "Impact of regulatory perturbations to disease spread through cattle movements in Great Britain". In: *Preventive Veterinary Medicine* 105.1-2 (2012), pp. 110–117. DOI: 10.1016/j.prevetmed.2011.12.016.

[116] F. Vial et al. "Bovine Tuberculosis Risk Factors for British Herds Before and After the 2001 Foot-and-Mouth Epidemic: What have we Learned from the TB99 and CCS2005 Studies?" In: *Transboundary and Emerging Diseases* 62.5 (2013), pp. 505–515. DOI: 10.1111/tbed.12184.

[117] V.V. Volkova et al. "Potential for transmission of infections in networks of cattle farms". In: *Epidemics* 2.3 (2010), pp. 116–122. DOI: 10.1016/j.epidem.2010.05.004.

[118] Erik Volz and Lauren Ancel Meyers. "Epidemic thresholds in dynamic contact networks". In: *Journal of The Royal Society Interface* 6.32 (2008), pp. 233–241. DOI: 10.1098/rsif.2008.0218.

[119] Erik Volz and Lauren Ancel Meyers. "Susceptible–infected–recovered epidemics in dynamic contact networks". In: *Proceedings of the Royal Society B: Biological Sciences* 274.1628 (2007), pp. 2925–2934. DOI: 10.1098/rspb.2007.1159.

[120] R Whitlock et al. "ELISA and fecal culture for paratuberculosis (Johnes disease): sensitivity and specificity of each method". In: *Veterinary Microbiology* 77.3-4 (2000), pp. 387–398. DOI: 10.1016/s0378-1135(00)00324-2.

[121] R. J. Whittington et al. "Survival and dormancy of Mycobacterium avium subsp. paratuberculosis in the environment". In: *Appl Environ Microbiol* 70.5 (May 2004), pp. 2989–3004.

[122] R.J Whittington and E.S.G Sergeant. "Progress towards understanding the spread, detection and control of Mycobacterium avium subsp para-tuberculosis in animal populations". In: *Australian Veterinary Journal* 79.4 (2001), pp. 267–278. DOI: 10.1111/j.1751-0813.2001.tb11980.x.

[123] Richard Whittington et al. "Control of paratuberculosis: who, why and how. A review of 48 countries". In: *BMC Veterinary Research* 15.1 (June 2019). DOI: 10.1186/s12917-019-1943-4. URL: https://doi.org/10.1186/s12917-019-1943-4.